Performance and Environmental Sustainability Assessment of an Integrated Solar Water Heater Designed for Disassembly

by

RUTH M. SAINT
BSC, MSC

Thesis submitted in partial fulfilment of the requirements

of Edinburgh Napier University, for the award of

Doctor of Philosophy

School of Engineering and the Built Environment

Edinburgh Napier University

February 2021

Abstract

Recent amendments to the Climate Change (Scotland) Bill set an ambitious target of net-zero by 2045 and the Scottish Government has highlighted the need for policy reform to decarbonise heat. Minimum requirement for hot water provision through renewable technologies are already included in Section 7 (Sustainability) of the Scottish Building Regulations. However, with growing demand for affordable housing in Scotland, and modular construction becoming increasingly popular due to its affordability, energy performance and sustainability, there is an urgent need to identify solutions for a renewable provision of heat that aligns with construction trends and societal requirements.

This research aims to optimise a unique integrated collector-storage solar water heater (ICSSWH) design for integration into buildings under Scottish weather conditions, underpinned by a lifecycle perspective and incorporating circular economy principles. The ICSSWH evaluated was specifically engineered for integration into modern roof structures, to be compatible with offsite modular construction as a plug-and-play, fit-and-forget system, and designed for disassembly to improve reuse potential at the end of its useful life. Two design configurations were evaluated, baffled and finned, alongside two heat retention methods, additional insulation and a night cover.

Extensive field tests were conducted, with the designs embedded into a structural insulated panel, under a realistic draw-off profile to mimic practical application and quantitively assess real-life, seasonal performance. The baffled system outperforms the finned in every scenario and the night cover offers the greatest improvement in heat retention. Life cycle assessment (LCA) complemented field tests to establish whether operational savings achieved by the system would outweigh the embodied impacts. LCA showed that the ICSSWH can recoup both its embodied energy (3.7-5.5 years) and carbon (4.9-13 years) within its useful life. Additionally, the cost analysis demonstrated the economic viability with payback times of 5.8–7.7 years when replacing an electric system.

These analyses demonstrates the environmental sustainability of the system, and the element of integration into the roof structure, as part of a pre-built package, illustrates the benefits of its practical application. With extensive uptake of this technology, significant carbon savings could be achieved. If ICSSWHs were integrated into 10,000 new builds, the potential carbon savings would be approximately 13,200 tonnes of CO_{2e}, bringing the operational carbon emissions associated with the hot water demand of the new homes down by 42%. This work advances existing knowledge through: innovative design for disassembly and integration into the roof structure; a circular approach, considering sustainability at the design stage and promoting reuse over disposal; a feasible prototype evaluating real-life performance using a seasonal testing method and realistic draw-off profile.

Acknowledgements

This thesis would not have been possible without the help and support of my family, friends and colleagues. I would like to thank my supervisory team for always being there to give me advice and stem the moments of panic. Professor John Currie for being my director of studies and guiding me through the new terrain. Dr Francesco Pomponi for training me in the art of life cycle assessment and always making himself available to help. Dr Celine Garnier for believing in me and for not sugar-coating anything. I would also like to thank the technicians who helped me through the maze of DIY and for being patient with my lack of technical know-how.

Thank you to all of my friends and colleagues at Edinburgh Napier, past and present, who helped me in various ways and just provided a nice working environment. I would like to especially thank Niaz who made his LaTex template freely available for everyone to have a beautiful thesis and Faqhrul who spent hours and hours helping me understand how to use it.

Finally, I would like to thank my family. Shenando, who came out of nowhere but who has helped me through everything since. Rebecca, my person, who has helped me through everything my whole life. My mum, for supporting me and picking up the typos in the final stages. My dad, who never got to see me finish but I know he is still proud of me.

Author's declaration

I declare that this thesis has been composed solely by myself and that it has not been submitted, in whole or in part, in any previous application for a degree. Except where states otherwise by reference or acknowledgement, the work presented is entirely my own.

SIGNED: RUTH SAINT..... DATE: 29.06.2020.....

List of publications

Peer-reviewed journal articles and conference papers related to this PhD:

Saint, R.M., Pomponi, F., Garnier, C. and Currie, J. (2019). Whole life design and resource reuse of a solar water heater in the UK. *Engineering Sustainability*, **172**(3), pp. 153-164 ; doi:10.1680/jensu.17.00068.

Saint, R.M., Garnier, C., Pomponi, F. and Currie, J. (2018). Thermal Performance through Heat Retention in Integrated Collector-Storage Solar Water Heaters: A Review. *Energies*, **11**, 1615; doi:10.3390/en11061615.

Saint, R.M., Pomponi, F. and Currie, J. (2018). A method for a cradle-to-cradle life cycle assessment of integrated collector-storage solar water heaters. In: *Proceedings of the 9th International SOLARIS Conference 2018, Chengdu, China, 30th-31st August.*

Saint, R.M., Currie, J. and Garnier, C. (2017). Technological development of integrated collector storage solar water heaters: A review. In: *Proceedings of the 8th International SOLARIS Conference 2017, London, UK, 27th-28th July.*

TABLE OF CONTENTS

List of Tables

List of Figures

FIGURES **Page**

Nomenclature

Abbreviations

CED	Cumulative Energy Demand
CV	Coefficient of variation
DHW	Domestic hot water
EPD	Environmental Product Declaration
EPDM	Ethylene Propylene Diene M-class rubber
ETC	Evacuated tube collector
FPC	Flat-plate collector
FU	Functional unit
GWP	Global warming potential
ICSSWH	Integrated collector-storage solar water heater
LCA	Life cycle assessment
LCI	Life cycle inventory
LCIA	Life cycle impact assessment
MMC	Modern methods of construction
SD	Standard deviation
SIP	Structural insulated panel
SWH	Solar water heater

Scientific symbols

T_h	temperature at any given height in the water column	°K
T_b	temperature at the bottom of the tank	°K

h	length of the collector at any given height in the water column	m
H	total length of the collector	m
Q	Useful energy delivered	kWh
m	mass of water required	kg
C_p	specific heat capacity of water	J/kg· °K
ΔT	temperature difference between inlet and outlet water	°K
T_i	hourly bulk water temperature from the start of the cooling period	°K
T_{final}	bulk water temperature at the end of the cooling period	°K
Q_{req}	total energy required	kWh
I_{ave}	average solar insolation during the collection period	W/m^2
Q_{inc}	total incident energy on the absorber surface	Wh
T_w	bulk water temperature in the tank	°K
T_{out}	hot water outlet temperature	°K
η_{col}	collection efficiency	%
η_{ret}	heat retention efficiency	%
Q_{col}	total solar energy collected by the absorber surface	Wh
$T_{initial,c}$	initial bulk water temperature at the start of the cooling period	°K
T_{amb}	average ambient temperature	°K
U	U-value, heat loss coefficient	W/m^2°K
d	material thickness	m
k	thermal conductivity	W/m· °K
U_{system}	heat loss coefficient of a system	W/m^2°K
mc_{system}	thermal mass of the system	J/°K
A_{unit}	area heat is being lost from	m^2
Q_{lost}	energy loss from a system	J
Δt	duration of the cooling period	s

First Chapter

Introduction

1.1 The energy scenario

Current trends of global population growth will dramatically increase the energy demand worldwide, which is still largely met by fossil fuels (BP, 2019). At the current rate of extraction, reserves of coal, crude oil, and natural gas will be exhausted in 119, 46, and 63 years, respectively (Wang et al., 2015). These projections are susceptible to numerous factors including an ever-changing market and political and social conditions. Running out of energy is not the only concern; global warming from greenhouse gas (GHG) emissions and the resultant climate change poses a real and global threat. Society's reliance on fossil fuels is shifting towards more renewable and sustainable forms of energy but this shift must be accelerated to meet climate targets.

The Kyoto Protocol came into force in 2005 in a bid to mitigate the damaging effects of global warming and climate change and by 2016 192 countries had ratified it (UNFCC, 2016). The Protocol is an international agreement where member countries commit to internationally binding emission reduction targets. These member countries opted to accelerate and intensify current efforts against climate change, a global reduction target of 18% below 1990 levels, which manifested in the Paris Agreement. This Agreement states that global temperature rise must be limited to below 2°C by 2100, compared to preindustrial levels (United Nations, 2015). The definition of 'pre-industrial' is ambiguous, but the approach is clear; less, ideally zero, energy derived from fossil fuels

and more from renewable sustainable sources.

The EU is becoming a leader in the battle against climate change despite only contributing 10% of global GHG emissions (European Commission, 2012). The EU was apportioned 8% of the burden-sharing agreement of the first Kyoto commitment period for the reduction target. Certain countries within the EU shoulder more of the burden than others such as Finland, France, Greece, Ireland, Sweden, and the UK. The UK remained on track, below or close to their Kyoto Protocol target path, and achieved domestic emissions reductions of 12.5% below 1990 levels (European Commission, 2003). The UK then set a statutory emissions reduction target of at least 80% below 1990 levels by 2050, strengthening their role as an international leader in tackling climate change (DECC, 2015). In a further push to combat climate change, the UK has put forth legislation to set a net zero emissions target, by 2050, in law (DBEIS, 2019a).

In addition to the targets set by the UK, Scotland introduced an interim target for 2020 aimed at reducing domestic emissions by at least 42%, compared to 1990 levels, which remains in line with the EU and UK 2050 roadmap (European Commission, 2012). By 2014, Scotland achieved a 45.8% reduction in their adjusted emissions, exceeding the 2020 target six years early (Scottish Government, 2017). The Scottish Government sporadically publishes a report on policies and proposals (RPP) to ensure the satisfactory delivery of the statutory annual targets set through the Climate Change (Scotland) Act 2009. The most recent is the RPP3, released in January 2017, which sets a reduction target of 66% below 1990 levels by 2032 (Scottish Government, 2017).

The reductions to date have been achieved by the reduced use of coal in the power sector alongside increased renewable energy generation. However, the RPP3 also states that "*there has been little progress in reducing emissions from transport and agriculture and land use, and there is much further to go for renewable heat uptake. To meet high ambition and tighter targets beyond 2020 there is a need for stronger policies in the Climate Change Plan*" (Scottish Government, 2017, p.7). This admonition highlights the need for policy reform regarding renewable heating and the need to decarbonise heat. Additionally, in response to the ambitious net zero target for the UK, Scotland has lodged amendments to the Climate Change (Emissions Reduction Targets) (Scotland)

Bill. These amendments aim to reduce greenhouse gas emissions in Scotland to reach net-zero by 2045. Therefore, the drive towards a renewable future must be accelerated (Scottish Government, 2019).

1.2 The solar resource

Fundamentally, all sources of energy on Earth can be attributed to the sun. Solar energy fuels life through photosynthesis, provides warmth, generates wind, waves and rain by heating the land and sea creating a pressure differential, as well as generating tidal energy through the gravitational pull of the moon and sun. Barring nuclear and geothermal energy, the sun is the basis of renewable energy resources; wind, solar, marine/hydro, and bioenergy. Solar energy is the greatest potential resource, with 120,000 terawatts striking the Earth's surface (Philibert, 2006). The amount of solar radiation that reaches Earth's atmosphere is known as the solar constant and is 1367 W/m^2, on average (Zombeck, 2007). Global solar radiation comprises two components, direct and diffuse radiation (Figure 1.1). Direct radiation describes solar radiation that travels in a straight line from the sun to the surface of the earth without being scattered. Diffuse radiation is the solar radiation that arrives at the earth's surface after it has been scattered by molecules and particles in the atmosphere and can travel in any direction. This global radiative energy is termed 'insolation' and is the energy per unit area measured in J/m^2 or kWh/m^2.

Scotland receives a peak solar radiance of 900 W/m^2 in the summer months with daylight lasting approximately 16 hours. In the winter months there are fewer daylight hours and much weaker insolation, averaging 400 W/m^2 (Currie et al., 2008). Weather conditions in Scotland are not perfect for solar technologies due to the relatively low solar insolation levels compared to other temperate regions. Scotland also suffers from high levels of cloud cover, particularly in the afternoon due to the maritime climate. This means that solar technologies must work with diffuse radiation as well as direct. The limitations of the Scottish climate can be overcome if solar energy systems are designed efficiently, implemented effectively and fit for purpose. Solar water heating systems do

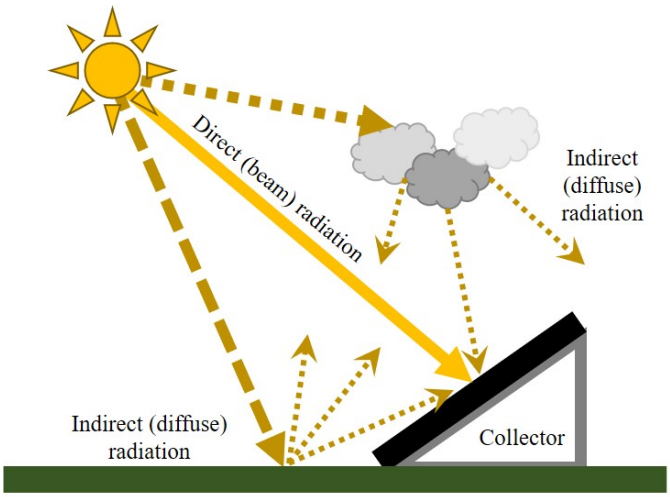

Figure 1.1: Illustration of direct and diffuse solar radiation

not rely solely on direct radiation, they can also absorb diffuse radiation. This allows greater flexibility in their use as they are not as constrained in terms of orientation and inclination, i.e. the position relative to north and the angle relative to the horizontal plane, respectively. Solar water heaters (SWHs) are not a new technology, they have been studied and adopted for decades. There are numerous commercial models for domestic application, but they are mainly evacuated tube or flat plate collectors (Figure 1.2). These are dispersed systems where the collector is separate from the water storage tank. Another style of SWH is the integrated collector-storage solar water heater (ICSSWH) which combines the collector and storage tank into a single, compact unit (Figure 1.2). The ICSSWH offers several benefits over commercially available SWHs:

- Simple, low-cost design
- Passive system with no working parts (e.g. heat exchanger, pumps)
- Compact design reduces heat loss points with fewer conduits and connecting pipes
- Fewer parts means reduced complexity and manufacturing costs
- Reduced space requirement as an external water storage tank is not needed
- Lower environmental impact due to fewer components
- 'Plug-and-play' design reduces user error.

Evacuated tube collector Flat plate collector ICSSWH

Figure 1.2: The main types of solar water heaters. The evacuated tube and flat plate collectors require an external water storage tank while this is integrated in the ICSSWH variant

Substantial research on ICSSWH systems has already been conducted at Edinburgh Napier University (Birley et al., 2012; Garnier, 2009; Henderson et al., 2007; Junaidi, 2007) presenting evidence that SWHs are a feasible contributing solution to the energy crisis in Scottish weather conditions. A major drawback with these systems remains unaddressed in the Scottish context; as the collector is in contact with the water store, the system suffers heavy heat losses, especially at night. The current research builds upon this foundation with the aim to optimise the system further by altering its design and by adding heat retention methods to combat night-time heat losses. This novel ICSSWH design offers additional improvements over previous iterations. The system has been designed for disassembly, with a strong influence from circular economy principles and resource reuse. The materials were chosen not only based on their thermal performance but also their reuse and recycle potential, reducing the environmental impact and increasing the sustainability of the system. Also, the ICSSWH has been designed for integration into warm roof timber construction, negating the need for an insulated housing and further reducing the materials required.

The following section outlines the rationale behind this research and the scope of the study.

1.3 Research rationale and scope

There is an identified need for decarbonised heat, not just in Scotland but globally. Given the immense solar resource available, development and optimisation of renewable heating technologies harnessing this resource is justified. One such technology is the ICSSWH and, with its simple, low cost, space-saving design, it offers a potentially

contributing solution. However, in climates like Scotland, a major drawback is night-time heat loss. Additional, for any technology to meaningfully contribute to a zero-carbon future, their impact across the whole life-cycle must have a net benefit in terms of emissions, i.e. their operational savings outweigh the emissions invested in their production. After a thorough literature review, there is an extensive knowledge base on the operational performance of conventional solar water heating technologies, i.e. flat plate and evacuated tube collectors. However, limited research has been conducted in northern maritime climates, where there is a greater need for heat, for these ICS-type collectors and even fewer studies evaluate the sustainability of these systems. Therefore, the rationale behind this research is to fill the identified gaps in knowledge highlighted through the literature review and evaluate the practical application of a novel ICSSWH design under Scottish weather conditions.

The scope of this work covers the performance and environmental sustainability assessment of two ICSSWH design configurations, under different heat retention methods to combat the night-time heat losses. These design configurations and heat retention methods were informed by the literature. A critical element of the ICS is its design for disassembly; considering sustainability in the design stage, highly reusable materials were chosen and the system was specifically designed to be easily dismantled at the end of its useful life. A real-life experimental testing method is employed to determine the seasonal operational performance under a realistic hot water draw-off profile. In terms of the environmental sustainability, a cradle-to-cradle life cycle assessment is carried out to highly the importance of material and resource reuse as opposed to disposal.

The following section outlines the aim and objectives of this thesis, highlighting the contribution to knowledge this work will provide.

1.4 Aim and objectives

The **aim** of this research is the optimisation of a unique integrated collector-storage solar water heater (ICSSWH) design for integration into buildings under Scottish weather conditions, incorporating circular economy principles. This aim will be achieved through

the following **objectives**:

1. Optimise the ICSSWH design for integration into modern offsite modular construction
2. Establish the impact/improvement external heat retention methods have on thermal efficiency without significantly increasing the complexity of the unit
3. Evaluate the overall performance of the design (considering Objectives 1 and 2) when it is used in a direct draw-off configuration (i.e. hot water use)
4. Determine the environmental impact and energy and carbon payback times for the ICSSWH system using Life Cycle Assessment (LCA).

Through the aim and objectives, this thesis offers the following **contributions to knowledge**:

1. Development and thermal performance evaluation of a more sustainable ICSSWH system, designed to be disassembled
2. The environmental impact/benefit of the ICSSWH due to its unique design for disassembly, considering a circular economy ethos
3. Extended field tests for the ICSSWH under a realistic draw-off profile and how the system performance is impacted by transient discharge and recharge cycles
4. Real-life performance assessment of different heat retention methods on the current ICSSWH design under Scottish weather conditions.

1.5 Thesis roadmap

Chapter 1 provides the background for this research, giving an introduction to the broader energy scenario, focusing on the UK and Scottish context to highlight the emission reduction targets that have been set. Solar energy as a resource is explored along with the potential of solar water heating in Scotland, specifically integrated

collector-storage solar water heater systems. This chapter also provides the research rationale and scope and the aim and objectives that will be referred to throughout the thesis. Finally, the structure of the thesis is outlined.

Chapter 2 presents the literature review which is divided into four main sections: an introduction to SWHs, heat retention methods, domestic hot water draw-off, and life cycle assessment. The first section has a specific focus on heat retention strategies and design parameters to target Objectives 1 and 2. Section 2 looks at draw-off to address Objective 3 and the final section reviews the literature surrounding life cycle assessment to set the scene for Objective 4.

Chapter 3 reviews the research approach, design and methods used throughout the thesis and is divided into three main sections: the research approach, field experiments and life cycle assessment. The field experimental work details the test-rig set-up and testing regime, equipment calibration, and the data measurement, collection and analysis. Experimental considerations are also presented, evaluating the equipment error and uncertainty, as well as operational errors. This section also includes the draw-off profile and seasonal test method that was used during the field testing. Finally, the life cycle assessment method is outlined and discussed.

Chapter 4 is the first part of the analysis and results, based on the field experiment work, which provides evidence for Objectives 1, 2 and 3. This chapter is broken down into a baseline comparison of the two ICSSWH design configurations under evaluation, both with and without draw-off. This is followed by the analysis of the heat retention methods, informed by the literature review, that were applied to each base configuration. These design conditions were tested under a direct draw-off profile and compared against each other, as well as across the two configurations. Also, a comparison of an insulated frame versus integration into a structural insulated panel (SIP) as a housing for the ICSSWH is presented.

Chapter 5 is the second part of the analysis and results, based on the life cycle assessment aspect, and provides evidence for Objective 4. This chapter presents a comprehensive analysis of the environmental and energy impacts of the two base configurations both with and without the design conditions (heat retention methods)

applied. Also, the carbon and energy impact of housing the ICSSWH system in an insulated frame versus a SIP are compared.

Chapter 6 provides the discussion of the findings and ties together the two previous chapters, adding new insight and understanding to the collected data. The chapter discusses how the ICSSWH performs under the different design configurations and conditions. How the ICSSWH ranks in terms of environmental impact and sustainability and whether it can be successfully integrated with timber MMC. Also, where the unique designs evaluated in this thesis sit in the larger context of commercially available solar water heaters and existing literature. Based on this discussion of the findings, this chapter concludes with the benefits of such systems in a Scottish context and recommends an optimum arrangement.

Chapter 7 is the final, concluding chapter. It highlights the contributions this thesis makes to current knowledge and draws important conclusions from each of the elements within the work. Here, the outcome of the research aim and objectives are summarised. The limitations are also reiterated, making way for future work and recommendations.

Second Chapter

Literature Review

The context of the present study is the use of an integrated collector-storage solar water heater (ICSSWH) design in a Scottish climate. To enable the optimisation of this system, three key aspects are focused on throughout this literature review. First is their adaptation to, or suitability for, Scottish weather conditions. Second, is the importance of performance and efficiency during domestic application when subject to domestic hot water demand. Finally, the energy and environmental benefits of using solar water heaters (SWHs), namely ICSSWH, over conventional energy sources.

This chapter reviews the literature surrounding these core aspects and is sub-divided accordingly. Section 2.1 gives a brief background on SWHs, the different systems available and their defining characteristics. Section 2.2[1] focuses on the various heat retention methods reviewed throughout the literature, highlighting ways solar water heating can be adapted to a Scottish climate. Section 2.3 reviews the draw-off profiles presented by different government bodies and academic studies to derive a robust method for evaluating performance during domestic application. Section 2.4[2] provides a comprehensive summary of the literature concerning life cycle assessment (LCA) and SWHs. The primary focus throughout this literature review is on studies surrounding ICSSWHs.

[1] Section 2.2 of this chapter is adapted from the following paper: Saint, R.M., Garnier, C., Pomponi, F., Currie, J. (Saint et al., 2018). Thermal performance through heat retention in integrated collector-storage solar water heaters: A review. *Energies*, **11**(6), 1615. https://doi.org/10.3390/en11061615

[2] Section 2.4 of this chapter is adapted from the following paper: Saint, R.M., Pomponi, F., Garnier, C., Currie, J.I. (Saint et al., 2019). Whole life design and resource reuse of a solar water heater in the UK. *Engineering Sustainability*, **172**(3), pp. 153-164. https://doi.org/10.1680/jensu.17.00068

2.1 Solar water heaters

The first SWH of its kind, 'The Climax Solar-Water Heater', was patented by Clarence M. Kemp in the US in 1891 and the evolution of SWHs has been an impressive journey. However, once extensive oil and gas reserves were discovered, research into these systems halted until the early 1970s (Smyth et al., 2006). Japan, a country devoid of fossil fuels but with a high demand for hot water, continued the development of solar water heating. Japan patented several ICSSWH designs (Smyth et al., 2006; Tanishita, 1955) which, along with global concern for alternative energy sources to replace OPEC-embargoed Arabian oil, revitalised the research and development of these systems in other countries such as the US, South Africa and Australia (Smyth et al., 2006). Interest in solar water heating has also been revived in response to global initiatives aimed at the promotion of renewable energy technologies to mitigate greenhouse gas (GHG) emissions (IPCC, 2014a; United Nations, 1998).

There are many different models of SWH systems, but they all have the same goal; to deliver hot water to the end-user when required, efficiently and at a reasonable cost. Figure 2.1 illustrates five of these SWH designs. Focusing on the built-in storage type of SWH, Figure 2.2 shows an ICSSWH and illustrates the general key components of any SWH: an absorber surface to collect incident solar radiation, a storage tank (either combined with the collector or a distributed system), glazing with high transmission, insulated housing for the collector/storage unit, and cold-water inlet and hot-water outlet pipes.

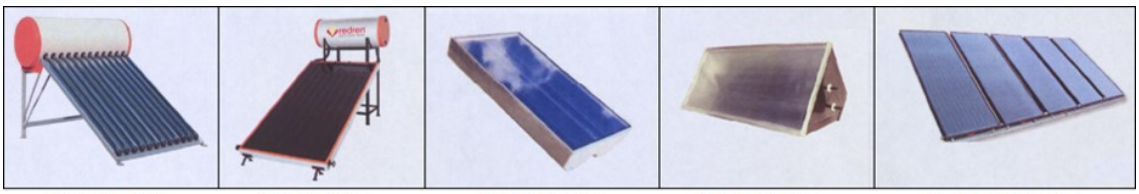

Figure 2.1: Different solar water heater designs. Adapted from Junaidi (2007)

The concept of a SWH is very simple, sunlight is used to heat a body of water which is then stored until required by the end-user. Solar radiation strikes an absorbing surface

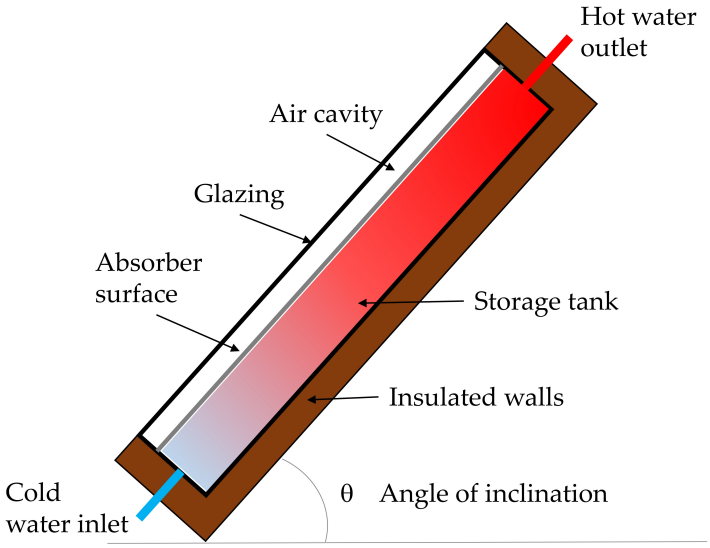

Figure 2.2: Diagrammatic representation of the key components of an ICSSWH

which is in contact with a heat transfer fluid, such as water or glycol, causing the heat to pass into the fluid thus raising its temperature. SWHs can be direct or indirect and active or passive. In a direct system, water is heated and then stored directly. A system using a heat transfer fluid, for example a glycol/water mixture, is indirect as this fluid is unpotable. It is continuously recycled through the system, transferring its heat via a heat exchanger to water in an external storage tank.

Active systems, also known as forced circulation systems, can be direct or indirect and require an electric pump to circulate the water/heat transfer fluid. Active systems also require a control system which monitors the temperature inside the collector and storage tank. When the water temperature at the top of the storage tank is sufficiently higher than at the base, the electric pump begins to circulate water, this is usually controlled by a differential thermostat. In passive systems, this circulation is achieved through natural convection; the storage tank is positioned above the collector thus promoting buoyant flow. Like active systems, passive systems can also be direct or indirect; the difference being there is no requirement for a pump or control system.

In terms of design and operational principles, SWHs can be divided into the following categories: (a) thermo-syphonic; (b) forced circulation type SWHs; (c) ICS systems; (d) direct circulation; (e) indirect water heating systems (using a heat transfer fluid); (f)

hybrid system (back-up electric heating). Types (a) and (c) are passive systems while the other categories are termed active (Singh et al., 2016).

A comparison of passive versus active systems, under the similar weather conditions, shows that active systems have efficiencies between 35-80% higher than natural circulation, passive systems (Khalifa, 1998). Also, in passive systems, e.g. thermo-syphonic, the storage tank must be above the collector for natural convection to occur. This is not necessary in active systems due to the use of a pump, making them more suited to multi-story buildings. However, the active system is much more complex due to its additional components and dependency on electricity (Wang et al., 2015). Not only does this detract from the zero-carbon aim of solar water heaters but it also requires experienced personnel to operate it, greatly increasing the running costs. Passive systems do not require these additional components, such as pumps and control systems, so they have lower installation costs. Overall, passive systems are the most commonly used SWHs for domestic applications (Wang et al., 2015).

The three most common SWH designs are concentrating collectors, evacuated tube collectors, and flat-plate collectors. The choice of which design to employ can be determined by the environmental conditions and the heating requirements of the end-user. Flat-plate collectors are the cheapest of the three options and are used extensively for domestic water heating applications due to the performance advantages relative to cost (Currie et al., 2008). They have varying designs, such as serpentine, parallel tubes or ICSSWH, and they collect both direct and diffuse radiation. This is advantageous in overcast conditions and solar tracking is not required thus lowering system cost and complexity. As a subset of flat-plate collectors, ICSSWH systems combine the collector and storage components into a single unit making their design the simplest, able to supply heated water for instantaneous use. This design has no need for pumps, heat exchangers or moving parts, under certain configurations, with natural circulation of the water through the system occurring when water is drawn off, i.e. whenever there is demand.

Many studies of these systems aim to evaluate and optimise their performance, including optical efficiency, thermal efficiency, and heat retention. A major drawback

of integrated collector-storage (ICS) systems is the substantial heat losses experienced during non-collection periods, such as heavy overcast conditions and at night. There have been many papers over the last decade aiming to review heat loss reduction strategies and to appraise the work being conducted in the area of thermal performance. Table 2.1 provides a summary of recent papers reviewing ICS systems and details the design factors considered, i.e. design elements beyond the key components that aim to improve performance. Smyth et al. (2006) present the most comprehensive review of the technical aspects of ICSSWH systems. Kumar and Rosen (2013) also review numerous optimisation strategies, collating key literature.

Table 2.1: Summary of papers reviewing the current research and outcomes surrounding design factors of ICS systems

Reference	**Title**	**System(s) Reviewed**	**Design Aspects Reviewed**
Smyth et al. (2006)	Integrated collector storage solar water heaters	ICSSWH	Additional insulation; Baffles; Cavity evacuation; Collector material; Glazing; phase change material (PCM); Reflectors; Selective absorber surfaces
Kumar and Rosen (2013)	Review of solar water heaters with integrated collector-storage units	ICSSWH	Additional insulation; Baffle Plates; Glazing; Inlet valve configuration; PCM; Reflectors; Selective absorber surfaces
Raisul Islam et al. (2013)	Solar water heating systems and their market trends	ICSSWH; Thermo-syphon; Direct/ indirect circulation; Air	Additional insulation; Baffle plates; PCM; Reflectors
Ibrahim et al. (2014)	Review of water-heating systems: General selection approach based on energy and environmental aspects	ICSSWH; Thermo-syphon; Active; PV/T; PCM	Fins; PCM; Reflectors; Selective absorber surfaces
Souliotis et al. (2015)	Integrated collector storage solar water heaters: Survey and recent developments	ICSSWH	Additional insulation; Baffle plate/inner sleeve; PCM; Thermal diodes
Colangelo et al. (2016)	Innovation in flat solar thermal collectors: A review of the last ten years experimental results	Flat-plate; ICSSWH; PV/T	Additional insulation; Collector material; Fins; Nanofluids; Selective absorber surfaces
Jamar et al. (2016)	A review of water heating system for solar energy applications	Flat-plate; Evacuated tube; Concentrating; ICSSWH	Auxiliary immersion heating; Nanofluids
Singh et al. (2016)	Recent developments in integrated collector storage (ICS) solar water heaters: A review	ICSSWH	Additional insulation; Baffle plate/inner sleeve; Thermal diodes

2.2 Heat retention

ICSSWH systems are the simplest of the SWH designs, combining the collector and storage tank into one compact unit. As a result, ICSSWH are subject to heavy heat losses, especially during overcast and non-collection periods (Grassie et al., 2006). Figure 2.3 illustrates the heat transfer mechanisms in a typical ICSSWH system showing the number of ways heat can be lost. The collector surface absorbs solar radiation and converts it to heat which is then transferred directly to the water through conduction. This heat is transmitted throughout the water body via convection. Due to the buoyancy effect, thermal stratification (i.e. distinct layers of different temperatures) builds up in the water body with the hottest water at the top of the tank where most heat is lost through convection, conduction and radiation.

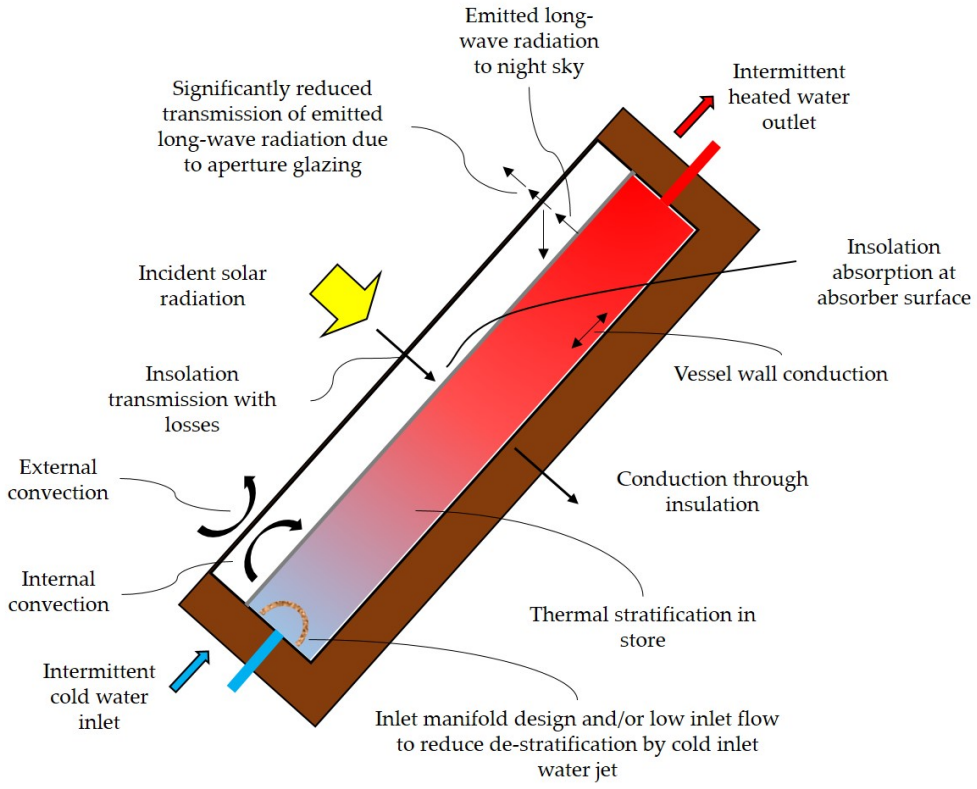

Figure 2.3: Illustration of the heat transfer processes in an ICSSWH. Adapted from Smyth et al. (2006)

Convective heat losses occur between the absorber plate and the glazing, so the air cavity needs to be optimised to act as an insulating gap, suppressing convective heat transfer to the collector to minimise losses when ambient temperatures drop.

Conductive heat loss from the back and side walls, as well as the absorber surface, is a major problem for ICSSWH systems and they need to be heavily insulated. Long-wave radiative heat losses have the largest impact and occur between the absorber plate, the glazing, and the night sky. The glazing needs to have a very high transmissivity to ensure as much incident solar radiation can reach the collector surface as possible whilst again minimising radiative losses.

2.2.1 Design factors

Many strategies exist to overcome heat loss and this section discusses the research surrounding these methods, with a focus on ICSSWH systems. Within this work, these strategies are termed 'design factors' as they are additional performance aides to the key design components of a solar thermal system.

2.2.1.1 Insulation

Insulation is a simple and effective way of retaining heat, particularly at night. Opaque and transparent are the two main types of insulation. Opaque insulation is primarily used around the back and sides of the systems where ambient heat losses through conduction and convection are high but there is no need for transmittance of solar radiation (McCracken, 1978; Muneer et al., 2006). A large percentage of heat is lost through the glazing as this needs to transmit solar irradiance. This loss can be alleviated by insulating the air cavity, using opaque or transparent insulated glazing materials, and/or by applying an insulating cover during the night and non-collection periods.

Transparent insulation materials (TIMs) TIMs are a new class of thermal insulation used to reduce unwanted heat losses from air gaps and evacuated spaces. TIMs are transparent to solar irradiation yet they can provide good thermal insulation. Early attempts to use these materials, such as experimental work by McCracken (1978), led to overall decreases in system efficiency, by 20% during daytime collection, due to their poor solar transmittance (0.85 in this case). However, research and development of these materials has led to greater collector performances and they could be beneficial

for heat retention in thermal energy systems. TIMs include organic-based transparent foams, honeycomb or capillary structures, and inorganic glass foams (e.g., silica aerogel). There are several configurations available in terms of cellular geometry, as illustrated in Figure 2.4 (Kaushika and Sumathy, 2003).

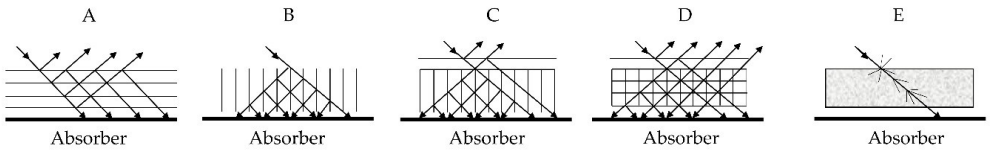

Figure 2.4: Diagrammatic representation of different cellular geometries. (A) Absorber-parallel; (B) Absorber-perpendicular; (C) Mixed configuration; (D) Cavity structures; (E) Homogeneous. The arrows indicate the absorptance and reflectance of the different TIMs in terms of incident solar irradiance. Adapted from Kaushika and Sumathy (2003)

Kaushika and Sumathy (2003) conducted a review of solar TIMs. They found that using a honeycomb material produced the highest efficiencies when compared to a single- and double-glazed system and a transparent slab of methyl methacrylate (MMA). Another outcome was that efficiency increases with TIM thickness; a thicker insulating layer retains enough heat to offset the negative impact on solar transmittance. For the honeycomb cover system, increasing TIM thickness from 25 mm to 50 mm had the greatest impact with an 8% efficiency increase. Increasing from 50 mm to 100 mm only offers a 4% so this must be balanced against production cost.

Schmidt and Goetzberger (1990) evaluated a single-tube absorber mounted in an involute reflector. They determined that the ICS performance was almost constant for a TIM with a polycarbonate honeycomb structure and thickness ranging from 50–150 mm. Chaurasia and Twidell (2001) compared two identical ICS units, one with TIM and the other without. The system with TIM had a total heat loss factor of 1.03 W/m^2K, with hot water at temperatures 8.5–9.5°C higher the next morning, compared with 7.06 W/m^2K for the glass only system. The study found that, by using TIM, storage efficiency was 24.7% higher; 39.8% compared to 15.1% without the TIM.

Reddy and Kaushika (1999) conducted a series of comparative studies on the effect of different TIM configurations for a rectangular ICSSWH. They reported that an absorber-perpendicular configuration, with a transparent honeycomb structure

immersed in an air layer, exhibited superior efficiencies over corresponding absorber-parallel configurations, with multiple covers of glass/plastic films. These findings were later corroborated by Kaushika and Reddy (1999) and Ghoneim (2005). Reddy and Kaushika (1999) concluded that the double-wall structured polycarbonate TIM sheet was the most effective configuration and a system with a thickness of 10 cm can achieve average solar collection and storage efficiencies in the range of 20–40% and bulk water temperatures between 40 and 50°C.

Research into TIMs has progressed since the early work by McCracken (1978) and they are capable of significantly improving the heat retention of SWHs without too much impact on solar transmittance. This is important for adaptation of ICSSWHs in Scottish weather conditions as a solution to night-time heat losses. However, TIMs are not yet cost effective for low cost solar thermal solutions; their performance improvement is outweighed by their cost.

Opaque insulation Several studies have experimentally reviewed the collector performance of fully versus partially exposed designs. Tripanagnostopoulos et al. (1999) evaluated the performance of two double-vessel systems using asymmetric compound parabolic concentrator (CPC) reflectors where one had both tanks fully exposed while the other was partially exposed. The latter showed improved heat retention during non-collection periods, but the fully exposed design exhibited greater collection efficiency. Smyth et al. (2003) investigated two ICSSWH systems enclosed within a concentrating collector. One system was a fully exposed, 1.0 m long cylindrical tank and the other a 1.5 m long tank with the top third heavily insulated. Unlike Tripanagnostopoulos et al. (1999), the insulated system exhibited a 13% increase in collection efficiency and increased thermal retention of up to 37% in the upper insulated section due to stratification. However, these results are perhaps reflecting the greater storage capacity and lower average water storage temperatures of the 1.5 m tank.

Chaabane et al. (2014) also found, through a numerical CFD study, that a partially insulated tank effectively retained heat during non-collecting periods. For the studied CPC mounted ICS system, they found that the additional insulation did affect the op-

tical efficiency, with slightly lower water temperatures observed; up to 7.5°C difference between the insulated and non-insulated systems. However, this trade-off was worthwhile with higher temperatures (by up to 7°C) at the start of the collection period and an approximately 25% reduction in thermal losses.

Using an experimental set-up, Souza et al. (2014) and Swiatek et al. (2015) studied a parallelepiped ICSSWH system which was partially heated. Souza et al. (2014) looked at the effect on thermal stratification within a cavity with a heat flux applied only to bottom 0.2 m. Swiatek et al. (2015) later adapted this and applied the heat flux to a 0.2 m section in the middle of the cavity. Beyond the heated zone, the front plate of the cavity in both studies was entirely insulated with extruded polystyrene. Souza et al. (2014) found that by only heating a short section at the bottom of the cavity the evolution of thermal stratification within the tank was unsatisfactory and reported a maximum temperature difference of only 4.2°C. The adaptations made in the later study yielded enhanced levels of stratification, with a maximum temperature difference of 20.1°C (Swiatek et al., 2015).

Despite the reduction in solar transmittance, partial insulation of the absorber area offers a simple solution with good improvement in performance. If the material is low-cost with a high thermal resistance, the reduced absorption during the collection period can be outweighed by the higher temperatures at the end of the non-collection period without significantly increasing the cost.

Night cover As well as insulating the air cavity, an insulating night cover can be used to reduce night-time heat losses. Kumar and Rosen (2011a) undertook a comparative performance investigation of rectangular ICSSWHs, assessing various heat loss reduction strategies. The following five cases were assessed: (1) single glazed without night insulation cover; (2) single glazed with night insulation cover; (3) double glazed without night insulation cover; (4) TIM with single glazing; and (5) insulating baffle plate with single glazing. They found that the TIM covered system reached lower absorber plate temperatures than single- and double-glazed cases due to the system receiving 10–15% less solar radiation. However, the TIM layer did help retain heat in the water store

during the night, more so than the double glazing and significantly more than the single glazing. The single and double glazing perform in a similar manner during periods of insolation but at night the double-glazed systems exhibits greater heat retention. Figure 2.5 illustrates the bulk water temperatures of the ICSSWH systems over a 24 h period showing that all five cases perform well. In terms of efficiency, Cases 2 and 3 exhibit almost identical performance, 57.1% and 57.6%, respectively. In all cases, efficiency increased with increasing flow rate. Therefore, of the five cases, 2 and 3 maintain the highest temperatures and collector efficiencies with little difference in performance; the choice of which solution to use becomes a matter of cost and complexity.

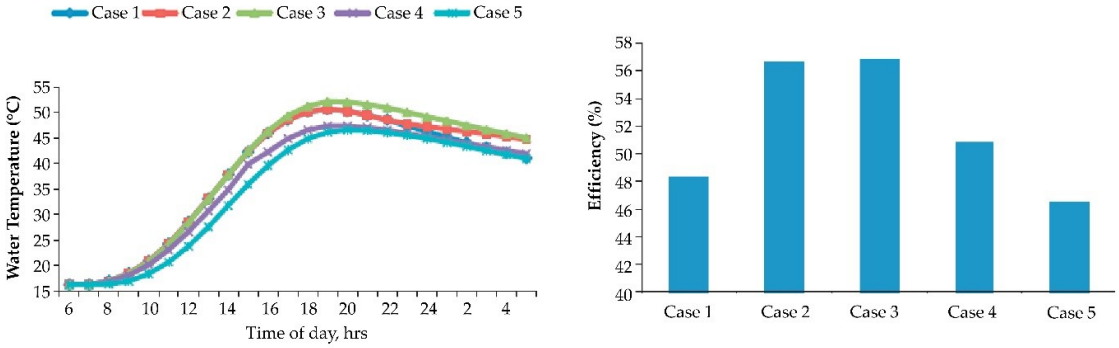

Figure 2.5: Daily variation in the bulk water temperature (left) and collector efficiencies (right) for the five reviewed cases. Adapted from Kumar and Rosen (2011a)

Applying a night cover may add complexity to the system, either through having to apply it manually or installing an automated system. However, the performance is comparable between a single-glazed system with a night cover and a double-glazed system with no night cover. Therefore, the single glazed system would be a suitable low-cost option as double-glazing is more expensive than a solar powered blind, for example a VELUX Solar Blackout Blind.

2.2.1.2 Auxiliary heating

In a Scottish climate, average total hot water demand cannot be met by SWHs alone due to their diurnal nature. Garnier (2009) tested the thermal performance of an ICSSWH with a 1 m^2 absorber area and 50 litre capacity. They discovered that the amount of energy required to supply a three-person household with a domestic hot water demand of 50 l/person/day at 55°C is approximately 7.5 kWh/day, 2747 kWh/year. The amount

of energy that the studied ICSSWH could contribute to this demand is shown in Figure 2.6; 1107 kWh, or 40% of the yearly energy demand. Therefore, the remaining 60% would need to be supplied by an auxiliary heater for diurnal demand.

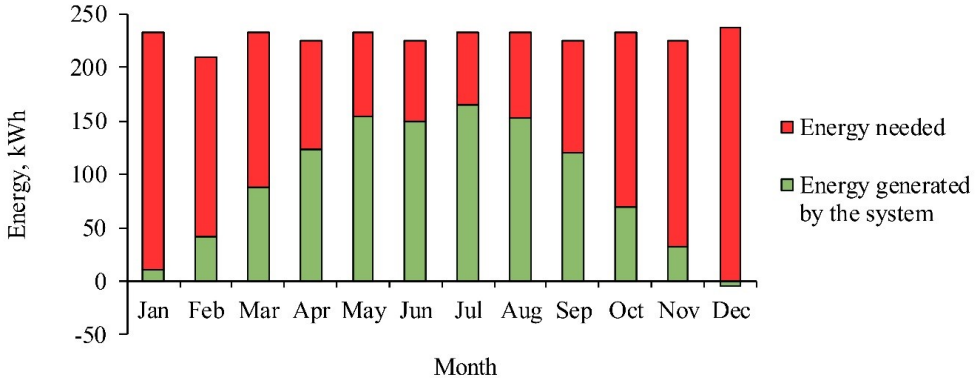

Figure 2.6: Domestic hot water energy requirement and ICSSWH contribution for a three-person household in 2007. Adapted from Garnier (2009)

A solar combi system (SCS) is one way to provide this additional heat requirement, if multiple solar thermal panels are unfeasible. Sarbu and Sebarchievici (2017) summarise the major studies surrounding SCSs in the literature. Drück and Hahne (1998) conducted a comparative study of four hot water stores, each connected to a 10 m^2 flat-plate collector area, where the back-up heat method was an immersed heat exchanger. The authors found that, for a well performing SCS, the most important factors are good thermal insulation and the optimal configuration of the hot water and auxiliary heating loops. By using an SCS over a conventional boiler, fractional energy savings of up to 21% can be realised.

A study in Jordan by Kablan (2004) looked at the techno-economic feasibility of a SWH system with a built-in electric coil as an auxiliary heater compared to a gas geyser system. The author found that the SWH with the integrated auxiliary heater was more economic due to the longer operational life expectancy and the number of days where the use of the electric coil is not required. If the number of days that electricity is used to provide the full daily hot water needs of a family is 120 or less the actual cost of the SWH system is less than the gas system, over the operational life.

Garnier et al. (2018) conducted a numerical and empirical analysis of an ICSSWH

under Scottish weather conditions. The novel design incorporated an immersion heater inside an outlet manifold within the storage tank (Figure 2.7). When water is drawn-off, it is taken from the top, hottest, part of the tank and down the manifold to the outlet at the bottom of the tank. This configuration allowed the outlet water to pass over the immersion heater, which added auxiliary heat if necessary. Therefore, most heat losses from the immersion heater would transfer back into the bulk water inside the storage tank. A drawback of this design is that the hot outlet water runs down through the stratified layers where heat transfer occurs through conduction, thus reducing the final outlet temperature. The magnitude of this cooling reduces at higher rates of draw-off, but then has a knock-on effect on stratification as the higher rate of influx promotes mixing. However, the efficiency of the immersion heater was found to increase with faster flow rates and a higher energy input with minimal impact on mixing.

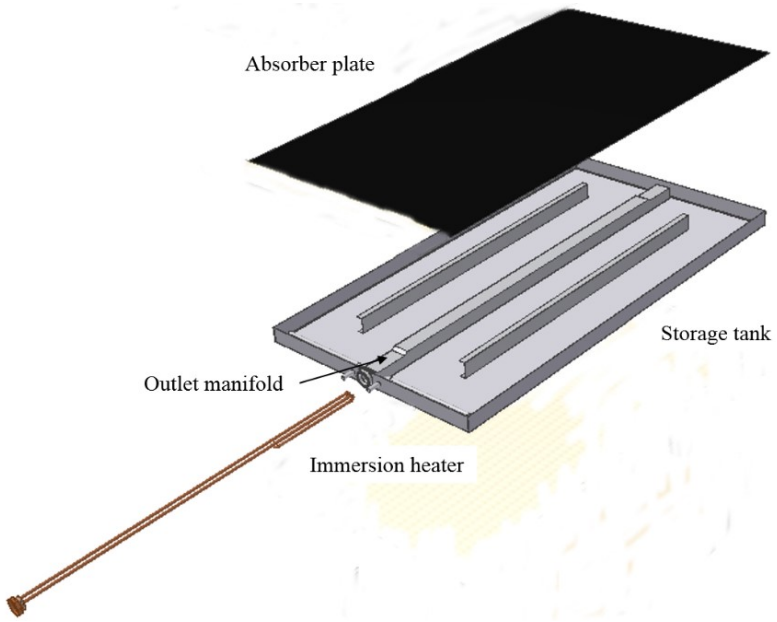

Figure 2.7: Illustration of the components in the studied ICSSWH design, showing the location of the immersion heater and outlet manifold. Adapted from Garnier et al. (2018)

Legionella/Freezing Due to bacterial growth and freezing potential, most ICSSWHs are currently connected to a secondary auxiliary heating system. Hot water consumed by the end-user must be at a temperature that is high enough to kill any bacteria that may have formed in a system, the biggest concern being *Legionella pneumophila*. A review on behalf of the WHO (2007) states that Legionella thrives at 36°C and within a

range of 25–50°C. Water temperatures are required to exceed 60°C for several minutes, at least once a day, to kill off any bacteria. Alternatively, draw off temperatures could be increased to 70°C which destroys the bacteria instantly. This is potentially unattainable through solar insolation in a temperate climate such as Scotland, especially in winter months. Therefore, methods of back-up heating that work in conjunction with SWHs need to be incorporated.

Freezing is also an issue for ICSSWHs due to their high level of exposure to the elements. Smyth et al. (2006) suggested that systems less than 100 mm deep were at greater risk of freezing and to prevent damage to the collector and storage tank the depth should be greater than this. Schmidt and Goetzberger (1990) predicted that, for Northern European climates, the risk of freezing only occurs for ICS systems with a specific collector volume lower than $70\ \mathrm{l/m^2}$ and that damage due to freezing only occurs if more than 20% of the ICS water content is frozen.

ICSSWHs offer a positive energy saving contribution but are unfeasible as standalone systems in a Scottish climate. Given the risk of bacteria and the inability of ICS systems to meet the required temperatures, and the risk of freezing in the winter months, a back-up energy source is essential.

2.2.1.3 Baffle plate/inner store

Baffle plates have been successfully implemented in numerous ICSSWH designs as a method of improved thermal performance and heat retention. Various studies (Faiman et al., 2001; Kaushik et al., 1995; Mohamad, 1997) have used an insulating plate, inserted parallel to the absorber plate, which creates a narrow channel with a thin layer of water which can reach much higher temperatures than the main water body. This system separates the downward and upward flow, thus decreasing mixing in the storage tank and promoting stratification. Once the water is heated it is deposited at the top of the tank, allowing colder water to be drawn up into the channel. Souza et al. (2014) studied an ICS system incorporating a stratification plate running parallel to the absorber surface, which was only heated over the bottom 0.2 m. No significant improvement in thermal stratification was found, with a maximum temperature difference of 4.2°C being

achieved. A follow-up study by Swiatek et al. (2015) found that a shorter stratification plate (0.75 m compared to 0.9 m) in the 1.3 m rectangular system improved thermal stratification, with a maximum temperature difference of 20.1°C. In contrast to Souza et al. (2014), Swiatek et al. (2015) heated a 0.2 m section in the middle of the tank and reduced the channel gap from 8 mm to 5 mm.

Ziapour and Aghamiri (2014) looked at the effect of the channel width on collector efficiency in a two trapezoid ICSSWH system and found that a gap of 6 mm had the highest performance. Kumar and Rosen (2011b) studied a rectangular ICSSWH with an insulating baffle plate and single glazing. They found that absorber plate temperatures peaked at 63°C during the day then suffered heavy losses during the night, dropping by approximately 30°C. However, in the cylindrical ICSSWH configuration presented by Smyth et al. (1999, 2001, 2003) it was found that, by perforating the baffle plate, night-time heat losses could be reduced by 20% as the plate prevents reverse flow in the absence of a heat source. The operating principle of this perforated baffle plate is illustrated in Figure 2.8.

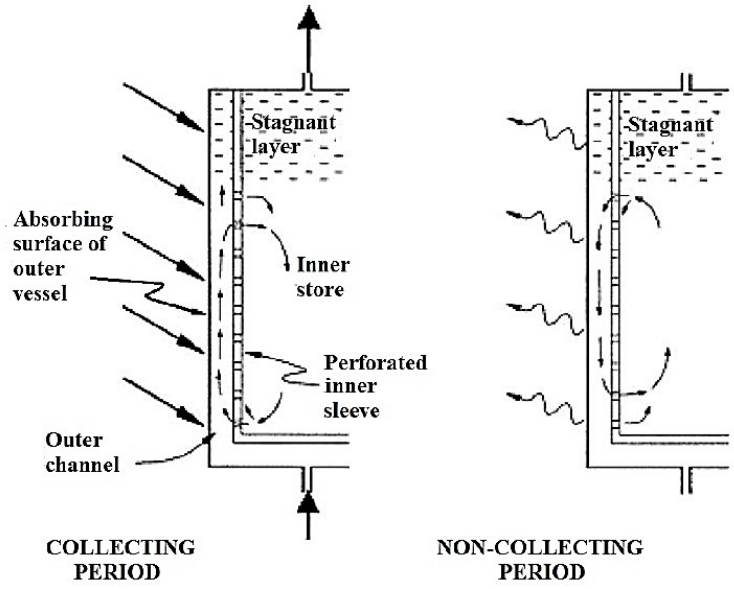

Figure 2.8: Operating principle of the heat retaining ICSSWH design during collection (left) and non-collection (right) periods. Adapted from Smyth et al. (1999)

Sokolov and Vaxman (1983) and, in a follow-up study, Vaxman and Sokolov (1985) assessed a triangular system with a baffle plate and achieved an efficiency of 53%. Smyth

et al. (2003) presented results on an experimental analysis of a 1.5 m cylindrical ICS vessel, mounted within a reflector cavity, with the upper third heavily insulated and a perforated inner sleeve acting as a baffle. They showed that 60% of the thermal energy stored within the vessel could be retained over a 16 h non-collection period. The most efficient configuration was the 1.5 m vessel, with the top third insulated, no insulated cover during the non-charging phase, and a perforated inner sleeve. It outperformed the same configuration without the inner sleeve by 1.3% and the 1 m vessel with no insulated upper section and no inner sleeve by almost 7%.

El-Sebaii (2005) studied the thermal performance of a shallow solar-pond, a batch system similar to ICSSWH, with an integrated baffle plate. Thermal performance was found to improve with the inclusion of the baffle plate. The highest daily efficiencies, up to 64.3%, were achieved using a plate without vents and positioned at approximately two-thirds of the total height of the collector. However, when a baffle plate with vents was used the performance is less dependent on its position within the pond. It was also shown that the baffle plate material had a negligible impact on water temperature throughout the pond, ranging from 58°C to 59.1°C to 60.3°C for mica, aluminium and stainless steel, respectively. These results conformed to those previously reported by Kaushik et al. (1995). The baffle plate also allowed the pond to retain hot water overnight, reaching temperatures of 71°C in the late afternoon and providing water at temperatures of 43°C in the early morning the following day.

Baffle plates can be a simple, effective contributing solution to the heat losses suffered by ICS systems given the improvement in performance demonstrated throughout the literature and the negligible impact of material type. Different shapes, sizes and set-ups have been considered and all offer an element of increased performance.

2.2.1.4 Fins

In 1907, Charles L. Haskell (Haskell, 1907) patented a solar heater design incorporating 'struts' for improved heat conduction as well as structural stability (Figure 2.9). Since then, 'struts', or fins/extended surfaces, are commonly used in commercial evacuated tube and flat-plate collectors, protruding out from the collector pipes to enhance heat

transfer to the working fluid. In ICSSWH systems, these fins can be placed directly into the water body, i.e. storage tank, and extend throughout the full depth allowing heat to be transferred through conduction to the areas that are not in close contact to the absorbing surface. Youcef-Ali (2005) conducted an optimisation study evaluating the impact of fin length and various glazing types on thermal performance. The author studied a solar air collector with offset rectangular plate fin absorbers and found that they generated a higher heater transfer versus a flat-plate alone. The flat-plate collector, with double glazing, produced an efficiency of 38% against 64% for the offset absorber plate with 50 mm fins.

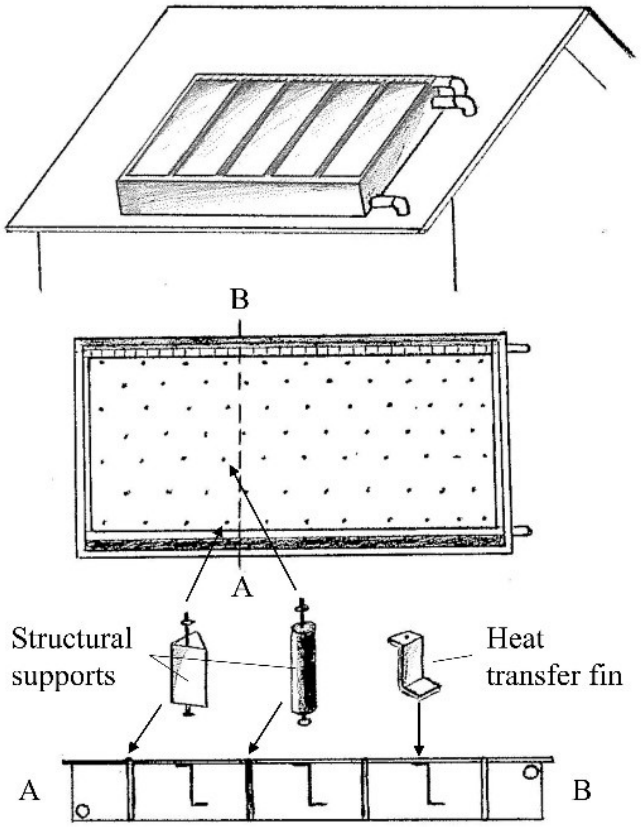

Figure 2.9: Solar water heater incorporating fins patented in 1907 by Charles L. Haskell. Illustrated is the mounted collector and a cross section (A-B) to show the internal configuration. Adapted from Haskell (1907)

Gertzos and Caouris (2008) optimised the arrangement of structural and functional parts in a flat-plate ICSSWH experimentally and numerically. Their aim was to eliminate the stagnation area near the geometrical centre of the stored water body and provide structural stability. The authors found that the presence of fins had no effect on the

outlet water temperature as the increase in heat transfer rate was insignificant due to their small area, which was dwarfed by that of the tank. Li and Wu (2015) studied the effect of extended fins on improving heat performance in shell-tube thermal energy storage units with phase change materials (PCMs). They found that by incorporating fins into the tube design the charging time could be shortened by up to 20%, depending on the PCM material used.

Work conducted by Muneer et al. (2006), which was later validated by Junaidi (2007), led to the inclusion and optimisation of elongated fins inside a box-type ICSSWH to improve heat transfer throughout the water body. Junaidi carried out simulations on both a finned and un-finned SWH and determined that the finned collector performed significantly better. Currie et al. (2008) analysed the optimisation of fin length and thickness for an even heat distribution throughout the storage tank without disrupting flow patterns. The prototype subsequently tested by Garnier (2009) incorporated four 3 mm-thick aluminium fins mounted vertically in a square shaped collector. These were found to improve both the thermal performance and structural strength of the ICSSWH (Figure 2.10). A 13% increase in heat transfer was found, as a direct result of the fin installation. Mohsen and Akash (2002) also studied the performance of a box-type ICSSWH with extended heat transfer fins. They found that the use of fins can improve the cumulative efficiency of the system by 9%, during the month of November in Jordan.

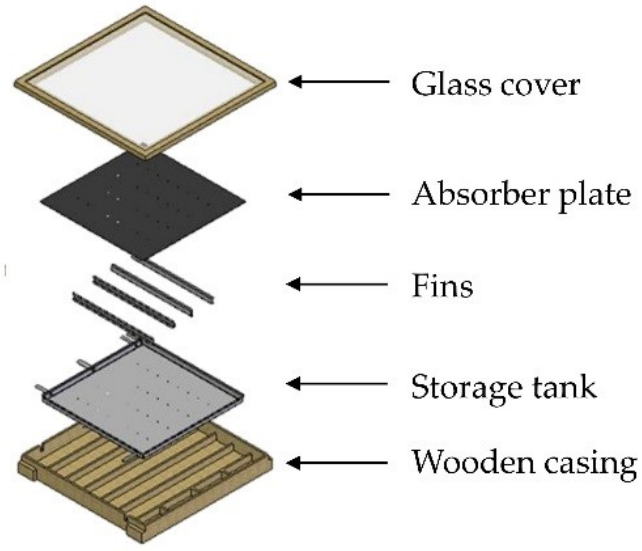

Figure 2.10: Exploded view of the ICSSWH studied. Adapted from Garnier et al. (2008)

Following a numerical study by Chaabane et al. (2013), the thermal performance of a cylindrical ICSSWH, mounted in a CPC, was improved by the inclusion of rectangular radial fins. This work was based on, and validated by, the experimental data presented by Chaouachi and Gabsi (2006). The fins create a modified surface that enhanced the convective heat transfer due to their higher characteristic length. This resulted in a double-edged sword with higher water temperatures and reduced thermal losses during the charging period but higher thermal losses during non-collection periods. The authors also noted a significant correlation between fin length and average water temperature, convective heat transfer, and heat retention. Three fin lengths were modelled, 15, 30 and 45 mm, and in all cases the 45 mm fins produced the best results during day-time operation. As the fin depth increases so does the availability of hot water; temperatures over 50°C were maintained for 6.5 h and more than 10 h for a fin length of 15 mm and 45 mm, respectively. During night-time operation, the thermal loss coefficient is higher for the cases with fins, with a slight increase in the coefficient with increasing fin depth. However, the higher temperatures and longer heat retention gained during the day means a better overall performance for the finned ICS over un-finned. The author suggests a night insulation cover to combat the radiative heat losses.

2.2.1.5 Glazing

Solar water heaters generally include a glazed aperture over the absorber area with an optimised air gap to suppress upward convection and minimise heat losses, whilst maintaining a high transmissivity (Duffie and Beckman, 2006). Glass is the most commonly used material as it is resistant to degradation from ultraviolet (UV) radiation and it has a very good transmittance to solar radiation (up to 90%), as well as a low transmittance to the thermal radiation emitted by the absorber (Kumar and Rosen, 2013; Norton and Lo, 2006). Still, approximately 60% of heat loss in residential buildings can be attributed to the glazed areas (Cuce and Riffat, 2015a) and this is no less important in an ICSSWH system. There are numerous ways to improve thermal performance and heat retention through the type and configuration of the glazed aperture including multilayer, vacuum,

aerogel, and PCM glazing as well as low-emittance coatings. The most common options are reviewed below.

Glazing layers The study by Kumar and Rosen (2011a), reviewed in Section 2.2.1.1, looked at various heat retention strategies for a rectangular ICSSWH system. They found that a double-glazed system maintained the highest temperatures and collector efficiencies which shows that thermal retention can be improved with multiple glazing layers. However, the amount of insolation transmitted to the absorber plate is reduced. Despite this, Bishop (1983) studied a high-volume ICS water heater (two 170 litre tanks), designed for use in freezing climates, which incorporated six glazing layers - one top sheet of low-iron glass and five sheets of high transmission polyester film with an overall solar transmittance of 70%. It was concluded that a twin-tank system with a total area of 2.88 m^2 produced enough water at 50°C, in January, for a family of four in the climate of Denver, Colorado, USA. This suggests that the reduced heat gain due to lower transmittance is, at least, balanced by the heat retained due to the greater thermal resistance of the multiple layers. In freezing climates, where solar insolation is presumably weak, this is highly beneficial as heat loss to the ambient environment will cripple any ICSSWH system. However, in locations where temperatures remain above freezing, with sufficient solar insolation, multiple glazing layers may reduce collector efficiency as well as significantly increase the cost of the unit.

Youcef-Ali (2005) also advocated for a multi-glazed system in a study of a solar air collector. The author experimentally compared two types of transparent cover; double and triple glazed. The triple glazed system produced a better thermal performance reaching efficiencies up to 68% while the double-glazed system peaked at 64%. The triple glazing shows a reduced transmission of solar energy, but this is outweighed by the greater heat retention. AL-Khaliffajy and Mossad (2011) reviewed the optimisation of air cavities between glazing layers for a solar water heater with double glazing. This air gap has a strong influence on heat loss as it determines the level of convective motion between the absorber plate and subsequent layers of glazing. In the simulation, the air gap spacing between the absorber and the lower glass cover (L1) and between the lower

and top glass cover (L2) ranged from 15 - 50 mm. It was found that the lowest heat loss was achieved with the combination of L1 = 40 mm and L2 = 25 mm.

Another addition to multiple layers is vacuum glazing which offers a low heat loss, high transmittance solution. A double-glazed system with a vacuum gap between the glass sheets aims to eliminate conductive and convective heat transfer (Cuce and Riffat, 2015a). The issue of the glass layers collapsing in on themselves due to the high pressure of the vacuum can be combatted by inserting support pillars that have a minimal impact on optical performance (NSG Group, 2003). Han et al. (2012) found an overall heat transfer coefficient of 2.55 W/m^{2}K for a 1 m^2 double-glazed sample with a vacuum gap. The experiments considered the heat conduction through the support pillars and edge seal and the radiation between two glass sheets. As reported by Jelle et al. (2012), SPACIA-21 a product from the Pilkington Company (Tokyo, Japan) (Figure 2.11), shows excellent promise with an overall heat loss coefficient of 0.70 W/m^{2}K and a small external thickness of 21 mm, as opposed to a comparable multilayer glazing configuration at 40 mm. Cuce and Riffat (2015b) included translucent aerogel support pillars into a vacuum glazing design and modelled their impact on thermal performance and found a 44% reduction in the panels U-value. The authors indicated that a lower U-value could be reached if the number and distribution of the support pillars is optimised.

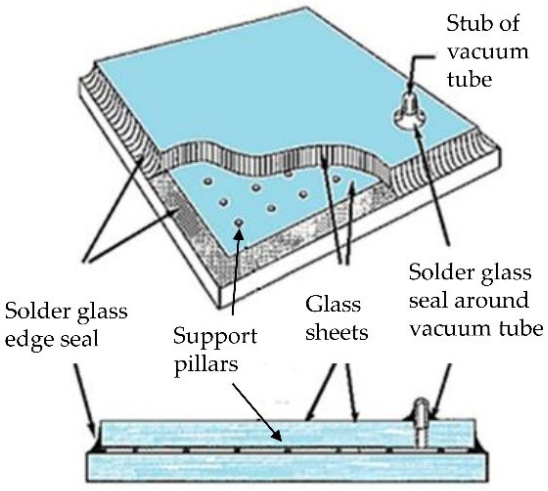

Figure 2.11: Schematic of a vacuum glazing panel detailing the edge seal and support pillars. Adapted from NSG Group (2003)

Vacuum glazing appears to be a promising option, however, there is an issue with conductive heat loss through the contiguous seal enclosing the glass sheets. Fang et al. (2010) conducted a study on triple vacuum glazing and the impact of the edge seal on overall thermal transmission. They found that with smaller glazing size there is a larger ratio of heat conduction through the edge seal to that of the total glazing area. A 1 m^2 sample demonstrated a total thermal transmission of 0.49 W/m^2K compared to 0.65 W/m^2K for 0.5 m^2, equating to a 24.6% decrease. The width of the edge seal also made a significant impact on heat transmission. Increasing it from 3 mm to 10 mm resulted in a 24.7% and 25% increase in thermal transmission for indium and solder glass edge seals (with no frame rebate), respectively.

Selective coatings/glazing material Several studies investigated the use of selective coatings on glass apertures (Ahmadzadeh and Gascoigne, 1976; Bainbridge, 1981; Lefkow and Lee, 1980; Teixeira et al., 2001; Wozniak, 1979). A low-emissivity selective coating is designed to suppress infrared radiation exchange and acts as a selective reflector. Commonly used materials for these coatings have a transmission near zero for longwave infrared, i.e. energy radiated from warm objects, and low reflectivity for shortwave infrared, i.e. solar energy. Therefore, solar energy will be able to penetrate due to the low reflectance of the coating whilst heat emanating from a solar collector will be blocked by its low transmissivity. Bainbridge (1981) found that double glazing with a selective transmission film worked as well as a night cover in reducing night-time heat losses. However, infrared reflective coatings reduce the transmission of solar radiation and Ahmadzadeh and Gascoigne (1976) suggested that, for most operating conditions, the overall performance is better with plain glazing. Although, Muneer et al. (2000) state that a low-emissivity coating has little effect on daylight transmissivity with a 5% reduction, from 80% to 75% transmission, when one layer is added to a double-glazed window. This may seem like a significant decrease but when compared to the almost 50% reduction in the U-value it may be a fair trade.

These selective coatings can aid transmission and retention of solar radiation, however, they come with a high production cost and the cost-benefit ratio is low (Cuce and

Riffat, 2015a). Also, the coatings are susceptible to abrasion and dust accumulation over time, thus reducing solar radiation gain and overall system performance, as well as increasing maintenance (Kumar and Rosen, 2013). It is possible to use plastic films or sheets instead of glass for the glazing material as they have high transmittance and low emittance of solar radiation. However, they are prone to deform at high temperatures and become opaque due to yellowing from UV radiation (Norton and Lo, 2006). A polycarbonate sheet can also be used as it is weather-proof and UV-resistant (Frid et al., 2016). A review by Kumar and Rosen (2011a) shows that either a double-glazed system or a single-glazed system with an insulated night-time cover are the most advantageous options in terms of heat gain and retention as well as economic feasibility.

2.2.1.6 Inlet pipe configuration

Thermal stratification within a water store is an essential contributor to overall efficiency. A fully mixed water body not only has a lower maximum temperature but also less capacity for heat gain. The level of stratification within a storage tank depends on the charging and discharging cycles of the SWH; the flow rates and water velocities; the size and shape of the system and; the size and location of the inlet and outlet pipes (Smyth et al., 2006). The design and configuration of the inlet pipe can have a significant impact on thermal stratification as it can be used to control flow velocities and thus reduce turbulent mixing (Carlsson, 1993; Lavan and Thompson, 1977; Zurigat et al., 1988). Diffuser designs differ greatly and include slotted tubes, pipes with inverted cups, solid baffle plates, perforated circular plates, radial-flow disks, distributed nozzles, and perforated tubes (Hegazy and Diab, 2002). Hegazy (2007) experimentally tested three inlet geometries (Figure 2.12) and found that all the designs promoted good thermal stratification. The slotted inlet slightly outperformed the perforated and wedged pipes and the design is also simpler and cheaper to manufacture.

Chung et al. (2008) analysed the impact of diffuser configuration on the thermal stratification within a rectangular water storage tank. The three diffuser types were studied—radial plate, radial adjusted plate, and H-beam. The results ratified the knowledge that diffuser shape has a significant impact on thermal performance and that the

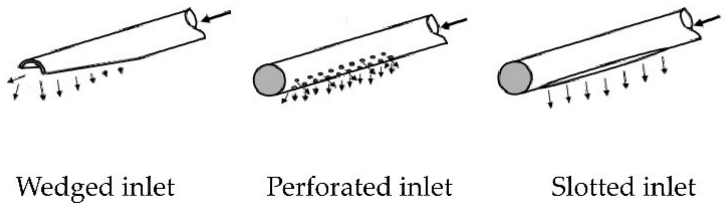

Figure 2.12: Examples of inlet designs. Adapted from Hegazy (2007)

design should be tailored to the aspect ratio of the storage tank. In this case, the H-beam produced a thicker thermocline (and therefore higher thermal stratification) than the radial diffusers. The difference between the radial plates was minimal. Dragsted et al. (2017) compared a new inlet diffuser design with well-established ones, illustrated in Figure 2.13.

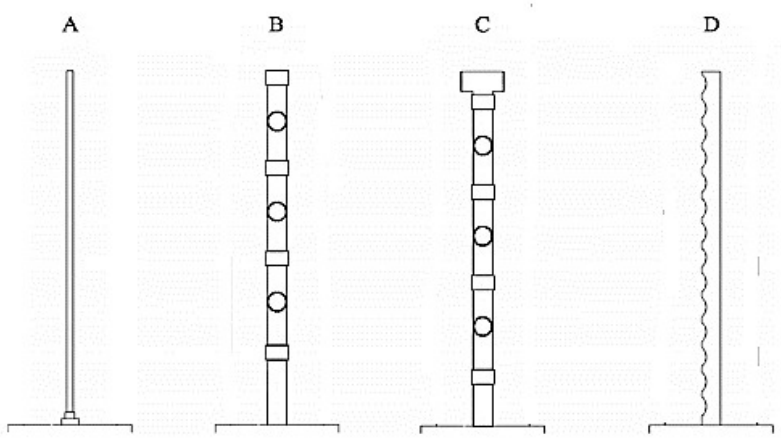

Figure 2.13: Different inlet diffusers tested. (A) a simple rigid polymer pipe; (B, C) a polymer pipe with three "non-return" valves ((B) open-ended, (C) with a T-piece endcap); (D) a flexible perforated pipe. Adapted from Dragsted et al. (2017)

The results found that performance depended on flow rate. At higher flow rates (4 l/min) designs B and C performed the best while design D worked better at lower flow rates (1 and 2 l/min). During charging periods design D showed the best performance due to the greater number of perforations. Therefore, to help reduce mixing and promote thermal stratification, inlet diffusers are beneficial, particularly perforated or slotted designs.

2.2.1.7 Phase Change Materials (PCM)

Latent heat storage materials, also known as Phase Change Materials (PCMs), are an increasingly popular method of extended heat energy storage and can be applied in many solar energy applications (Pandey et al., 2018; Pereira da Cunha and Eames, 2016; Prabhu et al., 2012). During daytime charging the PCMs store excess thermal energy as latent heat by changing phase. During non-collection periods, as hot water is withdrawn for domestic use fresh, cold, water replaces it with no solar energy for heat gain. Therefore, the stored latent energy is released as the PCMs change phase and revert to their original state. There are different classes of PCM including organic compounds, inorganic materials, and eutectic mixtures (Hamed et al., 2017). One of the benefits of PCM is that, by storing excess energy, the heat losses that occur when the collector is at its highest temperature are reduced, thus enhancing system efficiency (Haillot et al., 2012).

With regards to PCM integration into ICSSWH, a few studies have been conducted to determine the thermal performance (Al-Kayiem and Lin, 2014; Souliotis et al., 2015; Tarhan et al., 2006). Tarhan et al. (2006) investigated the effect of PCM on the temperature distribution within the water tank. Three trapezoidal ICSSWH systems were analysed, one without PCM to act as a reference heater and two with different configurations of organic PCM (Figure 2.14).

The first set-up used myristic acid, in a PCM storage tank, as an absorber plate (Figure 2.14 [b]) and in the second set-up lauric acid in the PCM storage tank was used as a baffle plate (Figure 2.14 [c]). The configuration with myristic acid proved to have the highest overall performance with water temperature differences up to 4°C after the cooling period. This is due to the solidification temperature of the myristic acid, it solidifies at 51–52°C and acts as a thermal barrier so the absorber plate essentially becomes a night cover. The reference collector, with no PCM, reached higher peak temperatures during the collection period but this heat was lost during the night.

Chaabane et al. (2014) carried out a numerical study of a CPC mounted ICSSWH system with two different PCMs - myristic acid and RT42-graphite. The authors also

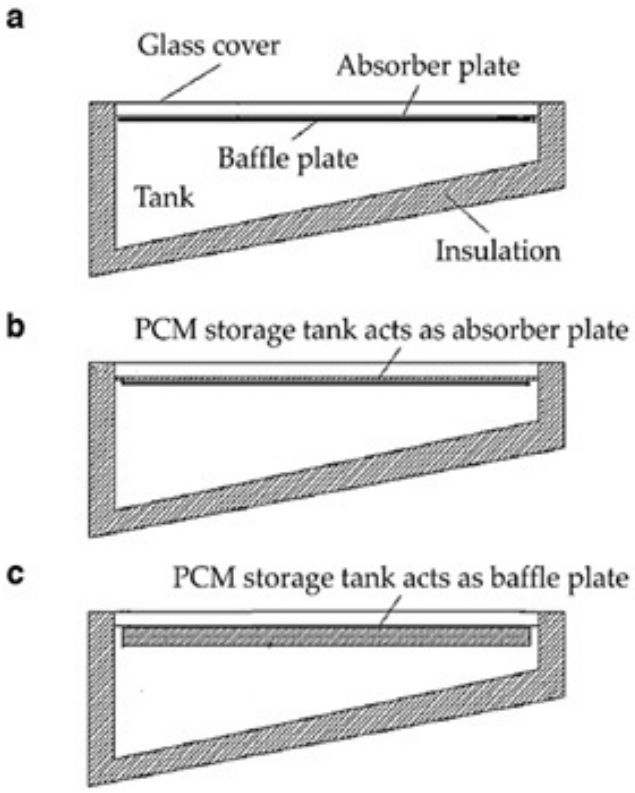

Figure 2.14: Cross sectional view of the three trapezoidal ICSSWH systems studied. (a) reference collector; (b) PCM storage tank filled with myristic acid, acting as an absorber plate; (c) PCM storage tank filled with lauric acid, acting as a baffle plate. Adapted from Tarhan et al. (2006)

found myristic acid to be the most beneficial as it reaches higher maximum temperatures during the day and allows better heat preservation during the night, with water temperatures almost 30°C higher than a non-PCM system after 18 h of operation. The thermal efficiency of the system without PCM is only slightly higher during the collection period but drops below the PCM configurations overnight. Hamed et al. (2017) also did a numerical study, analysing the charging and discharging performance of a rectangular ICSSWH. The type of PCM used in the calculations was not stated, only the thermophysical properties. As with the other studies the inclusion of a PCM resulted in a longer charging time, reaching lower peak temperatures, and higher available temperatures during the non-collection period with a maximum temperature difference of almost 9°C.

However, the use of PCMs in thermal energy storage is limited and often unavailable on a commercial market due to economic and environmental constraints (Pandey et al., 2018). Choosing the right type of PCM and the position within an ICS system is crucial

to its effective function (Chaabane et al., 2014). Also, the evaporation associated with certain types of PCM requires enormous changes in volume of the storage materials making storage complex and impractical (Hamed et al., 2017). Many organic PCMs have a low rate of heat transfer as well as low thermal conductivity and for small scale applications, such as domestic solar water heating, the cost of this technology is still too great (Pandey et al., 2018).

2.2.1.8 Reflectors

ICSSWH systems can absorb both diffuse and direct solar radiation and an easy way to enhance the level of solar radiation collected is to apply strategically positioned reflective surfaces. In terms of ICS systems, the most common configuration of collector and reflector is the compound parabolic concentrating (CPC) collector. A cylindrical water store is set into a reflective trough which reflects incident radiation to the absorber.

The design and geometry of CPC collectors are very important parameters to optimise the collection of incident radiation, both direct and diffuse. Souliotis et al. (2011) conducted an optical analysis on an ICSSWH with an asymmetric CPC reflector; to determine optical efficiency, the factor of diffuse solar radiation (γ) must first be defined, as shown in Equation 2.1.

$$\gamma = \frac{G_b + G_d \cdot CR^{-1}}{G_t} \tag{2.1}$$

Where, G_b, G_d, and G_t are the beam (direct), diffuse and total intensity of the incident solar radiation, respectively. CR is the concentration ratio, which is defined as the aperture area divided by the absorber area. Therefore, the proportion of diffuse radiation collected by a CPC is a function of the CR; a smaller CR, i.e. smaller aperture area and/or larger absorber area, means a greater proportion of diffuse radiation is collected.

Devanarayanan and Kalidasa Murugavel (2014) conducted a comprehensive review of the development and progress surrounding ICSSWH with integrated CPC. The authors classified the different configurations of integrated compound parabolic concentrator storage solar water heater (ICPCSSWH) systems based on the associated

absorber. The main conclusions from this review were that ICPCSSWH systems are cost-effective and simple to construct with a satisfactory thermal efficiency that can compete with flat-plate thermosyphonic units (FPTU). Also, they have a short response time across discharging and recharging. Drawbacks, however, include their lower optical efficiency, especially at lower sun angles, i.e. winter, high heat losses, particularly during non-collection periods, and only moderate thermal stratification within the water store.

Souliotis et al. (2013, 2011) carried out research studies on ICSSWH systems mounted in CPC reflector troughs with the aim of assessing the thermal performance and enhancing the night-time heat retention. The authors found that seasonal variation has little impact on optical efficiency for the experimental location (Patras, Greece) with values ranging from 77% in winter to 79% in summer (Souliotis et al., 2011). When compared with a FPTU, the ICS system has poorer heat retention with the bulk water temperature, after 24 h, being 7°C lower. However, during the charging period the ICPCSSWH has a greater system efficiency and thermal stratification due, in part, to the partial vacuum in the annulus between the absorber and storage of the ICS unit. This added thermal diode improves the operation of the system, but high thermal losses, poor stratification, and optical efficiency are still observed. These results were reiterated in a later study with a bulk water temperature difference of 12°C between the FPTU and ICS models, after 24 h (Souliotis et al., 2013). However, thermal losses can be improved by incorporating double glazing into the design.

Varghese and Manjunath (2017) carried out a study on a cylindrical ICPCSSWH in Delhi, India, with the aim of improving heat retention by including an air gap in the side walls (the arms of the CPC). They found maximum experimental efficiencies of 38% and water temperatures of 53°C. By introducing an air gap, the maximum outlet temperature can be enhanced and continues to rise even after collector efficiencies drop. This is due to the thermal barrier, created by the air gap, between the absorber and the ambient air which decreases the thermal loss coefficient by up to 52.5%, depending on water temperature.

Not all reflector mounted ICS systems use cylindrical collectors, however. Ziapour

et al. (2016) analysed the performance improvement of a rectangular PV/T system which incorporated reflectors that acted as removable insulation covers (Figure 2.15). The findings of the numerical model showed that the reflectors effectively reduced the night-time heat losses whilst increasing the level of solar radiation incident on the absorber plate. With reflectors, peak diurnal temperatures reach 69.2°C; 9.5°C higher than a system without reflectors. Water temperatures in the morning (6 am) are also much higher with values up to 54°C compared to 31°C, thus offering a 43% improvement. The angle at which the reflectors are mounted has a strong influence on the total solar radiation incident on the absorber plate and a model optimising these angles was presented.

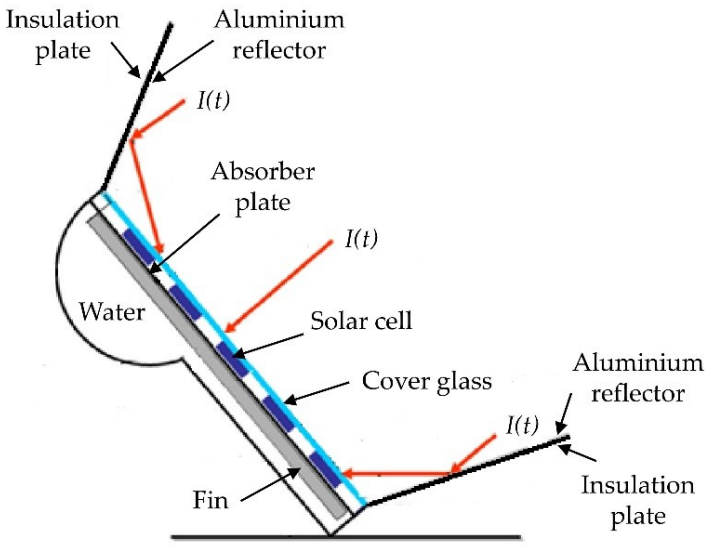

Figure 2.15: Schematic representation of the passive PV/T system studied. I(t) denotes the incident solar radiation. Adapted from Ziapour et al. (2016)

Although reflectors have potential, their shape and size are not practical for mounting on a pitched roof. The impact on the aesthetics of the structure might be off-putting for prospective consumers. The issue of wind loading is also magnified with these ICS configurations as their bulky and protruding nature makes them more susceptible to higher wind loads. This would be especially prominent in the case of the latter study as the reflectors, which are open during the day, could be damaged in high winds. Ziapour et al. (2016) made no mention of the impact of wind in their numerical study, however, this would be an important consideration under practical application.

2.2.1.9 Selective absorber surfaces

An absorbent coating is often used to enhance the absorption of solar radiation. Black paint is commonly used as it is a good absorber of radiation within the visible and infrared part of the spectrum and therefore absorbs the most heat. Due to the low emittance of a black object it can absorb up to 96% of incident insolation (Incropera et al., 2013; Norton and Lo, 2006). For greater absorptivity and lower emissivity, a spectrally selective absorber surface can be employed. Smyth et al. (2006) conducted a thorough review of several studies that have verified the benefit of selective absorber coatings (Bainbridge, 1981; Burton and Zweig, 1981; Cummings and Clark, 1983; Fasulo et al., 1987; Stickney and Nagy, 1980; Tiller and Wochatz, 1982). Bainbridge (1981) tested ICS vessels with and without a selective absorber surface and concluded that the water temperature in a single-glazed unit with a selective absorber was 9°C higher than the same systems painted black. Tiller and Wochatz (1982) used a selective surface paint with a solar absorptance of 0.94 and long-wave emittance of 0.45–0.60 and found that a single-glazed, shuttered design reached temperatures 2.8°C higher than the un-shuttered, selective absorber design. This suggests that the influence of a night cover on heat losses is greater than the selective absorber surface. However, a coating with a lower emittance could make up this small temperature difference thus indicating the importance of the spectral emittance of the absorber (Teixeira et al., 2001).

Cummings and Clark (1983) performed a set of computer simulations on selective absorber surfaces in conjunction with various glazing materials. The selective surface was simulated with an absorptance of 0.95 and an emittance of 0.10. They showed that the average annual delivered energy for a single-glazed selective absorber design would increase in the range of 26–44% compared with a basic design. Fasulo et al. (1987) showed that, by using a selective absorber coating, night-time heat losses were reduced by 3 MJ/night compared to a vessel painted matt black. Tripanagnostopoulos and Yianoulis (1992) further emphasised the importance of a low emissivity coating in their study. They compared the performance of asymmetrical reflector ICSSWH designs with simple black paint (α=0.92 and ε=0.9) against a selective black coating

(α=0.95 and ε=0.11). The systems with the selective coating had a significantly improved performance though these improvements were partly due to the optimised reflector material.

Teixeira et al. (2001) presented a numerical model that allows the selectivity of absorber coatings to be correlated with the collector efficiency. The study focused on the microstructure, crystalline structure, and optical properties of composite cermet thin coatings deposited on glass, aluminium and copper substrates. The analysed coatings have high spectral selectivity, with absorption in the range of 0.88 to 0.94 and emissivity ranging from 0.15 to 0.04 and were subject to three different sputtering conditions; single layer, multilayers and gradient coatings. The study showed that a graded coating had much higher absorptivity, due to reduced reflectance, than a pure cermet film. Layered coatings also had much lower reflectance, and therefore greater absorptivity, for aluminium and copper surfaces, although glass did not follow this behaviour. For both cases reflectance is less than 10%, over the visible range of 380–780 nm associated with the luminance of daylight (Ghosh and Norton, 2017).

The type of coating used for the absorber surface is not the only consideration but also the profile; for example, whether it is planar or corrugated. Kumar and Rosen (2010) reported on the thermal performance of an ICSSWH with a corrugated absorber surface. This surface has a higher characteristic length and, therefore, a higher surface area exposed to solar radiation. It was concluded that the corrugated surface had higher operating temperatures for a greater period than the plane surface but a marginally reduced system efficiency, as a result. As the corrugation depth increases from 0.4 mm to 1 mm, the maximum temperature of the water increases from 53 to 64°C while the efficiency decreases from 46.8% to 42.4% (with night-time insulation) and 40% to 35% (without night insulation). At a corrugation depth of 1 mm average water temperatures are 5 to 10°C higher than with a plane surface during collecting periods.

2.2.1.10 Storage tank/collector material

Metals Traditionally, SWHs have been constructed from metals due to their strength and durability. The most common are copper, stainless steel, and aluminium. Copper

has the highest thermal conductivity at 385 W/m·K but it is also the most expensive. Therefore, in the interests of developing a cost-effective solution, stainless steel or aluminium are more often used (Gardner, 2005). In terms of structural strength, stainless steel outperforms aluminium which is a 'soft' metal and can deform at high temperature and pressure. Aluminium can also suffer galvanic corrosion when connected to conventional copper pipework whereas stainless steel is resistant to corrosion (Gardner, 2005). Aluminium does, however, have a much higher thermal conductivity at 237 W/m·K compared to 14.9 W/m·K for stainless steel (Incropera et al., 2013). Heat transfer and the thermal conductivity of the vessel material have a significant impact on thermal stratification within the water store. Vertical conduction in the tank walls, coupled with losses to the ambient environment, induces convective currents that rapidly degrade thermal stratification (Smyth et al., 2006). This suggests that a material with a lower thermal conductivity could be beneficial in reducing the convective heat motion, thus enhancing stratification. However, there is the trade-off of reduced transfer of absorbed heat to the water body.

Ziapour and Aghamiri (2014) simulated and compared four different types of absorber for passive PV/T systems. Here, PV panels were mounted onto different absorber plate types of an ICSSWH - an aluminium plate with fins; aluminium without fins; Tedlar (a highly versatile polyvinyl fluoride polymer material) and; black painted glazing. The simulation results showed that the aluminium absorber plate with fins had the highest electrical and thermal efficiencies, with combined PV/T efficiencies up to 88% (Ziapour and Aghamiri, 2014). Garnier (2009) modelled the impact of stainless steel versus aluminium on heat transfer, comparing aluminium thicknesses of 3 mm and 1.5 mm and 1.5 mm thick stainless steel, and found heat transfer rates of 67.3%, 63% and 25.3%, respectively. These computational results were found to be in close agreement with experimental data. Garnier (2009) also conducted a monetary analysis and life cycle assessment of stainless steel versus aluminium systems. ICS systems strive to be a "green" technology; therefore, the embodied energy, embodied carbon, and recyclability must be taken into consideration. The author found that the embodied energy of stainless steel was 66% less than aluminium and, likewise, the embodied

carbon was 26% lower with stainless steel over aluminium. This difference could be reduced if the percentage of recycled material in the aluminium is increased.

Polymer and composite materials The use of solar thermal energy systems has increased dramatically in last decade yet the metal-based collectors, despite a high thermal performance, are still relatively expensive to buy and install (Buker and Riffat, 2015). More recently, research has been undertaken on the use of polymer and composite materials for the ICSSWH components (Frid et al., 2016; Oshchepkov and Frid, 2016; Popel' et al., 2013). These have the potential to simplify ICSSWH construction as well as decrease the cost of the unit as a whole (Frid et al., 2016). Polymers are light-weight and non-corrosive, which cannot be said for metal-based materials (Shukla et al., 2013). The manufacture of the system would need to be altered in terms of welding, soldering, mechanical treatment, and assembly (moulding and gluing of the polymer composite). Frid et al. (2016) looked at the use of polymer composite materials in ICSSWH construction, incorporating only three components - glazing, absorber plate, and storage tank/SWH casing (Figure 2.16). The glazing is weather-proof, UV-resistant, plate-type polycarbonate and the absorber plate is manufactured from a fibreglass or carbon-filled plastic and coated with a selective absorber coating. The storage tank is a series of troughs and is integrated with the outer wall of the system (Figure 2.16), with the area between the two filled with thermal insulation, to reduce the number of parts in the unit.

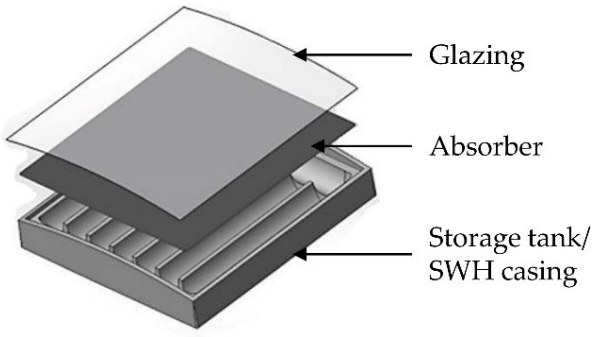

Figure 2.16: Schematic of experimental polymer composite ICSSWH design with only 3 components. Adapted from Frid et al. (2016)

This prototype demonstrated its in-situ operability, however, the engineering solutions applied in its construction are suitable only for low volume production, and thermal vacuum moulding of the polycarbonate glazing gave no guaranteed result (Popel' et al., 2013). This brings into question the mass reproducibility of the unit as well as its structural integrity. Also, the estimated minimum service lifetime for the casing, absorbing panel, and glue joints was 7 years at a cost of \$70 - 90/m^2 (receiving surface), an average or maximum expected lifetime was not mentioned (Frid et al., 2016). While this is approximately half the cost of traditional materials, which are in the range of \$150 - 200/m^2 (prices commonly fluctuate), the unit also has half the lifetime with stainless steel and aluminium systems offering satisfactory performance for up to 20 years. There is an international effort to advance the use of polymer materials in SWH systems to lower the initial cost. However, more research needs to be done in terms of the structural integrity of the unit, their ability to resist UV degradation, and overheat protection of the absorber to prevent overrunning the maximum allowable temperature of the polymer (Buker and Riffat, 2015; Smyth et al., 2006). Despite the flexibility and freeze tolerance of polymers they have a lower thermal conductivity than metals and a much shorter lifetime so in terms of the cost to benefit ratio metals still have the upper hand (Shukla et al., 2013).

2.2.1.11 Thermal diodes

A thermal diode is a device which causes heat to flow preferentially in one direction and is a method of heat retention during the night and non-collecting periods, offering improved efficiencies and higher temperatures. Mohamad (1997) introduced a simple thermal diode into triangular ICS systems with incorporated baffle plates. The thermal diode design is located at the base of the vessel, at the entry to the baffle channel, and consists of a light weight plastic 'gate' that prohibits reverse flow (Figure 2.17). Mohamad (1997) showed that reverse circulation at night-time is prevented, particularly when storage temperatures are high, thus producing storage efficiencies of 68.6% and 53.3% with and without the diode, respectively.

Sopian et al. (2004) introduced a thermal diode into their ICS design and the temper-

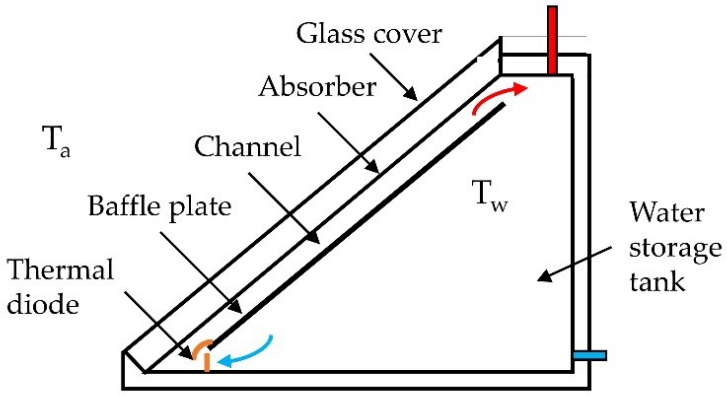

Figure 2.17: Schematic detail of the ICSSWH with a baffle plate and a thermal diode. T_a - ambient air temperature; T_w - bulk water temperature. Adapted from Mohamad (1997)

ature drop in the storage tank overnight was reduced from 20°C without a thermal diode to 10°C with a diode. Creating an evacuated layer between the absorber plate and water cavity is another form of thermal diode. Souliotis et al. (2011) studied an ICS vessel design mounted in a CPC reflector trough where an annulus between the cylinders is partially evacuated and contains a small amount of water, which changes phase at low temperature and produces vapour. This phase change creates a thermal diode transfer mechanism from the outer absorbing surface to the inner storage tank surface. Experimental results showed that the systems performance, when compared with a FPTU, is as effective both during day and night-time operation. More recently, Souliotis et al. (2017) did a follow-up study on this CPC mounted ICSSWH system where extensive experimental data was collected over more than two years. The authors found that the PCM vapour pressure was a crucial parameter and the temperature increase during diurnal collection periods, at the optimal pressure, reaches 39°C while the maximum heat loss during night-time operation is 13°C with a thermal loss coefficient between 1.60 and 1.62 W/K. This performance was shown to be better than a commercial FPTU.

Smyth et al. (2017) also conducted an experimental evaluation of a novel thermal diode in an ICSSWH to be used as a pre-heater. The collector was tested using a solar simulation facility and consisted of three concentric cylinders - the outer glazing, the middle absorbing surface and the inner storage tank (Figure 2.18). As in the latter study, the annular cavity between the absorbing surface and the storage tank is partially

evacuated and contains a small amount of liquid/vapour PCM which acts as a thermal diode.

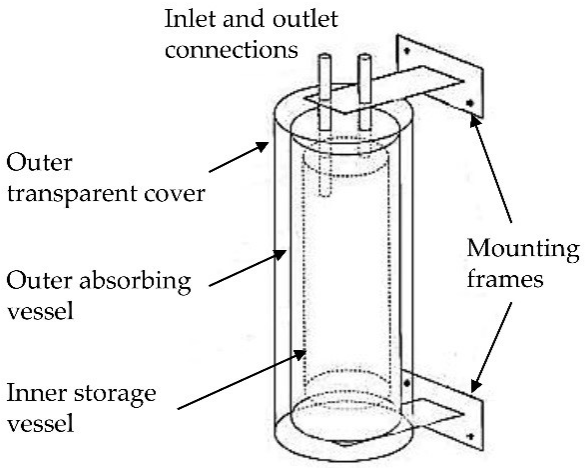

Figure 2.18: Conceptual design illustrating the three concentric cylinders with the thermal diode mechanism working between the inner and outer vessels. Adapted from Smyth et al. (2017)

The importance of a transparent aperture cover and cavity back insulation was highlighted as they are crucial in achieving the saturation temperature which promotes heat transfer through convection as opposed to radiation only. For the thermal diode mechanism to work effectively certain temperatures need to be reached and maintained to facilitate the evaporation-condensation cycle. Overall efficiencies reached a maximum of 36% and the impact on heat retention was considerable with a reduction in thermal losses of approximately 40%, compared with conventional ICS systems.

2.2.2 Design parameters

ICSSWH incorporate the collector and storage tank in a single unit creating direct contact between the working fluid (e.g. water) and absorber plate. This negates the need for a heat exchanger and has the potential to achieve high efficiencies given its all-in-one design. Also, the absence of additional conduits and connecting pipes, which are major heat loss areas, eliminates bulk heat losses as well as reducing manufacturing costs (Currie et al., 2008). ICS systems are easily adapted giving them an advantage when considering their integration into buildings, as the construction industry dictates the rules and restrictions. The structure of buildings is difficult to adjust without

compromising structural stability and increasing cost; therefore, the adaptability of ICS designs allows them to integrate seamlessly into roof structures, dependant on optimised design parameters.

Certain design parameters are constrained, to an extent, by this integration and the roofing panels being used, for example timber frame structural insulated panels (SIPs). These parameters are reviewed in the following sections.

2.2.2.1 Aspect ratio of the storage tank

Nelson et al. (1999) conducted a study on thermal stratification in cylindrical chilled-water storage tanks, varying certain experimental parameters such as the aspect ratio, defined in the study as the height to diameter ratio (H/D) where the diameter is both the width and thickness. They demonstrated that by increasing the aspect ratio the thermal stratification also increased. More specifically, increasing the distance between the inlet and outlet areas, i.e. the top and bottom of the tank, decreases the mixing coefficient, thus maintaining a stronger thermocline. Also, a lower H/D ratio promoted thermal degradation due to axial wall conduction. These results suggest that long, thin vessels stimulate greater thermal stratification than short, wide ones. In the same study, Nelson et al. (1999) concluded that performance improves when increasing the H/D ratio from 2 to 3, beyond 3 any change is insignificant. Hahne and Chen (1998) carried out a similar, numerical, study again looking at the effect of altering the H/D ratio of a cylindrical hot water system. Through their simulation they demonstrated that charging efficiency increased sharply as the H/D ratio varied from 1 to 4, beyond 4 efficiency plateaued. They, along with Lavan and Thompson (1977) who also studied a cylindrical system, concluded that a H/D ratio between 3 and 4 would be a reasonable compromise in practical application.

Studies testing rectangular ICSSWH systems also advocated that a higher aspect ratio, defined here as the height to thickness ratio (H/L), promotes greater thermal stratification and improved overall thermal performance. Polentini et al. (1993) showed that the effect on heat transfer is negligible for H/L ratios between 2.5 and 7.5. Tou et al. (1999) go even further, showing that the aspect ratio effect is practically neglected for

values between 5 and 20. As the H/L ratio decreases from 20–1, the heated surface and back wall are farther apart and flow becomes confined to the opposite walls, leaving the central region almost stagnant (Tou et al., 1999). Therefore, a higher H/L ratio, where the water cavity is shallower, generates greater convective flow in the storage tank which results in improved heat transfer. Simulations conducted by Eames and Norton (1998) showed that a height to width ratio of 3:1 performed more efficiently than a ratio of 1:3. Tiller and Wochatz (1982) carried out a study on integrated passive solar water heaters under varying design conditions in the US and suggested that, in cooler climates, a storage volume to absorber area ratio of 51 – 69 l/m^2 gives a better thermal performance.

Previous studies have suggested that ICS systems with a triangular design enhance solar collection and exhibit greater heat transfer due to increased natural convection (Ecevit et al., 1990, 1989; Kaushik et al., 1994; Prakash et al., 1992). A study conducted by Soponronnarit et al. (1994) compared two ICSSWH systems, one rectangular and one triangular, under identical experimental operating conditions. They showed a 4% higher thermal efficiency, at 63%, in the triangular system with reduced heat loss during non-collecting periods. However, this shape is not as suited to embedment in a roofing panel as a rectangular configuration. Smyth et al. (2006) reviewed several studies on cylindrical designs and found that rectangular systems perform and operate just as effectively in an ICSSWH configuration.

2.2.2.2 Aspect ratio of the air cavity

Changing the aspect ratio of the storage tank impacts upon the aspect ratio of the air cavity. The storage tank dimensions can be adjusted for optimal performance, but this inescapably impacts upon the aspect ratio of the air cavity. Henderson et al. (2007) published a comprehensive review of previous studies on inclined cavities along with an experimental and CFD investigation of an ICSSWH at various inclinations. This study showed that the optimal design of an air cavity requires the lowest possible value for the Nusselt number without severely impacting the Rayleigh number. Therefore, optimal cavity thickness is the maximum thickness for which the Nusselt number would remain

close to 1. Henderson et al. (2007) state that, in terms of convection, the behaviour of the water cavity is nearly opposite to that of the air cavity for any given angle of inclination. This contrast, in fact, favours the required heat transfer; a lower Nusselt number in the air cavity for less convective flow and less heat loss to the ambient environment and a higher Nusselt number in the water cavity for greater heat gain and transfer. The authors also compare CFD results for an aspect ratio of 28.5 against data from Elsherbiny et al. (1982) for an aspect ratio of 40. This higher aspect ratio proved to have lower average Nusselt numbers and showed a steady decline with increasing inclination angle (discussed in Section 2.2.2.3). Therefore, there is a very fine balance to be found for the dimensions of the system in terms of thermal performance. These characteristics of the systems design need further consideration as well as discussion and collaboration with the construction industry to ensure successful commercial uptake.

2.2.2.3 Angle of inclination

In a previous study by Junaidi et al. (2006) the performance of a finned, 1.5 mm stainless steel ICSSWH was investigated experimentally for heat fluxes of 100 – 400 W, increasing at 50 W intervals, and varying angles of inclination. The authors proved that system performance and efficiency differ at various inclination angles which could be attributed to the combined effect of the impact on heat loss from the air cavity, due to increased convective motion, and heat gained by the absorber, due to increased solar incidence. Theoretically, efficiency at a 0° angle should be lower than all other inclinations as the peak value of convective heat losses occurs in a horizontal position (Junaidi et al., 2006). Another study by Junaidi (2007) showed that thermal optima increased with increasing angle of inclination and that a 45° inclination gave the best global results with higher temperatures and efficiencies achieved. Based on these results, Garnier (2009) and Currie et al. (2008) adopted an inclination angle of 45° for their finned, 3 mm aluminium ICSSWH and tested system performance at varying heat fluxes. These studies demonstrated the potential of SWH in the Scottish climate.

Henderson et al. (2007) processed 27-year irradiance data for Edinburgh and showed that peak value irradiance falls at an angle of 35°. A study conducted by Kumar and

Rosen (2011a) analyses a rectangular ICSSWH that is coupled with an extended, heavily insulated, upper storage section and based on the climatic conditions of Toronto; a slightly lower latitude than Edinburgh. The study demonstrated that maximum water temperature was achieved at a 30° angle of inclination as well as the greatest level of incident solar irradiance on the absorber surface. As the tilt angle was increased from 15° to 45°, the natural convective flow rate that developed within the system increased continuously. However, the amount of incident solar irradiance decreased once the tilt angle surpassed 30°. This results in a trade-off between thermal gain and convective flow. A higher tilt angle means greater convective flow which aids the heat transfer throughout the storage tank and thus thermal stratification. It also means reduced incident solar radiation and heat gain thus any improvement in efficiency is minimal at higher latitudes (Henderson et al., 2007).

Souza et al. (2014) also showed an optimum angle of inclination of 30° through experimental studies in France showing that systems with a lower tilt angle, e.g. 30° as opposed to 60°, had improved thermal stratification with higher temperatures at the top of the storage tank. Their rectangular system had a high aspect ratio of 13 (height = 1.3 m, thickness = 0.1 m) and the applied heat flux was concentrated on the bottom 0.2 m of the absorber surface. They studied three heat flux densities (1800, 3600, and 5400 W/m^2) at three inclination angles (30°, 45°, and 60°). They concluded that an angle of 30° and a heat flux of 5400 W/m^2 showed a maximum temperature difference of only 4.2°C. It was recommended that a baffle plate should be used to promote stratification. Following this, Swiatek et al. (2015) demonstrated that an angle of 45° and a lower heat flux of 3400 W/m^2 was optimal for a similar system configuration. As with Souza et al. (2014), their system had the same aspect ratio of 13 but included a short stratification (baffle) plate and the heat flux was only applied to the middle 0.2 m section of the absorber plate. This demonstrates the benefit of a higher inclination angle, in terms of thermal stratification, but the lower heat gain from reduced incident radiation must also be considered.

However, in support of the findings by Henderson et al. (2007), NASA data based on the monthly averaged radiation incident on a south-facing, inclined surface shows

that, at the latitude of Edinburgh, a tilt angle of 40° is the best overall (annually) (Figure 2.19). This angle of inclination also fits well with the range that best suits thermal stratification, as optimised by Junaidi (2007). Additionally, Scottish roofs are generally angled between 33° and 36° for optimum performance in terms of passive heating. Therefore, considering the optimum angle for incident solar radiation and the angle of existing Scottish roof structures, an angle of 35° would be suitable for Scotland.

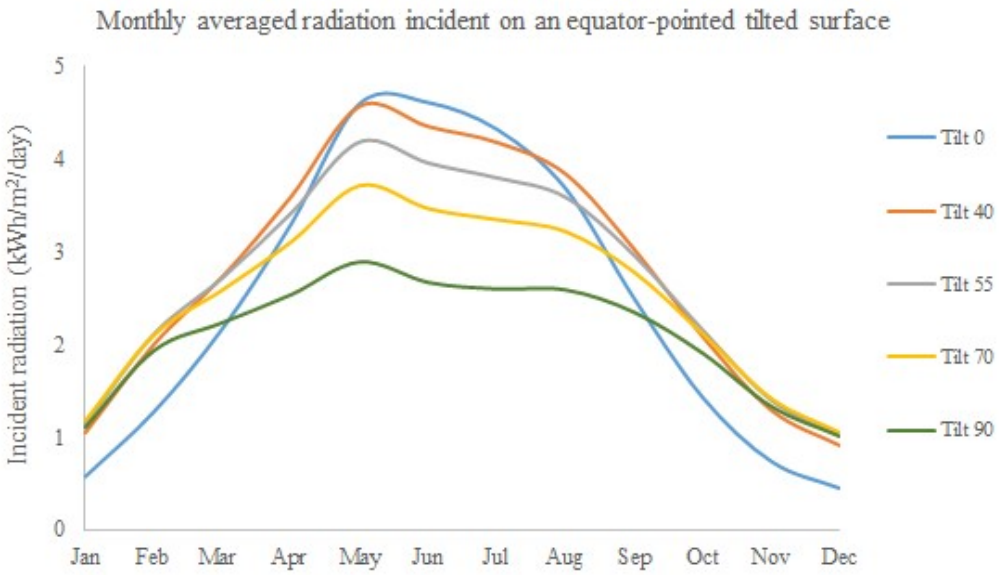

Figure 2.19: Monthly average solar radiation incident on a south-facing tilted surface at the latitude of Edinburgh. Data taken from NASA (2008)

2.2.3 Summary of heat retention methods

This review highlights novel methods that are available to prevent heat losses, optimise the system design and improve overall performance. The radiative losses to the ambient and sky can be combatted by insulated sections of the collector surface, night-covers, and/or using a glazed aperture with low emissivity yet high transmittance. Heat losses at night or during non-collection periods can be reduced using a thermal diode which prevents reverse flow of heated water. Conduction losses through the back wall and sides can be reduced with more efficient insulation materials or embedding the system into the building envelope so the temperature difference across the thermal bridge is smaller. Heat loss through pipes and joints can also be reduced by integration into the roof structure, having fewer working parts, and localising the plumbing connections

so there are fewer holes in the building envelope. Of the methods reviewed, some are less complex and expensive solutions that can be easily adapted to a chosen ICS design. The heat loss mechanisms associated with the various heat retention strategies that have been discussed are summarised in Table 2.2.

Table 2.2: Heat retention strategies and the associated heat loss mechanisms

Heat Gain/Retention Strategy	Heat Loss Mechanism Impacted
Additional insulation	Reduces convective, conductive, and radiative heat losses
Baffle plate/inner sleeve	Reduces convective heat losses and promotes thermal stratification
Fins	Promotes heat transfer to the bulk water body through conduction
Glazing	Impacts on radiative heat losses and transmissivity, creates an air cavity which suppresses internal convection
Inlet pipe configuration	Impacts on thermal stratification and therefore heat gain
Phase change materials	Can impact on conductive, convective and radiative heat losses depending on their use. Provides stored heat during non-collection periods
Reflectors	Impacts on the level of incident radiation, can reflect radiative heat losses
Selective absorber surfaces	Enhances the absorption and reduces the emission of solar radiation
Storage tank/collector material	Impacts on conductive heat losses
Thermal diodes	Reduces convective heat losses

The burden of performance improvement does not rest solely on heat loss reduction; improving the collection of solar energy and internal heat transfer efficiencies are also essential. For example, selective coatings on the absorber surface can maximise collector performance. The insertion of a baffle plate parallel to the absorber surface can produce higher temperatures and greater thermal stratification through convection. An evacuated layer between the absorber surface and the glazing can both improve heat transfer and reduce heat loss. Extended fins along the length of the tank improve heat transfer through conduction and provide structural stability.

Alongside all these methods to improve collector performance, the system must be

able to contribute to the hot water demand required by the end-user and it must be fit for practical application. Therefore, any potential designs should be tested under a realistic hot water draw-off profile. Also, given the nature of ICSSWHs, hot water draw-off improves the efficiency of the system as hot water, which has a relatively low capacity for heat gain, is removed and replaced by cold water, which has a high capacity for heat gain. So, instead of letting the system reach equilibrium and losing heat to the ambient environment, drawing off water makes better use of the system. The following section reviews various draw-off profiles proposed in the literature and by standardisation bodies, focusing on required end-user temperature, hot water consumption and the time of day the water is drawn-off.

2.3 Draw-off

Here, "draw-off" is a term that simply means to remove hot water from the collector. This removal is based on the domestic hot water (DHW) consumption pattern, which varies from household to household. Therefore, it is not possible to have a truly representative demand profile. There are various test procedure standards for domestic hot-water stores that use several DHW profiles such as CEN & CENELEC (European Commission, 2002), BS ISO 9459 (BSI, 2013), EN 12977 (BSI, 2012), and BRE (Building Research Establishment). These vary between three large draw-off events or several smaller ones across a 24-hour period attempting to mimic a realistic profile. CEN & CENELEC developed three draw-off profiles, referred to as 'tapping cycles', in the mandate for European measurement standards; a light cycle, EU1, a moderate cycle, EU2 and a heavy cycle EU3. The EU1 tapping cycle assumes a daily hot water consumption of 52 litres across 11 draw-off events with a modest shower in the evening. EU2 assumes a 157 litres consumption across 23 draw-offs, including two showers, and EU3 is 323 litres across 24 draw-offs, including two baths and one shower. All profiles run from 07:00 to 21:30 hours. Different draw-off rates are suggested ranging from 3.5 l/min to 9 l/min, the inlet temperature is assumed to be 10°C with required delivery temperatures of 40 and 55°C, depending on the type of draw-off.

The BS ISO 9459 standard uses a load pattern from ASHRAE 90.2 and proposes load volumes ranging from 50 to 600 l/d. A flow rate of 10 l/min is applied and the hot water load for each hour is the daily load volume multiplied by a predefined factor for that hour. This standard assumes that there is a certain level of hot water draw-off within every hour across a 24-hour period, which is not a realistic representation of DHW use. The EN 12977 daily load cycle consists of three draw-offs at 40%, 20% and 40% of the daily load volume, respectively, at a constant flow rate of 10 l/min. These tests were conducted indoors, and the timings of these draw-offs were based on when the cycle started, t_0. The first draw-off occurred at t_0 + 12 hours, the second at t_0 + 17 hours and the final one at t_0 + 22 hours. For example, in practical application this could equate to 07:00, 12:00 and 17:00 hours. The inlet temperature is assumed to be 10°C with a required delivery temperature of 45°C.

BRE adopt their own DHW consumption profiles for system testing and performance comparison and they are divided into three profiles, 'light', 'medium' and 'heavy' (Spur et al., 2006). All three are comprised of 9 draw-off events, spread from 07:15 to 21:30 hours, at different load volumes and flow rates. The total volumes for each profile are 168 litres, 298 litres, and 383 litres for the 'light', 'medium' and 'heavy' profiles, respectively. Hot water demand is based on the number occupants, N, following the relationship 38+25N (l), and delivery temperature is 55°C above inlet temperature. Figure 2.20 shows a comparison of the CEN & CENELEC, EN 12977, and BRE (Building Research Establishment) higher demand profiles, all around a 300-litre daily DHW load. CEN & CENELEC is the most dispersed, with smaller, more regular draw-offs throughout the day and the larger draw-offs concentrated in the morning and night, i.e. for showering and bathing. The BRE profile has fewer draw-offs, all equal volume, with no early morning DHW use but more concentrated across midday and in the evening. The EN 12977 profile simply has three large draw-offs; one in the morning, at noon and in the evening. Of these the patterns, only CEN & CENELEC accommodate for the smaller 'dishwashing' cycles of 6, 8, and 14 litres.

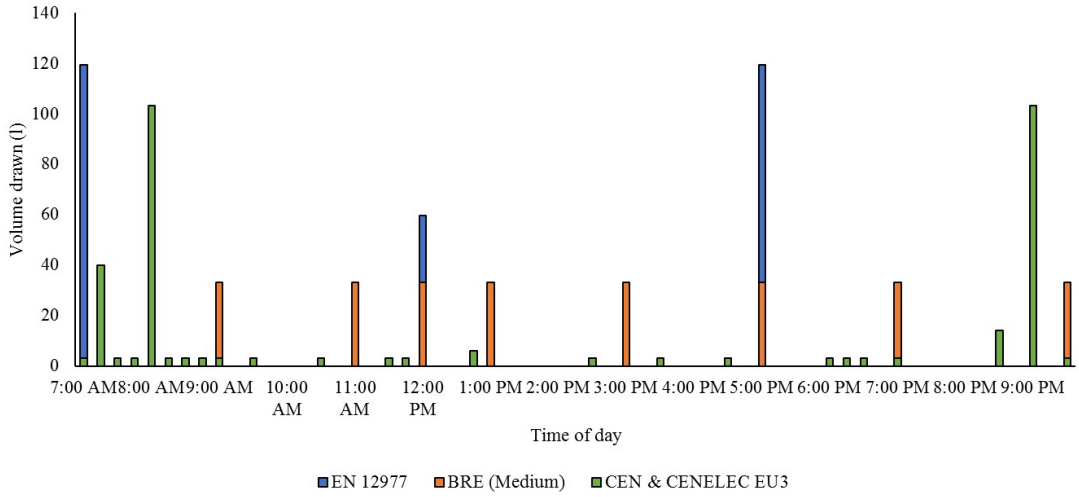

Figure 2.20: Comparison of the EN 19277 (based on a daily load of 300 litres), BRE (under the 'medium' load) and CEN & CENLEC (EU3 profile) DHW draw-off profiles

Alongside these patterns used by standardisation bodies, other studies have been conducted to determine DHW consumption (Energy Saving Trust, 2008; McLennan, 2006; Spur et al., 2006). McLennan (2006) conducted a survey of 32 Scottish homes, monitoring hourly DHW activity for one week and found that the average weekday hot water consumption was approximately 50 l/person/day, based on a delivery temperature of 55°C. This demand profile ran from 05:00 hours to midnight with the largest draw-offs concentrated in the morning, between 08:00 and 10:00 hours, and the evening, between 19:00 and 21:00 hours, with small and medium draw-offs throughout the rest of day. The survey also determined the average persons per household as 2.44, comparable to the 2001 UK-Census average of 2.4 and slightly higher than the latest UK-Census data of 2.3 persons (Office for National Statistics, 2013). However, given that there are 2.4 million households in Scotland, McLennan's study had a relatively small sample size.

Spur et al. (2006) proposed and developed three daily profiles that best represent the use of DHW of European homes, based on statistical analysis of a whole year's data. These profiles, termed realistic daily profiles (RDPs), are built upon data collected by Jordan and Vajen (2000) and found high probability of large draw-off events around 07:00 and 19:00 hours, for showers and baths, and a low probability of any draw-off between 23:00 and 05:00 hours. The RDPs are categorised into RDP1, 'light' load of 100

l/day for a two-person household, RDP2, 'medium' load of 180 l/day for a 3.5-person household, and RDP3, 'heavy' load of 320 l/day for a 3.5-person household. The inlet temperature is assumed to be 10°C and the required delivery temperature is 45°C. RDP1 consists of 26 draw-offs, including one shower, RDP2 has 42 draw-offs, including two showers, and RDP3 has 43 draw-offs, including two showers and one bath. All three profiles run from 05:00 to 23:00 and the flow rate depends on the type of draw-off; 1 l/min for short and 6 l/min for medium draw-offs, 8 l/min for showers and 14 l/min for baths. This study showed that by using a more realistic consumption pattern to test DHW stores, system performance was 13% higher for the RDP2 profile versus a single high-volume draw-off.

Garnier (2009) assessed an ICSSWH under a draw-off pattern adapted from McLennan (2006) as the ICS system was designed as 50 litres, or the consumption of one person. The adapted profile ran from 07:00 to 23:00 hours, providing 79 l/person/day of DHW with a desired delivery temperature of 55°C. Figure 2.21 shows a comparison of the discussed draw-off profiles presented in the literature, based on the DHW demand of varying occupancy. Unlike the profiles proposed in the standards above, the ones presented here all follow a similar pattern; high demand in the morning and evening and low, steady demand throughout the rest of the day. Only the CEN & CENELEC profile follows a similar pattern.

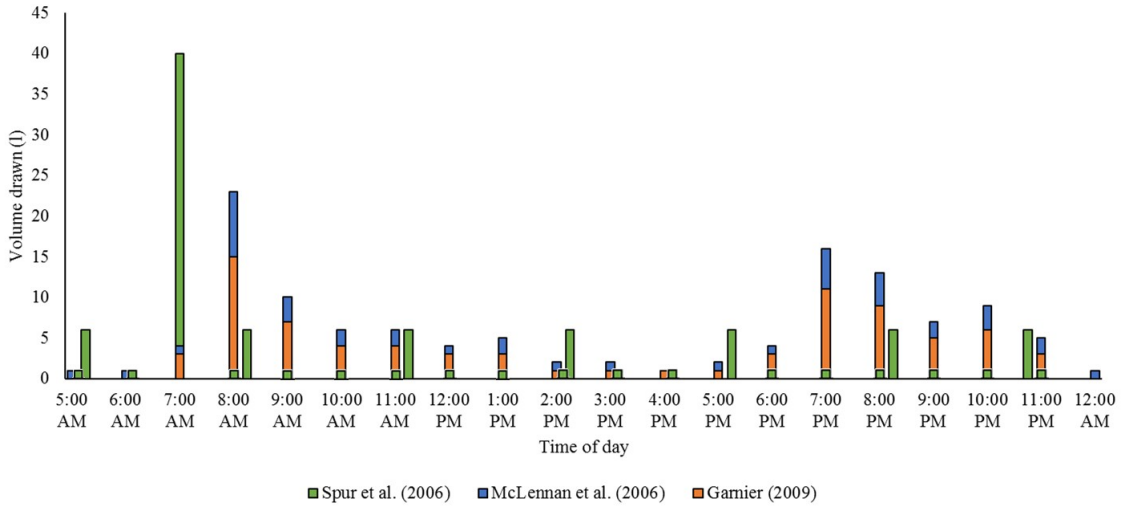

Figure 2.21: Comparison of DHW profiles reported in the literature. Spur et al. (2006) shows realistic daily profile 1 (RDP1) based on a two-person household, McLennan (2006) is based on a 2.44 person household and Garnier (2009) is based on a single occupancy dwelling

The timings of the highest DHW demand and the volumes suggested for varying levels of occupancy are supported by the findings of a study conducted by the Energy Saving Trust (2008). The report analysed data from approximately 120 domestic dwellings in the UK with the aim to measure volumetric consumption of DHW and identify heating patterns in terms of times and temperatures. This study found that the mean household DHW consumption is 122 l/day, based on 2.3 occupants per household, and each person takes 4.4 showers and 1.3 baths each week, on average. The mean delivery temperature was 51.9°C with an average heating time of 2.6 hours/day, and the often assumed 10°C inlet temperature is lower than actual values. The overall pattern of consumption showed that water is heated between 08:00 and 10:00 hours and 18:00 and 23:00 hours. Therefore, the CEN & CENELEC and McLennan profiles appear to be the most accurate representation of realistic DHW use and required delivery temperatures. Therefore, they would be recommended to test the thermal performance of DHW systems.

Having reviewed the importance of system design and efficiency and an accurate DHW consumption pattern, another vital factor in the development of a renewable technology is whether it is sustainable. A system designed to save or offset damaging carbon emissions throughout its useful life should also be as carbon efficient as possible in its design, construction and disposal/reuse. Therefore, conducting a thorough life cycle assessment of any potential contributing solution to the energy crisis, in fact all products in general, is a vital stage in assessing its practical application and sustainability. The following section reviews the literature surrounding life cycle assessment, focusing on ICSSWH.

2.4 Life cycle assessment

The literature surrounding ICSSWH systems is largely focussed on improving performance and efficiency and reducing cost (Colangelo et al., 2016; Jaisankar et al., 2011; Kumar and Rosen, 2013; Singh et al., 2016). Relatively few studies are concerned about the environmental impact throughout the whole life cycle of the product. ICSSWHs

can be branded as a carbon-free renewable technology due their passive functionality. However, if the whole life cycle of these systems is properly evaluated, they have an impact that should not be overlooked. Due to the multiple materials used, their manufacturing processes, a lifespan that is usually shorter than that of a building a system is applied to, and the waste generated when it has reached the end of its useful life, a more holistic approach to the design and performance of these systems should be adopted. When it comes to 'green' renewable technologies, it is nonsensical to develop systems that generate more environmentally harmful impacts during their production, maintenance and disposal than they can recoup and save over their useful life. Therefore, the improvement of performance and efficiency must be balanced with the environmental impact, not just throughout the product's useful life but also at the end-of-life stage, considering disposal and reuse. This makes life cycle assessment (LCA) such an important tool as it allows these impacts to be quantified and a products sustainability to be evaluated.

Given the sheer volume of research surrounding solar thermal systems and, in turn, ICSSWH, there are very few corresponding LCA studies. Even fewer studies focus on the UK and its climate, which affects the efficiency of a system and thus its energetic impact. This shows a short-term focus, where the system performance and efficiencies are prioritised over the actual life cycle of the product. However, there are a handful of relevant studies focussed on LCA of SWH systems. Most of these studies use electric or gas boilers as a basis for comparison and focus on commercially available systems (Greening and Azapagic, 2014). Uctug and Azapagic (2018) conducted a cradle-to-grave LCA for a passive, flat-plate thermosiphon SWH in Turkey. The authors considered two scenarios; a linear LCA approach where the system components were processed as waste and a circular approach where they were recycled at the end of the service life. The construction stage proved to be the most energy intensive and had the biggest environmental impact and, of the components, the water storage tank had the highest overall impact. However, environmental impacts are still 1.5–2 times lower when compared to gas boilers and the SWH could provide 80% of the annual hot water requirement.

Kylili et al. (2018) carried out an environmental assessment of SWHs for industrial

use in various European countries and found that 85% of the total environmental impact stems from the production and construction phases. They also found that SWHs could avoid over 70% of energy and carbon used/emitted when using conventional thermal systems. Similar energy results and environmental savings are found in other studies across the world with different types of SWH systems (Balaji et al., 2018; Fertahi et al., 2018; Moore et al., 2017). Further studies focus on the economic aspects of SWHs, showing their potential to replace conventional systems as well as justifying the need for government incentives (Araya et al., 2017; Chen et al., 2018; Rout et al., 2018). However, these studies concentrate on hybrid systems (i.e. incorporating photovoltaics) or indirect, active systems, not ICSSWH.

Table 2.3 summarises the European studies found when searching 'life cycle assessment' and 'solar water heaters' and shows that only six have been conducted in the UK (Allen et al., 2010; Garnier, 2009; Greening and Azapagic, 2014; Menzies and Roderick, 2010; Piroozfar et al., 2016; Smyth et al., 2000) and only two on ICSSWHs (Garnier, 2009; Smyth et al., 2000). As a result of the increasing concern over our use of finite resources, the circular economy has emerged as a new paradigm which aims to decouple resource consumption from economic growth. A key element of the circular economy is to keep resources in the loop for as long as possible, thus maximising the re-usability of products, elements, and components. Whilst the concept is gaining momentum in many sectors, its uptake in the construction industry is lagging (Pomponi and Moncaster, 2017).

Table 2.3: Summary of literature surrounding LCA and SWHs in terms of payback times, LCA stages assessed and methodologies and databases used

		Payback Times (years)								
		Energy		**Environment**		**Economy**				
Paper	**Country of study**	Best	Worst	Best	Worst	Best	Worst	**Lifespan (years)**	**LCA Stages**	**Method used**
Smyth et al. (2000)	*UK*	>2							A 1-3	TRANSYS simulation and correlation program (Polysun 2000)
Tsilingiridis et al. (2004)	*Greece*			50%*	38%*			15	A-C	GaBi software; CML 2001
Ardente et al. (2005)	*Italy*	>2		>2	2			15	A-C	ISO 14040
Battisti and Corrado (2005)	*Italy*	0.42	1.3	0.42	1.6			15-20	A-C	Eco-it software; Eco-indicator 99
Tripanagnostopoulos et al. (2005)	*Italy*	1.3	1.6	1.2	2	14.2	22.1	15-25	A-D	SimaPro 5.1 software; CML 2 baseline 2000; Eco-indicator 95
Kalogirou (2009)	*Cyprus*	1.1		0.6	3.2	2.7	4.5	20	A 1-3	TRANSYS simulation and correlation program (Polysun 2000)
Garnier (2009)	*UK*	1.5	2.6	0.7	3.1	15	30	20	A-D	University of Bath Inventory of Carbon and Energy v.1.6a
Allen et al. (2010)	*UK*	1.3	5.2	1.2	2	15	85	25	A 1-5	SimaPro v.7.1 software; data directly from manufacturers
Menzies and Roderick (2010)	*UK*	2.6	6.1	3.5	8.2			20	A-C	University of Bath Inventory of Carbon and Energy v.1.6a
Laborderie et al. (2011)	*France*	>1	1.5	0.42	0.5			20-25	A-D	Impact 2002+ (v2.04); SimaPro 7.1; Eco-invent 2.0 database

Continuation of Table 2.3

		Energy		Environment		Economy				
Paper	**Country of study**	Best	Worst	Best	Worst	Best	Worst	Lifespan (years)	**LCA Stages**	Method used
Koroneos and Nanaki (2012)	*Greece*					4	6	20	A-C	ISO 14040; GEMIS software; Eco-indicator 99 and Eco-indicator 95
Carnevale et al. (2014)	*Italy*	0.7	1.2	0.65	1.1			25	A-D	ISO 14040; Eco-invent 2.2; Eco-indicator 95
Comodi et al. (2014)	*Italy*	0.2	1	0.1	2.5	3	13	10	A-C	Tolomeo software; GaBi database; Eco-indicator 99 (E199-EE)
Greening and Azapagic (2014)	*UK*	93%*	82%*	94%*	87%*			25	A-C	ISO 14040 and 14044; GaBi software v.4.4 and CML 2001
Chen et al. (2015)	*Ukraine*	3.8	8.3	1.9	7.2			10-15	A-C	SimaPro v.7.0; Eco-indicator 95
Lamnatou et al. (2015)	*France/ Spain*	0.5	2					30	A-C	Impact 2002+; Eco-indicator 99
Zambrana-Vasquez et al. (2015)	*Spain*	0.6	4.35	72%*	30%*			20	A-C	CHEQ4 v.1.3 software; METASOL
Piroozfar et al. (2016)	*UK*	62%*		<6				20	A-C	SimaPro 8.0.3.14; Eco-invent (2013) database
Arnaoutakis et al. (2017)	*Greece*			96%*				10	A-C	SimaPro 8.2; Eco-invent v.3.3; Eco-indicator 99
Kylili et al. (2018)	*Greece*	75%*	71%*	74%*	68%*			20	A-B	ISO 14040; GaBi software

**Did not calculate payback in years but expressed as % avoided compared to conventional systems. Arnaoutakis et al. (2017) compared against a flat-plate unit*

2.4.1 Life cycle assessment as a tool

LCA is an environmental management tool that allows the environmental impact of a product to be evaluated. It allows the quantitative or qualitative description of the energy and materials used and associated environmental waste, and their assessment (Consoli et al., 1993). There are different stages that make up a complete LCA, specific to buildings and construction products, which are shown in Figure 2.22, as stated in the British Standard EN 15978 (BSI, 2011). Stages A-C, cradle-to-grave, are the most commonly evaluated with the final supplementary Stage D often neglected. Stage D allows a cyclic, holistic view of the full impacts of a product. It closes the loop and transforms an LCA from a linear analysis to circular, from cradle-to-grave to cradle-to-cradle. Cradle-to-cradle can have a very positive influence on LCA results as both reuse and recycling greatly reduce the environmental impact (Allen et al., 2010).

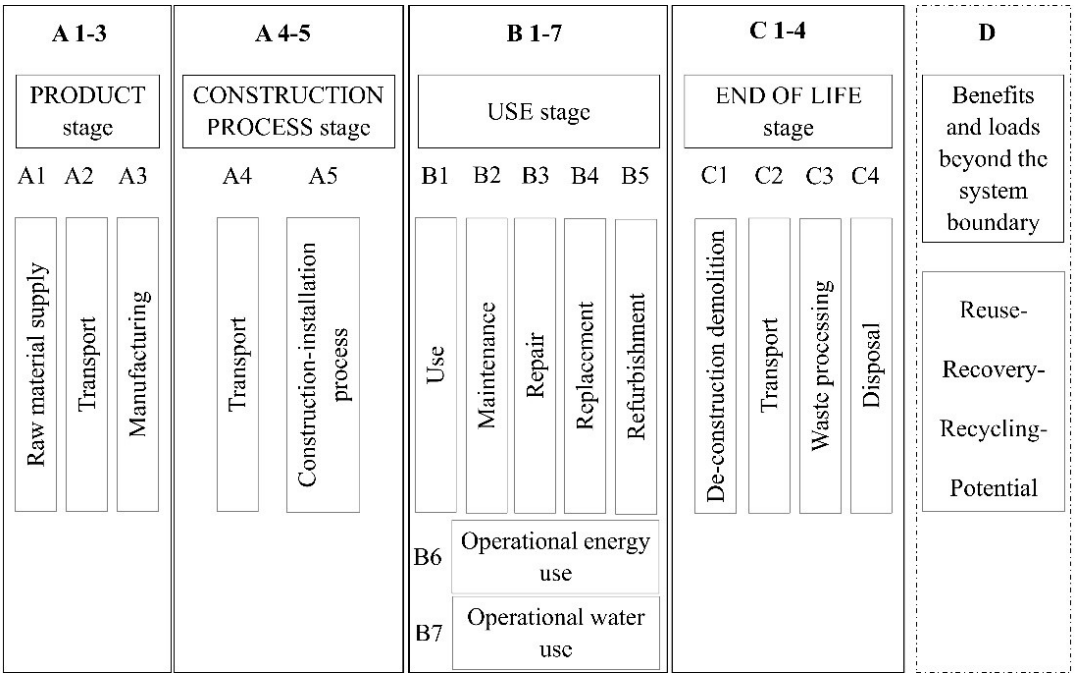

Figure 2.22: Different stages of the building life cycle (stages A-C) and supplementary information beyond (D). Adapted from BSI (2011)

The most common methodology employed for an LCA is the ISO14040 (2006) framework which consists of four main steps. First, it is necessary to define the goal and scope of the study which includes defining the system boundaries, the functional unit (FU; to allow comparability and reproducibility), and the depth and breadth of the

assessment. Second, the life cycle inventory (LCI) stage requires the necessary data collection. Third, the life cycle impact assessment (LCIA) allows the quantification of potential environmental impacts based on the data collected for the LCI stage. Finally, an improvement analysis can be done to assess any possible solutions to the environmental issues that arise such as, changes in production design, materials, energy use, waste management, reuse and recycling, etc. In the goal and scope, the FU is a quantified description of the performance requirements that a product system fulfils, and it provides a reference to which all other data in the assessment are normalised. The LCIA assesses the environmental impacts in terms of ecological systems, human health, climate change, and resource depletion.

Climate change is a commonly used impact category in LCIA methodologies (ILCD, 2010) and it is used to quantify the total set of GHG emissions caused directly and indirectly by a product (Carbon Trust, 2017). It uses global warming potential (GWP) as an assessment method (IPCC, 2014b), giving the impact in terms of cumulative radiative forcing of GHG emissions, in $kgCO_{2e}$ (carbon dioxide equivalent). Carbon impact can be used as a shorthand for GWP and $kgCO_{2e}$, thus accounting for the six main GHGs defined by the Kyoto Protocol (Carbon Trust, 2017). In terms of the whole life cycle of a product, GWP can be categorised in to 'embodied' and 'operational' carbon. Embodied carbon is the hidden carbon generated in the extraction and production of raw materials, the manufacture of the system components, the construction of the product and its deconstruction at the end of its useful life, and the transportation required between each of these stages (Figure 2.22). The operational carbon is the carbon generated throughout the products service life. For renewable systems such as the ICSSWH, the operational carbon is negative as they offset carbon emissions through reduced use of conventional fossil fuel systems.

However, GWP through GHG emissions is not the only environmental impact category that can be assessed through an LCIA. LCA, and life cycle thinking (LCT), are rapidly growing paradigms in the context of Sustainable Consumption and Production. Within an LCA, the emissions and resources associated with a specific product are documented in the LCI. Using this, an LCIA can be undertaken to analyse the impact of

emissions into water, air and soil as well as the consumption of natural resources. Every product or system has an associated impact pathway and category indicators are measurable points along this pathway. One set of measurable points are impact categories at midpoint level, which are links in the cause-effect chain before an endpoint is reached, i.e. the impact on areas of protection. An LCIA allows the contribution the impact of a product or system makes on the main areas of protection, i.e. endpoint indicators (human health, the natural environment and availability of resources), to be assessed. The emissions and resources documented in the LCI are assigned to certain impact categories for the LCIA, i.e. midpoint categories. These midpoint impact categories include climate change as well as ozone depletion, eutrophication, acidification, human toxicity (cancer and non-cancer related), respiratory inorganics, ionizing radiation, ecotoxicity, photochemical ozone formation, land use, and resource depletion. These are then converted into indicators, using factors calculated by impact assessment methods which represent the contribution to an impact per unit emission or resource consumed. Figure 2.23 gives a visual representation of the midpoint and endpoint impact categories and their relation to the three areas of protection.

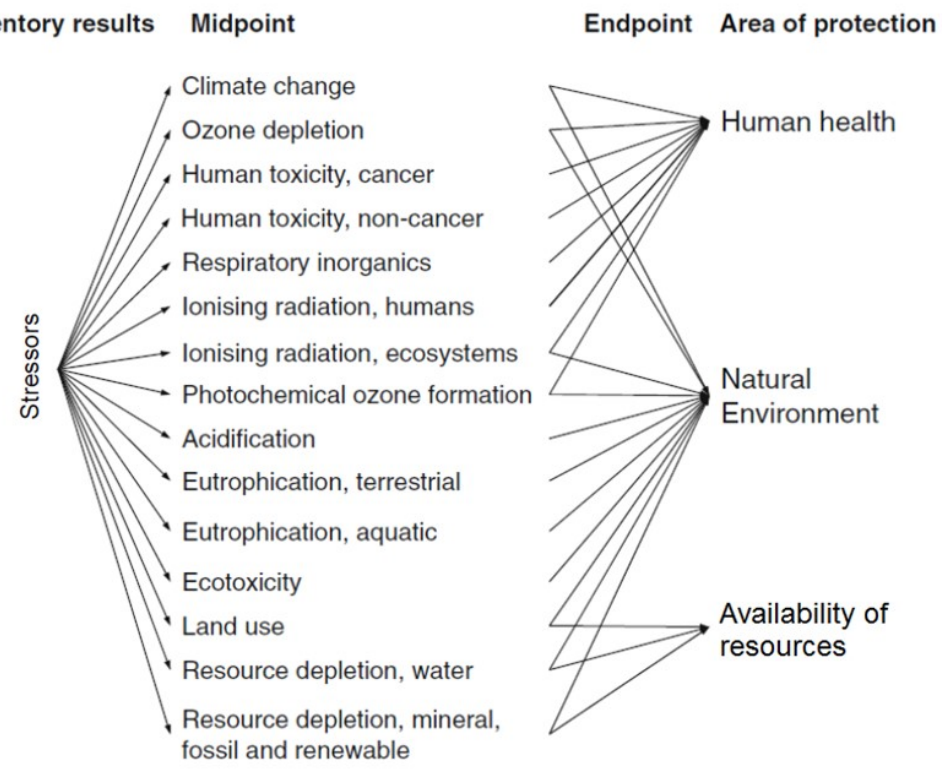

Figure 2.23: Framework of LCIA, linking stressors from the LCI to impact categories at midpoint and endpoint level and finally to the three areas of protection (adapted from ILCD (2010))

Figure 2.23 is derived from the impact categories reported in the International Reference Life Cycle Data System Handbook (ILCD, 2010), a guidance document to use alongside the ISO14040 (2006) framework. The ILCD handbook is recommended by the European Commission Joint Research Centre (EU-JRC) to help LCA practitioners maintain consistent, robust and high-quality results; it is the most comprehensive research project in this area. This technical guidance reports on impact categories at both midpoint and endpoint (points along the impact pathway). There are 16 midpoint impact categories reported in the ILCD documentation and they are presented in Table 2.4.

Table 2.4: Impact categories at midpoint and the recommended LCIA method and indicator (taken from ILCD (2011))

Impact category	LCIA method	Indicator
Climate change	Baseline model of 100 years (IPCC, 2014b)	Radiative forcing as Global Warming Potential (GWP100, $kgCO_2$-eq)
Ozone depletion	Steady-state ODPs 1999 (WMO, 1999)	Ozone Depletion Potential (ODP, kgCFC-11-eq)
Human toxicity (cancer effects)	USEtox model (Rosenbaum et al., 2008)	Comparative Toxic Unit for humans (CTU_h)
Human toxicity (non-cancer effects)	USEtox model (Rosenbaum et al., 2008)	Comparative Toxic Unit for humans (CTU_h)
Particulate matter/ respiratory inorganics	RiskPoll model (Rabl and Sparado, 2004)	Intake fraction for fine particles (kg $PM_{2.5}$-eq)
Ionising radiation (human health)	Human health effect model (Frischknecht et al., 2000)	Human exposure efficiency relative to U^{235} (kgU^{235}-eq)
Ionising radiation (ecosystems)	No methods recommended	
Photochemical ozone formation	LOTOS-EUROS (Zelm et al., 2008)	Tropospheric ozone concentration increase (kgC_2H_4-eq)
Acidification	Accumulated Exceedance (Posch et al., 2008; Seppälä et al., 2006)	Accumulated Exceedance (AE, mole H^+-eq)
Eutrophication (terrestrial)	Accumulated Exceedance (Posch et al., 2008; Seppälä et al., 2006)	Accumulated Exceedance (AE, mole N^+-eq)
Eutrophication (aquatic)	EUTREND model (Struijs et al., 2013)	Fraction of nutrients reaching freshwater (kgP-eq) or marine end compartment (kgN-eq)
Ecotoxicity (freshwater)	USEtox model (Rosenbaum et al., 2008)	Comparative Toxic Unit for ecosystems (CTU_e)
Ecotoxicity (terrestrial and marine)	No methods recommended	
Land use	Model based on Soil Organic Matter (SOM) (Mila i Canals et al., 2007)	Soil Organic Matter (kg, deficit)
Resource depletion (water)	Model for water consumption (as in Swiss Ecoscarcity) (Frischknecht et al., 2009)	Water use related to local scarcity of water (m^3)
Resource depletion (mineral, fossil and renewable)	CML 2002 (Guinée et al., 2002)	Scarcity (kg antimony [Sb] -eq)

Based on the ILCD handbook, most of the midpoint impact methods have a classification level of I or II, i.e. 'recommended and satisfactory' or 'recommended but in need of some improvements'. However, none of the endpoint impact methods meet the level I classification and only a couple meet level II. This is because the further along the impact pathway, the greater the uncertainty. Midpoint impacts are more transparent and have lower uncertainty than endpoint impacts (PRé, 2016). Despite this, endpoint impacts are often used as they are easier to interpret and less complex than their midpoint counterparts.

Along with this environmental impact assessment, often focusing only on GWP, many of the studies reviewed also evaluate the energy and economic impacts. Combing these three aspects allows a detailed view of a products overall impact. Energy refers to the performance of the system and how much operational energy it can save over its useful life; this can pay back the system's embodied energy. The operational energy is an important factor for determining the operational carbon impacts as the latter is derived from the former and converted into CO_{2e} using conversion factors based on the current and predicted energy mix. Economy is also heavily influenced by this as a better system performance will reward more savings to the end-user in terms of avoided conventional energy consumption.

By using a solar, passive system, a proportion of conventional fossil fuels are replaced. The embodied energy can usually be recouped in under 2 years and embodied carbon varies depending on the energy mix and the delivery system being replaced (Table 2.3). The economic payback periods (PBP) are reported to be much longer due to the higher capital costs of solar thermal systems compared to gas or electric boilers, for example. A life cycle cost analysis is beyond the scope of this thesis, however, PBP reported in the literature are shown to give an idea of the potential of such systems. Table 2.3 reviews the country of each study (geographic location playing a large role in system performance), payback times (where reported), the lifespan considered in each study, the stages of LCA covered (i.e. system boundaries), and the methodology employed. Only European studies have been presented here as the databases and software used are more relevant to the current study, as discussed below.

The same methodology is rarely used throughout the literature, and this is not new in LCAs in the built environment (Pomponi and Moncaster, 2016). Many consider the ISO 14040 standard as the procedure to follow but use different databases and analytical software. The accuracy of the LCA relies on the integrity and applicability of the database used. There are numerous available however it is important to choose one that is most representative of the source and type of construction material used. Databases are often specific to geographic regions; for example, European databases include Ecoinvent, GaBi, and European Life Cycle Database whilst American databases include Athena and U.S. Life Cycle Inventory. Martínez-Rocamora et al. (2016) reviewed LCA databases focused on construction materials and presented a clear, informed selection process for researchers. The authors emphasised the high quality of Ecoinvent and GaBi Database for European studies and SimaPro as a software package. Software tools are used to minimise the time and effort required for a LCIA and common tools include CML 2001, Eco-indicator 99, and Impact2002. Martínez et al. (2015) evaluated seven software tools through a case study involving a wind turbine. The authors found that, although LCIA results across the different tools could vary markedly, CML and Eco-indicator 99 tools provided a robust and accurate comparison for most categories. The choice of database as well as the software tool is therefore a crucial consideration.

The spread in databases and software used makes direct comparison, as well as replicability, difficult. This inconsistency across the literature makes it hard to identify the steps within the LCA that have the greatest impact and, therefore, the greatest improvement potential (Ardente et al., 2005). Many studies also claim to conduct a cradle-to-grave LCA which translates to stages A to C in the EN 15978 standard. However, results are often presented as aggregated indexes, i.e. aggregating multiple subsequent or different activities in a supply chain, not considering the truncation error inherent in many material databases (Lenzen and Dey, 2000). Every component included in the final FU has its own lifecycle and impacts though this is rarely considered, with the analysis only extending a short way into the components supply chain. Therefore, the more disaggregated the results, the more transparent and comprehensive the LCA.

2.4.2 Life cycle assessment methods: advantages and limitations

Three main methods for LCAs exist in the built environment: process, input-output, and the hybrid analysis. A process-based analysis refers to a mix of processes, products, and location-specific data to calculate and establish the environmental impact of a product system. Input-output analysis is an economic technique, which uses input-output tables (matrices of sector-based monetary transactions) to map resource consumption and pollutants release throughout the whole economy (Crawford, 2011). Both process and input-output LCAs suffer from incomplete and unreliable inventory data sources which impacts upon hybrid LCA, albeit with less severity (Crawford, 2008). Process LCA has inherent truncation errors due to the definition of system boundaries and the limited process data available (Lenzen, 2001). Input-output LCA has issues associated with data aggregation, though, if done correctly, the impact of this is typically much less than the truncation error in process LCA (Crawford and Stephan, 2013). Input-output LCA also suffers a downstream truncation error (Majeau-Bettez et al., 2011) as it does not consider the 'gate-to-grave' period of the life cycle. However, this is easily overcome by using input-output-based multipliers (Lenzen, 2001).

Hybrid analysis aims to combine the strengths of the previous two by filling missing, process-related information with input-output data, and it has been demonstrated that it is likely to yield more accurate results (Pomponi and Lenzen, 2018). However, combining process and input-output data in a hybrid LCA remains a highly manual and time-consuming process (Crawford et al., 2017). Therefore, in the LCA of buildings, where each of the materials used has its own specific life-cycle and all interact dynamically in both space and time (Collinge et al., 2013; Erlandsson and Borg, 2003), the process-based analysis appears as the most reasonable choice and is also suggested by European and International Standards that are specifically developed for the construction sector (Moncaster and Song, 2012).

2.4.3 Summary of LCA

LCA is a valuable tool for the environmental management of products and processes. There is strong inconsistency throughout the research in this field as to the methodology, software and databases that are used. This makes direct comparison and reproducibility difficult. Therefore, when comparing products or processes, it is essential that the any life cycle impact analyses follow the same methodology, consider the same functional unit, and use the same software and databases. It is also important to use databases that are relevant to the geographic region of the study as this has a large impact on the results of an LCA.

2.5 Concluding remarks

This chapter began with a review of the various heat retention strategies and design parameters applicable to ICSSWH systems currently being researched. Section 2.1 provided a brief introduction into solar water heaters, focusing in on ICSSWH. Section 2.2 highlighted several innovative ways to improve heat retention, thermal performance and overall system efficiency without significantly increasing the complexity or cost of the system. Several of the reviewed studies noted the importance of draw-off frequency on system efficiency. As such, this is an important consideration for the optimisation of any ICSSWH system and a review of the literature and standardisation bodies surrounding draw-off patterns is presented in Section 2.3. Finally, 'green' renewable technologies carry a heavy burden to offset carbon emissions and contribute towards emissions reductions targets. Therefore, a holistic review of the life cycle of any product is important to be able to claim environmental sustainability. Section 2.4 describes the concept of life cycle assessment as an environmental management tool and highlights current research surrounding ICSSWHs and LCA. Only two studies have been conducted on the LCA of ICSSWH in the UK (Garnier, 2009; Smyth et al., 2000).

This chapter highlights certain gaps in knowledge that the remainder of this thesis aimed to fill through the research objectives (RO) presented in Chapter 1. First, research

into ICSSWH in the UK is sparse and most studies focus on laboratory experiments with only short periods of transient field testing. This thesis evaluates and compares two rectangular ICS systems with different heat retention strategies incorporated into the base design. Beyond this, two additional heat retention strategies are experimentally tested to determine their practical application and contribution to system performance (RO 2). Second, these heat retention strategies are applied under a realistic DHW consumption pattern (RO 3). Third, ICSSWHs, and SWHs in general, are additional units applied to domestic dwellings once they have been constructed. This thesis aimed to highlight the benefits of integrating the ICS system into warm roof timber construction; improving heat retention due to embedment into the building fabric as well as the overall aesthetic as it would be flush to the roof surface (RO 1). Finally, LCA of ICSSWH in the UK has rarely been done and never on the proposed designs. An LCA that considers the reuse and recycle potential, the supplementary stage D, is rarer still. This thesis presents a comprehensive LCA of the two base configurations, with the additional heat retention methods, both with and without a circular economy approach (RO 4).

The following chapter describes the research methodology employed for both the field experiments and the LCA.

Third Chapter

Research design, approach and methods

Following the extensive literature review presented in the previous chapter, and pursuant to the aim and objectives of the current research, this chapter outlines the materials and methods used throughout this work. The design and construction of the systems under evaluation, as informed by the literature, is outlined followed by a detailed description of the methods used for the field experiment phases. The methodology employed for the life-cycle assessment (LCA) aspect of the current research is also laid out. Firstly, however, it is important to understand the different schools of thought and philosophical stances conceptualised by researchers in this field, and justify the chosen research approach.

3.1 The research approach

This section presents a reflection on the theoretical underpinnings of research focussed on the built environment. Given the breadth and depth of subjects included in this area, a wide range of approaches are adopted. However, they can be explained through four paradigms: ontology, epistemology, methodology and methods/techniques. Each level can be further subdivided and related, as shown in Figure 3.1. The overarching research approach taken for the current research is also highlighted in the figure. To achieve the research objectives of this work, an objective ontology is required as the research is objective, independent of thoughts/beliefs, and quantifiable. Within that umbrella, a positivist epistemology approach is taken as this work deals with credible

facts, rigorous scientific inquiry, and empirical observation and measurement (Creswell, 2014). Further along the research route, a deductive methodology is applied, with the following stages: theory, based on existing knowledge; objectives, based on gaps in knowledge; operationalise, i.e. specify what is required of the researcher to measure a concept; testing, through empirical observation or experimentation; and examine outcomes, i.e. achieve, or fail to achieve, the research objectives (Gray, 2011).

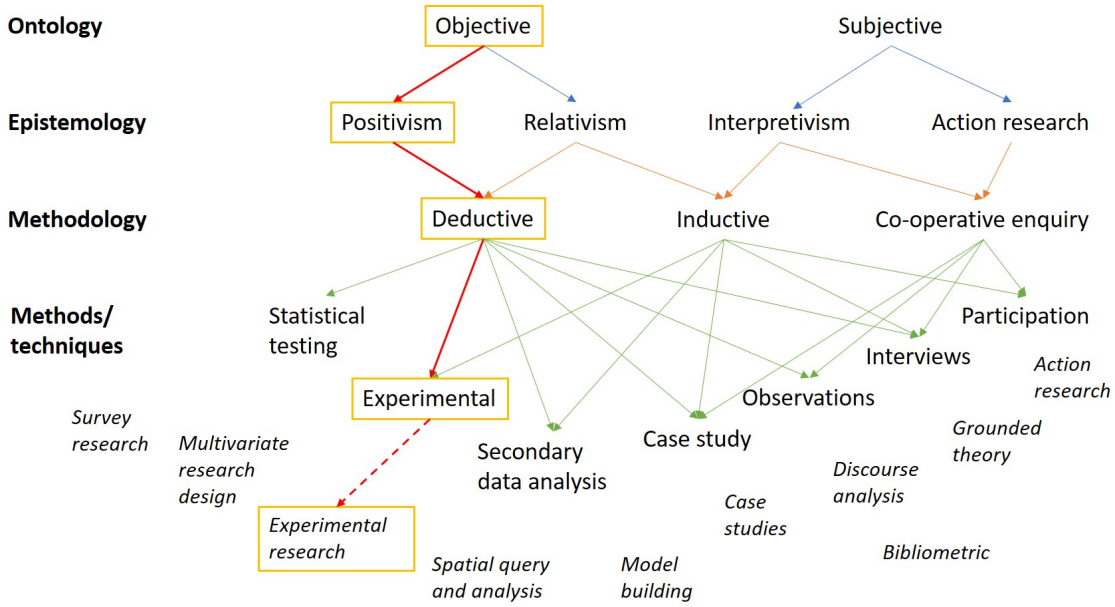

Figure 3.1: Approaches and routes in research. The research approach taken for the current research is highlighted. Adapted from Ates (2008)

However, despite every desire for research to be objective, quantified and quantifiable, and free from beliefs, the nature of the work presented in this thesis nevertheless lends itself to blurry theoretical and methodological boundaries. This lack of distinct boundaries is widely recognised in built environment research, so it cannot be defined as "a discrete discipline with its own standard approaches to philosophy, methodology, and methods" (Knight and Turnbull, 2008, p.72). While field experiments are more strictly bound to rigorous experimental procedures, an example of where the subjectivity steps in and possibly influences the outcome of this research, without the opportunity to assess its impact on the results, is the choice (or lack thereof) the solar panel's location. Different positions would have likely led to different energy yields and possibly unveiled other patterns in performance. Of course, it is not possible to test

every possible combination of position and orientation but it is nonetheless important to be aware of the subjective choices made and offer evidence as to where they came from (the literature review, for instance, in the case of this research).

As far LCA is concerned, there is long-standing recognition of the value-ladenness that characterises it. Seminal work, credited to Hertwich et al. (2000), joined (and possibly resolved) an ongoing methodological debate in the late 1990s around the role of value judgements in LCAs (e.g. Finnveden, 1997; Heijungs, 1998). This was sparked by the ISO LCA committee who place LCA as a discipline within the natural sciences, arguing these are free from value judgements (e.g. Owens, 1998). One side posited that objective truth can be achieved by the rigorous application of the LCA method to obtain results that are scientifically and technically valid. The other side, while still supporting the usefulness of the method, showed that in carrying out an LCA the assessor's ethical, ideological and subjective valuations regularly affect the choice of calculation methods, data collection, data choices, etc. Hertwich et al. (2000) resolved this by demonstrating the value-ladenness of LCA on one of the most widely used impact assessment indicators, the Global Warming Potential (GWP). They concluded, and proposed, that LCA should be seen as a component of the environmental decision making progress rather than "a disinterested aggregation of facts" (Hertwich et al., 2000). It is through this lens that LCA is seen and applied in this thesis.

Figure 3.2 provides an overview of the research design, the conceptual framework of this study. First, an extensive literature review was carried out to identify gaps in knowledge and inform the new ICSSWH designs, alongside the existing iterations that were subsequently adapted. From here, the research objectives (ROs) were developed, based on a deductive methodology, and the system design and operation were experimentally tested. The new system design seeks to achieve RO1 and the results obtained from this experimental phase aim to achieve ROs 2 and 3. The design itself, and its practical performance, feed into the LCA work which aims to achieve RO4. These strands then all come together to achieve the overall research aim.

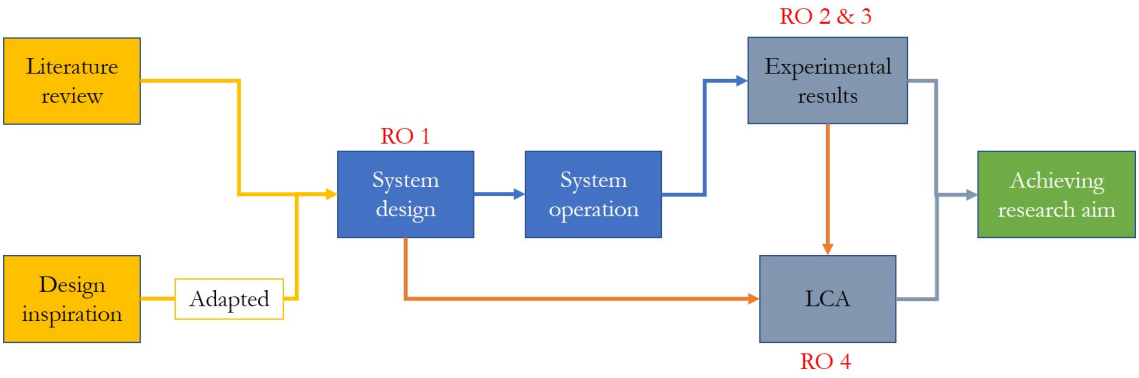

Figure 3.2: Overview of the research design

The following sections outline the materials and methods used for the design and construction of the ICSSWH systems and the LCA method.

3.2 Field experiments

3.2.1 Design and construction

A new ICSSWH design was commissioned that would be tested under two design configurations. The internal tank dimensions are the same for both configurations whereas the design and the materials used in their construction differ, as detailed in the following sections. A major adaptation from previous designs is that the new prototypes are designed to be disassembled so the collector components can be cleanly separated and reused at the end of their useful life. The absorber plate can be detached from the storage tank as reuse and recycle potential had a heavy influence on the collectors' design.

3.2.1.1 Proposed prototypes

The proposed new ICSSWH designs incorporate elongated heat transfer fins and an internal baffle plate, labelled "finned" and "baffled" respectively. These configurations were informed by the literature and the justification for their adoption can be found in Chapter 2. Heat transfer fins are an effective, low-cost method of improving the conductive transfer of heat to the bulk water body. Baffle plates can be used in a variety

of different ways and configurations. They act to promote the convective transfer of heat from a thin layer of water, trapped between the baffle and absorber plates, to the main water store.

These base design configurations form the basis for comparison throughout the experimental and LCA work and this inter-system comparison requires that each system is the optimal paradigm of its type. These design configurations were chosen based on the results of existing optimisation studies; the finned configuration was optimised by Garnier (2009) and Birley et al. (2012) while the baffled design was optimised by Souza et al. (2014) and Swiatek et al. (2015). A system is optimised for a specific set of climatic and user conditions and for this work, the geographic study area is Scotland and the user conditions constitute the storage volume per square meter of absorber area and angle of inclination. Therefore, the conditions under which the design configurations were optimised must be in the same climate classification and operate under similar user conditions as the present study. Table 3.1 states the climate classification and user conditions for this study and the optimisation studies. The climate classification is taken from the Köppen-Geiger World Map (Kottek et al., 2006) which is widely used, globally, as it defines the global climate at a fine resolution through a three-layer classification. These three layers are: the main climate; precipitation; and temperature. Both optimisation studies used in this research fall under climate category *C*, warm temperate, precipitation level *f*, fully humid, and temperature band *b*, warm summer. The user conditions are the acceptably similar for the optimisation of the fins while the study optimising the baffle plate has double the storage volume per square meter of absorber area. This is still within an acceptable range as the absolute volume is 80 litres versus 48 litres in this study. Additionally, the angles of inclination are well aligned.

Table 3.1: Climate classification and user conditions of the present study and optimisation studies. C: warm temperate, f: fully humid, b: warm summer; based on the Köppen-Geiger World Map (Kottek et al., 2006)

Study	Climate classification	User conditions
Birley et al. (2012) and Garnier (2009)	Cfb	50 l/m^2; inclined 45°
Souza et al. (2014) and Swiatek et al. (2015)	Cfb	100 l/m^2; inclined 30°, 45° & 60°
Present study	Cfb	50 l/m^2; inclined 35°

Figure 3.3 and Figure 3.4 illustrate the exploded view of each proposed design. These prototypes are designed to be disassembled allowing the use of different materials which can be adapted for optimal thermal performance and environmental sustainability. The collector components are discussed in the following section.

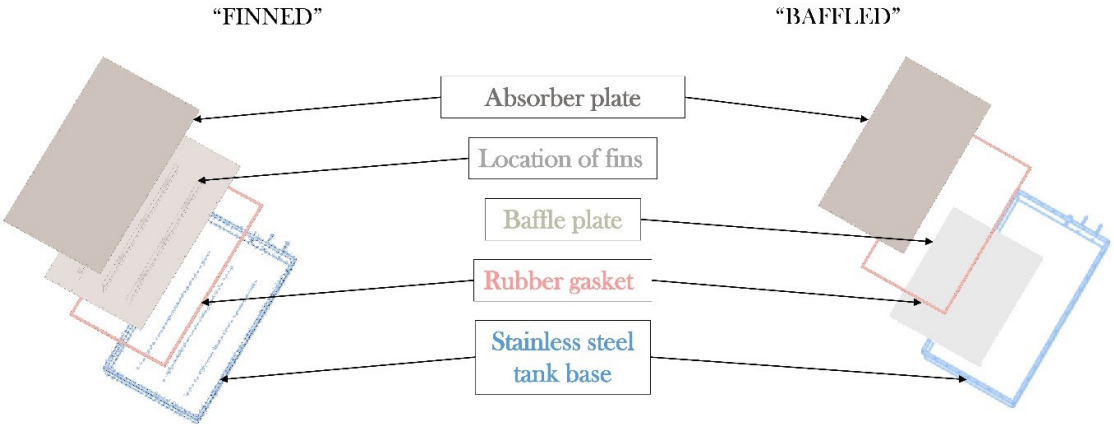

Figure 3.3: Exploded view of the proposed prototypes – the "finned" and "baffled" collector designs

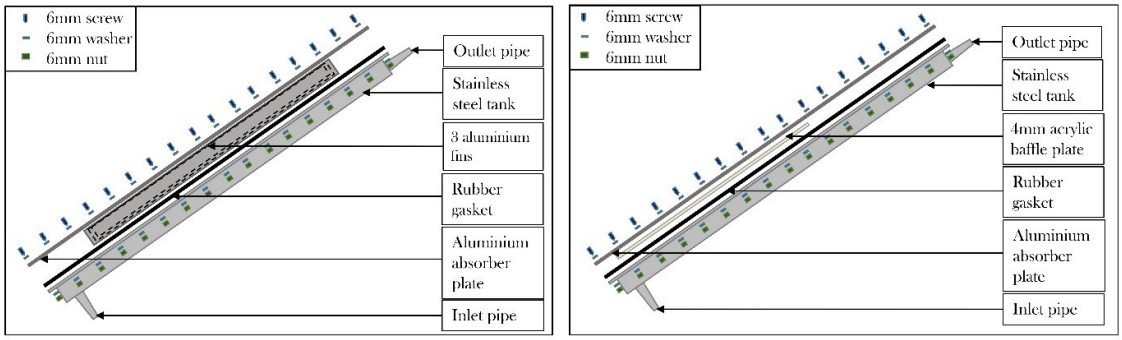

Figure 3.4: Side exploded elevation of the proposed prototypes with details of collector components. Left: "finned" design; right: "baffled" design

3.2.1.2 Collector components

The two designs have the same basic collector set-up, as shown above, consisting of a stainless-steel tank base and an aluminium absorber plate. The tank base includes four pipes extending from its surface; an inlet pipe located at the bottom of the tank, an outlet pipe at the top of the tank, and two pipes to hold the thermocouple rods (discussed in Section 3.2.3.1). The tank was made using 1.5 mm thick 304 stainless steel. For the baffled design, the absorber plate is a plain sheet of aluminium while for the finned design, 3 elongated aluminium fins were welded to the underside of the absorber plate, evenly spaced across its width (see Appendix A for technical drawings). The aluminium used was 3 mm thick. The baffled design includes a 4mm thick pane of polycarbonate that is secured at a depth 5mm below the absorber plate. Table 3.2 lists all the components required to produce the two ICSSWH designs under evaluation. Dimensions and technical details can be found in the next section. The materials used for the heat retention strategies and the frame/insulation are detailed in Section 3.2.3.

Table 3.2: Collector components for the baffled and finned ICSSWH designs

Baffled			**Finned**		
Component	*Material*	*Quantity*	***Component***	*Material*	*Quantity*
Tank base	1.5 mm, 304 Stainless steel	1	**Tank base**	1.5 mm, 304 Stainless steel	1
Absorber plate	3mm aluminium	1	**Absorber plate**	3mm aluminium	1
Baffle plate	4mm polycarbonate	1	**Fins**	3mm aluminium	3
Absorber plate coating	Black spray paint (matte)	4 coats	**Absorber plate coating**	Black spray paint (matte)	4 coats
Sparge tube	Copper	1	**Sparge tube**	Copper	1
Gasket	EPDM rubber	1	**Gasket**	EPDM rubber	1
Gasket sealant	Hylomar	1	**Gasket sealant**	Hylomar	1
Compression reducing coupling	Copper with brass finish	1	**Compression reducing coupling**	Copper with brass finish	1
Compression straight coupling	Copper with brass finish	1	**Compression straight coupling**	Copper with brass finish	1
Hose fitting	Copper with brass finish	1	**Hose fitting**	Copper with brass finish	1
6 mm screws	Steel	44	**6 mm screws**	Steel	44
6 mm Nylock nuts	Steel	44	**6 mm Nylock nuts**	Steel	44
6 mm washers	Steel	88	**6 mm washers**	Steel	88
Sparge tube supports	Polycarbonate	2	**Sparge tube supports**	Polycarbonate	2
Baffle plate supports	Polycarbonate	3			

3.2.1.3 Collector fabrication

The main components of the new collector designs, i.e. the storage tanks and absorber plates (one including fins), were manufactured externally by Pentland Tech Metal Fabrications, an Edinburgh based company. The internal sparge tube, EPDM gasket and baffle plate were produced in-house at Edinburgh Napier University. The collector

was assembled onsite at the custom-made solar laboratory on a roof of Edinburgh Napier University.

Each collector had internal dimensions of 1325 x 725 x 50 mm, giving a volume of 48 litres, with a 20 mm lip to accommodate the gasket that allows a watertight seal between the storage tank and absorber plate. The baffle plate dimensions were 855 x 725 x 4 mm and was set 50 mm from the base of the tank, to avoid disrupting the flow from the inlet sparge tube. The dimensions and placement of the baffle plate were informed by studies conducted by Souza et al. (2014) and Swiatek et al. (2015) which were discussed and evaluated in Chapter 2. The three fins were T-shaped aluminium plates welded to the underside of the absorber plate and each fin had dimensions of 1000 x 3 x 50 mm. The sizing and placement of the fins was based on previous work by Garnier et al. (2008) and Birley et al. (2012).

The following is a series of photographs of the collector design and assembly (Figure 3.5, Figure 3.6, and Figure 3.7).

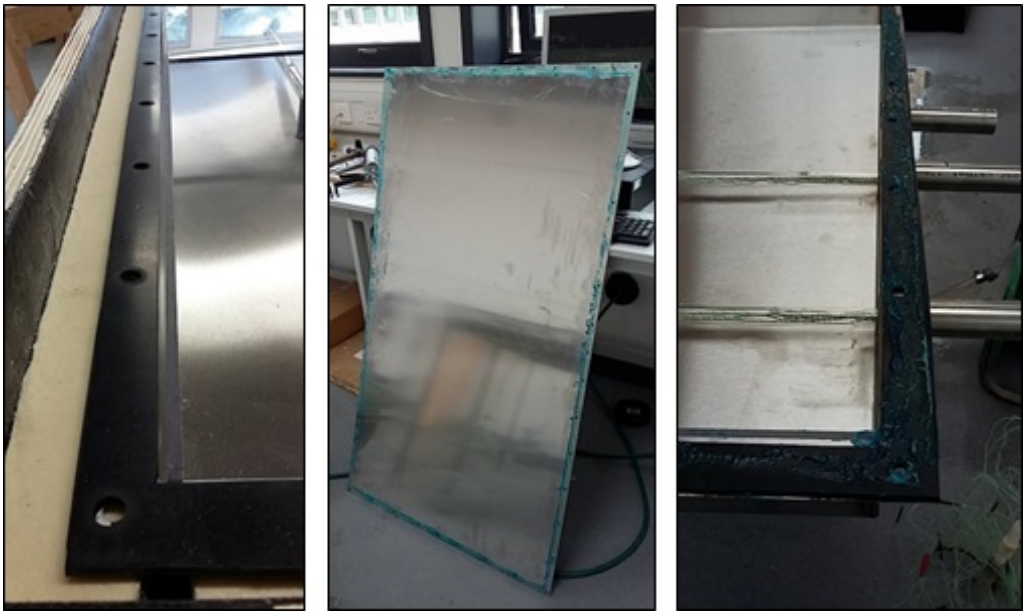

Figure 3.5: The EPDM gasket and the Hylomar gasket sealant

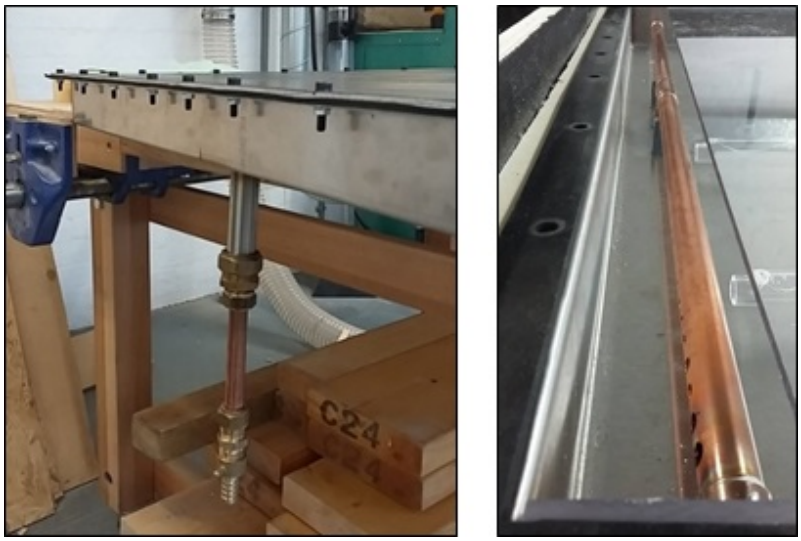

Figure 3.6: Situation of the inlet pipe and internal sparge tube

Figure 3.7: Configuration and placement of the internal baffle plate, with the supporting pillars, and the storage tank and absorber plate bolted together

3.2.1.4 Evolution of the ICSSWH design

This novel solar water heater began with Muneer et al. (2006) who compared a plain against a 5-finned ICSSWH design, both were 1 m^2, 80 mm deep and constructed from 1 mm thick stainless steel. Following this work, Henderson et al. (2007) modelled the system to determine the optimal angle of inclination for Edinburgh and the optimal sizes of the air and water cavities. The authors validated their model with laboratory studies using a 1.5 mm stainless steel collector which was 1 m^2, 50 mm deep. Thus, the original design was adapted to thicker steel, for increased structural stability, and a shallower storage tank, for faster heat transfer.

Garnier (2009) also modelled collector performance, however, the author compared stainless steel against aluminium and a 4-finned versus 5-finned design. The adaptations here being the introduction of aluminium as the absorber (and storage) material

and varying the number of fins to determine the impact on the internal thermal dynamics. Garnier used the same dimensions, 1000 x 1000 x 50 mm, and evaluated various metal thicknesses; 1.5 mm stainless steel, and 1.5 mm and 3 mm aluminium. Informed by and building upon this, Birley et al. (2012) developed a collector entirely constructed of aluminium with a 4-finned design. However, the two central fins were joined to create an outlet manifold to encase an immersion heater. This evolution brought together the optimal fin number, the use of aluminium with its higher thermal conductivity albeit weaker structural stability, and an immersion heater as an auxiliary heat source (Garnier et al., 2018). The authors also adapted the dimensions of the system, making it longer and narrower to better suit MMC, and conducted a CFD analysis to determine the influence on the thermal dynamics. Figure 3.8 illustrates the evolution of these novel ICSSWH designs up to the iteration preceding the current study.

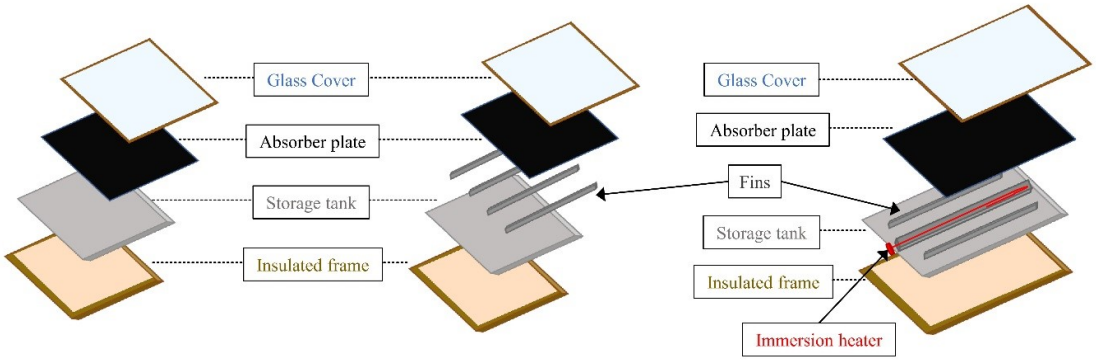

Figure 3.8: Evolution of the novel ICSSWH developed at Edinburgh Napier University, from an unfinned, stainless steel design, to a finned aluminium design incorporating an immersion heater

The design iteration in the current study improves upon its predecessor in that it can be dismantled; the absorber plate can be detached from the storage tank. This allows the use of different metals which cannot be welded together. The absorber plate is made from aluminium while the storage tank is made from stainless steel. Aluminium was chosen for its high thermal conductivity and specific heat capacity; both are greater than that of stainless steel. Stainless steel was chosen for its lower thermal conductivity and heat capacity which translates to reduced heat losses from the back and side walls compared to a collector made entirely of aluminium. Stainless steel is more expensive than aluminium but has a longer lifespan and greater structural stability. It can also

be easily worked with at lower thicknesses, e.g. 1.5 mm, and retain its strength while aluminium is difficult to weld when that thin and thus a greater volume is needed.

The two design configurations evaluated in this work were tested as stand-alone water heaters and any auxiliary heating is assumed to be provided by other direct heating solutions. The fins use 3 mm thick aluminium as opposed to the 2 mm thick sheets used by Birley as the fabricator could not guarantee a watertight weld with aluminium thinner than 3 mm. Indeed, in the initial phases of testing, when using the collector manufactured for Birley's research, the collector suffered numerous small leaks around the spot welds.

3.2.2 Experimental equipment – assessment and calibration

3.2.2.1 Thermocouple calibration

K-type thermocouples were used for all temperature measurements for the field experiments carried out throughout this work. The K-type thermocouples used in the current study have a temperature range of -75 to 250°C. Given the temperatures reached in non-concentrating solar thermal systems, this type of thermocouple is suitable for work with ICSSWH systems.

Calibrating the thermocouples required a 'boil' and 'ice' test. The boil test is done to ensure all the thermocouple readings are consistent over a gradually increasing temperature range. The ice test ensures all thermocouples consistently read 0°C, ±0.5°C given their accuracy. These calibration tests were done to make sure the data measured during the experimental work would be accurate and reliable and to check that the thermocouples were functioning properly. The results of these tests were subject to a linear regression analysis to ensure a strong correlation between recorded and expected temperatures. The equipment used for the calibration tests is outlined in Table 3.3.

Table 3.3: Apparatus used for experimental calibration

Apparatus	Specification	Number of units
Data logger type 2F16	Grant Instruments Squirrel SQ2040 Series Data Logger. Accuracy: 0.05%	2
Thermocouples	Single, K-type, 2.8 m long. Accuracy: ±0.5°C; Temperature range: -75 to 250°C	58
Thermos flask	Insulated flask filled with ice, used for ice test	1
Hot water bath	Constant temperature, electrothermal water bath, used for boil test. Maximum temperature: 150°C	1
Software	SquirrelView, SQ2040 logger configuration. Excel, to export data directly from SquirrelView	
Computer	Computational analysis of logged data	1

Boil and ice test For the boil test, the thermocouples were grouped into batches, placed into an electrothermal water bath and connected to the data loggers to be used throughout future experimental work. Using a Variac to control the temperature of the water bath, the temperature was increased by 10°C intervals up to a maximum temperature of 100°C. At each increment, the test was left until the water reached the required temperature and the thermocouple readings stabilised, to ±0.5°C of each other. For the ice test, the thermocouples were grouped into batches and connected to the data loggers to be used during all experimental work. They were then placed in a thermos flask filled with ice and left to settle, i.e. until the thermocouples consistently recorded 0°C, ±0.5°C. The installations for both calibration tests are shown in Figure 3.9.

Figure 3.9: Boil and ice test apparatus. From left to right: hot water bath; Grant SQ2040 data logger; thermos flask

3.2.2.2 Data loggers

Grant Instrument Squirrel 2040 series, type 2F16, data loggers were used to record all temperature and solar insolation values. The channels are compatible with K-type thermocouples for a temperature range of -200 to 1372°C. Each channel converts the voltage measured by the K-type thermocouple to a temperature reading, using a polynomial relationship for current conversion to temperature defined by British Standards (BS EN 60584.1). These loggers are 24-bit analogue-to-digital convertors with an accuracy of 0.05% and a sensitivity specification of 0.1°C.

3.2.2.3 Pyranometer

A Kipp and Zonen CMP10 pyranometer was used to accurately measure the global solar radiation incident on the absorber surface of the ICS systems under evaluation. Insolation was recorded as a voltage and required a correction factor to be applied to convert it to power, W/m^2. The pyranometer had a sensitivity of 8.99μV/W/m^2. The pyranometer was mounted to the frame of the ICSSWH, parallel to the absorber plate, to determine the irradiance incident on the inclined plane.

3.2.2.4 Solenoid valve and draw-off timer

To evaluate the ICS systems under realistic conditions, the performance of the system must be monitored under a representative hot water draw-off profile. The details of the draw-off profile adopted and justification behind it are given in Section 3.2.4. To implement the chosen profile a Burkert Solenoid Value was used, connected to a timer which opened the valve at the time specified. Initially, a Grasslin Digi 20 Series timer was used which allowed the valve to be opened for 1-minute increments, sufficient in this stage of testing for the desired flow rate and volume. However, in the later stages of testing a more sensitive timer was required to allow 30-second increments so that the volume at each draw-off could be kept constant (the need for this adaptation is discussed in Section 3.2.6). For this, an Arduino Uno microcontroller was used which was programmed to open for multiples of 30-second time steps.

3.2.2.5 Weather station

To support the data gathered by the thermocouples for ambient temperature and the pyranometer, and to occasionally replace missing data, a weather station was erected on the roof of the Solar Lab. This is an all-in-one weather data collection unit designed by Logic Energy which allows remote access and monitoring with their LeNET data logging and GPRS transmission system. The weather station specifications are detailed in Table 3.4 but only the temperature and wind data were ever used.

Table 3.4: Weather station specifications

Sensor name	Measurements	Accuracy
Temperature probe	Dry bulb (°C)	±0.5°C typical
Barometric pressure	Atmospheric pressure (mbar)	±1.0 mbar
Humidity	Relative humidity (RH%)	±3%
Solar radiation	(W/m^2)	±5%
Anemometer and wind vane	Wind speed (m/s) and direction (° from north)	Direction: ±3° ; Speed: ±1 m/s

3.2.3 Experimental testing

The previous studies this work builds upon were heavily focused on computational modelling and laboratory tests. The current research aims to bring a real-life component to assess how these ICS systems work in real-time and under realistic conditions, for the Scottish climate. Therefore, extended field experiments were conducted for the two design configurations under evaluation and for the additional heat retention methods that were chosen from the literature review; additional insulation and a night cover. This enhances the breadth and depth of the assessment surrounding this ICS design; computational and laboratory studies have proven the effectiveness of these systems and the extended field tests presented in this work will allow the feasibility of their practical implementation to be evaluated.

At the start of the testing phase, the two base design configurations, the finned and baffled collectors with no additional heat retention strategies applied, were tested side-by-side under 'no-flow' conditions, i.e. without draw-off. This created a baseline for

system performance and how each configuration performed relative to the other. Next, the configurations were tested under 'flow' conditions, i.e. with draw-off, to determine the impact on performance. Implementing a realistic draw-off profile allows the most efficient use of the system; to steadily use the hot water so that fresh cold water can be heated.

Following this initial system performance classification, the transient testing phases continued to allow the impact of the heat retention methods to be quantified. These phases followed a seasonal testing method (described in 3.2.5) to ensure as accurate a comparison as possible during the field experiments. Baseline steady and transient state tests were done to evaluate the impact of drawing water from the system and three testing phases were done to determine the impact of the heat retention methods. Under transient conditions, i.e. the standardised draw-off profile defined in Section 3.2.4, each collector configuration (finned and baffled) was tested under three design conditions – base (as designed); with additional insulation covering the top third of the absorber plate and; a night cover. The choice of these methods was informed by the literature and the justification can be found in Chapter 2.

3.2.3.1 Thermocouple placement

Pursuant to the objectives of this research, the thermal performance of the ICS systems needs to be measured. Using the calibrated thermocouples, the temperature profiles within the inclined storage tanks can be monitored. The strategic placement of these thermocouples was to ensure as comprehensive a view of the internal thermodynamics of the system as possible. As the system is symmetrical along its vertical axis, only half of the tank needs to be observed. The finned tank is symmetrical around its middle fin and the baffled tank is symmetrical around the pillars supporting the baffle plate. The thermocouple placement was identical for the two ICS designs.

Figure 3.10 shows the placement of all the thermocouples used, built upon and adapted from previous work (Garnier, 2009). Thermocouples 1–18 are located inside the water tank and measure the thermal stratification; thermocouples 19–27 are attached to the absorber plate and the glass cover as well as suspended in the air cavity, to observe

the extent of heat loss when employing the heat retention methods; thermocouples 28 and 29 measure the inlet and outlet water temperature and; thermocouple 30 measures the ambient air temperature. The control volumes, outlined in Figure 3.10 with dotted lines, were spaced so they are clustered closer together at the top and bottom of the tank as well as the tips of the fins, to see the influence of internal wall conduction and convective eddies. A wider spacing is used in the middle section of the tank as there is less interaction with the tank walls and therefore less important in terms of internal thermal dynamics.

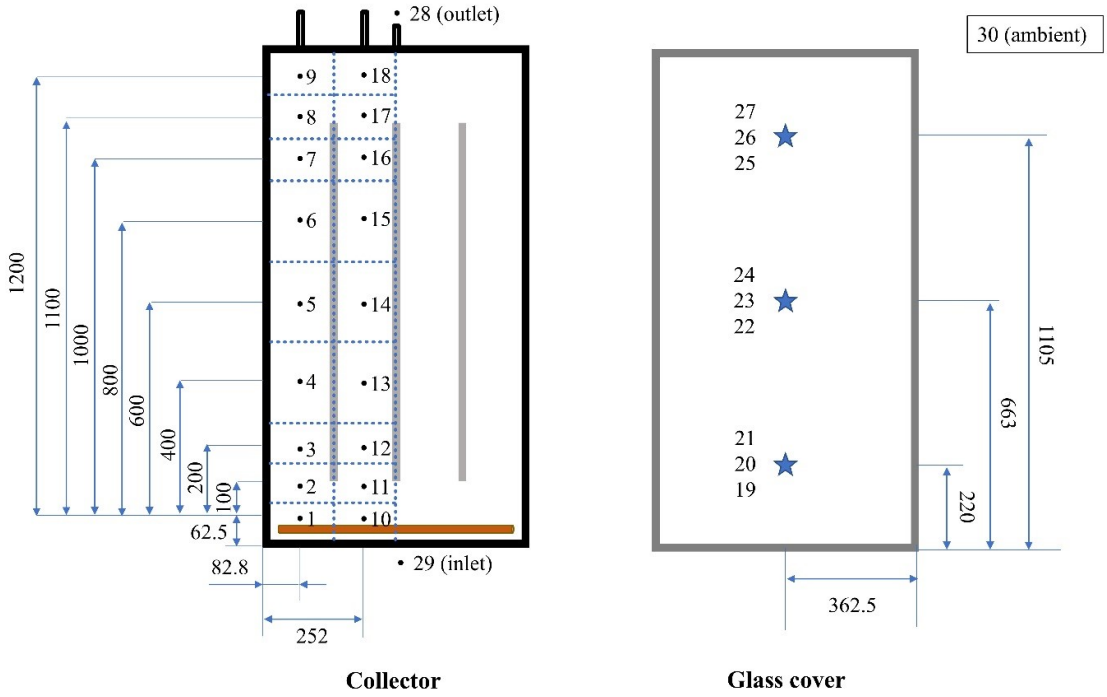

Figure 3.10: Placement of the thermocouples (numbered 1 – 30) and the associated control volumes (defined by the dotted lines), illustrated using the finned design

To achieve the necessary spacing and placement of the thermocouples, polycarbonate tubes with an external diameter of 12 mm and an internal diameter of 8 mm were used. With a high resistance to heat deformation, these rods can withstand the temperatures reached inside the water body and retain their shape. However, they bowed due to their length (1.5 m) and had to be supported to ensure they measured the water temperature in the centre of the control volumes. This was done using plastic supports as shown in Figure 3.11. The supports were kept as small as possible to not disrupt the internal flow dynamics. Figure 3.11 also shows the thermocouples inserted

in the rods. Small holes were drilled into the rods for each thermocouple, so the tip was exposed to the water, and they were secured with silicon.

Figure 3.11: Thermocouples inserted into polycarbonate tubing to keep them stable within the water body. The photo on the right shows the thermocouple placement inside the baffled tank, the rods supported with small plastic supports

3.2.3.2 SIPs and frame

Given that the aim of the current work is to optimise the ICS design for integration into buildings whilst considering MMC, the ICS system was made to be embedded in structural insulated panels (SIPs) used in warm roof, timber construction. SIPs are a composite building material and consist of an insulating layer of rigid core sandwiched between two layers of structural board. The board can be sheet metal, plywood, cement, magnesium oxide board (MgO) or oriented strand board (OSB). The core, either expanded polystyrene foam (EPS), extruded polystyrene foam (XPS), polyisocyanurate foam (PIR), polyurethane foam (PUR) or composite honeycomb (HSC). Pitched SIP roofs generally consist of different layers, illustrated in Figure 3.12.

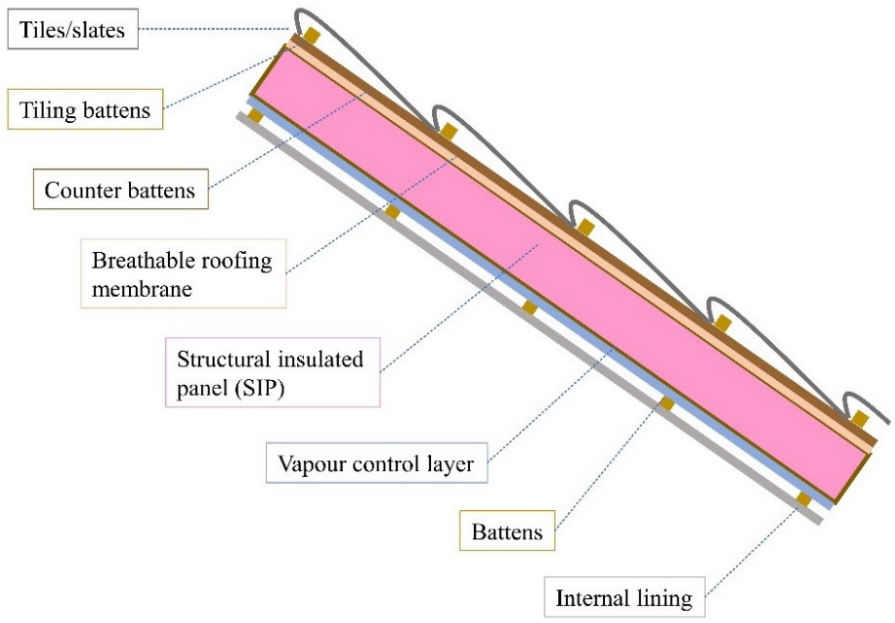

Figure 3.12: General composition of a SIP roof

Experimental testing of the new design configurations, finned and baffled, began in the summer of 2017. During the initial stages, the systems were mounted in custom-made wooden frames lined with 40 mm Celotex insulation. In the spring of 2018, the systems were incorporated and tested in SIPs Eco Panels. Figure 3.13 shows the initial collector set-up, with the wooden frame, compared to the final set-up, embedded in the SIP. The wooden frame was painted with black, weather-proof paint to help it withstand the elements and the SIPs were coated with a weather-resistant membrane; Wraptite. The same glass cover was used for both set-ups.

Figure 3.13: Pictures of the empty frame (top-left) and empty SIP (top-right), showing the different extent of insulation. The ICS collector in-situ is shown in the frame (bottom-left) and the SIP (bottom-right)

Changing the supporting frame, specifically the level of insulation, is presumed to have a significant impact on the heat lost from the back and sides of the collector. The thickness of the surrounding insulation is different (122 mm for the SIP with integrated ICS versus 40 mm Celotex) as well as its thermal resistance. The heat-loss coefficient of each set-up was therefore calculated and the contribution to heat loss reduction quantified (see Chapter 4).

3.2.3.3 Rig set-up

The finned and baffled ICS systems were constructed on the roof of Edinburgh Napier University, adjacent to the custom-built solar lab. The collectors were mounted at a 35° angle of inclination and the absorber surface was oriented due south-east, approximately 143° from north. The collectors could not be exactly south-facing due to the orientation of the university buildings and the location of the Solar Lab (Figure 3.14).

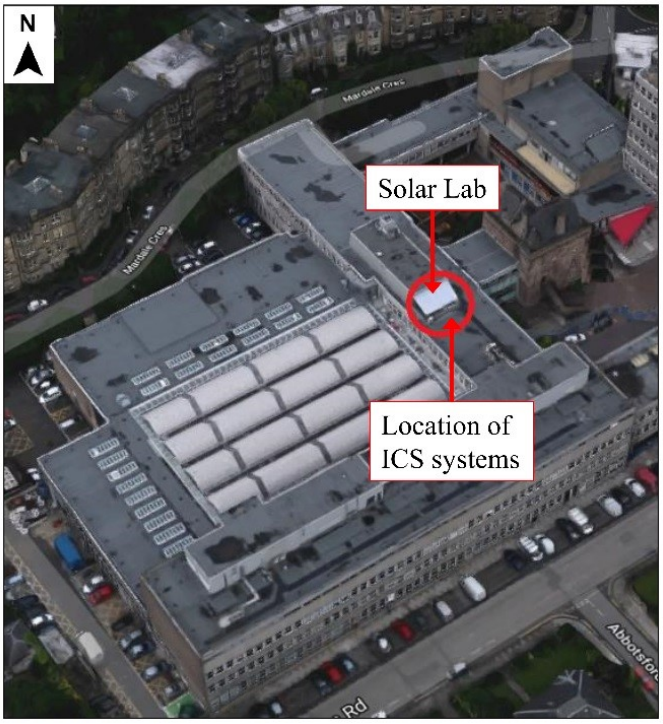

Figure 3.14: Location of the Solar Lab on the roof of Edinburgh Napier University. Picture is oriented north to illustrate that the location of the ICS system is not fully south facing. Screenshot adapted from Google Earth (2018)

Bringing together the aforementioned components, each ICS design configuration was placed in its insulated enclosure, i.e. wooden frame followed by SIP, and covered with a glass lid. This glazing created the necessary air gap that aims to reduce the convective loss of heat from the absorber plate. Based on a previous optimisation study by Henderson et al. (2007), this air gap was set at 35 mm. All pipework to the collector was insulated to combat possible freezing in the winter months. The experimental rigs were then set at an angle (θ) of 35°, again based on previous optimisation studies (Birley et al., 2012; Henderson et al., 2007), using a braced, wooden supporting frame. Figure 3.15 provides a simple illustration of this set-up, pictures of the rig in-situ are shown in Figure 3.13.

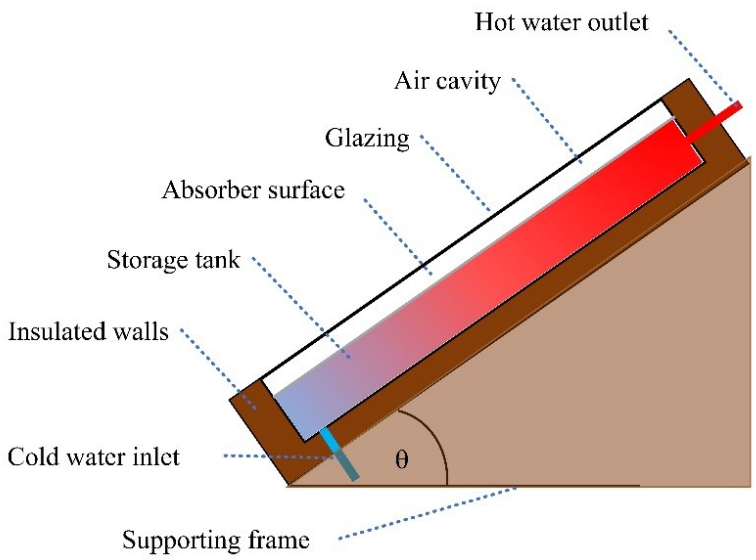

Figure 3.15: Schematic representation of the ICSSWH system rig installation

The thermocouples, described in Section 3.2.3.1, and the solar pyranometer were connected to the Grant data loggers used for the thermocouple calibration and set to log at 1-minute intervals (Figure 3.16). This time interval was chosen so that small scale temperature changes occurring at each draw-off could be monitored. The weather station logged the wind speed and direction as well as ambient air temperature, as a back-up and to ensure the readings corresponded with the allotted thermocouple.

Figure 3.16: Location of the thermocouples, connected to the data logger, entering the collector and the insulated hot-water outlet pipe

For the incoming cold water, both collectors were fed from the same mains tap inside the Solar Lab, a Y-shaped connector split the pipe into two and each fork was connected to a collector. A solenoid valve, placed before the fork in the inlet pipe

(closest to the tap), controlled by a pre-programmed timer, allowed cold water to flow into the collectors under mains pressure at the defined draw-off times (see Section 3.2.4). This incoming cold water forced out a volume of water from the hot-water outlet pipe of each collector, which was permanently open to mitigate any pressure build-up in the tank and allow a passive flow regime. The volume of each draw-off was determined by the length of time the solenoid valve was open for and the balance across the tanks was achieved using ball valves on each fork of the inlet pipe. Figure 3.17 shows the various connections and valves used to regulate the draw-off as well as the thermocouple monitoring inlet water temperature (Figure 3.17[b]).

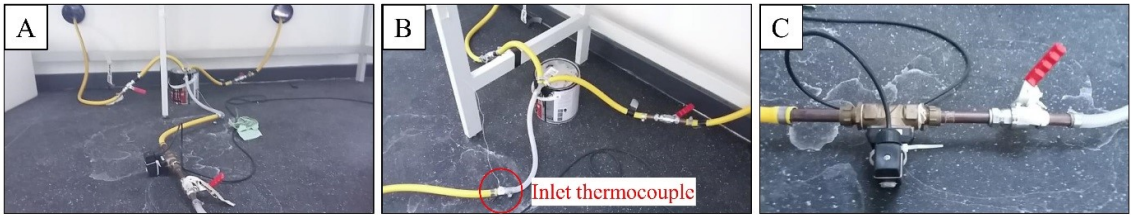

Figure 3.17: Pipework and valves required to control the cold-water input; (a) all pipework and connections between the mains water tap and the collectors, (b) Y-shaped connector to split the incoming cold water across the two collectors and ball valves to balance the flow rate, (c) solenoid valve to control draw-off timings and a ball valve to regulate the flow rate

A seasonal testing methodology was employed and is outlined in Section 3.2.5. It incorporates extended field experiments running from July–December (2017) and April–July (2018), evaluating the finned and baffled designs under different heat retention methods. A full years' worth of data was hoped for, however, due to a variety of factors (explained in Section 3.2.6) this was not possible. Three testing configurations were chosen; the base collector designs to evaluate the performance of the fins versus the baffle plate, additional insulation covering the top third of the absorber plate to retain heat in the hottest portion of the water body, and a night cover to prevent radiative heat losses during the non-collection period.

Based on the extensive literature review, additional insulation and a night cover were chosen due to their relative simplicity, ease of application and demonstrated performance improvement (Chaabane et al., 2014; Kumar and Rosen, 2011a; Smyth et al., 2003; Souza et al., 2014; Swiatek et al., 2015). Of the design factors reviewed these

methods offered the simplest potential solution at the lowest cost and effort/adaptation to the base design. By applying these heat retention methods to an experimentally validated system, their ability to improve heat retention, and therefore overall thermal performance, can be quantified and corroborated against existing studies. Additionally, these simple modifications have the potential to improve the life cycle impact of these systems. By improving the thermal performance, they can provide more energy to the end user thus further offsetting the use of conventional energy sources.

The insulation used to insulate the top third of the absorber tank is 10 mm Spaceloft®, a flexible, nanoporous aerogel blanket produced by Aspen Aerogels®. This was used due to availability and its superior thermal resistance. Table 3.5 shows the thermal properties of various types of insulation, highlighting the thicknesses required to achieve the minimum U-value needed for a rooflight on a pitched roof (for domestic homes in Scotland, Figure 3.18). Aerogel materials demonstrate the highest thermal resistance but are also the most expensive, by a significant margin. Celotex TB4000 appears the best choice when balancing insulation thickness and cost. That is the reason this material was chosen to line the original wooden frames before the introduction of the SIPs. Transparent insulation materials (TIMs) were not considered due to their high cost.

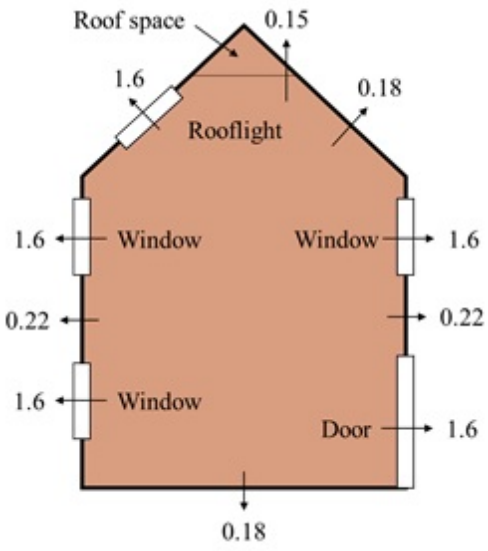

Figure 3.18: The U-values for building elements of the insulation envelope, adapted from Building Scottish Standards (2013)

Table 3.5: Matrix of different insulation materials, their R-values at different thicknesses (calculated from their thermal conductivity, k), the thickness required to achieve the minimum U-value for a roof-light and the price per square meter

Material	Thickness (mm)	k (W/m·K)	R-value (m^2K/W)	Thickness req. (mm)	Price (£/m^2)
ThermaBlok® Aerogel	10	0.015	0.714	21	250.51
	20		1.429		501.02
Aspen Aerogel Spaceloft®	10	0.014	0.67	23	35.09
	20		1.33		71.30
Kingspan TR27 Thermaroof	10	0.025	0.4	38	10.52
	20		0.8		
Kingspan TP10 Thermapitch	10	0.022	0.44	34	7.97
	20		0.88		
Rockwool Thermal Roll	10	0.044	0.23	66	4.98
	20		0.45		
Earthwool Universal Roll	10	0.044	0.23	66	2.05
	20		0.45		
Isover Cladding Roll	10	0.04	0.25	60	2.93
	20		0.5		
Celotex TB4000	10	0.022	0.45	33	5.58
	20		0.91		

For the night cover, Airtec aluminium foil bubble insulation was used due to its low cost (approximately £1.66/m^2) and minimal impact on the thermal performance of the system (R-value is 0.124 m^2K/W). The aim of the night cover was to minimise radiative heat losses from the absorber plate/glazing to the sky. It was applied to the glazing aperture like a roller blind and ran down two aluminium channels to protect it from the wind, as shown in Figure 3.19.

Figure 3.19: Night cover – aluminium foil bubble insulation secured to a roller blind and held in place, once rolled down, by aluminium channels

3.2.4 Draw-off

To truly evaluate system performance, the ICS designs must be subject to realistic and practical use. To achieve this, a standardised, representative draw-off profile was applied to the systems. A number of organisations and research groups have reviewed domestic water consumption in the UK and Europe (Energy Saving Trust, 2008; European Commission, 2002; Spur et al., 2006) and have developed profiles mimicking average domestic hot water (DHW) consumption. As it is impossible to define a profile that caters to the daily hot water and energy requirements of every individual, average profiles give a fair estimation of demand and can be used for system testing and comparison of performance. There are several DHW profiles that are commonly used; however, it is important to choose one that suits the system under evaluation and that the same profile is applied to all systems under comparison. An appraisal of these studies can be found in Chapter 2 and from this, the profile that was adhered to throughout this work was chosen.

The CEN and CENELEC EU reference tapping cycle 1, detailed in Table 3.6, was chosen as it appeared to be the most realistic for the system under evaluation, providing 52 l/day of hot water. The 48 litre ICSSWH system in the current study is assumed to provide DHW for one person, therefore, a light draw-off pattern would be the most suitable as a single occupancy dwelling is unlikely to use volumes as great as those quoted for heavier demand profiles.

Table 3.6: Summary of the CEN and CENELEC EU reference tapping cycle 1. *Energy is calculated based on a cold-water temperature of 10°C

EU reference tapping cycle 1					
Draw-off	*Start time*	*Energy (kWh)**	***Volume (l)***	*Type*	*Desired T (°C)*
1	07:00	0.105	3	Small	40
2	07:30	0.105	3	Small	40
3	08:30	0.105	3	Small	40
4	09:30	0.105	3	Small	40
5	11:30	0.105	3	Small	40
6	11:45	0.105	3	Small	40
7	12:45	0.315	6	Dish wash	55
8	18:00	0.105	3	Small	40
9	18:15	0.105	2	Clean	55
10	20:30	0.420	8	Dish wash	55
11	21:30	0.525	15	Large	40
	Total	**2.1**	**52**		

Once the draw-off profile was chosen and a delivery mechanism applied (see Section 3.2.2.4, the volumes required had to be equal across the two tanks for each draw-off volume as well as the daily total thus it was necessary to calibrate the systems. Figure 3.20 and Figure 3.21 plot the calibration curves for the ICS systems for both rig arrangements, i.e. the initial insulated wooden frame and the upgrade to SIPs, respectively. Figure 3.20 and Figure 3.21 show that the draw-off periods are significantly different between the two, yet the volumes remain the same. Using a linear regression analysis, the R^2 value suggests that the calibration curve conforms well to the observed data, ranging from 97% – 99.6%. Spot checks were also done throughout the testing phases to ensure that equal volumes across the systems were being drawn off. These spot checks were in line with the calibration curves thus it was assumed that all other, non-checked, draw-offs were also accurate.

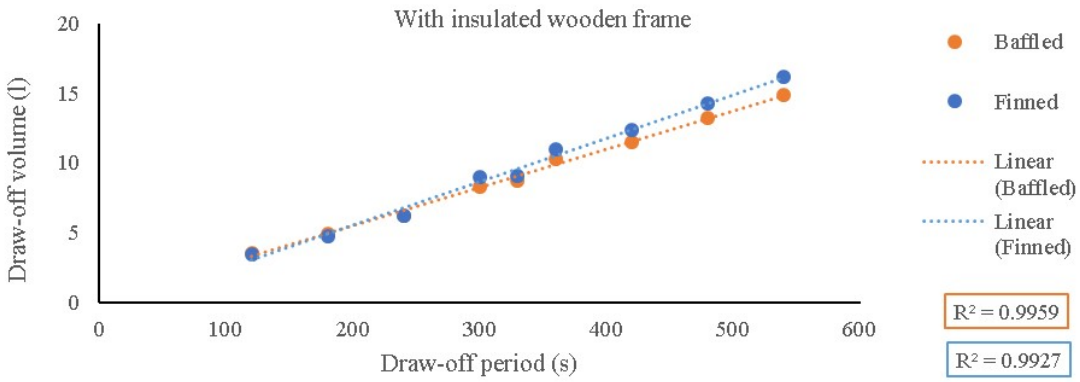

Figure 3.20: Calibration curve for the ICS systems in the insulated wooden frames, using a Grasslin Digi 20 Series timer to open the solenoid valve

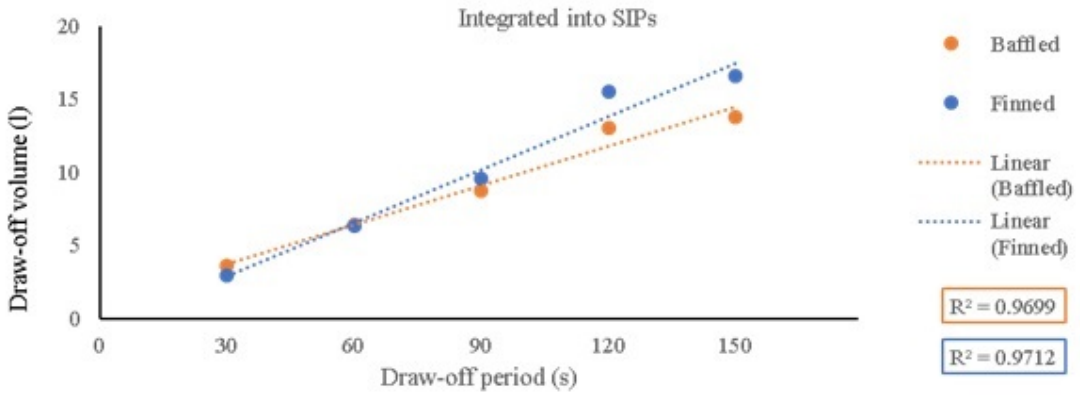

Figure 3.21: Calibration curve for the ICS systems integrated into the SIPs, using an Arduino microcontroller to open the solenoid valve

Table 3.7 provides more detail for the calibration test conducted for the ICS systems when integrated into the SIPs. Tabulated is the programmed time steps, in 30 second increments, the time taken for the water to start flowing from the outlet pipe, the length of time water flowed for, the expected volume for each draw-off and the actual volume drawn-off for each system. The different flow rates for ICS systems in the insulated frame versus integrated in the SIPs does not significantly impact upon the performance of the system. When the systems were integrated into the SIPs it was very difficult to balance the draw-off across the baffled and the finned collectors. The initial low flow rate of 1.5 l/min and timing programme, using the Grasslin Digi 20 Series timer, could not be followed as there was insufficient pressure to allow the systems to equilibrate. Therefore, the inlet water pressure was increased to generate a flow rate of 6 l/min and the timing programme had to be controlled by an Arduino microcontroller as it could

work at 30 second intervals as opposed to 1 minute. Despite the differing flow rates, the draw-off volumes remained the same which is the most important consideration with batch-style solar water heaters (SWHs).

Table 3.7: Calibration of the ICS systems integrated into the SIPs, using an Arduino microcontroller

Draw-off	**Time valve open for (s)**	**Time till flow starts (s)**		**Flow period (s)**		**Expected volume (l)**	**Actual volume (l)**	
		Finned	*Baffled*	*Finned*	*Baffled*		*Finned*	*Baffled*
1	30	9	9	26	29	3	3	3.7
2	30	9	9	27	31	3	2.9	3.5
3	30	9	9	28	31	3	2.9	3.5
4	30	9	9	28	32	3	3	3.6
5	30	9	9	27	31	3	3	3.6
6	30	9	9	27	30	3	3	3.6
7	60	9	9	56	56	6	6.3	6.4
8	30	8	7	28	30	3	3	3.6
9	30	9	9	27	30	3	2.9	3.5
10	90	8	8	85	93	9	9.4	8.8
11	150	9	9	145	145	15	16	13.5
						Total	**55.4**	**57.3**

With distributed SWH systems, e.g. FPC and ETC, flow rate is very important as it influences the heat gain and transfer to the storage tank. ICS systems are essentially a bulk water storage tank thus for every draw-off, a mass of water is removed as opposed to a constant slow and steady flow of water, so flow rate has a minimal effect.

3.2.5 Seasonal tests

An objective of the current research is to measure the impact/improvement the external heat retention methods have on thermal efficiency under ambient, transient conditions. As there are only two collectors, these design factors need to be applied in turn, they cannot be tested concurrently. This poses the problem of seasonal variability and how to test these factors under the same conditions so that any results will be comparable. No two days are the same, especially in a Scottish climate, therefore certain assumptions

must be made. The three testing phases – base (as designed), additional insulation, and a night cover – were applied using a round-robin method for three of the four seasons. The actual time plan is outlined in Table 3.8. At the start of this research, the intention was to gather a year's worth of data. However this was not possible, as discussed in Section 3.2.6.6.

Table 3.8: Actual timetable for the experimental testing phases. *Each phase was run for 7–10 days over autumn months

Season	Month	Base (as designed)	Additional insulation	Night cover
Summer	May	✓		
	Jun		✓	
	Jul			✓
Autumn	Aug*	✓		
	Sep*	✓	✓	✓
	Oct*	✓	✓	✓
Winter	Nov	✓		
	Dec			
	Jan			

The data used for allocating the seasons was taken from NASA Surface meteorology and Solar Energy (SSE) Release 6.0 Data Set (NASA, 2008). The global, direct and diffuse radiation values from 22-year monthly average data (July 1983 – June 2005) were plotted to identify periods of similar insolation levels (Figure 3.22). This data is consistent with other studies that review the variation in solar radiation at different latitudes and seasons (Muneer, 1999 [in Muneer et al., 2000]; Burgess, 2009). It is apparent that May, June, and July are well defined with relatively stable insolation levels, as are November, December, and January so these were labelled the "summer" and "winter" months, respectively. Therefore, during these months the testing methodology sees each experimental phase tested for an entire month (Table 3.8). It is assumed that the data gathered for one month would be representative of the whole season due to the consistent insolation levels.

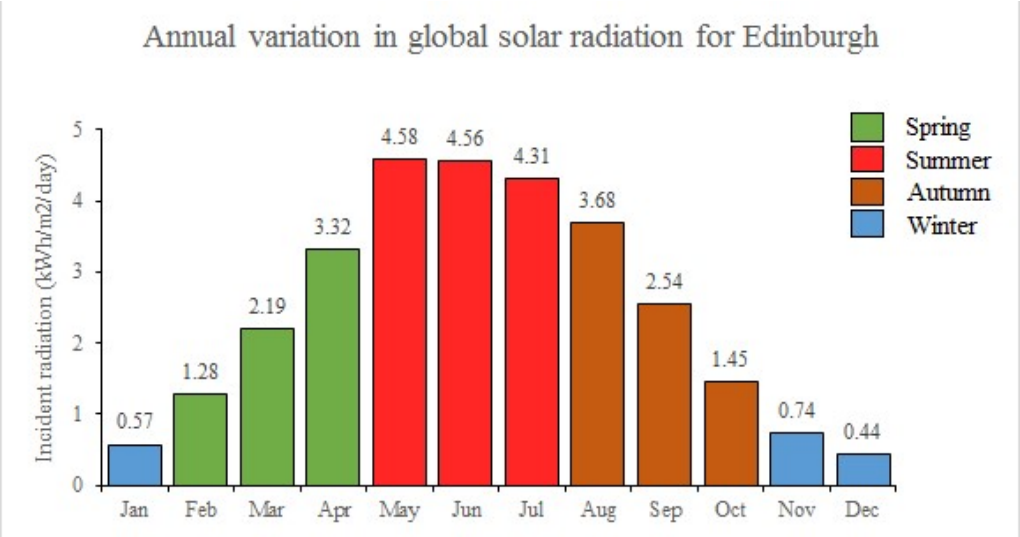

Figure 3.22: Annual variation in global solar radiation for Edinburgh, using data taken from NASA Surface meteorology and Solar Energy (SSE) Release 6.0 Data Set (2008)

During the remaining months, labelled “spring” and “autumn”, solar radiation is highly variable. Therefore, one month is not representative of the environmental conditions for the whole season and to run each set-up for a month would have a heavy bias, especially for the phases at the beginning of autumn. Therefore, during this season, all three design conditions were tested each month, for 7–10 days each, to ensure the data is as comparable as possible. It is assumed that the 7–10-day period is representative of the whole month.

Before each testing phase, the ICS systems were flushed with fresh cold water to ensure that each round of experiments began with the same water temperature in the storage tank to keep variables to a minimum. The systems were reset at roughly the same time of day. For the testing phase involving the night cover, the application and removal times were determined from the results of the base (as designed) testing phase within each round-robin. When the collection period began and ended during this base phase, i.e. when the water in the storage tank began to heat up or cool down, it was assumed that these times would be the same for the night cover phase. For summer months, removal times were determined as 08:00 hours and application times were 17:00 hours. Winter times were 10:00–14:00 hours and spring and autumn were 09:00–16:00 hours.

3.2.6 Experimental considerations

In any form of research, it is important to highlight potential errors that can occur due to the methodology employed and assumptions made throughout the work.

3.2.6.1 Design and construction

Based on previous work by Birley et al. (2012), it was identified that a new system should be constructed using the lessons learned from previous iterations as well as from the literature. Regarding the manufacture of the finned collector, the fabricator was unable to weld along the entire length of each fin as it would compromise the structural and mechanical integrity of the absorber plate. Therefore, they attached the fins to the underside of the absorber plate with three spot welds. This meant that, although the entire length of the fin was in contact with the absorber plate, the conductive transfer of heat may have been reduced. Optimising the way the fins are attached to the absorber plate would result in greater collector performance.

3.2.6.2 Experimental equipment – assessment and calibration

A few problems arose with the data loggers and thermocouples. Upon insertion into the tanks, via the pipes extending from the storage tank, a couple of the junctions were damaged resulting in "Open Circuit" readings on the data loggers. Also, during the experimental tests, the logger monitoring the baffled tank developed a fault whereby every even-numbered thermocouple in the first 4 ports began to record erroneous data. This logger was replaced and data collection continued. For the ambient temperature readings, weather station data was used as it had previously been calibrated against the logger data when it was working.

3.2.6.3 Experimental error

The experimental temperature measurements were made using 30 K-type thermocouples, discussed in Sections 3.2.2.1 and 3.2.3.1. These thermocouples have an associated error of ±0.5°C meaning that, for any given temperature reading, the actual

value may be 0.5°C higher or lower than that recorded. Therefore, when comparing data across the ICS systems, this tolerance must be considered when discussing experimental results. This is particularly important where differences are close to this margin of experimental error as interpretation of the results can only be considered indicative, not conclusive.

3.2.6.4 Experimental testing

There were several considerations and assumptions associated with the experimental testing phases, not least the location of the Solar Lab. Given the geometry of the Merchiston campus, shading was a significant issue for portions of the day, especially in wintertime due to low solar angles. The level of overshadowing in winter meant that the collectors were receiving little, if any, solar insolation thus it was very difficult to combat freezing. Therefore, the data collected could be considered a worst-case scenario for system performance, but it is also an important factor for domestic buildings which will often suffer from shading. To determine the detrimental extent of this overshadowing, a solar shading analysis of the surrounding buildings within the location was performed using IES-VE SunCast and Model Viewer; selecting the Edinburgh weather file and CAD drawing of Merchiston campus. Figure 3.23 presents an illustration of these shading profiles for the summer and winter solstices and autumn equinox. Partial shading occurs in the morning during summer and autumn and the collectors are completely shaded by the end of the day. In the winter months, the collectors experience almost no incident solar insolation. Spring was excluded as it follows the same pattern as autumn.

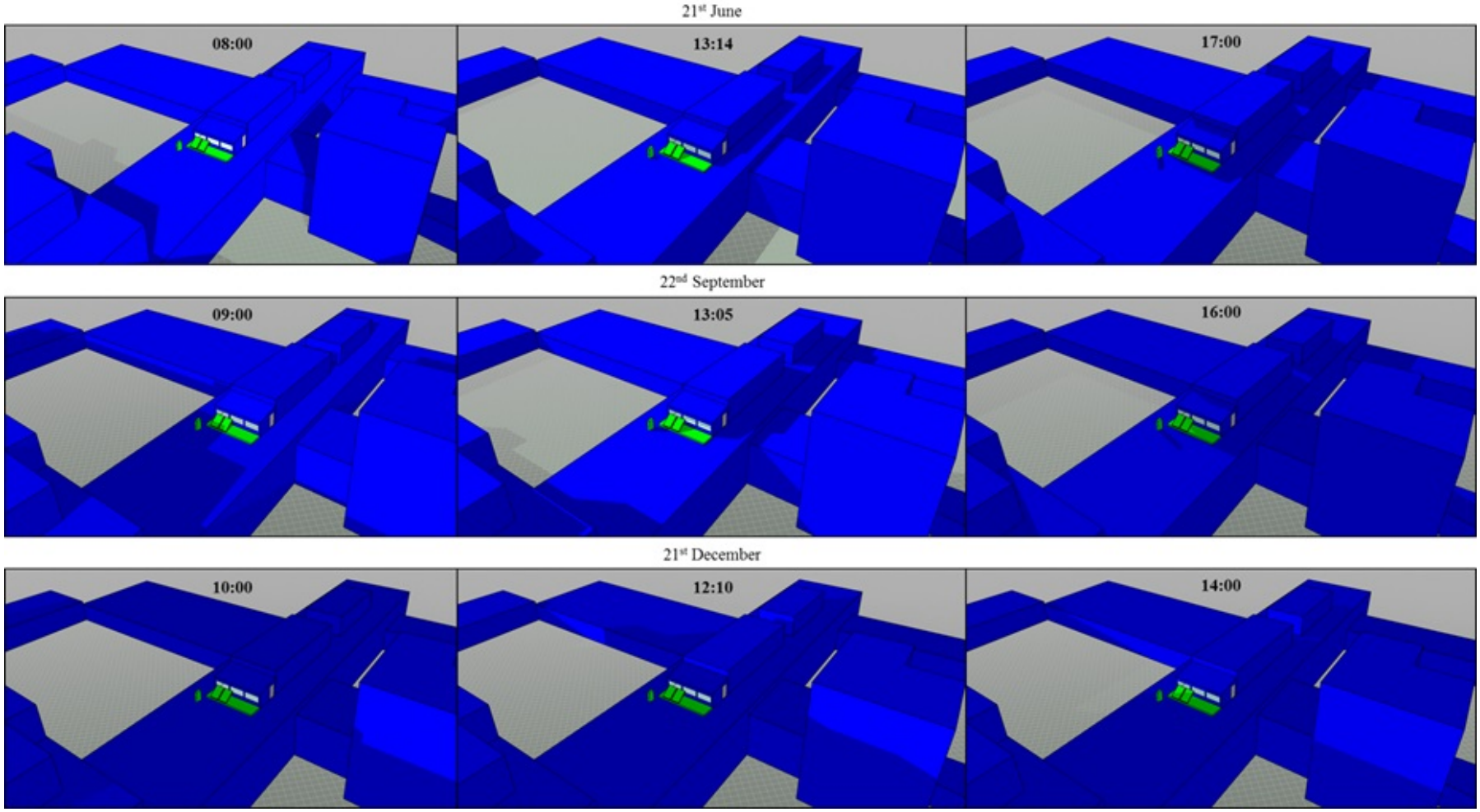

Figure 3.23: Shading profiles of the solar lab and ICSSWH locations for the summer solstice (21st June), autumn equinox (22nd September) and winter solstice (21st December). Three times of day are assessed; the start and end of the collection period for each season and solar noon for each day presented. The spring equinox is not included as it is very similar to autumn. Note, the stand-alone object is a ventilation unit that is on the roof

A further caveat is the variable nature of nature. For the end-use functionality of a system to be assessed, it must be tested under practical application and transient conditions. This research has no lab-based experimental component, purely empirical field testing. Given the variable nature of outdoor tests, a methodology for comparable testing is difficult and must be considered when evaluating the collected data, certain assumptions and limitations must be detailed. As discussed in Section 3.2.5, the break-down of the seasonal testing methodology was chosen to give as comprehensive, robust and comparable results as possible. Only so many variables can be controlled when testing in an outdoor environment and the methodology presented aimed to limit the margin for error to an acceptable level.

The transition from the insulated frame to the SIP resulted in a delay to experimental testing and great difficulty in calibrating draw-off. The draw-off equilibrated relatively easily when the ICS systems were in the insulated frames and a low flow rate could be maintained, allowing the thermocouples to pick up on temperature changes given their 1-minute logging intervals. However, when integrated into the SIPs, drawing off water at low flow rates resulted in highly variable flow across the two tanks; the baffled tank would run for a short time and stop, whilst the finned collector would continue. This phenomenon occurred due to a thermosyphon effect within the system which was combatted by creating a thermosyphon break so that, when flow ceased, the pipe would suck in air instead of syphoning out excess water.

Another consideration of the switch to SIPs is the impact on the thermal performance. Given the greater amount of insulation provided by the SIP over the frame, the heat retention attributed to the design factors across this transition must be calculated carefully. The heat loss coefficient of each rig set-up, i.e. frame and SIP, needs to be defined so that any contribution to performance can be decoupled from that of the heat retention methods.

3.2.6.5 Draw-off

To calibrate the draw-off, the tests were run back-to-back. For example, the solenoid valve was open for 1 minute, closed for 1 minute, opened for 2 minutes, closed for 1

minute, open for 3 minutes, etc. This was not representative of how the system would perform under practical application since it did not have time to settle as it would between the programmed draw-off events. This would potentially cause a bias in the calibration. However, the two systems need to consistently draw-off the same volume as each other and the flow needs to be balanced across them. Monitoring the draw-off following the profile used throughout testing would be impractical due roof access restrictions, therefore, this method was deemed acceptable. Also, random spot checks throughout the testing phases ensured the draw-off volumes were in line with the calibration curve.

3.2.6.6 Seasonal tests

The seasonal testing plan outlined in Section 3.2.5 hoped to give a comprehensive, year-long view of the practical performance of the ICS systems and chosen heat retention methods. However, an unfortunate setback occurred over winter (2017–2018) with the baffled tank reaching freezing temperatures. The water in the finned tank remained above 0°C during this time but that is most likely because the collector received sufficient sunlight to defrost. Due to the position of the baffled collector and the shading issue mentioned previously, solar radiation was not incident on the absorber plate (Figure 3.23). It was deemed prudent, to prevent damage to the systems from freezing, to drain both the collectors for the remainder of the winter period. Unfortunately, owing to the harsh and prolonged winter conditions experienced in the early months of 2018, it was not possible to resume testing.

At this stage, the SIPs were being prepared by Sips Eco Panels and it was decided to postpone testing until the ICS systems were integrated in the panels. However, as previously mentioned, the transition to the SIPs delayed testing for over a month due to problems with calibrating draw-off. Therefore, the vision of a years' worth of data was cropped to that presented in Section 3.2.5, Table 3.8. The base configuration has the most data with measurements for all seasons but spring. The additional insulation and night cover configurations, however, were only tested through summer and autumn months.

Using the data gathered from these seasonal testing phases, the annual energy provided by each system was extrapolated. This annual operational energy was then used to estimate the energy savings each system could make over their useful life; later used to determine their sustainability. Additionally, the embodied energy required to produce, maintain and dismantle the system is equally important to consider. Therefore, the following section outlines the methodology employed for the comprehensive life cycle assessment that was carried out for the ICSSWH systems under investigation.

3.3 Life cycle assessment

Passive systems are vital to reduce energy demand in the built environment as well as for future energy security and to truly evaluate the sustainability of such systems, it is important to compare the operational energy savings against the embodied energy. Scottish weather is not as forgiving as a Mediterranean climate, therefore, the energy benefits of a SWH system are likely to be lower than in other, hotter, parts of the world, despite the greater need for heat. Therefore, the lifecycle is important to be able to make any claim about the overall benefits of a system; operational energy must offset embodied energy for it to be considered sustainable and to actively contribute to Scotland's climate targets.

Chapter 2 reviewed the literature surrounding LCA and ICSSWHs, evaluating the numerous methods, software and databases used. Many studies consider the ISO14040 (2006) standard the procedure to follow and that methodology is also adhered to in this work. Based on the ISO 14040 framework, an LCA consists of four main steps; goal and scope definition, life cycle inventory (LCI), life cycle impact assessment (LCIA), and interpretation of results. These steps are all interdependent; the goal and scope define the LCI and LCIA in terms of what is included in the analysis and the type of analysis, for example, linear or circular. The following sections outline these four steps and how they apply to the current study.

3.3.1 Goal and Scope

The goal and scope include defining the system boundary, the functional unit (to allow comparability and reproducibility), and the depth and breadth of the assessment. The goal of the present research is to determine the environmental impact of an ICSSWH under different design configurations, with the heat retention methods, from a linear versus circular economy perspective. To make the system more attractive from an LCA point of view the absorber plate can be detached from the storage tank. This greatly improves the collector's recovery potential as they can be cleanly separated and reused. This design aspect was underpinned by circular economy principles.

The FU is defined as one ICSSWH unit designed to provide domestic hot water for a single occupancy dwelling, based on a consumption of 52 l/day, over a service life of 20 years. One FU includes the collector and associated fittings but pipework to and from the collector is excluded as it is assumed that this is already in place before its installation. The collectors have been considered with both the insulated frame and the SIPs. When the collectors are placed in the insulted frame, this becomes part of its FU, but when the collectors are integrated into the SIPs this aspect is excluded. The SIP is assumed to be a part of the buildings FU, not that of the ICSSWH. This comparison was done to highlight the benefit of incorporating this system into the building fabric as opposed to securing it on to its surface.

Figure 3.24 illustrates the system boundaries of the current study, in terms of the LCA stages, considering both a linear (Stages A–C) and circular (Stages A–D) analysis. The difference between the baffled and finned systems will have an impact across the whole lifecycle; Stage A will depend on the embodied carbon and energy associated with materials, Stage B will depend on the operational performance throughout the useful life of the collectors, and Stages C and D will depend on the recycle potential of the different materials. The following section details the materials and fabrication process flows involved in the manufacture of the collectors.

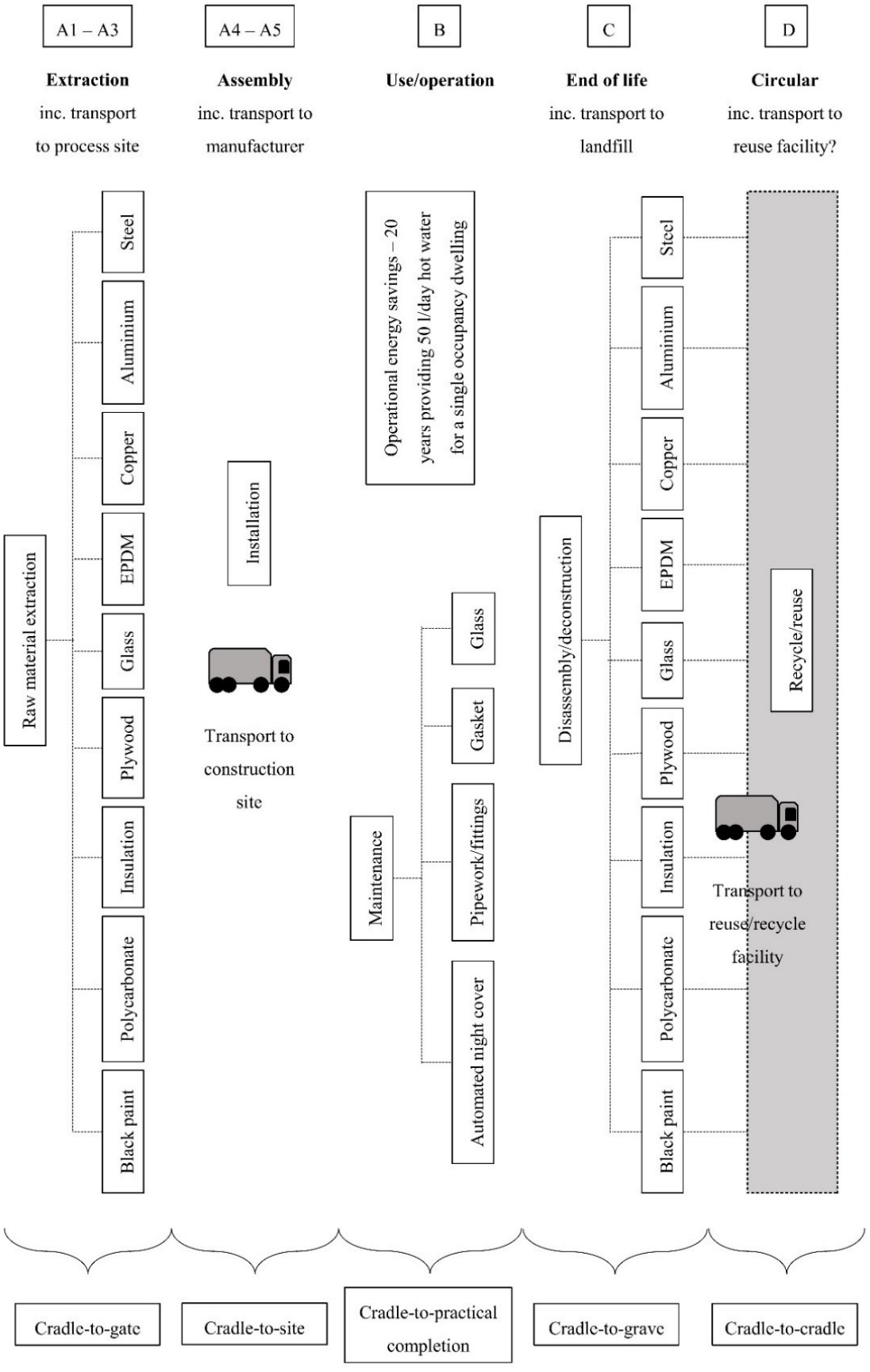

Figure 3.24: System boundaries of the present analysis for both a linear and circular approach. The circular aspect of the LCA is represented in the grey box

3.3.2 Life cycle inventory

The LCI brings together all the materials used in the construction of the product and the creation of the FU. The fabrication process flow for the ICSSWH systems is shown in Figure 3.25, considering both the baffled and finned designs and whether it is in a wooden frame or integrated into a SIP. The LCI presented in Chapter 5 shows the quantity and total mass of each component, from which the percentage of the overall product weight was calculated. The ISO standard states that any component whose mass is less than 1% of the overall weight has a negligible effect in the analysis and can thus be neglected. However, to disaggregate the results as fully as possible and generate a more transparent and comprehensive LCA, a cut-off criterion of 0.5% has been applied for this study.

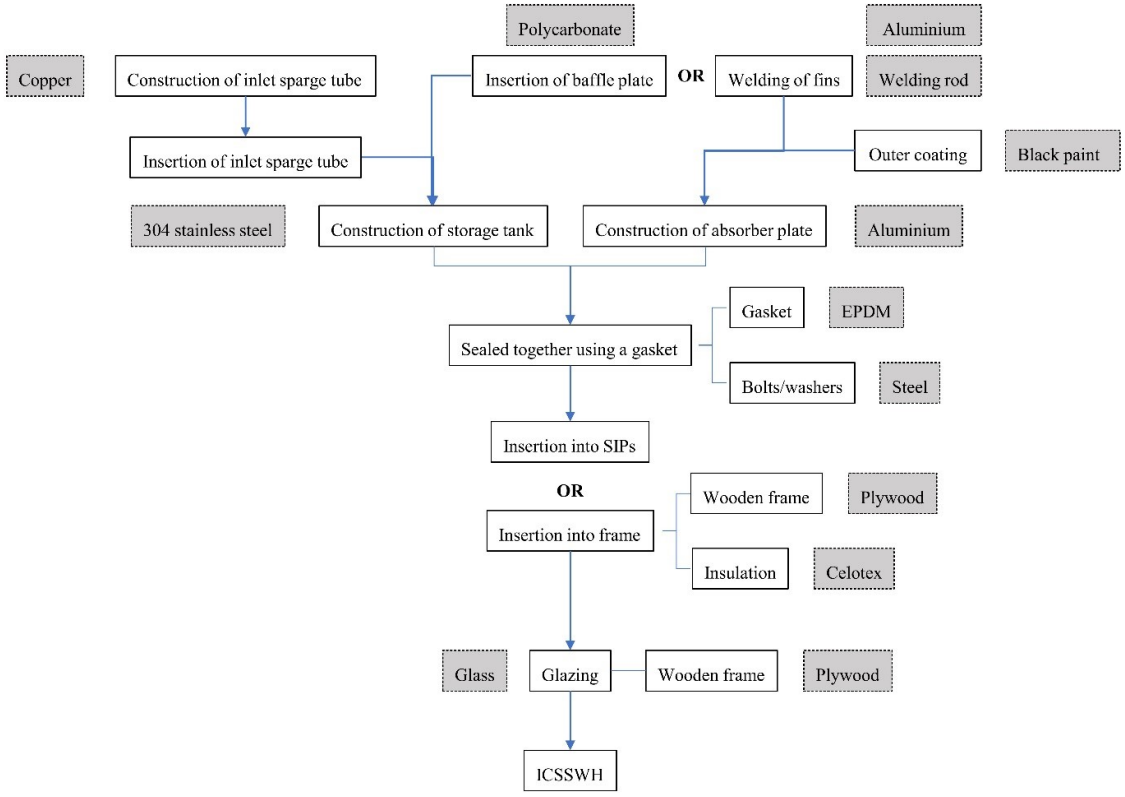

Figure 3.25: Fabrication process flow for the ICSSWH, considering both baffled and finned designs and a wooden frame or SIP. Necessary input materials are shown in the grey boxes

3.3.3 Life cycle impact assessment

The LCIA allows the quantification of potential environmental impacts in terms of embodied energy and operational energy, based on the data collected for the LCI stage. Embodied energy is the energy expended throughout the systems useful life (i.e. from sourcing raw materials to the deconstruction of the FU) and is added to give a positive impact on the total energy; the energy needed. Operational energy, which is the useful energy generated by the FU during its useful life, is added to give a negative impact on total energy; the energy generated by the system.

An LCIA of the ICSSWH FUs has been done for both operational and embodied energy, considering both a linear and circular economy to determine the positive (or negative) impact of the final supplementary stage of the LCA, Stage D. The ICSSWH system is being compared against itself under the different design configurations and with the three different heat retention methods.

The LCA tool used in the analysis is SimaPro v 9.0 equipped with the Ecoinvent database v3.5, using European data. SimaPro is the most commonly used LCA software package and is fully compatible with the ISO standards LCA methodology used for this research (PRé, 2016). The impact assessment method used to determine the embodied carbon was IPCC 2013 GWP 100a (v1.03) and for the embodied energy, the Cumulative Energy Demand (v1.10). To characterise the midpoint environmental impacts and determine the damage to the endpoint impact categories, CML-IA baseline (v3.05) and ReCiPe 2016 Endpoint (H, v1.02) were used, respectively. A discussion of midpoint and endpoint impact categories is provided in Chapter 2, Section 2.4.1. These tools were adopted based on the types of analytical software and databases that are commonly used throughout European studies. The accuracy of the LCA relies on the integrity and applicability of the database used and they are often specific to geographic regions. Ecoinvent is a high-quality database for European studies and the CML and IPCC GWP (100) impact assessment methods provide robust and accurate results (Martínez et al., 2015).

3.3.4 Interpretation of results

Pursuant to the goal and scope of the present LCA, embodied energy and carbon were compared against the operational energy and carbon savings to determine the energy and carbon payback times for all the scenarios listed in Table 3.9. Additionally, other environmental impact categories will be assessed such as, human health, ecotoxicity and resource availability. Alongside this interpretation, sensitivity and uncertainty analyses will be conducted. Sensitivity analysis is a method of measuring the effect that changes in inputs will have on the output, e.g. changing the amount or type of a material or the lifespan of the product (Saltelli et al., 2004).

Table 3.9: Scenarios being evaluated through LCA

Scenario	Configuration	Heat retention method	Frame or SIP	Linear/circular analysis
1	Baffled	Plain (as designed)	Frame	Linear
2	Baffled	Plain (as designed)	Frame	Circular
3	Baffled	Additional insulation	Frame	Linear
4	Baffled	Additional insulation	Frame	Circular
5	Baffled	Night cover	Frame	Linear
6	Baffled	Night cover	Frame	Circular
7	Baffled	Plain (as designed)	SIP	Linear
8	Baffled	Plain (as designed)	SIP	Circular
9	Baffled	Additional insulation	SIP	Linear
10	Baffled	Additional insulation	SIP	Circular
11	Baffled	Night cover	SIP	Linear
12	Baffled	Night cover	SIP	Circular
13	Finned	Plain (as designed)	Frame	Linear
14	Finned	Plain (as designed)	Frame	Circular
15	Finned	Additional insulation	Frame	Linear
16	Finned	Additional insulation	Frame	Circular
17	Finned	Night cover	Frame	Linear
18	Finned	Night cover	Frame	Circular
19	Finned	Plain (as designed)	SIP	Linear
20	Finned	Plain (as designed)	SIP	Circular
21	Finned	Additional insulation	SIP	Linear
22	Finned	Additional insulation	SIP	Circular
23	Finned	Night cover	SIP	Linear
24	Finned	Night cover	SIP	Circular

Uncertainty analysis is carried out in conjunction with the sensitivity analysis, particularly in fields such as environmental assessment, to account for the uncertainty of the inputs so a best estimate value for the output can be evaluated. Sensitivity is determined by calculating system derivatives, i.e. the variation of the inputs and outputs. Uncertainty is commonly achieved through the Monte Carlo method (Saltelli et al., 2004). SimaPro, as a software package, supports both analyses and offers relatively simple Monte Carlo calculations to give an indication of data uncertainty. This has been

used in this research. Sensitivity and uncertainty analyses are important to enhance the robustness of an LCA, providing a realistic range which includes the most probable values as opposed to a single deterministic output (Pomponi, 2015).

3.4 Concluding remarks

This chapter brings together the methodology for both the field experiments and the life cycle assessment. The design and construction of the proposed prototypes was described followed by the assessment and calibration of the equipment used throughout the experimental tests. The rig set up for the field tests and different design conditions was illustrated along with the seasonal testing regime and the calibration of the DHW consumption pattern. Important considerations for the experimental tests were outlined including issues with shading, equilibrating the draw-off across the two systems and the seasonal testing methodology. Finally, an account of the LCA methodology, as defined by the ISO 14040 (2006) framework, that is adhered to throughout this work was presented.

Chapter 4 presents the results of the field experiments, focusing on a comparison of the base configurations, the finned and baffled collectors, the heat retention methods, and the ICS system embedded in an insulated frame versus a SIP.

Fourth Chapter

Field Experiments: Results

The two base configurations under evaluation are a collector with three elongated heat transfer fins and a collector with an internal baffle plate. Fins were shown to improve the efficiency of the collector studied by Garnier (2009). However, the impact of the baffle plate in a collector of this design in a Scottish climate has yet to be assessed. Also, to combat the ongoing issue of night-time heat losses, two additional heat retention strategies are evaluated in combination with the base collector configurations.

This collector design has gradually evolved from its first iteration (Grassie et al., 2006), yet extended field studies have not been completed with the longest testing period being three summer months. This chapter presents the empirical results of extended field tests for both collector configurations. A baseline comparison of the finned and baffled collectors is presented followed by the energy performance of the base configurations. Next, the heat retention methods are analysed in terms of their ability to prevent night-time losses and their impact on the cooling profile within the storage tank. Finally, a comparison between the performances of the collectors in the wooden frame versus the SIP is undertaken. The analytical methods and equations used are stated throughout this chapter. Given that the methodologies and equations specified in standardisation bodies are intended for distributed solar water heating systems, the analysis carried out in this work is based on previous research surrounding integrated solar water heaters.

4.1 Baseline tests

To determine the baseline performance of the two configurations, finned and baffled, both collectors were tested side-by-side under 'no-flow' and 'flow' conditions. 'No-flow' here refers to there being no water draw-off; as these are field experiments, the environmental conditions cannot be controlled and are therefore inherently transient. 'Flow' conditions are experienced when water is drawn from the system and replaced. No heat retention methods were applied for the baseline tests.

4.1.1 Without draw-off

Figure 4.1 and Figure 4.2 show the difference in collector performance without draw-off over a week period and a daily cycle in July 2017, respectively. In Figure 4.1, the collectors are very closely matched with the baffled collector slightly outperforming the finned in terms of peak temperature. When considering cooling and heat retention, the performance is almost identical. The rate at which the bulk water temperature drops is similar in both collectors and is much more rapid when the peak water temperatures during the day were high. The bulk water temperature of the baffled collector is slightly higher than the finned after the cooling period. However, their ability to retain heat is very similar. With a maximum and minimum temperature difference of 2.2°C and 0.8°C, respectively, some values may fall within the range of experimental error (see Section 3.2.6.3) thus the better performance of the baffled collector is indicative, not conclusive.

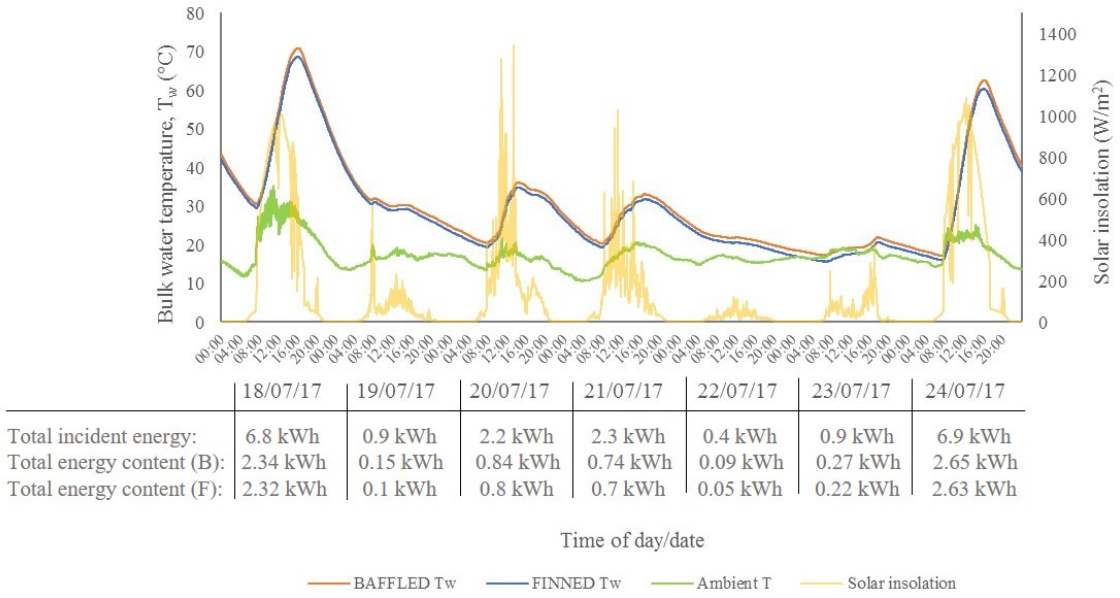

	18/07/17	19/07/17	20/07/17	21/07/17	22/07/17	23/07/17	24/07/17
Total incident energy:	6.8 kWh	0.9 kWh	2.2 kWh	2.3 kWh	0.4 kWh	0.9 kWh	6.9 kWh
Total energy content (B):	2.34 kWh	0.15 kWh	0.84 kWh	0.74 kWh	0.09 kWh	0.27 kWh	2.65 kWh
Total energy content (F):	2.32 kWh	0.1 kWh	0.8 kWh	0.7 kWh	0.05 kWh	0.22 kWh	2.63 kWh

Figure 4.1: Comparison of baseline 'no-flow' tests for the baffled and finned collectors over a week period in July 2017. Included is the total daily incident and collected energy to aid the visual representation

Figure 4.2 illustrates the comparative collector performance over a daily cycle on the 18th July 2017. Initially both collectors' bulk water temperatures are approximately 30°C at 07:30 hours. Over the course of the day, as a result of significant solar insolation levels, peak bulk water temperatures of 69°C and 71°C were reached at around 16:00 hours for the finned and baffled collectors, respectively. When considering these bulk water temperatures alongside the average absorber plate temperature for each collector, the same pattern is identified with the absorber plate temperatures being slightly higher than the bulk water during the collection period and lower during cooling.

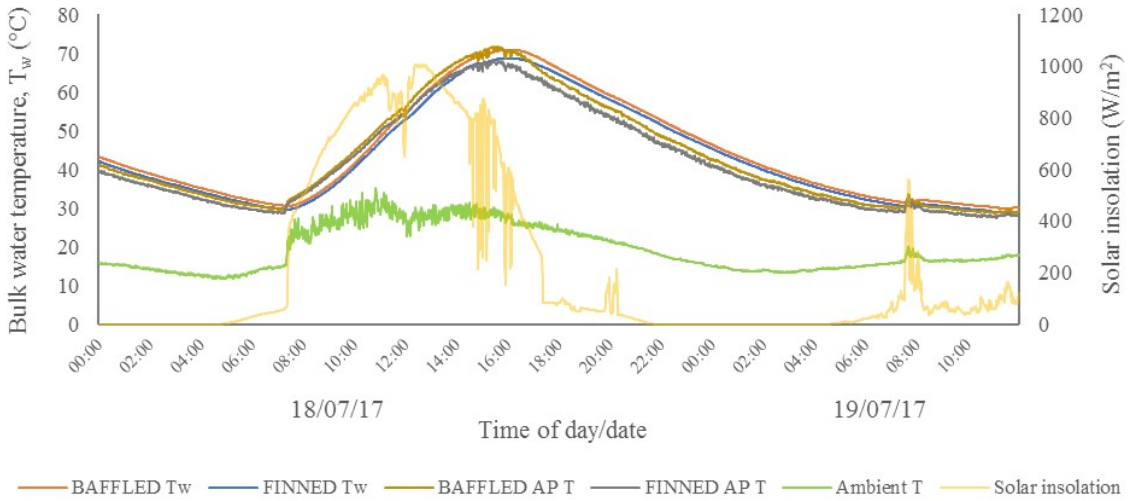

Figure 4.2: Comparison of baseline 'no-flow' tests for the baffled and finned collectors for a daily cycle on 18th July 2017. AP T – absorber plate temperature

The absorber plate collects the incident solar radiation, heats up and transfers that heat to the body of water. During this charging phase, the thermal properties of the aluminium absorber plate means that its temperature will always be higher than that of the water. Heat is passed into the water via conduction which is then distributed to the bulk water via convection within the water body. During the cooling period, solar radiation levels drop and radiative heat losses dominate which lowers the temperature of the absorber plate, drawing more heat from the bulk water.

4.1.2 With draw-off

Figure 4.3 and Figure 4.4 show the difference in collector performance with draw-off over a week period and a daily cycle in May 2018, respectively. During these tests, water is drawn off following the CEN & CENELEC EU1 draw-off profile outlined in Chapter 3, Section 3.2.4. Draw-off improves the efficiency of a solar thermal collector as the withdrawal of hot water allows the influx of cold water which has a greater capacity for heat gain. Therefore, these discharge and recharge cycles allow the best use of the solar energy. In contrast to Figure 4.1, Figure 4.3 shows that, while the collectors are again very closely matched, the finned collector reaches slightly higher peak bulk water temperatures than the baffled collector. However, it also has a higher rate of heat loss. During the collection period, a greater portion of the incident solar energy is being transferred to the bulk water body of the finned collector. This suggests that, while in a 'flow' state, the conductive heat transfer through the fins acts as a better conduit for heat gain whereas the convective heat transfer promoted by the internal baffle plate is less effective. However, when it comes to the cooldown period the baffle plate is more effective at retaining the heat gained during the day. This is due to the compartmentalisation created by the baffle plate which limits heat loss to the small body of water contained between it and the absorber plate. As the baffle plate does not extend the full length of the collector there is still substantial heat loss, as can be seen in Figure 4.3. However, looking at the bulk water temperatures, it can be inferred that the baffled configuration outperforms the finned in terms of heat retention. Again,

however, with a maximum and minimum temperature difference of 0.7°C and -1.3°C, respectively, some values may fall within the range of experimental error (see Section 3.2.6.3) thus the performance comparison is indicative, not conclusive.

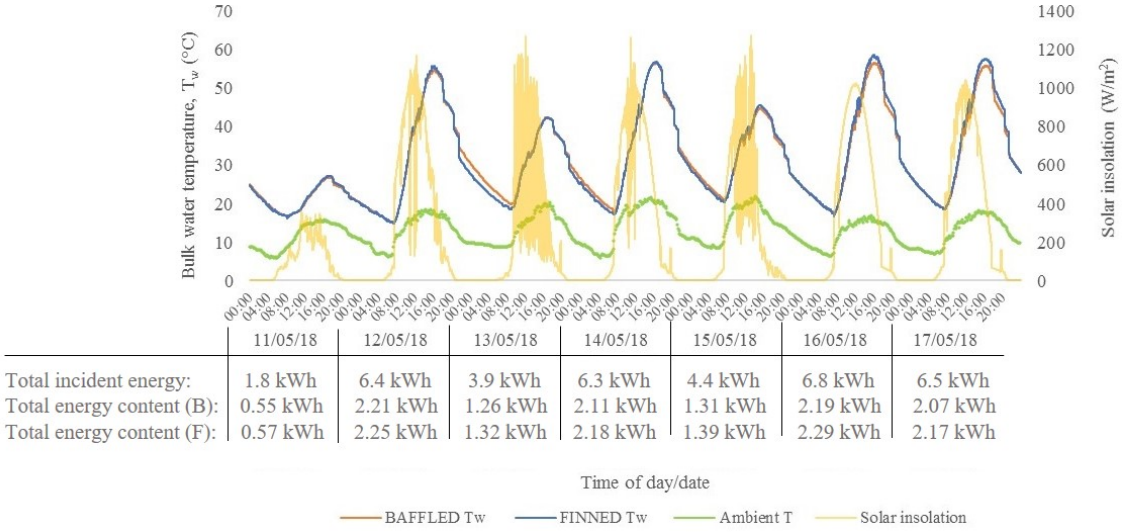

	11/05/18	12/05/18	13/05/18	14/05/18	15/05/18	16/05/18	17/05/18
Total incident energy:	1.8 kWh	6.4 kWh	3.9 kWh	6.3 kWh	4.4 kWh	6.8 kWh	6.5 kWh
Total energy content (B):	0.55 kWh	2.21 kWh	1.26 kWh	2.11 kWh	1.31 kWh	2.19 kWh	2.07 kWh
Total energy content (F):	0.57 kWh	2.25 kWh	1.32 kWh	2.18 kWh	1.39 kWh	2.29 kWh	2.17 kWh

Figure 4.3: Comparison of baseline 'flow' tests for the baffled and finned collectors over a week period in May 2018. Included is the total daily incident and collected energy to aid the visual representation

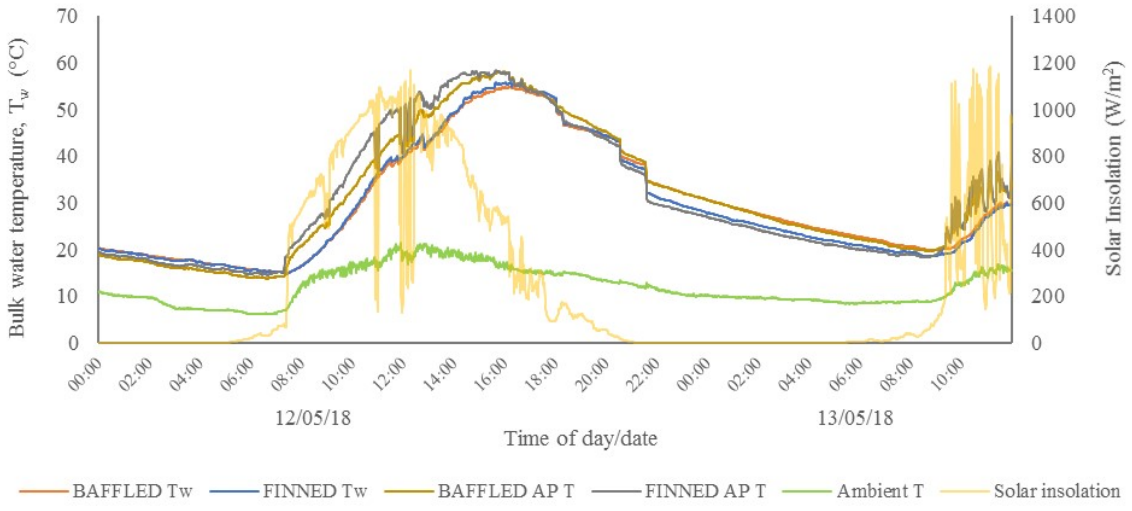

Figure 4.4: Comparison of baseline 'flow' tests for the baffled and finned collectors for a daily cycle on 12th May 2018. AP T – absorber plate temperature

Figure 4.4 illustrates the comparative collector performance over a daily cycle on the 12th May 2018. It shows that the difference in peak bulk water temperature is not significant, given the margin of experimental error. However, during the cooldown period, the finned water temperature drops below that of the baffled and then similar

cooling profiles are observed. This is an interesting reflection on system performance. The switch between which collector has the highest bulk water temperature comes after an evening draw-off when there is no insolation to top-up the energy in the system. This supports the observation that the baffled configuration has the greater ability to retain heat in the absence of incident radiation.

The absorber plate temperature behaves much differently when the system is subject to water draw-off. At the beginning of the collection period there is a rapid increase in absorber plate temperature due to the strength and consistency of the incident radiation levels. The finned and baffled plots steadily deviate from each other up until midday when solar insolation starts to drop off. This might suggest that the internal baffle plate is more efficient at transferring the heat, through convection, from the absorber plate to the bulk water than the elongated fins are through conduction where the heat remains in the plate. This is supported by the larger dip in the finned absorber plate temperature around the 12:45 water draw-off point. The bulk water is in closer contact with the absorber plate than in the baffled system as the baffle acts to compartmentalise the water body. Therefore, the incoming cold water can absorb the heat directly from the absorber plate, pushing the bulk water temperature above that of the baffled collector. During the cooldown period the bulk water and absorber plate temperatures are closely matched for both systems but after each draw-off the finned absorber plate temperature experiences a noticeable dip below bulk water temperature. This suggests that the incoming cold water comes into contact with the absorber plate and absorbs its heat.

4.1.3 Thermal stratification

The bulk water temperature gives a good indication of collector performance; however, it hides the more subtle interactions that occur in each collector. Figure 4.5 (a) and (b) plot the dimensionless stratification surrounding the evening draw-off periods, i.e. during the non-collection period, within the baffled and finned collectors, respectively. Stratification refers to the degree of temperature difference between the upper and lower portions of the water storage tank. To determine dimensionless stratification, so that

the different design conditions can be fairly compared, these temperature differences need to be scaled, resulting in the use of a temperature ratio (Garnier, 2009; Junaidi, 2007). Therefore, dimensionless stratification is obtained from the ratio between the temperature at any given height in the water column, T_h, and the temperature at the bottom of the tank, T_b . This ratio is plotted against dimensionless collector height which is derived from the ratio between the length of the collector at any given height in the water column, h, and the total length of the collector, H.

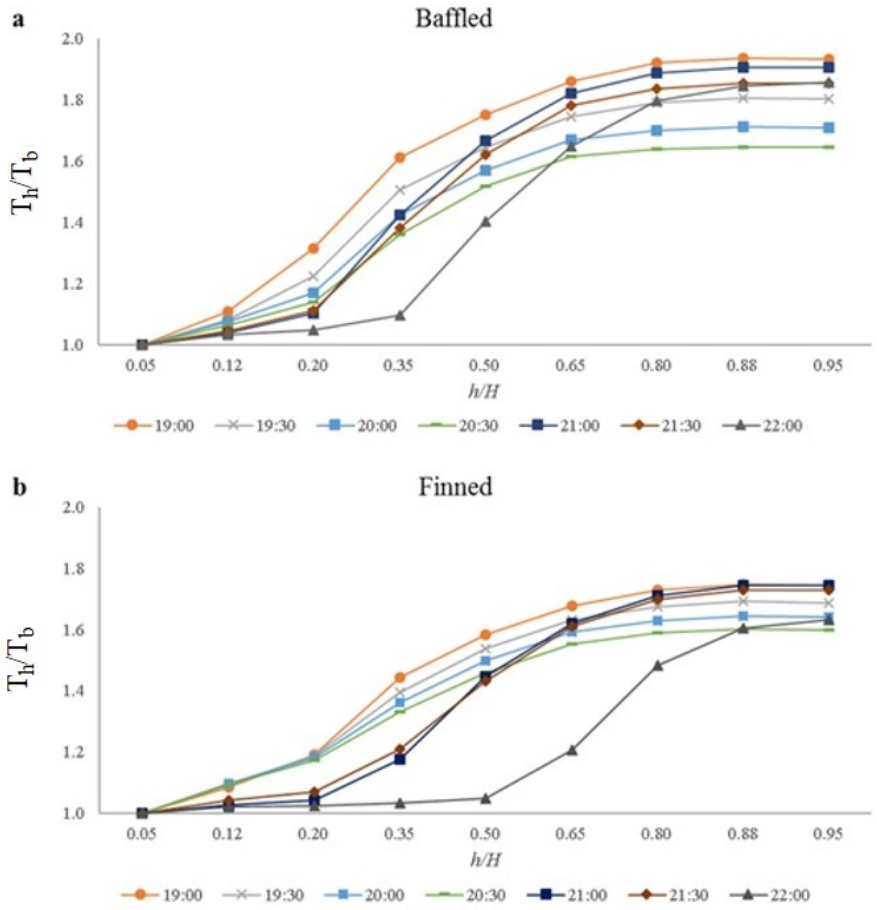

Figure 4.5: Thermal stratification in the (a) *baffled* and (b) *finned* collectors for evening draw-off periods (20:30 and 21:30) on 12th May 2018

The baffled collector shows greater levels of stratification than the finned but also a wider spread over the evening. Starting at 19:00 hours, both collectors show a smooth, gradual stratification along the length of the tank. The temperature ratio between the top and bottom water layers steadily reduces as heat is lost from the top, hottest part of the collector and gradual destratification (i.e. the breakdown or mixing of different temperature layers) occurs until the draw-off event at 20:30 hours. Following this, the

curve at 21:00 hours shows a sharper gradient in the mid-portion of the tank as the influx of cold-water mixes with the lower layers, increasing the temperature ratio along the length of the tank. The 21:30 hours curve shows that the water column is slowly recovering, and buoyant, convective mixing causes slight destratification and a softer gradient. Following the 21:30 draw-off, the 22:00 hours curve shows a larger impact than seen at the 20:30 draw-off; this is due to the larger volume of water being drawn from the system (8 l at 20:30; 15 l at 21:30). The lower layers are almost completely destratified in both systems and the finned system loses stratification for the entire bottom half of the tank. Stratification is maintained in the upper portion of both tanks.

Figure 4.6 shows a comparison between the finned and baffled collectors for the same evening, focusing on the final daily draw-off, at 21:30 hours. The stratification profiles prior to the draw-off are very similar albeit the finned collector shows a smaller dimensionless temperature ratio. Following the draw-off, the baffled collector maintains its stratification profile with some destratification in the lower portion of the tank. The finned collector suffers heavier destratification than the baffled, with mixing occurring in the middle layers of the tank and a smaller dimensionless temperature ratio compared to before the draw-off.

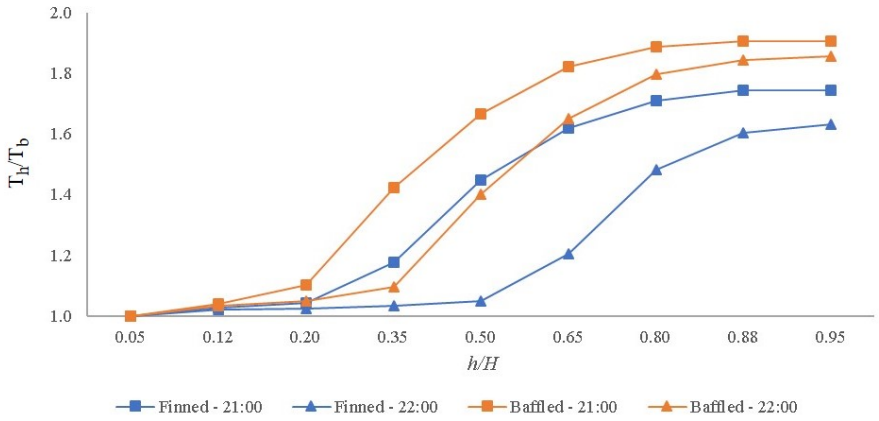

Figure 4.6: Dimensional stratification comparison of the finned and baffled collectors for the final evening draw-off (21:30) on 12th May 2018

The reason behind these differing stratification profiles, despite the same external conditions, is down to the collector design and the thermal properties of the incorporated materials. The fins create a conduit for conductive heat transfer along both the longitudinal length of the tank as well as its depth therefore a larger proportion

of the water body is affected. Conversely, the baffle plate only offers a heat transfer medium over a small portion of the water body, in the volume of water close to the absorber plate. Therefore, the conductive transfer of heat, and subsequently the extent of destratification, in the baffled design is much less impactful than in the finned design.

4.1.4 Summary of baseline performance

Reviewing the comparative performance of the base configurations, the finned and baffled collectors, it is apparent that they perform at a similar level when considering bulk water temperatures and the margin for experimental error (Section 3.2.6.3). Under a direct draw-off profile, the finned collector reaches higher bulk water temperatures during the collection period but also suffers greater heat loss at night. As the goal of an ICSSWH is to provide hot water as and when the end-user requires it, the baffled collector's greater heat retention outweighs the marginal negative difference in peak water temperature between the two collectors.

This conclusion is supported by the thermal stratification observed within the two systems. The baffled collector shows a high level of stratification over the times surrounding each evening draw-off (20:30 and 21:30 hours) and a lower level of destratification compared to the finned collector. The higher dimensionless temperature ratio along the longitudinal length of the tank means the baffled collector experiences less mixing between the stratified layers. Therefore, the heat is more effectively maintained in the upper portion of the tank. The breakdown of stratification in the finned collector results in lower temperatures in the top of the tank and thus less energy delivered to the end-user. However, these differences in collector performance are marginal with a deviation of only a few degrees temperature between the two. Therefore, the overall energy output of each base configuration, in a transient state, is reviewed in the following section to determine the contribution each system can make to the energy demand of a single person household.

4.2 Base collector energy contribution

Another way to analyse the performance of the ICS systems is to calculate the amount of energy they can provide. This section looks at the energy demand of a single person household with a hot water consumption of 52 l/day, based on the capacity of the ICS systems. After reviewing different demand profiles outlined by standardisation bodies and relevant literature (see Chapter 2, Section 2.3), the CEN & CENELEC EU1 cycle (European Commission, 2002) was chosen as it appeared to be the most realistic for the system under evaluation. Many of the other sources generate demand profiles based on averages across all monitored dwellings which results in a spread over the entire 24 hours of a day. Therefore, using data in the raw state presented in these studies to test or model a hot water system is illogical (Energy Saving Trust, 2008).

The CEN and CENELEC mandate stipulates a total draw-off volume of 52 l/day over 11 draw-off events with a mixture of small (3 l), medium (6/8 l), and large (15 l) draw-off volumes. This daily hot water demand is in line with other values in the literature, for example, McLennan (2006) monitored 32 Scottish households and concluded the average number of people per household and average weekday hot water consumption as 2.44 persons and 122 l/day, respectively. Scaling down to a single person dwelling, this equates to a comparable daily hot water demand of 50 l/day. Spur et al. (2006) developed 'Realistic Demand Profiles', the lightest of which was based on 50 l/day/person and the BS ISO 9459 standard (BSI, 2013) also offers a profile based on 50 l/day.

To determine the useful energy, Q, delivered by each collector to the end-user, the following equation was used:

$$Q = mC_p\Delta T \tag{4.1}$$

where m is the mass of water required (kg), C_p is the specific heat capacity of water (J/kg·K), and ΔT is the temperature difference between the mains inlet water and the collector outlet water (K) over 1-minute intervals. A conversion factor was applied to give a final value with units of kWh. Equation 4.1 was used for both the energy provided by the collector and the energy required by the end-user. In the latter case, ΔT is the

temperature difference between the mains inlet water and the final required water temperature. Applying this equation to the gathered data yielded the following results for the baffled and finned systems.

4.2.1 The baffled system

Based on the employed methodology (described in Chapter 3, Section 3.2.5), each condition was tested in a round-robin style, not side-by-side, due to experimental constraints. Figure 4.7 (a) and (b) shows the average energy and temperature provided by the baffled system, respectively, at each draw-off time. These values are plotted alongside the energy and temperatures required by the end-user, as stated in the CEN & CENELEC mandate (European Commission, 2002).

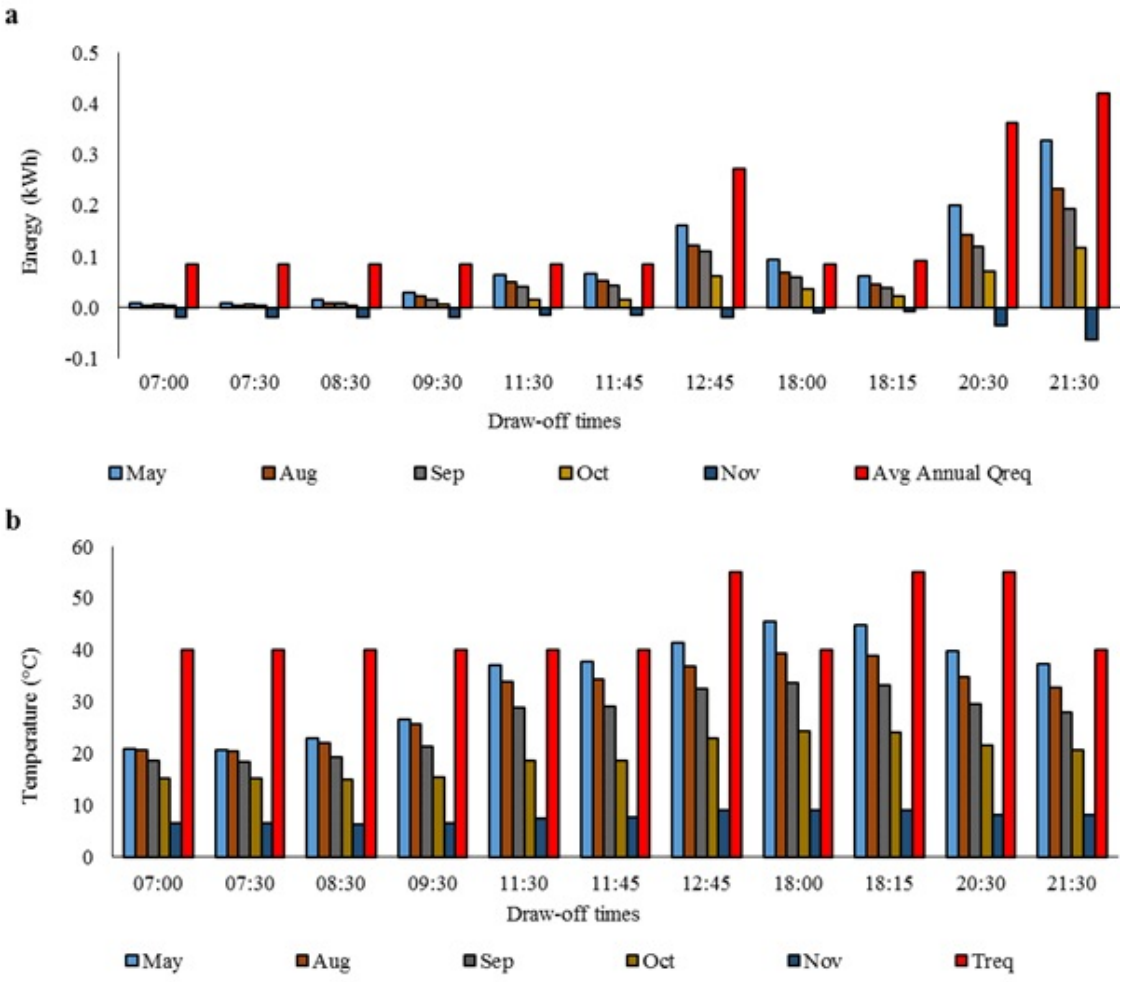

Figure 4.7: Monthly average (a) *energy* and (b) *temperature* provided by the *baffled* system against average annual energy and temperature required at each draw-off

The profiles observed across the year are expected with the summer months showing the highest contributions as longer, stronger solar insolation produces greater thermal performance. The winter months show poor performance not as a result of the colder ambient temperatures but due to the weaker insolation, lower sun angles (resulting in greater shading of the absorber, discussed in Chapter 3, Section 3.2.6.4), and shorter daylight hours. Due to the location of the collectors, there is very little to no incident solar radiation in the winter months (November to January) so the water body cannot recover during the day the heat losses suffered at night. All it can do is provide freeze tolerance as a result of its mass and thermal inertia. Therefore, the water temperature in the tank is often lower than the incoming cold water and by providing the hot water demand via the ICS, the system effectively cools down the mains water thus requiring a larger auxiliary heat input as shown by the negative values in Figure 4.7(a). As a result, in winter months, the ICS should be bypassed in favour of direct heating from the mains water.

Another observation is the energy and temperature at each draw-off time. When viewing the energy plots as a day as opposed to focusing on the months, an undulating pattern emerges. This pattern is a result of the temperature and volume requirements of the different draw-offs as well as the incoming cold-water temperature. The morning values are low due to the temperature difference between the outlet and the inlet water which impacts the energy provided as per Equation 4.1. Due to the set-up of the experimental test rig, the incoming cold water is sitting in insulated pipes in a well-heated building. Therefore, the often-assumed cold water temperature of 10°C, indeed the temperature assumed in the CEN & CENELEC mandate, is largely inaccurate. Only in the winter months is the recorded temperature, at 12°C, close to this assumed temperature; the rest of the year ranges from 14 – 19°C. Towards the end of the day, when water temperatures are higher, the biggest impact on energy provision switches to the required volume and temperature. For example, the 12:45, 18:15 and 20:30 draw-offs require temperatures of 55°C and thus the corresponding energy demand is greater.

When viewing the temperature plots as a day, an overall bell curve profile with a skewed distribution is observed (Figure 4.7[b]). The draw-off events show the lowest

temperatures in the morning, rising throughout the day to peak at the 18:00 and 18:15 periods and then dropping off slightly to the 21:30 draw-off. The morning draw-offs come after a long non-collection period where a large portion of the stored heat has been lost and solar insolation has yet to replenish the system. As incident solar radiation heats the water throughout the day, the system can provide higher outlet temperatures. The thermal inertia of the water drives the continued heating to a point where it can no longer be maintained, at around 17:00-18:00 hours, and then heat is gradually lost through conductive and radiative processes. The cold water introduced during the evening draw-off events works to drive the tank water temperature down and the observed outlet temperatures subsequently decline.

When following the CEN & CENELEC guidelines, the required temperature varies depending on the type of draw-off, either 40°C or 55°C. Applying these temperatures to Figure 4.7 allows a comparison of what is provided against what is required in terms of both energy and temperature. To raise the water temperature from the inlet to required temperature, the baffled collector's daily energy contribution ranges from -12% in the winter months to 65% in the summer months (Figure 4.8). A maximum average energy contribution of 125% is found at 18:00 hours in the summer months (May). It is important to note that the required draw-off temperatures do not meet the conditions required to control Legionella. If the system does not reach temperatures of 60°C for several minutes (or 70°C which destroys the bacteria instantly) each day, auxiliary heat would be required to kill any bacteria in the water tank.

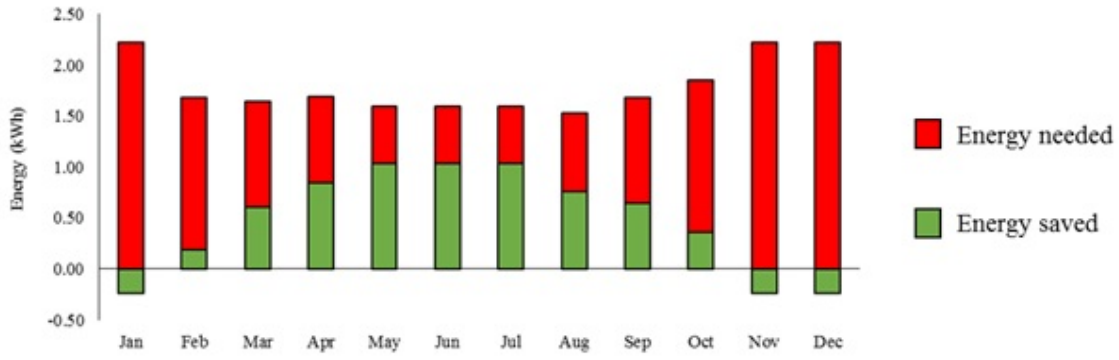

Figure 4.8: Annual average daily contribution versus demand for the *baffled* collector across all 11 draw off events

Table 4.1 provides a complete breakdown, by draw-off time, of the solar fraction of the baffled collector across the year. Solar fraction is the amount of energy the ICSSWH can provide divided by the total energy required by the end user. A 'traffic-light' ranking system has been used to distinguish between a high, moderate or low contribution with each level assigned an arbitrary value of 33%. Thus, anything less than 33% is classed as low, 33% – 66% is moderate, and any value greater than 66% is classed as high. Any negative values have been left unassigned as they present a negative contribution. Bar the winter months, the baffled ICS does make a significant energy contribution, especially in the latter stages of the day. The alternation between amber and green can be attributed to the different water temperature and volume required. For example, the 11:45 draw-off requires 3 l at 40°C while at 12:45, 6 l at 55°C is required and thus there is a correspondingly greater energy requirement that the ICS cannot cater to as effectively.

Table 4.1: Solar fraction of the *baffled* system for each average monthly draw-off (%). An arbitrary 'traffic-light' system is used to identify periods of high (>66%; green), moderate (33% – 66%; amber), and low (<33%; red) contribution. Negative values have been left black

	Draw-off time										
	07:00	**07:30**	**08:30**	**09:30**	**11:30**	**11:45**	**12:45**	**18:00**	**18:15**	**20:30**	**21:30**
May	11	10	21	38	86	89	63	125	72	59	87
Aug	6	6	13	31	70	72	49	97	55	43	65
Sep	8	7	11	20	52	53	41	73	43	34	48
Oct	5	4	3	6	18	18	22	40	25	19	26
Nov	-19	-19	-19	-19	-16	-15	-6	-10	-7	-9	-13

4.2.2 The finned system

The following figures detail the same information as presented above for the baffled system but for the finned system. Almost identical patterns are seen here due to the very similar level of collector performance. The main difference lies in the slightly lower values observed for the finned configuration, overall. Figure 4.9 (a) and (b) show the monthly average energy and temperature provided by the finned system at each draw-off time, respectively.

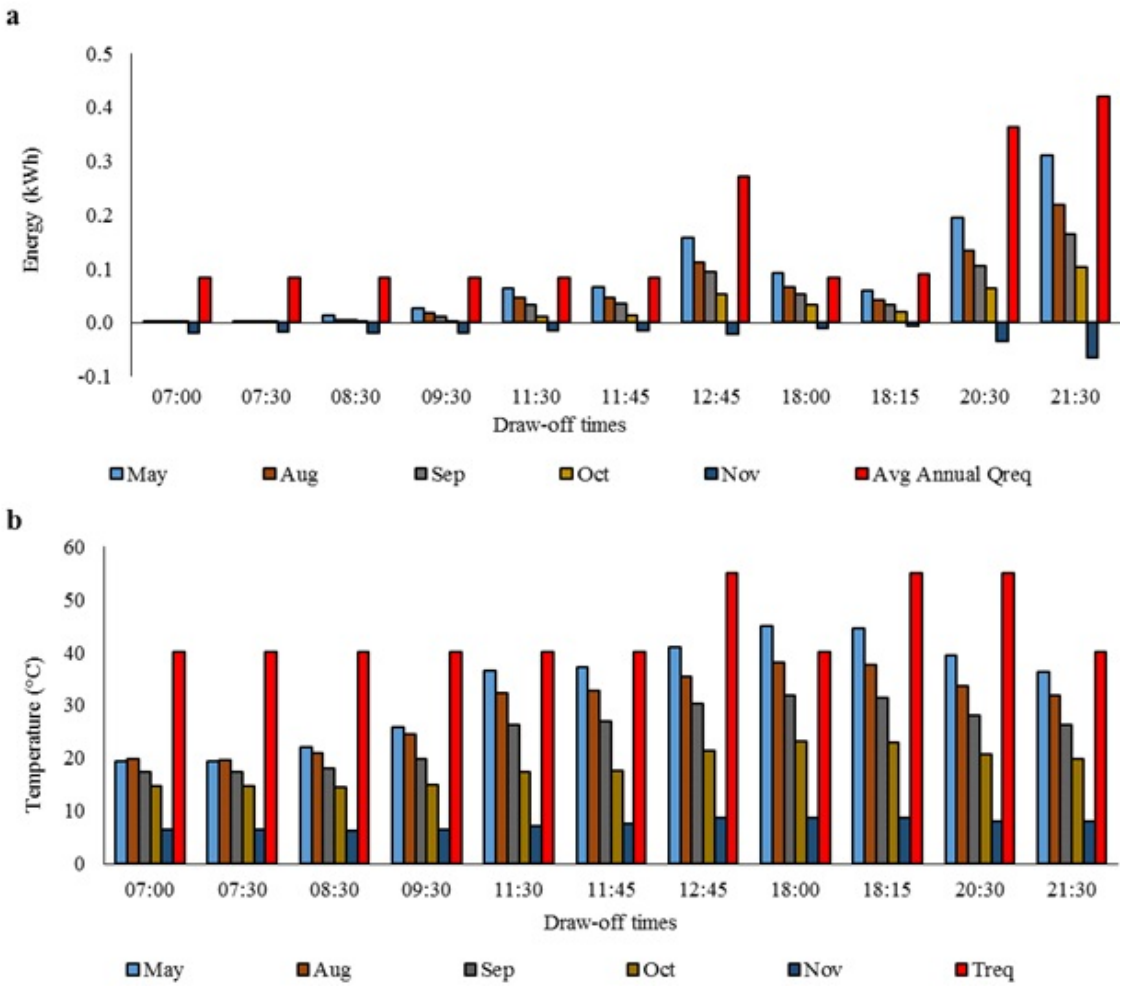

Figure 4.9: Monthly average (a) *energy* and (b) *temperature* provided by the *finned* system against average annual energy and temperature required at each draw-off

Figure 4.10 shows, for each month of the year, the daily energy contribution made by the finned collector stacked against the auxiliary energy that would need to be supplied to fulfil the energy demand of the end-user. The percentage of the daily energy requirement that the finned collector can provide ranges from -12% in the winter months to 63% in the summer months, where a maximum average energy contribution of 123% is found at 18:00 hours.

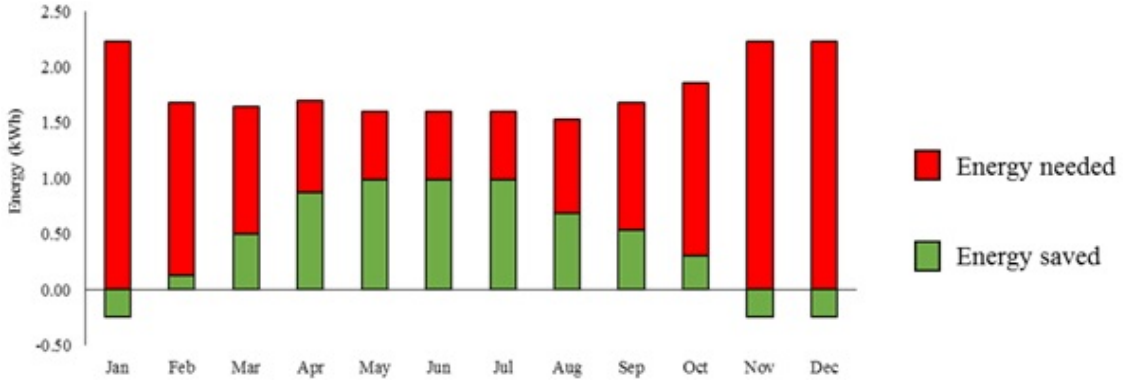

Figure 4.10: Annual average daily contribution versus demand for the *finned* collector across all 11 draw off events

Table 4.2 provides a complete breakdown, by draw-off time, of the solar fraction of the finned collector across the year, i.e. the percentage of required energy that the system can provide. Following the same 'traffic-light' ranking system as introduced in Table 4.1, the finned ICS is also shown to make a significant energy contribution, comparable to that of the baffled ICS. The same patterns seen there are also witnessed for the finned system.

Table 4.2: Solar fraction of the *finned* system for each average monthly draw-off (%). The 'traffic-light' system is used again here

	Draw-off time										
	07:00	**07:30**	**08:30**	**09:30**	**11:30**	**11:45**	**12:45**	**18:00**	**18:15**	**20:30**	**21:30**
May	4	5	17	34	84	87	62	123	71	57	83
Aug	2	2	8	25	63	65	45	91	51	40	61
Sep	3	2	5	13	41	44	35	65	38	29	41
Oct	3	3	2	4	13	14	18	36	22	17	23
Nov	-19	-18	-19	-19	-16	-15	-7	-11	-7	-9	-13

4.2.3 Configuration comparison

In terms of the energy provision offered over the year by the two configurations under investigation, the baffled system outperforms the finned; an overall trend that has been emphasised throughout this section. In the summer months, the baffled system can provide 3% more energy than the finned. In the autumn months, the percentage difference in energy provision ranges from 4%, 6%, and 3% in August, September and

October, respectively. In the winter months, there is no difference in performance as neither system can contribute to the energy demand. This trend can be further verified by evaluating the cooling profiles of each configuration.

Figure 4.11 illustrates a comparison between the cooling profiles for the baffled and finned collectors in May, under poor and good weather conditions. This characterisation of 'poor' and 'good' weather conditions (and any instance hereafter) was chosen to reflect the range of conditions experienced during testing and allow some visual interpretation; collected data was used to determine a range of weather profiles (i.e. solar insolation and ambient temperatures) where 'poor' weather was at the bottom of the range and 'good' weather was at the top. This range resulted from the assimilation and objective evaluation of gathered data and enables a broader understanding of the collector solar thermal performance. Note that, in Figure 4.11, different experimental durations are used, i.e. the start and end of the cooling periods are different. This is because the start of the cooling period was defined as when the water temperature in the storage tank began to decrease. Vice versa, the end of the cooling period was when the water temperature started to rise. Due to the differing external conditions, these times are slightly different.

These figures further highlight the similarity in performance of the two configurations. Additionally, they clearly show how bulk water temperature impacts the cooling profile. The higher the bulk water temperature at the start of the cooling period, the more rapid and extreme the heat loss as demonstrated by the steep gradient observed in Figure 4.11(b). Here ΔT is defined as the difference between the hourly bulk water temperature from the start of the non-collection period, T_i, and the bulk water temperature at the end of the non-collection period, T_{final}. The temperature profiles are normalised this way to present a more accurate comparison of the heat losses across the two collector configurations.

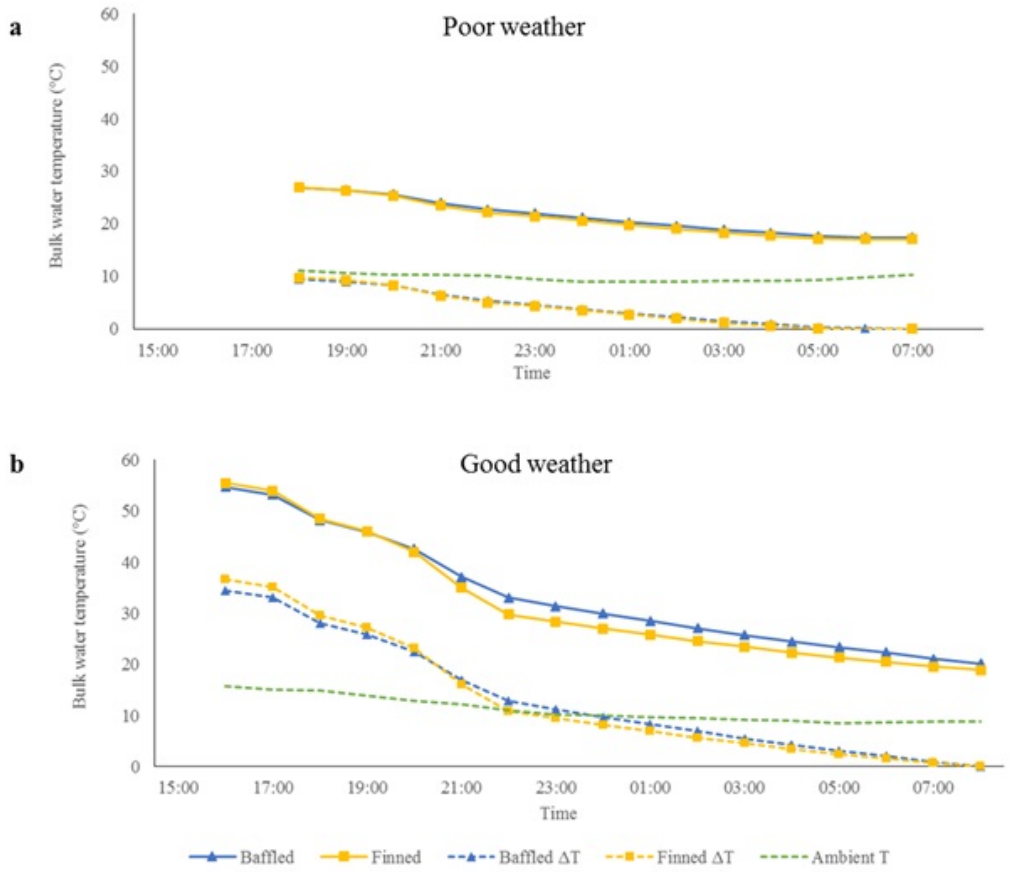

Figure 4.11: Cooling profiles for the base baffled and finned collectors under (a) poor weather conditions on *27/05/18*, (b) good weather conditions on *12/05/18*. $\Delta T = T_i - T_{final}$

Despite the similarity in performance, the finned collector exhibits greater heat loss, especially when the initial temperature is higher. This is to be expected due to characteristic differences between heat transfer fins and an internal baffle plate, designed to suppress reverse water flow at night. Note, the value of the y-axis is kept the same in both figures to emphasise the greater heat loss with higher initial temperature. Using Equation 4.1 to determine the energy lost from the water over the cooling period, the baffled base configuration loses 2% less energy than the finned under the poor weather conditions shown in Figure 4.11(a). This difference increases slightly with improving weather conditions; 6% less energy lost under good weather conditions.

4.3 Heat retention methods

As a main component of the experimental research, this section focuses on the heat retention methods that have been applied to the base collector configuration. The

additional insulation covering the top third of the absorber area and the night cover applied during the non-collection period were chosen, based on the extensive literature review, as a simple, low-cost potential improvement. The following results provide a breakdown of performance, in terms of energy contribution and heat retention, for the two applied methods followed by a comparison of the finned and baffled collectors and their three system set-ups; base collector, insulated, and night cover. This comparison aims to quantify the difference in system performance in order to identify a superior collector configuration.

4.3.1 Insulated performance

Due to setbacks with the experimental tests, less data was collected for the insulated condition with only September, October, and June recorded, i.e. autumn and summer.

4.3.1.1 Energy contribution

This section presents the energy contribution of the baffled and finned systems under the insulated condition. Figure 4.12 shows average daily energy provided and required, it is not split across the draw-off periods. The energy provided by the base configurations is also plotted to show the difference in performance and this comparison is discussed in Section 4.3.3. Like the base configuration, when averaged across the daily cycle, the insulated system cannot meet the total daily energy demand. Also, with additional insulation, the baffled configuration again outperforms the finned. September and October show poor performance during the collection period, reflecting the reduced absorber area resulting in a smaller level of incident solar insolation. There is a stark difference in performance between the summer and autumn months and even between September and October showing the importance of the strength of insolation. Similar profiles as seen in the individual draw-off events presented for the base configuration (Section 4.2) are observed in this aggregated data.

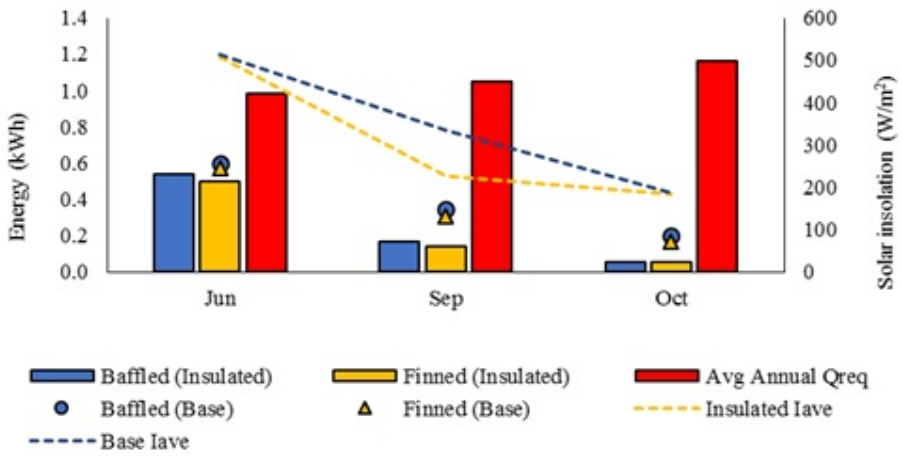

Figure 4.12: Total average daily energy provided by the finned and baffled systems with additional insulation across the 11 draw-off periods against the total daily energy required, "Avg Annual Q_{req}". I_{ave} – average solar insolation during the collection period. Base collector energy is provided for comparison

4.3.1.2 Cooling profiles

Figure 4.13 illustrates a comparison between the cooling profiles for the baffled and finned collectors with additional insulation in June, under poor and good weather conditions. Ambient temperature is relatively consistent across the two days. Note that the same reasoning for the start and end of the cooling period applies here as in Section 4.2.3. The difference between the finned and baffled systems is more noticeable with better weather conditions. The cooling profiles in Figure 4.13(a) show virtually no difference in performance, bar the very slightly higher temperature in the finned collector at the start of the cooling period. However, this falls within the range of experimental error (see Section 3.2.6.3). At the end of the cooling period, the collector temperatures are matched indicating the baffled collector again shows better heat retention. Figure 4.13(b) shows higher levels of deviation between the two systems, with the baffled clearly retaining more heat than the finned.

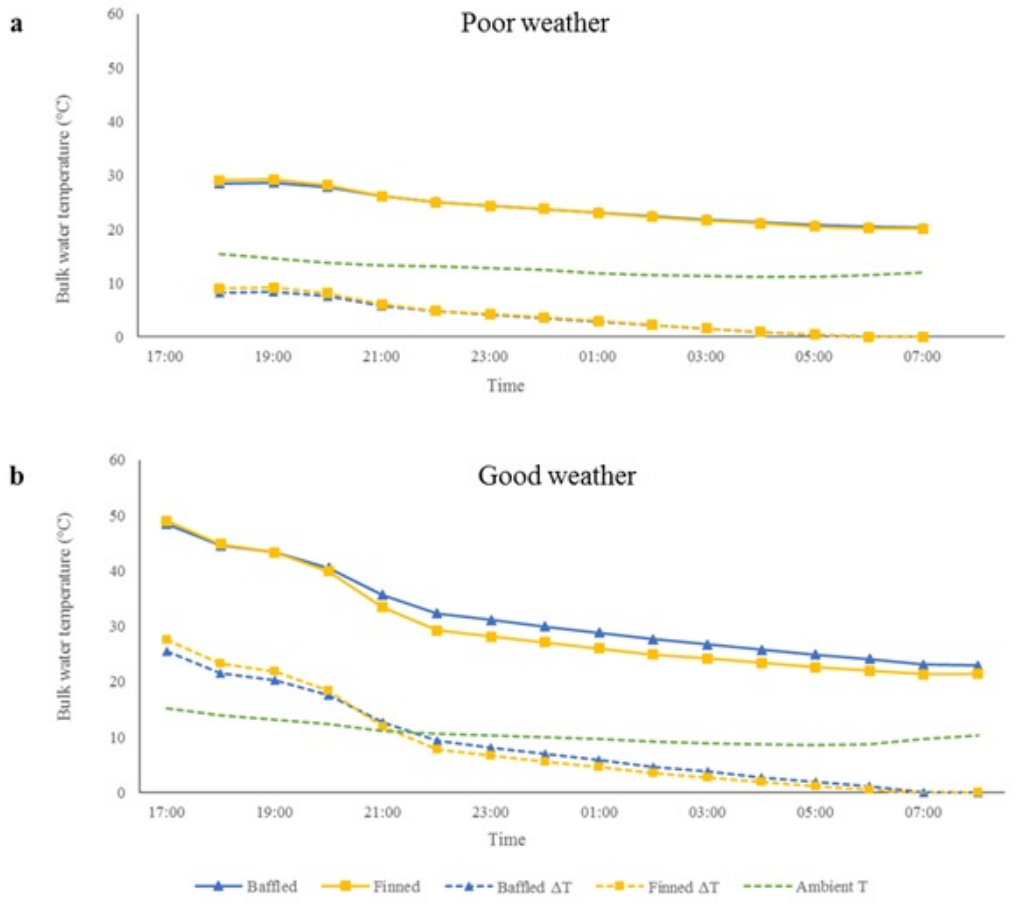

Figure 4.13: Cooling profiles for the insulated baffled and finned collectors under (a) poor weather conditions on *11/06/18* and (b) good weather conditions on *05/06/18*. $\Delta T = T_i - T_{final}$

In terms of energy lost, the finned system loses 8% more energy than the baffled. This improved heat retention is also reflected in the ΔT plots, the difference in bulk water temperature from the start to the end of the cooling period is smaller for the baffled system in both weather conditions. The choice of poor and good weather conditions is based on the collection period immediately prior the plotted cooling period. To allow as accurate a comparison as possible given the testing methodology, the days that have been compared throughout this section and Section 4.2.3 were chosen based on the similarity of the external and system conditions. Table 4.3 summarises the parameters that were considered.

Table 4.3: Summary of the environmental and system conditions for the days chosen for heat retention comparison. I_{ave} – average solar insolation over the collection period, Q_{inc} – total incident solar energy on the absorber surface over the collection period, T_w – bulk water temperature in the tank

	Parameter	**Base**	**Insulated**	**Night cover**
Poor day (Base - 27/05/18) (Ins. - 11/06/18) (N.C. - 13/07/18)	I_{ave} (W/m^2)	230	266	233
	Q_{inc} (Wh)	1766	1788	1792
	T_w (start) (°C)	28	29	32
	T_w (end) (°C)	17	20	23
	Ambient (day) (°C)	11	14	19
	Ambient (night) (°C)	10	13	16
Good day (Base - 12/05/18) (Ins. - 05/06/18) (N.C. - 03/07/18)	I_{ave} (W/m^2)	743	777	753
	Q_{inc} (Wh)	6425	6716	6508
	T_w (start) (°C)	54	49	57
	T_w (end) (°C)	20	23	29
	Ambient (day) (°C)	17	16	21
	Ambient (night) (°C)	11	11	16

4.3.2 Night cover performance

4.3.2.1 Energy contribution

As with the insulated performance presented above, Figure 4.14 shows average daily energy provided by the base configuration with a night cover applied. Again, the energy provided by the base configurations is shown here and discussed in a following section. The results differ here in that the insolation levels are much different in October. For these plots, the average insolation (I_{ave}) is that of the collection period only for the data presented; it is not a monthly average as that would not be representative. Based on the methodology for these field experiments, the night cover was tested at the end of October and insolation levels are clearly not stable across the whole month. Therefore, the round-robin style of testing suffers bias in the spring and autumn months thus not allowing a fair performance comparison. However, based purely on the baffled and finned configurations, which can be fairly compared as they were tested side-by-side, the baffled again outperforms the finned in terms of energy provision. For example, in

July, Figure 4.14 shows that the baffled system, on average, can provide 0.07 kWh more energy than the finned. A similar difference is observed in September with the baffled generating 0.06 kWh more energy. There is a negligible difference in October.

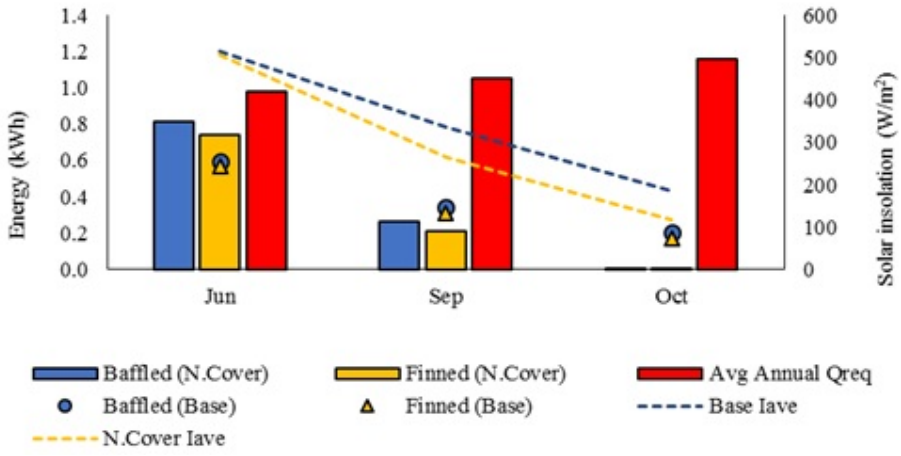

Figure 4.14: Total average daily energy provided by the finned and baffled systems with a night cover across the 11 draw-off periods against the total daily energy required, "Avg Annual Q_{req}". I_{ave} – average solar insolation during the collection period. Base collector energy is provided for comparison

4.3.2.2 Cooling profiles

Figure 4.15 illustrates a comparison of the cooling profiles for the baffled and finned collectors with a night cover in July, under poor and good weather conditions. Note that the same reasoning for the start and end of the cooling period applies here as in Section 4.2.3. Similar profiles are observed here as with the base configurations and with additional insulation. The following section offers a comparison of these design conditions versus the base configuration.

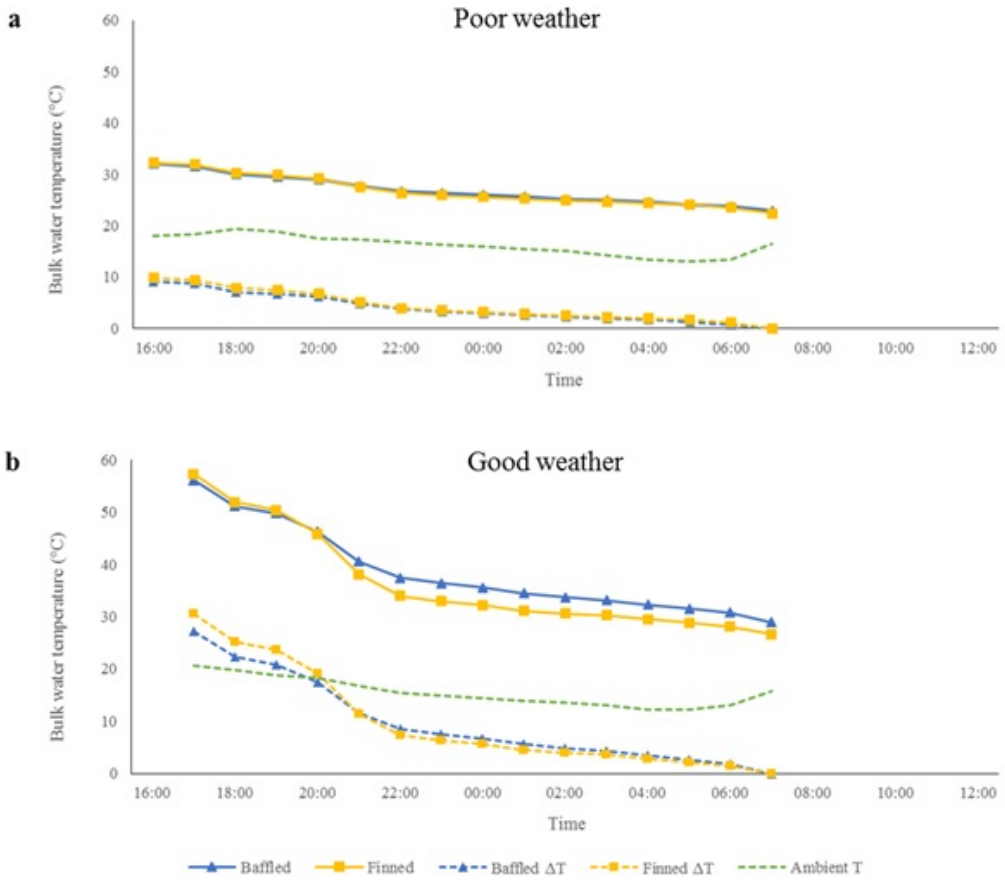

Figure 4.15: Cooling profiles for the baffled and finned collectors with a night cover under (a) poor weather conditions on *13/07/18* and (b) good weather conditions on *03/07/18*. $\Delta T = T_i - T_{final}$

4.3.3 Comparison of the design conditions

To compare the design conditions, i.e. additional insulation and a night cover, against the base configuration, different days were chosen from those presented in Table 4.3. As this section is comparing both the collection and heat retention performance, the environmental conditions need to be as closely matched as possible for two consecutive days. Note that due to the unpredictable nature of daily weather conditions, it is not possible to find days with identical environmental conditions. For this section, only a good weather scenario is considered and Table 4.4 summarises the details of the chosen days. Additionally, as the baffled system has consistently outperformed the finned, considering the range of experimental error (see Section 3.2.6.3), and the focus here is on the design conditions not configurations, only baffled data will be presented for this comparison.

Table 4.4: Summary of the environmental and system conditions for the days chosen for the comparison of the design conditions. I_{ave}, Q_{inc} and T_w are the average solar insolation and total incident solar energy on the absorber surface and bulk water temperature in the tank, respectively, over the collection period

	Parameter	**Base**	**Insulated**	**Night cover**
Day 1 (Base - 16/05/18) (Ins. - 21/06/18) (N.C. - 06/07/18)	I_{ave} (W/m^2)	788	756	819
	Q_{inc} (Wh)	6814	6534	6291
	T_w (start) (°C)	18	16	30
	T_w (end) (°C)	56	46	60
	Ambient (day) (°C)	16	17	23
Day 2 (Base - 17/05/18) (Ins. - 22/06/18) (N.C. - 07/07/18)	I_{ave} (W/m^2)	749	723	819
	Q_{inc} (Wh)	6474	6249	4911
	T_w (start) (°C)	19	23	30
	T_w (end) (°C)	55	48	55
	Ambient (day) (°C)	16	20	24

4.3.3.1 Bulk water temperature

Figure 4.16 shows a side-by-side comparison of the design conditions for the baffled collector; base (as designed), insulated and night cover. This plot illustrates the difference in heat gain and heat retention performance of the two heat retention methods against no change in the base design. The base and night cover configurations reach the highest bulk water temperatures during the day as both have the full absorber plate area open for heat gain during the collection period. The insulated design shows significantly lower daytime bulk water temperatures due to the top third of the absorber plate being covered by opaque insulation. The dip observed in the peak of the night cover plot is due to the sudden drop in solar insolation compared to the steady decline in the base plot.

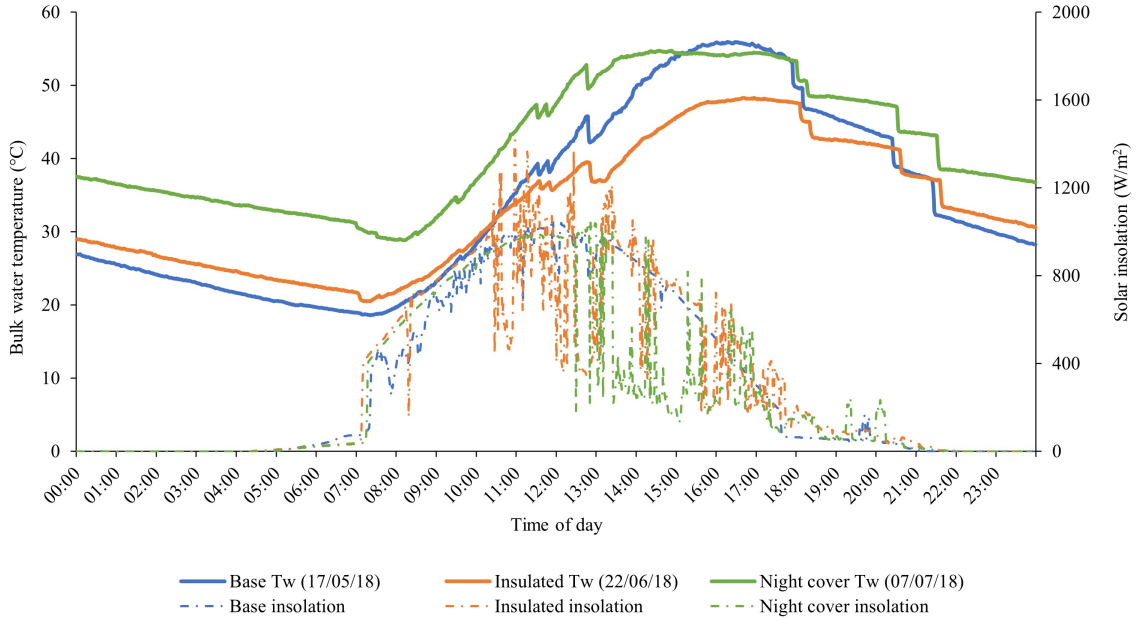

Figure 4.16: Bulk water temperature and solar insolation profiles for the three design conditions on Day 2. Note that they are not tested side-by-side but separately over the summer months and the environmental and system conditions are given in Table 4.4

Figure 4.17 (a) and (b) show the comparison between the base condition and the insulated and night cover conditions, respectively. The green hatched areas indicate the improvement in bulk water temperature provided by the heat retention strategies. The red hatched areas indicate the top-up energy required by the base collector; the additional energy required for the insulated system is left blank (Figure 4.17[a]). It is evident from Figure 4.17(a) that the insulated system offers an improvement in heat retention. Bulk water temperature reaches a maximum of 3°C, outlet temperature 6°C, higher over the non-collection period. However, this may be an artefact of higher heat gain during the day resulting in higher heat losses in the base system.

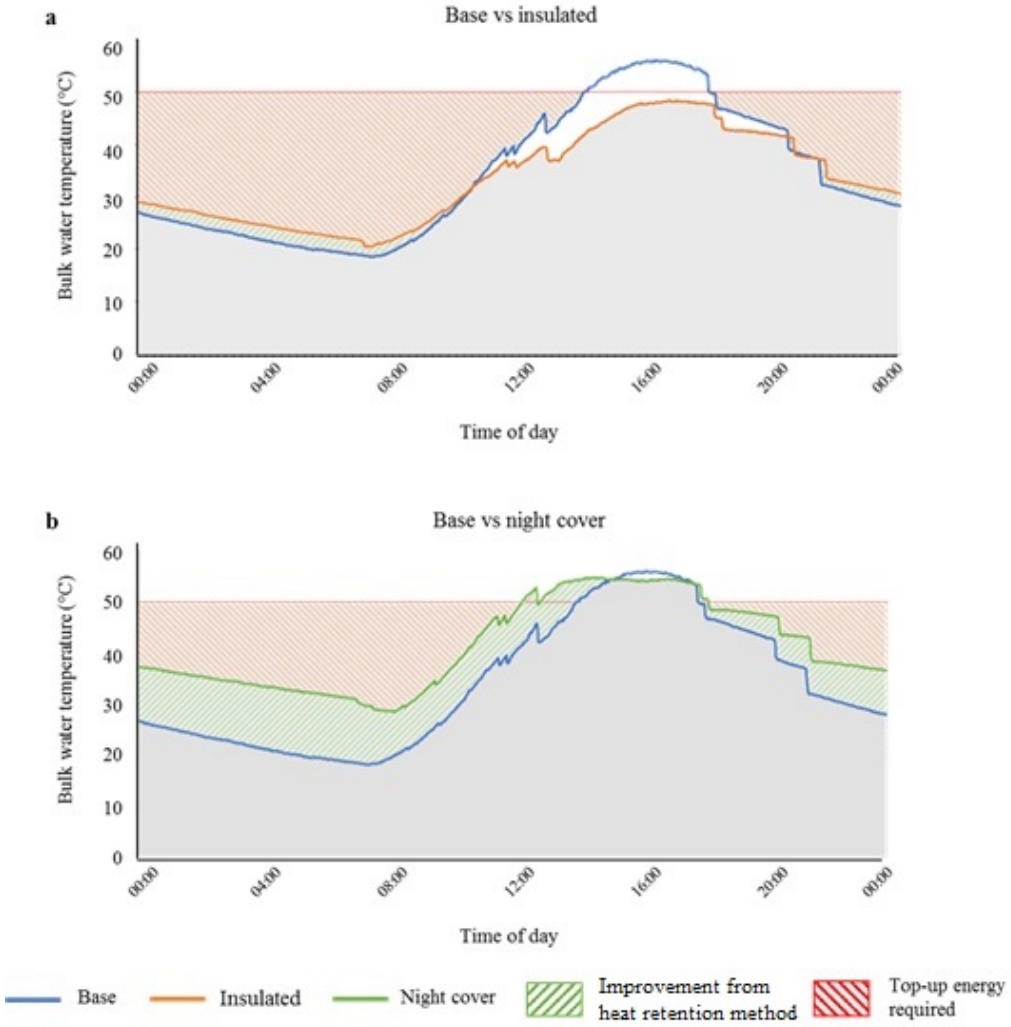

Figure 4.17: (a) Base versus insulated and (b) base versus night cover designs showing the difference in temperature, i.e. improvement in thermal performance, and the top-up energy required over the 24-hour period of Day 2

Figure 4.17(b) shows a significant improvement in heat retention due to the night cover. Also, the higher initial water temperature does not impact system performance as the night cover system reaches similar bulk water temperatures during the collection period. The base condition starts to heat up before the night cover condition, but temperature rise is subsequently inline. During the non-collection period, a maximum temperature difference of 22°C and an average of 16°C is observed. Additionally, both systems can achieve the required delivery temperature for a large portion of the day and the maximum useable temperature, as specified in the CEN & CENELEC mandate, for significantly longer. Figure 4.18 also shows the performance of the three design conditions alongside the CEN & CENELEC draw-off profile.

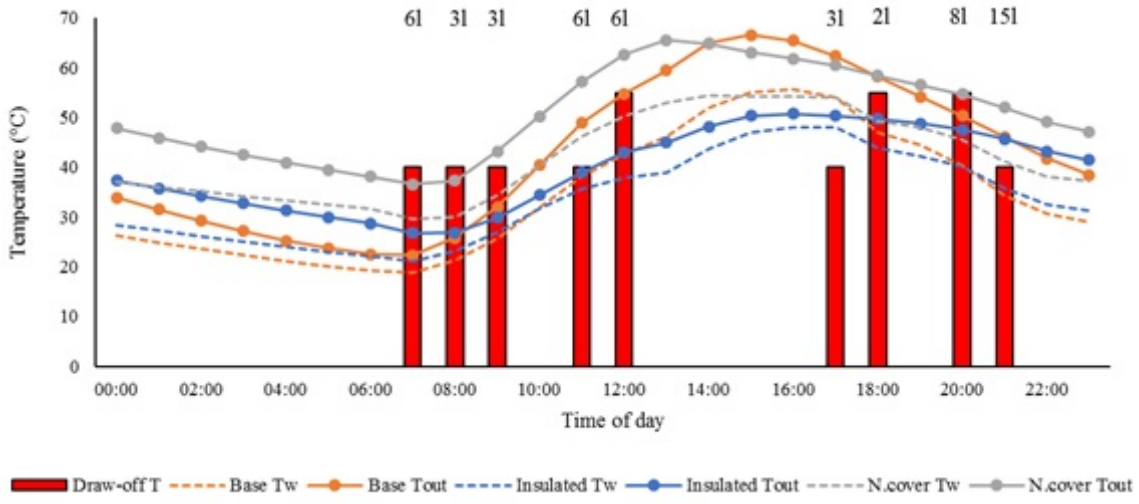

Figure 4.18: Performance of the three design conditions alongside the required temperatures for the implemented draw-off profile, the volumes required are shown at the top of the graph. Note: 07:00 and 07:30 and 11:30 and 11:45 have been grouped. T_w – bulk water temperature, T_{out} – outlet temperature

An additional point to note from Figure 4.17 is the temperature drop at the draw-off events. The smaller, 3l, draw-offs that occur during the collection period barely impact the bulk water temperature and the systems recover quickly. The larger 6l draw-off at 12:45 causes a 3-4°C drop but, again, the systems recover quickly, and higher bulk water temperatures are reached throughout the afternoon. The evening draw-offs suffer a slightly larger impact due to the lack of solar energy available to top-up the systems. The base system experiences a 3°C drop during the small draw-offs at 18:00 and 18:15 hours, and the insulated and night cover systems show a 2°C drop. For the larger events at 20:30 hours (8l) and 21:30 hours (15l), all systems are noticeably affected and do not recover as they occur during the non-collection period. The systems suffer a 3-4°C drop during the 20:30 draw-off and a 4-5°C drop at 21:30. Despite the systems being unable to recharge, the rate of cooling in the insulated system is slightly slower than the base condition and significantly slower in the system with the night cover. This is illustrated by the gradient of the cooling profiles shown in Figure 4.19. On Day 2 (Table 4.4), the base condition demonstrates a heat loss of 64%, for the insulated condition 54% is lost and the system with the night cover only loses 44% of the heat gained.

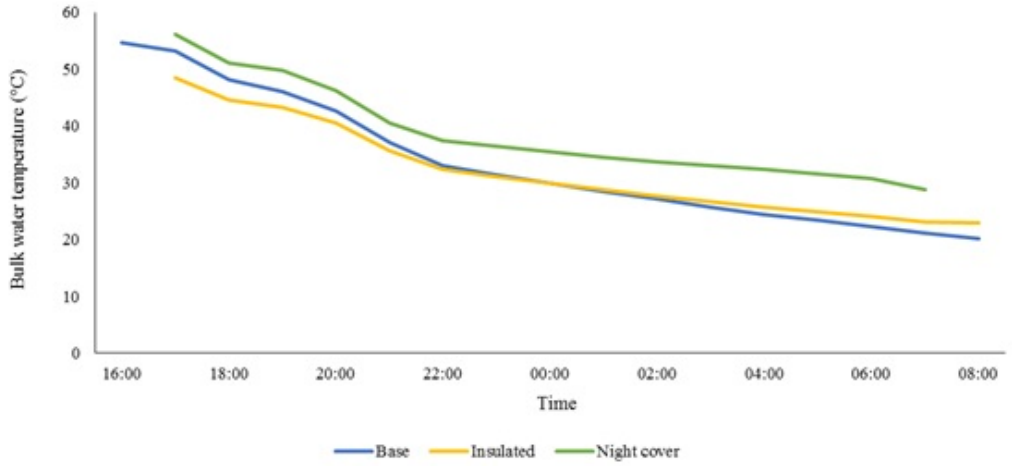

Figure 4.19: Comparative cooling profiles for the base, insulated and night cover conditions

4.3.3.2 Cooling profiles

The influence of the heat retention methods can also be observed by reviewing the thermal interactions occurring between the water, absorber plate, air cavity and glass cover over the cooling period. Figure 4.20 provides an interesting comparison between the three design conditions. The data plotted is from the upper third portion of the tank as this houses the hottest water and where the insulated condition is most relevant; ambient temperature is relatively consistent. Figure 4.20(a) shows the base condition and the observed profiles are to be expected; the water and absorber plate temperatures decline at the same rate, with the latter at slightly lower temperatures. The air cavity and glass cover temperatures also follow the same pattern, albeit at a shallower gradient. The glass cover has the lowest temperature, after ambient, as it is in direct contact with the ambient environment. It maintains higher temperatures than the ambient because of convective and radiative heat losses. However, the rate of heat loss is low due to the dampening effect of the air cavity which suppresses convective heat transfer. This explains the higher temperatures found there; the heat escaping from the absorber plate is trapped.

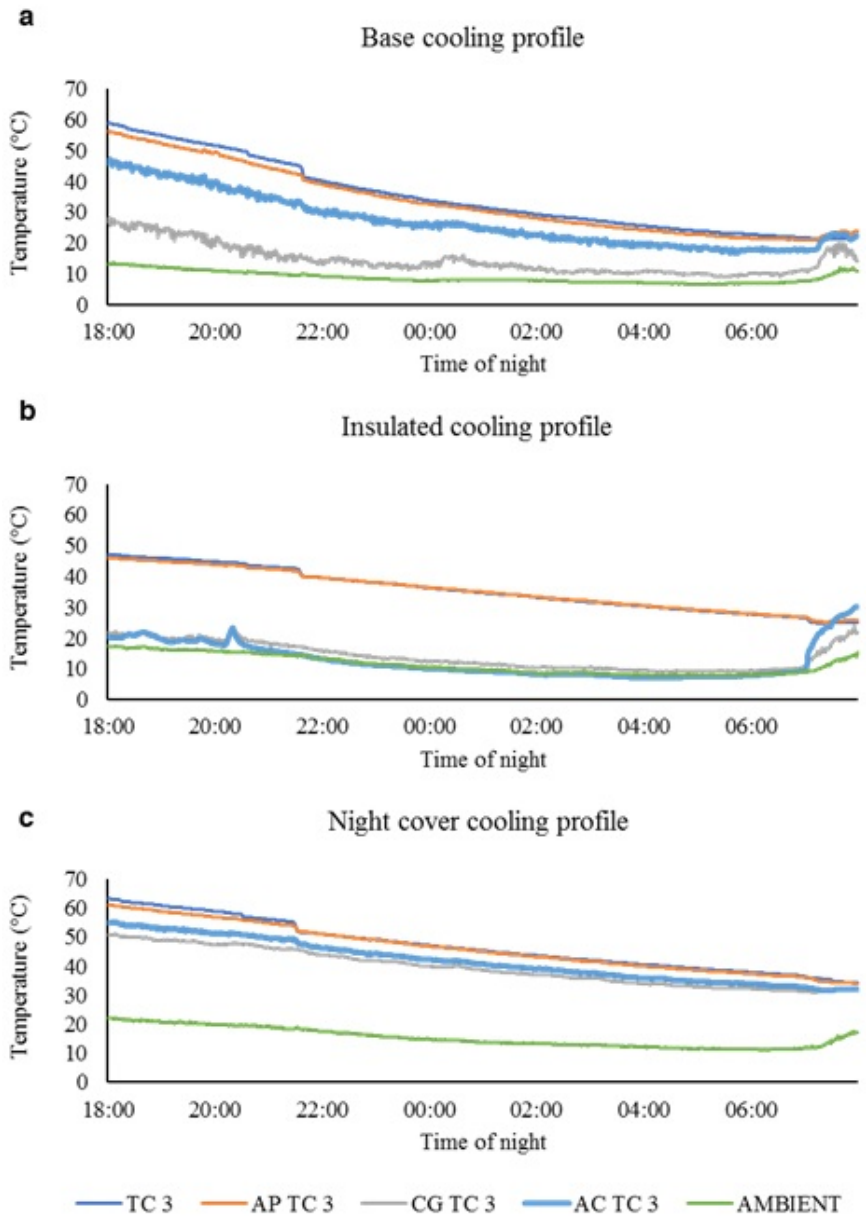

Figure 4.20: Cooling profiles for the upper third portion of each condition for the baffled configuration; TC - thermocouple in the water body, AP TC - thermocouple on the absorber plate, CG TC - thermocouple on the glass cover, AC TC - thermocouple in the air cavity

Figure 4.20(b) shows a very different profile for the insulated condition. The water and absorber plate temperatures are again aligned but the latter has fractionally higher temperatures, illustrating the insulating effect of the additional insulation. The glass cover temperatures show a similar pattern to the base condition, but the air cavity is significantly different. In the insulated condition, the additional insulation is set below the air cavity thermocouple. The large deviation between the absorber plate and air cavity temperatures shows how effective the insulation is. The heat is being trapped

beneath it and the portion of the air cavity above it is left to cool at the same rate as the glass cover, having minimal impact on the water temperature. Figure 4.20(c) also tells an interesting story about the night cover condition. All four of the measured parameters are similar; the water and absorber plate temperatures follow the same trend as the base condition, but the air cavity and glass cover temperatures are far higher than the ambient. This illustrates the impact of the night cover as heat is being lost from the absorber plate via convection, but it is not being transferred as effectively via radiation. As radiative heat losses have the most damaging influence on night-time heat loss, the night cover clearly offers an effective solution.

4.3.3.3 Thermal stratification

In terms of thermal stratification, Figure 4.21 plots the three designs across a 19-hour period, from midnight to 19:00 hours. Stratification varies across the three conditions, but similar patterns emerged with the strongest stratification experienced around midday, 13:00 hours for the base and night cover systems and 12:00 hours for insulated, and strong destratification in the afternoon. This breakdown of thermal layers in the afternoon can be explained by the lack of water draw-off. Draw-off promotes stratification as it prevents the tank from reaching thermal equilibrium; as the water store charges, i.e. after draw-off periods, stratification is strong. However, over the afternoon the system reaches a quasi-steady state where the temperature in the upper layers of the tank are established. This creates a density gradient between the top and bottom of the tank which drives buoyant convection, allowing the lower layers to achieve similar temperatures. This decreases the density gradient, i.e. the stratification. Additionally, due to the maritime climate, solar insolation is more intermittent in the afternoon, after being relatively consistent in the morning (see Figure 4.16).

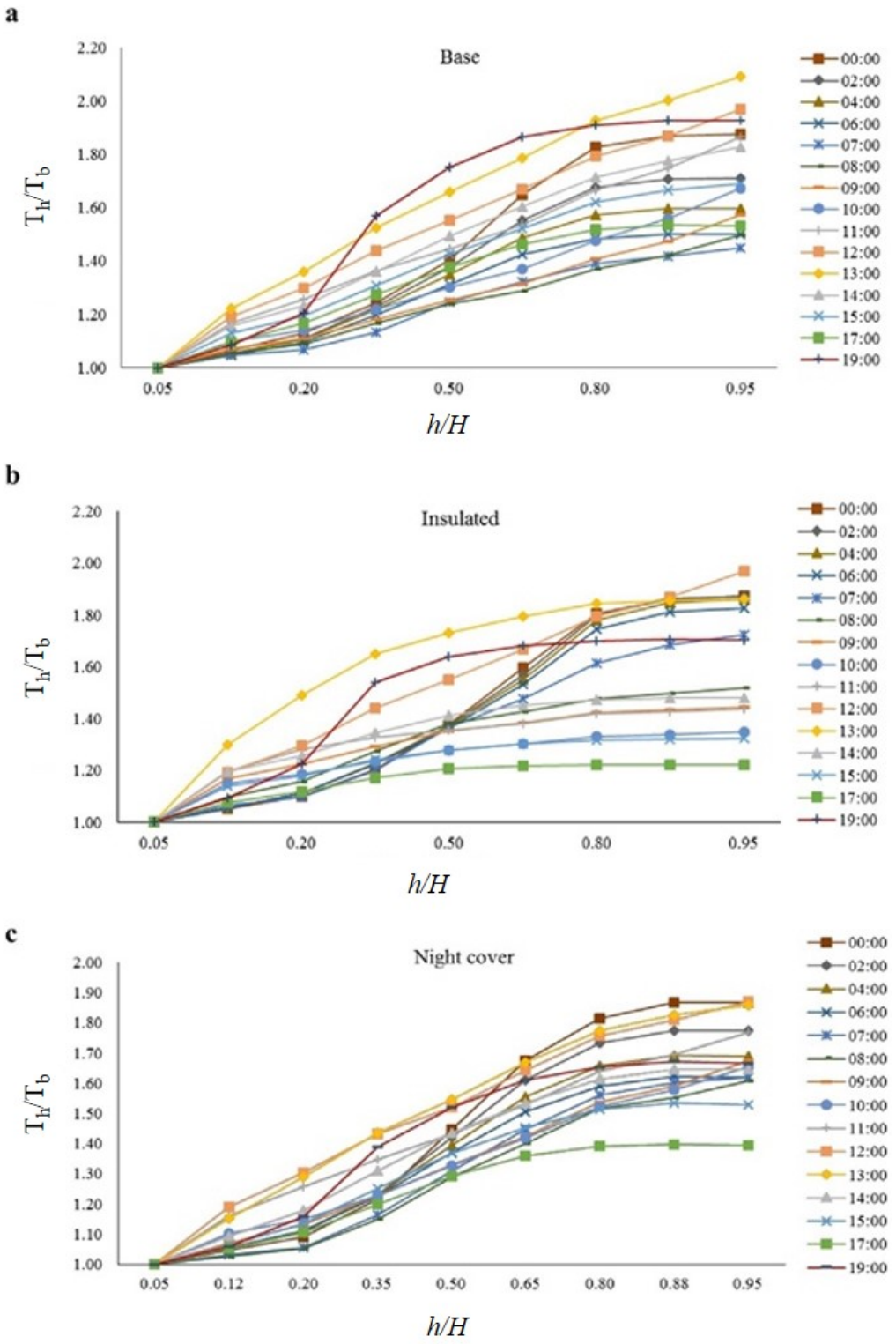

Figure 4.21: Thermal stratification in the three design conditions of the baffled collector over 19 hours. Dimensionless longitudinal stratification, T_h / T_b versus dimensional collector height, h / H

The base and night cover systems suffer steady destratification overnight, but the base condition is impacted more heavily with the weakest stratification occurring at 07:00 hours whereas the weakest stratification occurs at 17:00 hours for the insulated

and night cover systems. This further illustrates the heat retention properties of the latter two conditions; in the base condition, heat is steadily lost to the ambient environment reducing the density gradient. However, in the insulated system, stratification is relatively consistent from midnight to 06:00 hours, experiencing stronger destratification at 07:00 hours due to the first draw-off of the day with no potential to recharge. The only deviation from the observed pattern is in the insulated system which experiences destratification between 08:00–10:00 hours while the other two conditions steadily build stratification. This could be due to a sudden drop in solar insolation or the additional insulation covering the top third of the absorber plate. The upper water layers are not subject to any direct solar gain thus they rely on convective heat transfer. This means that the lower layers will heat up, reducing the temperature difference between the top and bottom of the tank, until the buoyancy effect becomes noticeable.

4.3.3.4 Energy

A final comparison is the energy contribution, illustrated in Figure 4.22, and the overall collection and heat retention efficiencies. Figure 4.22 shows that, for the summer months, the system with the night cover provides the most energy due to the improved heat retention; there is more energy available for the early draw-off events. However, in the autumn months, a limitation in the testing methodology emerges due to the variability in solar insolation for each of the three cases. Despite this, in September the insulated and night cover systems receive similar insolation levels, lower than the base condition, and the latter still significantly outperforms the former. Therefore, the night cover is a more effective heat retention method due to the greater available absorber area. In October, the insolation declines significantly across the month meaning the round-robin style of testing did not allow a fair comparison. However, the base and insulated conditions have the same insolation and the latter is again outperformed. The system with the night cover showed barely any energy gain as the inlet temperature was often close to the tank temperature, as it was heated by the ambient building and solar insolation was too weak.

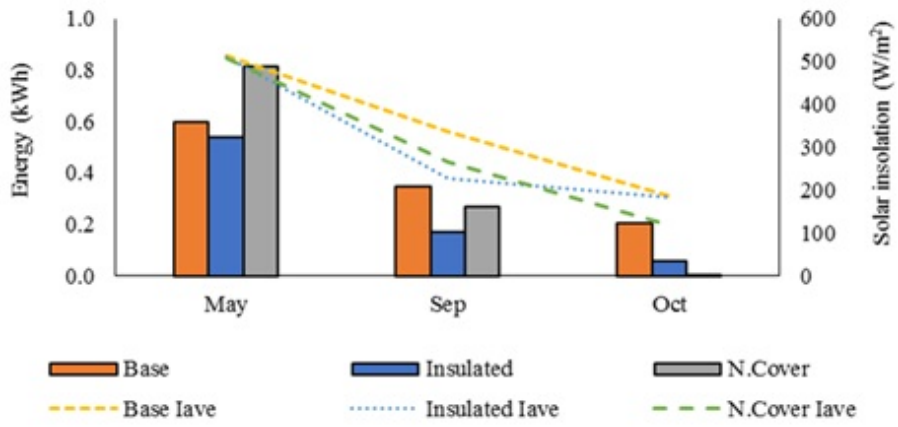

Figure 4.22: Total average daily energy provided by the three design conditions across the 11 draw-off periods and the average incident solar radiation across the collection periods of the data presented

To determine collection (η_{col}) and heat retention (η_{ret}) efficiencies, the following equations were used (Smyth et al., 2019), and the results are presented below:

$$\eta_{col} = \frac{Q_{col}}{Q_{incident}} x100 \tag{4.2}$$

$$\eta_{ret} = \left(\frac{mC_p(T_{final} - T_{amb})}{mC_p(T_{initial,c} - T_{amb})} \right) x100 \tag{4.3}$$

where Q_{col} and $Q_{incident}$ are the thermal energy collected by and incident on the absorber plate, respectively. m is the mass of water required (kg), C_p is the specific heat capacity of water (J/kg·K), and T_{final}, $T_{initial,c}$ and T_{amb} are the final and initial temperatures and average ambient temperature of the cooling period (K), respectively. Note that Equation 4.3 can only be applied for conditions where the initial water temperature is above ambient temperature.

Overall, available energy is more dependent on incident radiation than heat retention as draw-offs occur during the day. However, based on the performance in the summer months, where all three conditions experience the same level of solar insolation, it is assumed that the same pattern would continue across all seasons if side-by-side testing was conducted. In terms of collection and heat retention efficiency, the base collector demonstrated an average collection efficiency of 32% and heat retention efficiency of 24%. The insulated collector showed collection and heat retention efficiencies of 25% and 35%, respectively, and for the night cover 30% and 36%, respec-

tively. All efficiency values are for the summer months as they provide the most reliable comparison. The 2% difference between the base and night cover collection efficiencies could be due to the application and removal of the night cover, at 17:00 and 08:00 hours respectively, which could have lost the tail-ends of solar gain.

4.3.4 Summary of heat retention methods

System performance, in terms of heat retention, can be clearly ranked with the night cover condition at the top, followed by the insulated and finally base conditions. Despite achieving the lowest bulk water temperatures during the collection period, the insulated system can retain heat more effectively than the base configuration. The insulation covers the hottest portion of the water body and heat loss would mainly be due to destratification and heat loss from the bottom two-thirds of the absorber plate. The base configuration suffers steady heat loss from the entire absorber area. The night cover has the best overall performance; not only does it achieve the highest temperatures during the collection period, on par with the base condition, but it also provides the highest temperature in the morning by a significant margin. The higher bulk water temperature would be enough for this condition to have the poorest heat retention; the hotter the water, the faster heat is lost due to the temperature difference between the water and the ambient environment. However, the addition of the night cover offers an effective barrier against radiative heat losses thus a substantial proportion of the heat gained is retained. Throughout the day, the base collector offers the highest thermal stratification and efficiencies, followed closely by the night cover conditions, and the insulated system has the poorest due to its reliance on convective heat transfer to the upper layers as opposed to direct solar gain.

4.4 Integration in roof structure

Both the frame and SIP systems have the same basic construction; the ICS backed by insulation and covered with a glass lid. However, notable differences lie in the type and thickness of insulation and the level of integration in the building fabric. For the

SIP system, the ICSSWH is embedded directly into it, whereas the frame system sits on top of the pre-existing roof structure. The latter has the advantage of being a simple retrofit solution, but the SIP system offers more protection and greater insulation. Table 4.5 outlines the components of the two options that contribute to the heat loss from the back of the collector, along with the thermal properties. As both the frame and SIP systems have the same front cover construction, that element is not reviewed for this comparison. The rate of heat lost from an object is a function of its U-value, the heat loss coefficient, U. Therefore, the heat loss coefficient for the frame and SIP can be determined from the inverse of the total thermal resistance, where d is the material thickness and k is its thermal conductivity.

Table 4.5: Components for the frame and SIP that contribute to heat loss from the back of the system

Frame				**SIP**			
Material	***d* (m)**	***k* (W/m·K)**	**R-value (m^2·K/W)**	**Material**	***d* (m)**	***k* (W/m·K)**	**R-value (m^2·K/W)**
Stainless steel	0.0015	14.9	0.0001	Stainless steel	0.0015	14.9	0.0001
Celotex	0.04	0.022	1.82	EPS	0.122	0.031	3.94
Plywood	0.018	0.13	0.14	OSB	0.004	0.13	0.03
U-Value (W/m^2·K)		**0.51**		**U-Value (W/m^2·K)**		**0.25**	

The values determined from this method, 0.51 and 0.25 W/m^2·K for the frame and SIP systems respectively, are comparable to the values calculated from the following more robust method. Visser and van Dijk (1991 [in Smyth et al., 2018]) reviewed test procedures for short term thermal stores and derived the following equation to determine the heat loss coefficient of a system:

$$U_{system} = \frac{mc_{system}}{A_{unit}\Delta t} \ln\left(\frac{(T_{initial,c} - T_{amb})}{(T_{final} - T_{amb})}\right) \tag{4.4}$$

where mc_{system} is the thermal mass of the system, a product of the mass and specific heat capacity of the individual units, A_{unit} is the area heat is being lost from, and Δt is the duration of the cooling period, in seconds. Based on this calculation the heat loss coefficients of the frame and SIP systems are 0.56 and 0.21 W/m^2K, respectively.

Energy loss from a system can be defined as the product of the area heat is being lost from, the heat loss coefficient, the log mean temperature difference ($\ln[\Delta T]$) between the start and end of the cooling period and the ambient temperature, and the duration of the cooling period, as shown by Equations 4.5 and 4.6 (Velraj, 2016):

$$Q_{lost} = A * U_{system} * \ln(\Delta T) * \Delta t \tag{4.5}$$

Where:

$$\ln(\Delta T) = \frac{(T_{initial,c} - T_{amb}) - (T_{final} - T_{amb})}{\ln\left((T_{initial,c} - T_{amb}) - (T_{final} - T_{amb})\right)} \tag{4.6}$$

By calculating Equation 4.6 and substituting into Equation 4.5, the energy loss across the cooling period, in kJ, from the back surface of the storage tank can be determined for each system. The thermal network shown in Figure 4.23 gives a visual representation of the thermal interactions between each surface in the system. For this comparison only the 'back losses' are considered. Based on the output of Equation 4.5, the energy losses from the frame and SIP systems are 261 and 118 kJ, respectively. The data used in the calculation was taken from the baseline testing phases with ambient environmental conditions as closely matched as possible, as with the comparisons presented in previous sections.

Therefore, in terms of U-value, the SIP system shows a 159% improvement and 145% for heat loss from the back wall, a significant heat retention contribution. These values are slightly misaligned due to the differing external conditions. As previously mentioned, due to the nature of the experimental testing phase it is not possible to have identical days for comparison. It should also be noted that in the final installation of an ICSSWH, the SIP will form part of the roof structure. Therefore, heat losses will be further reduced as heat loss through the back of the system is to the internal home, not the external ambient environment, so the temperature difference across the surfaces will be smaller.

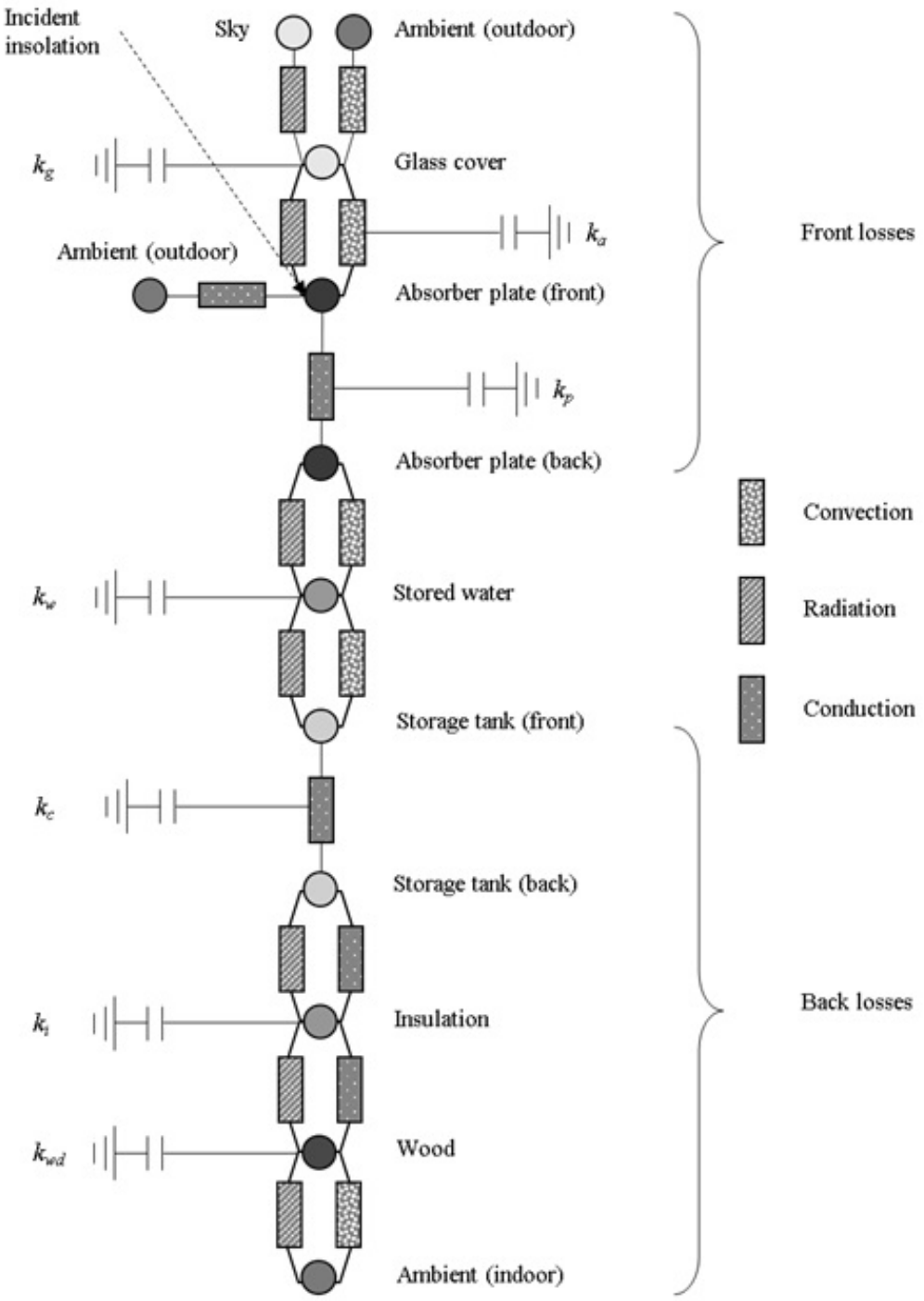

Figure 4.23: Thermal network of an ICSSWH, where k is the thermal conductivity of each component of the system

4.5 Concluding remarks

This chapter presented the results of the extended field experiments for the baffled and finned configurations under the three design conditions; base (as designed), additional insulation, and a night-time cover. First, the baseline performance of the finned and

baffled systems was compared which showed that the baffled system consistently outperformed the finned, providing an average of 4% more energy to the end user and 6% less energy loss during the non-collection period. Next, the heat retention methods were reviewed alongside the base condition. The addition of a night-time cover offered clear performance improvement with collection efficiencies comparable to the base configuration and 12% greater heat retention efficiency. Compared to the additional insulation, the heat retention efficiency is similar to the night cover condition, but the collection efficiency is 5% greater. Therefore, overall, a baffled configuration with a night cover offers the best thermal performance.

Chapter 5 discusses the environmental impacts of each design configuration and condition to determine whether the thermal performance and sustainability of the system can be balanced. A greater thermal performance may be at the cost of environmental sustainability which brings into question the suitability of the ICSSWH designs for commercial production. Therefore, Chapter 5 presents a detailed life cycle assessment, considering both disposal and reuse at the end of the systems useful life.

Fifth Chapter

Life Cycle Assessment

This chapter discusses the Life Cycle Assessment (LCA) of the proposed design configurations alongside the additional heat retention methods. Also, the difference between housing the collectors in a wooden frame versus embedding them in the building fabric, i.e. in structural insulated panels (SIPs) of warm roof timber construction. This LCA follows the methodology stipulated in the ISO14040 (2006) standard and discussed in Chapter 3. First, the goal and scope of the LCA is defined followed by an inventory of all the components required to fulfil the functional unit (FU). Then the Life Cycle Impact Assessment (LCIA) is presented and the environmental impact of the various design configurations and conditions is quantified. Finally, the results of the LCIA are interpreted and sensitivity and uncertainty analyses are carried out.

5.1 Goal and scope

The goal of the present LCA is to comparatively assess the environmental performance of a novel integrated collector-storage solar water heater (ICSSWH) under different design conditions and configurations. The aim is to determine whether this potential contributing solution to the current energy crisis is sustainable in terms of the energy and carbon investment required to produce these systems. If the capital energy and carbon cost cannot be offset within the product's useful life, then it is deemed unsustainable.

The product systems under evaluation are the finned and baffled base configura-

tions both with and without the heat retention methods and housed in an insulated frame versus integration into a SIP component of warm roof timber construction. The functional unit (FU) of the systems, i.e. the basis for comparison, is defined here as one ICSSWH unit designed to provide domestic hot water for a single occupancy dwelling, based on a consumption of 52 l/day, over a service life of 20 years. As discussed in Chapter 3, Section 3.3.1, one FU includes the collector and associated fittings but pipework to and from the collector is excluded as it is assumed that this is already in place before its installation. The system boundaries, specifying which unit processes are part of the product system, are defined in Chapter 3, Section 3.3.3. Unit processes are the smallest elements of the LCI for which input and output data are quantified. Both a linear and circular analysis are conducted as part of this research, thus stages A-D are considered. Additionally, different environmental impact categories will be reviewed to determine the impact of the product system on climate change, ecotoxicity, human health and resource availability.

For this LCA, the following assumptions have been made:

- The ICSSWH systems can function, without diminished performance, for a service life of 20 years, based on the review of existing research
- Transport within each relevant stage of the life cycle was taken to be 50 km as it is assumed that any necessary travel, such as from the manufacturer to the site or from the site to a landfill, is within a 50 km radius
- In terms of maintenance, the gasket is assumed to be replaced every 5 years. All other components are assumed to have a life span of 20 years, equal to the collector.

Limitations of the current LCA include:

- The data included in the Ecoinvent database is not geographically specific, European data is the highest level of accuracy for most materials in the inventory

- The lack of data available in the Ecoinvent database for the aerogel insulation (for the additional insulation condition) resulted in the use of an EPD which only models cradle-to-gate
- The energy analysis of the ICSSWH systems was limited due to the amount of experimental data collected. Extrapolating recorded data to provide an annual energy contribution is therefore considered a worst-case scenario.

5.2 Life cycle inventory

This assessment requires several LCIs to account for the different base configurations, heat retention methods and mounting system. Full material inventories are provided in Appendix B and a summary of the construction components is given in Table 5.1. The LCA tool used in the analysis is SimaPro v9.0 equipped with the Ecoinvent database v3.5, using European data The Ecoinvent processes used for the LCIs and the life cycle stages (i.e. production, transport, maintenance, and end-of-life treatment options) are provided in Appendix C.

Table 5.1: Summary of construction components required to create the different system scenarios. Configuration/condition specific components are indicated with additional information given in brackets, e.g. "Absorber Plate (*Baffled*)" is specific to the baffled configuration.

	Component	**Material**	**Mass (kg)**	**% Overall weight**
Collector	Tank base	1.5 mm Stainless steel	14.4	20.8
	Absorber plate (*Baffled*)	3 mm aluminium	8.5	12.3
	Absorber plate (*Finned*)	3 mm aluminium	9.7	14.1
	Absorber plate coating	Black spray paint	0.7	1.0
	Sparge tube	Copper	0.58	0.8
	Gasket	EPDM rubber	0.37	0.54
	Gasket sealant	Hylomar	0.1	0.14
	Compression Reducing Coupling 22mm-15mm	Copper with brass finish	0.1	0.14
	Compression Straight Coupling 15mm	Copper with brass finish	0.07	0.1
	Hose fitting	Copper with brass finish	0.01	0.02
	6 mm screws	Steel	1.01	1.46
	6 mm Nylock nuts	Stainless steel	0.13	0.19
	6 mm washers	Steel	0.26	0.37
	Sparge tube supports	Polycarbonate	0.002	0.003
	Baffle plate (*Baffled*)	4 mm Polycarbonate	1.55	2.2
	Baffle plate supports (*Baffled*)	Polycarbonate	0.001	0.001
Frame	Glazing	4 mm Glass	11.0	15.9
	Frame	18 mm Plywood	28.3	40.9
	Screws	Steel	0.02	0.03
	Sealant	Silicon	0.005	0.007
	Insulation	40 mm Celotex	2.0	2.9
	Waterproofing	Black paint	0.005	0.007
Heat retention	Absorber plate insulation (*Insulated*)	Spacetherm© Areogel	0.96	1.37
	Channels for night cover	Aluminium (Alloy 6082T6)	0.7	1.0
	Night cover insulation	Airtec aluminium foil bubble insulation	0.35	0.5
	Roller for night cover	Aluminium	0.28	0.39
	Supports for roller	Plywood	0.08	0.11
	Stabilising band	Polycarbonate	0.11	0.15
	Screws for night cover	Steel	0.005	0.007

5.3 Life cycle impact assessment

There are 24 scenarios evaluated in this section, as detailed in Chapter 3, Section 3.3.4 (Table 3.9). The design configurations (baffled/finned) and conditions (heat retention methods) are reviewed alongside the mounting system (SIP/frame) used from both a linear and circular perspective. Linear refers to cradle-to-grave, i.e. stages A-C of the ISO framework, and circular is cradle-to-cradle, i.e. stages A-D. This section is split into two parts. First, the 24 scenarios are analysed using IPCC 2013 Global Warming Potential (GWP) 100a (v1.03) and Cumulative Energy Demand (CED, v1.10) assessment methods to determine the carbon and energy impacts across the life cycle (whether linear or circular) of the different design set-ups. This was done using European data in Ecoinvent v3.5 where possible. Note that here carbon impact is used as shorthand for GWP and the six Kyoto GHGs that are considered within carbon dioxide equivalents (Carbon Trust, 2017). Second, the additional environmental impacts are presented for select design configurations and conditions to determine the impacts at midpoint, i.e. part-way along the cause-effect chain, and at endpoint, i.e. damage to the areas of protection. Here, the assessment methods used are the CML-IA baseline (v3.05) for the characterisation of midpoint impacts and ReCiPe 2016 Endpoint (H, v1.02) to determine the damage to the areas of protection.

For components made of the same material the total quantity was summed and added to the process flow. When a product, or a reasonably similar product, could not be found in the database an Environmental Product Declaration (EPD) was used. An EPD is a voluntary environmental impact statement for a product or system, allowing consumers to objectively compare the environmental performance of products. In the current analysis, only full life-cycle data for the additional insulation used for heat retention was not listed in the database. The EPD for this insulation (Renuables, 2015) was found and the values for the GWP 100 and CED were added to the final LCIA output. However, only data for Stages A1-A4 were included in the EPD thus the other stages are omitted from the analysis. Therefore, for the scenario with additional insulation, a

carbon impact of 4 $kgCO_{2e}$ was added to the plain configuration values for the carbon analysis and an energy impact of 83 MJ was added for the energy analysis.

5.3.1 Energy and carbon analysis

In this section, the carbon and energy impact of the 24 scenarios are quantified. The baffled and finned configurations are first evaluated separately in Sections 5.3.1.1 and 5.3.1.2 and then compared against each other in Section 5.3.1.3.

5.3.1.1 Baffled configuration

Figure 5.1 illustrates the carbon impact of the baffled configurations and Figure 5.2 details the energy impact, in order of increasing impact. For GWP, the linear scenarios always have a greater carbon impact than the circular as simply leaving the materials in a landfill has significant carbon impacts. There is no recovery or offset potential in a linear scenario. The difference between the circular SIP and linear SIP scenario is not as drastic as with the frame. This is because landfilling the frame causes the carbon sequestered in the timber to be released creating a much more significant carbon impact.

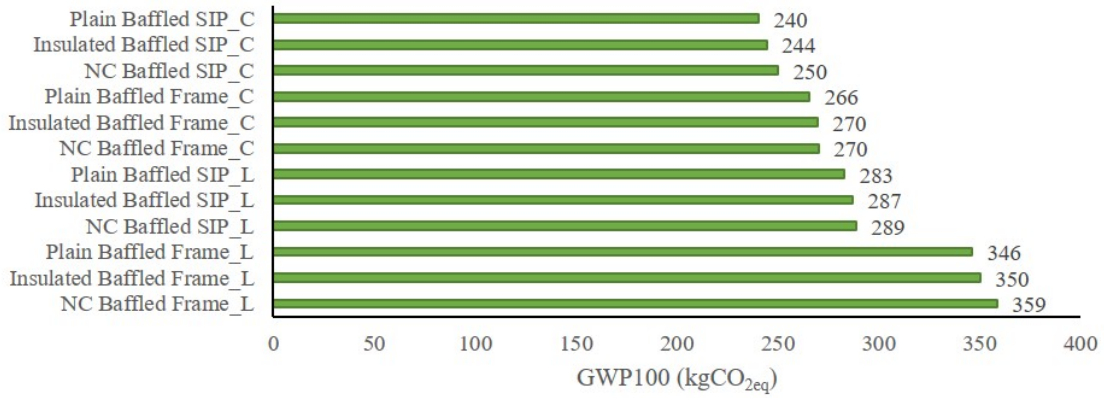

Figure 5.1: *GWP100* comparison for baffled configuration scenarios. NC – night cover, L – linear, C - circular

Figure 5.2: *CED* impact comparison for baffled configuration scenarios. NC – night cover, L – linear, C - circular

There is a clear hierarchy in the GWP results – recovering materials in a circular scenario is always the best option and within that, housing the collector into SIPs is the best case. In terms of the design conditions, the carbon impact increases in line with the complexity of the heat retention method. The plain, as designed, collector has the lowest impact, followed by the collector with additional insulation and finally the night cover set-up. This reflects the additional materials required in the assembly. However, the difference across the three design conditions is marginal.

However, when it comes to CED, different trends appear. The configuration with the SIP is always the best option and within that, the ranking is more mixed. Regarding energy consumption, the plain design is again the best-case scenario followed by the insulated system and then the night cover, as with GWP. Using a frame mounting system can consume, on average, 70% more energy than the SIP set-up.

The pattern seen in the circular and linear scenarios is explained by the modelling process. In the circular scenario, the end-of-life processing for reuse/recycling are not modelled as it is assumed that the materials simply exit the system. The burden of processing the waste falls on to subsequent life cycles as it is there that the benefit of avoided products is accounted for. For example, the ICSSWH is modelled using raw materials, it does not get the benefit of avoided products, i.e. recycled content. When dismantling the ICSSWH at the end of its useful life, the main components, i.e. steel, aluminium, glass and wood, exit the system boundaries. Future products using these

components then account for the processing of the waste materials as a new input into the life cycle, thus gaining the benefit of not using virgin materials which far exceeds the impacts associated with reuse/recycling. Therefore, the small difference seen between the circular and linear scenarios within each configuration and condition is down to the energy required to landfill the materials.

Due to new business models underpinned by circular economy principles (Lacy and Rutqvist, 2016), future life cycle scenarios will use the materials harvested from the end-of-life stage of the previous life cycle. Therefore, end-of-life energy would be much higher than that required to simply landfill the materials. However, the energy avoided in the production stages, Stage A1 (and potentially Stage A2) as virgin materials do not need to be extracted and processed, would more than compensate the reuse/recycling impacts due to the highly recyclable nature of the main system components. This circular scenario would result in net energy savings and the ICS systems' hierarchy would be similar to that of GWP.

Given the continuing decarbonisation of energy but increasing scarcity of resources and dangers of global warming, the greatest consideration lies with GWP. Despite the marginal difference in energy impact between the linear and circular scenarios, linear has significantly higher carbon impacts, particularly in the case with the collector housed in a frame. Recovery and processing of materials will become progressively more sustainable with the current trend of decarbonisation. Therefore, the focus should be on the final stage of the life cycle; recovery, reuse, recycle.

5.3.1.2 Finned configuration

Figure 5.3 illustrates the carbon impact of the finned configurations and Figure 5.4 details the energy impact. The same pattern as seen in the baffled configurations is also observed in the finned. For GWP, the linear scenarios always have a greater carbon impact than the circular while for the CED, configurations with the SIP is always the best option and within that, energy impact increases with the complexity of the heat retention method. With a SIP mounting system, a linear approach has a similar energy consumption as a circular one (0.3% more) while creating 18% more emissions (this

is because materials in landfill do not use energy but do instead emit GHGs, such as is the case with timber). With a frame mounting system, a linear approach consumes 0.2% more energy than a circular one and creates 30% more emissions. Therefore, the differences between a linear and circular approach are less stark when the system is mounted in a SIP. When using a frame, the plywood significantly contributes to life cycle impacts.

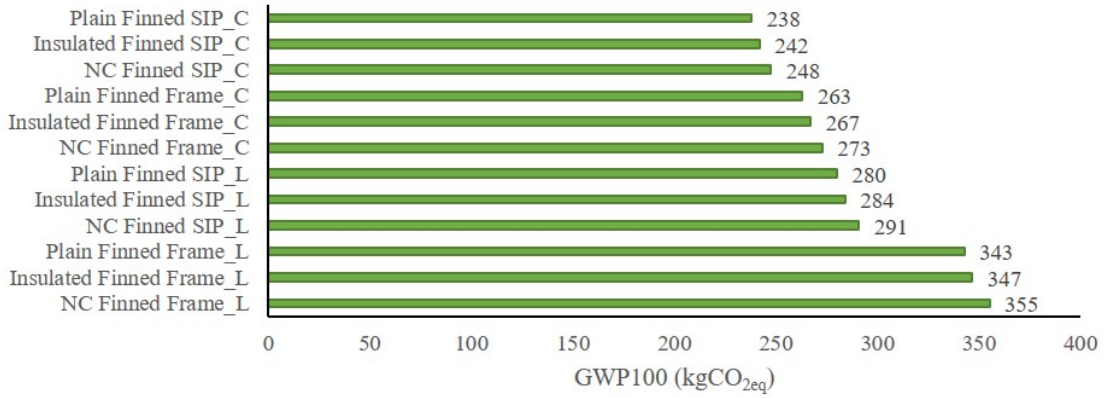

Figure 5.3: *GWP100* impact comparison for finned configuration scenarios. NC – night cover, L – linear, C – circular

Figure 5.4: *CED* impact comparison for finned configuration scenarios. NC – night cover, L – linear, C - circular

5.3.1.3 Baffled and finned comparison

This unique ICSSWH was designed to be integrated into warm roof timber construction. Therefore, for this comparison only the SIP scenarios will be used. Additionally, for both carbon and energy, the configurations incorporated into SIPs were the best-case

scenarios. First, the baffled and finned collectors will be compared at a system level, i.e. comparing each configuration and condition against the other. Following that, a comparison at the material level is presented, i.e. evaluating the impact of each component required to produce collector configuration/condition.

System level comparison Figure 5.5 and Figure 5.6 respectively show the carbon and energy impact of the baffled and finned collectors, integrated into the SIP mounting system and under the different heat retention methods. This comparison highlights how similar these two configurations are in terms of embodied GHG emissions. Figure 5.5 demonstrates the benefits of a circular approach when concerned with the carbon impact. The finned system consistently outperforms the baffled, albeit with a minimal difference, as the polycarbonate used for the baffle plate has a higher impact than the additional aluminium required for the fins. Also, by adopting a circular approach, that aluminium can be reused or recycled thus offsetting the carbon investment required when mining and extracting the raw materials for virgin aluminium for future products. If Stage D is not considered, the carbon impact of the system is much higher; an 18% increase with a linear approach over a circular one. As seen previously, with the additional materials and relative complexity of the heat retention methods, the carbon impact increases. Under a circular scenario, additional insulation creates 1.7% more emissions for both the baffled and finned collectors over the plain condition while incorporating a night cover increases emissions by approximately 4%. The process networks for the plain baffled and finned collectors integrated into the SIP, under both linear and circular scenarios, are presented in Appendix D, to highlight the major contributing stages to global warming potential.

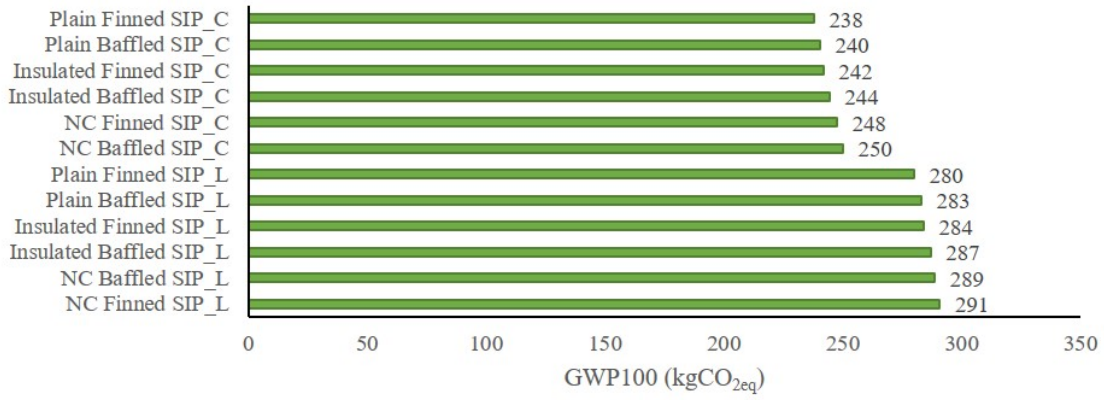

Figure 5.5: *GWP100* impact comparison for baffled and finned configuration scenarios, with a SIP mounting system. NC – night cover, L – linear, C – circular

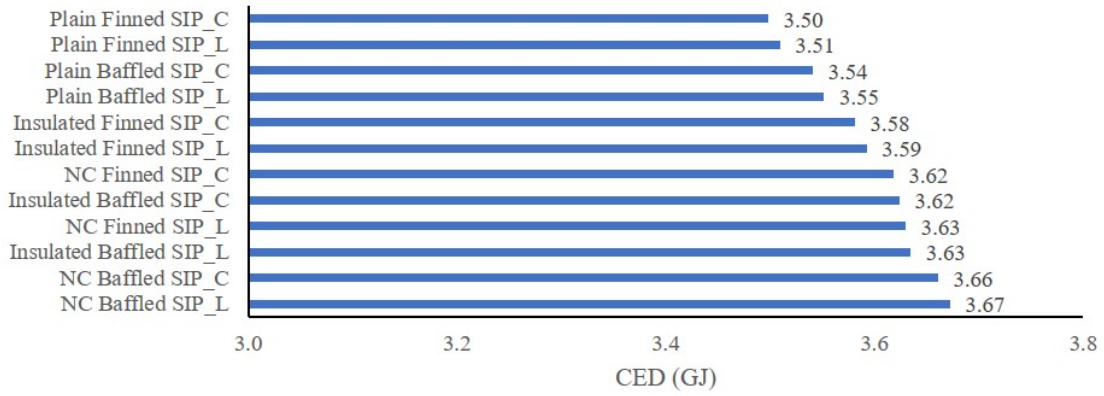

Figure 5.6: *CED* impact comparison for baffled and finned configuration scenarios, with a SIP mounting system. NC – night cover, L – linear, C – circular

In terms of embodied energy, the finned system again outperforms the baffled and the plain condition has the lowest energy requirement from both the linear and circular approaches (Figure 5.6). There is only a 0.3% increase with a linear scenario over circular due to the energy required to send the materials to landfill. Within both the linear and circular scenarios, the plain baffled system consumes 1.2% more energy than the plain finned. This is due to the inclusion of the polycarbonate baffle plate. Additional insulation consumes 2.3% and 2.4% more energy than the plain condition for the baffled and finned collectors, respectively. However, the data used for the aerogel insulation is incomplete as the EPD only considers Stages A1-A4, therefore the impact would potentially be greater if disposal was also considered. Adding a night cover to the baffled and finned collectors requires 3.4% more energy in both cases due to aluminium

used in its construction.

An interesting point to note is that there is less conformity when it comes to the embodied energy of the insulated and night cover conditions. When evaluating the embodied carbon there is a clear trend; plain produces the least emissions followed by the additional insulation, followed by the night cover. However, in terms of embodied energy, there is a more mixed trend. The differences between insulated baffled systems and the finned system with a night cover are marginal and can be attributed to the energy required to extract the collector materials; the polycarbonate used for the baffle plate significantly increases the energy impact. The contribution of the materials that make up the collectors is presented in the following section. The focus here is on carbon impact as this is deemed the more important metric, due to the scarcity of resources and current climate emergency discussed above.

Material level comparison On a material level, the components of both collectors are broken down into steel, aluminium, glazing, plywood, paint, copper, and rubber. For the baffled collector, polycarbonate is an additional material. Figure 5.7 shows the carbon impact share for the total mass of each of these components for both the baffled and finned collectors, without a mounting system. For both collectors, steel represents the highest impact share at 53% and 53.5%, respectively (Table 5.1). The higher share of steel in the finned collector reflects the absence of the polycarbonate used for the baffle plate. Aluminium ranks second at 31.9% and 36.6% of the impact share for the baffled and finned collectors, respectively. Aluminium in the finned collector has a higher impact as more of it is required to produce the fins. Despite having a lower carbon intensity per unit of mass (i.e. $kgCO_{2e}/kg$), the carbon impact of steel is greater than aluminium due to the greater mass used and the relatively small difference in emissions from their production. Also, even though the glazing contributes to a higher percentage of the overall collector weight than aluminium, the carbon impact is lower due to the much higher carbon intensity of aluminium production. Note that the data presented in this section is purely for the collector components and only the cradle-to-gate life cycle stage is considered.

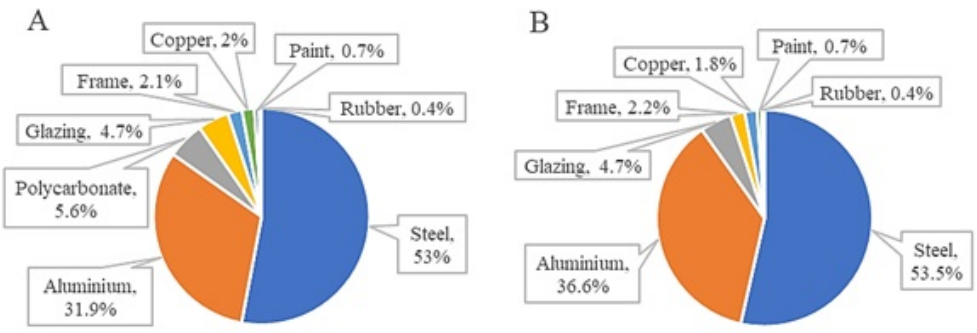

Figure 5.7: Carbon impact share for the total weight of each component for the baffled [A] and finned [B] collectors

Figure 5.8 presents these results after normalising them to account for the weight of each component and from this figure carbon hotspots can be identified. For the baffled collector, the polycarbonate used to create the baffle plate and the aluminium from the absorber plate contribute the most emissions per unit of mass, both at 23% of the impact share. This is followed by the steel from the tank, at 21%, then the copper for the pipework, at 15%. After normalisation, steel and aluminium have a similar carbon impact due to the Ecoinvent processes that were chosen and the percentage content of recycled material. Despite every effort to select appropriate processes that most accurately represent the material inputs and geographic location, there is still error and uncertainty associated with the software and databases.

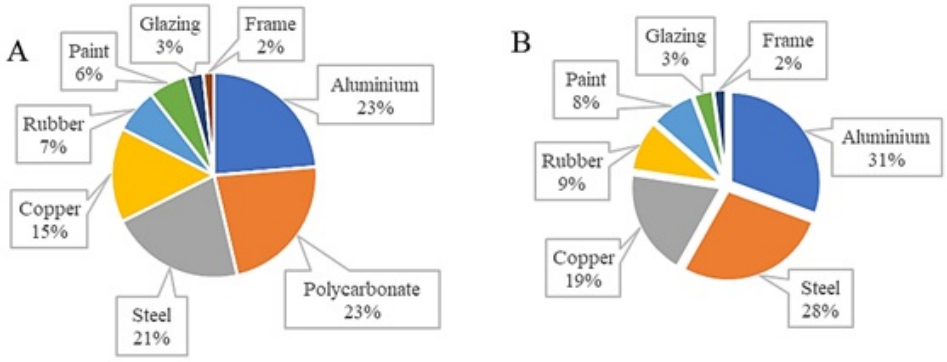

Figure 5.8: Cradle to gate carbon hotspots for plain baffled [A] and finned [B] collectors in SIP (best case scenario). Split is derived from embodied carbon values that have been normalised by weight

The identification of these hotspots allows the design to be re-evaluated and to potentially substitute or refine the materials or processes for a lower carbon impact. For example, in the baffled system, the baffle plate could be constructed out of a less

carbon intensive material like steel; its function is to create a separate layer of water and it does not matter if it has a thermal mass. Adapting other hotspots, such as steel, risk affecting the thermal performance of the ICSSWH system and would therefore need to be considered and modelled carefully. For example, the aluminium used for the collectors under evaluation has a thickness of 3 mm. Based on the analysis conducted by Garnier (2009), if this was to be reduced to 1.5 mm the embodied carbon would halve with minimal impact on the thermal performance (0.1%). However, as evidenced through the current research, using 1.5 mm aluminium sheet risks structural integrity and welding ability when incorporating fins.

When looking at the ICS systems from a cradle-to-cradle perspective, the life cycle hotspots can be identified. The life cycle stages are split into Stage A1-A3 (raw material extraction and manufacturing), A4 (transport), A5 (installation), B (maintenance/replacement), and C/D (end-of-life). Most emissions occur upstream, i.e. before the collector begins its useful life. Transport has a negligible impact and the end-of-life impacts are nil as that burden is passed on to subsequent life cycles, as discussed previously. The manufacture of the collector (Stage A3) has the highest impact share at 39% and 40% for the baffled and finned collector, respectively. Within that, the manufacture of aluminium accounts for 44% of the impact share, copper accounts for 31% and steel has the lowest share at 25%, when normalised per unit of mass. As evidenced by the greater normalised impact of aluminium over steel shown in Figure 5.8, this also highlights the greater carbon intensity of aluminium processing.

The extraction and transport of the raw materials (Stage A1-A2) required to produce the collector has the second highest impact share at 33% and 31% for the baffled and finned collectors, respectively. Maintenance, i.e. replacing the gasket, accounts for 28% of the impact share for both collectors. This shows that more than two thirds of the carbon impact occur upstream, in the extraction and manufacture of the materials. Therefore, efforts to minimise the carbon intensity of these ICSSWH collectors should be focussed here.

5.3.1.4 Uncertainty analysis

When conducting an LCA it is important to account for the uncertainty that characterises LCA data. Uncertainty analyses provide a probable range within which the impacts of the product or system being modelled with likely fall, as opposed to a single, definite value. SimaPro can deal with data uncertainty analysis through the Monte Carlo simulation approach. The Monte Carlo method generates an uncertainty range by randomly selecting a value within a given uncertainty range for each of the inputs and repeating this process with a different set of randomly selected values for a number of runs. This provides the mean, standard deviation and coefficient of variation for a given data set with a confidence interval of 95%. For the current uncertainty analysis, the software performed 1,000 runs and built up an uncertainty distribution, resulting in the data presented in Table 5.2. The probability distributions associated with this data are provided in Appendix E. Note that the insulated scenarios are not modelled here; as the aerogel insulation is not in the Ecoinvent database, the uncertainty analysis could not be done in SimaPro.

The mean values show the average carbon impact for each design configuration/ condition are randomly selecting values from within the uncertainty ranges associated with each of the materials in the LCI. The standard deviation (SD) indicates the spread of the values across the mean and here one standard deviation ranges from 12.18 for the 'Plain Baffled SIP C' scenario to 21.01 for the 'NC Baffled SIP C' scenario. Based on this, only four single point estimates fall within 1SD of the mean, four are within 2SD, five are within 3SD and three are significantly out with 3SD. The coefficient of variation (CV) is also known as the relative standard deviation, i.e. the SD relative to the mean. CV is important for comparing the results of different data sets, while SD ranges from 12.18 – 21.01, CV has a much smaller range of 5.05% to 6.37%. Therefore, each scenario has a similar level of variation relative to the mean value. Comparing the obtained results against the mean and SD of the uncertainty analysis show that, in a few of the scenarios, the difference is statistically significant. Therefore, the results of those analyses are not reliable.

Table 5.2: Uncertainty analysis for IPCC GWP 100. SD – standard deviation; CV – coefficient of variation; green indicates the actual value fails within 1SD from the mean, for amber they fall within 2SD, red are within 3SD and black are significantly out with 3SD

Scenarios	Single point estimate ($kgCO_{2e}$)	Mean ($kgCO_{2e}$)	SD ($kgCO_{2e}$)	CV (%)
Plain Finned SIP, L	280	278.6	14.57	5.23
Plain Baffled SIP, L	283	284.5	14.48	5.09
NC Finned SIP, L	291	327.4	17.11	5.23
NC Baffled SIP, L	289	330.1	16.07	6.35
Plain Finned Frame, L	**343**	269.1	14.47	5.38
Plain Baffled Frame, L	**346**	273.8	13.84	5.05
NC Finned Frame, L	**355**	279.3	14.72	5.27
NC Baffled Frame, L	359	319.0	17.29	6.34
Plain Finned SIP, C	238	212.8	12.51	5.89
Plain Baffled SIP, C	240	217.8	12.18	5.59
NC Finned SIP, C	248	222.1	12.60	5.67
NC Baffled SIP, C	250	253.2	21.01	6.37
Plain Finned Frame, C	263	238.6	13.44	5.63
Plain Baffled Frame, C	266	243.2	12.65	5.20
NC Finned Frame, C	273	247.1	13.59	5.50
NC Baffled Frame, C	270	272.8	17.70	5.55

This reflects the high level of uncertainty associated with life cycle modelling and the use of 'black box' software, i.e. viewing a system in terms of inputs and outputs without considering complicated process dynamics. Indeed, process LCA has inherent truncation errors due to the definition of system boundaries and the limited process data available (Lenzen, 2001), as discussed in Chapter 2, Section 2.4.2. However, the CV or relative SD is consistent across the scenarios and process LCA is the most reasonable choice for this analysis. Therefore, from a comparative standpoint, the results have a satisfactory level of reliability for the scope of this work.

5.3.2 Additional environmental impacts

This section is structured around the impact categories reported in the International Reference Life Cycle Data System Handbook (ILCD, 2010), as discussed in Chapter 2,

Section 2.4.1. This technical guidance reports on impact categories at both midpoint and endpoint. These are discussed below along with the results of the LCIA for the ICSSWH configurations under evaluation.

5.3.2.1 Midpoint impact categories

Using the CML-IA baseline (v3.05) method for the characterisation of midpoint impacts, the following impact categories are analysed: abiotic (non-fossil fuel and fossil fuel) depletion, climate change, ozone depletion, human toxicity, ecotoxicity, photochemical oxidation, acidification and eutrophication. Characterisation is a mandatory step in an LCIA and it allows the impact of different contributing substances to be quantified into a single comparable unit using equivalency or characterisation factors. These factors are determined by the impact assessment method. Beyond this, an optional step is to normalise the results which simplifies their interpretation. Normalisation offers the ability to interpret indicator results alongside each other; it sets a common reference, enabling comparison of different environmental impacts. The most common method for normalisation is to determine the impact category indicators for a region, over a year, and divide the result by the number of inhabitants in that area. This gives a result of 'impact potential per person per year' for each impact category, expressed in person equivalents (PE). However, normalisation requires additional subjective steps and decreases the transparency of the results; it should be applied and interpreted with caution.

The additional environmental impacts at midpoint are presented as both characterised results, to show the absolute impacts of the ICSSWH designs, and normalised results, to show how the impacts categories score against each other. Figure 5.9 shows the midpoint characterisation impacts for the design configurations/conditions when integrated into a SIP and using a circular approach. Characterisation is a comparison thus the y-axis represents the percentage impact of the systems in relation to the worst contributor, i.e. 100%. For three of the impact categories, the contribution of the finned system with the night cover is significantly higher than the other scenarios. In the case of abiotic depletion (non-fossil fuel) the finned system with the night cover has approx-

imately 70% more impact than the other scenarios. Also, it is significantly higher for GWP, terrestrial ecotoxicity and photochemical oxidation at around 13%, 27% and 31%, respectively. However, in the case of abiotic depletion (fossil fuels) and acidification the difference is marginal at around 10%.

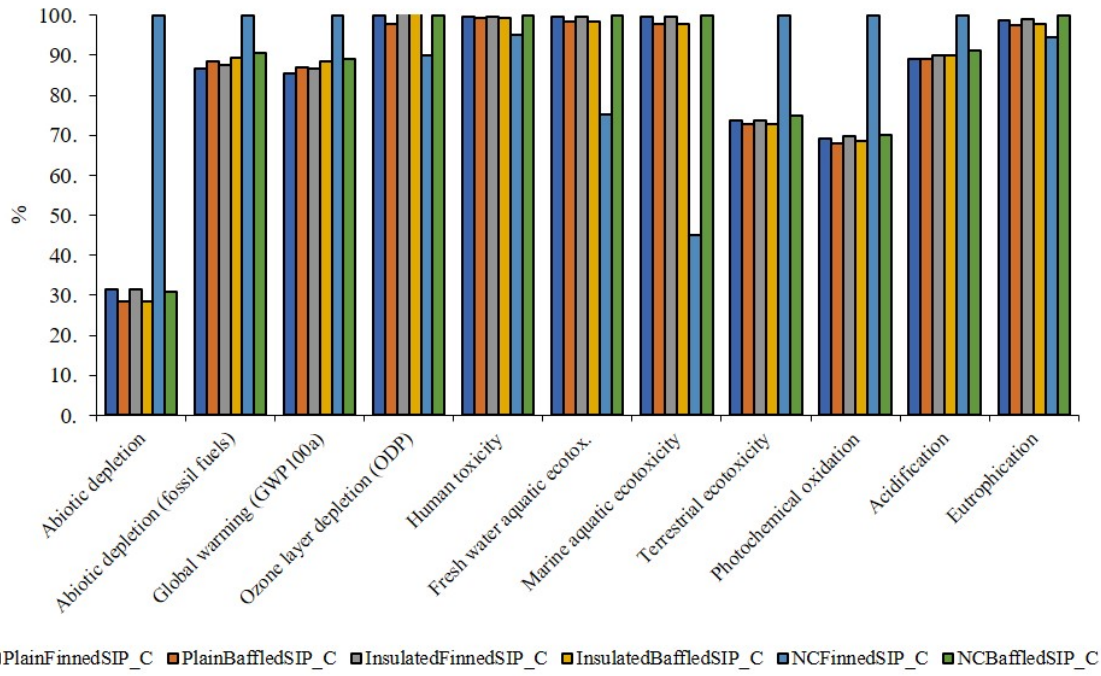

Figure 5.9: Midpoint characterisation impacts for the ICSSWH design configurations and conditions

Additionally, in the fresh water and marine aquatic ecotoxicity categories, the finned system with the night cover is significantly less impactful than the other configurations. In the other categories all the systems exhibit a similar impact with marginal, insignificant difference. As evidenced through the uncertainty analysis presented in Section 5.3.1.4, LCA modelling does not support the level of accuracy that would deem a 10% difference to be significant. There is a lot of uncertainty in LCA therefore the margin for error is higher than in other types of modelling (Bamber et al., 2020). This shows that there is no one right answer that LCA, as a tool to support decision making, can give but it provides information to allow an informed decision to be made.

Figure 5.10 shows the midpoint normalisation impacts for the design configurations when integrated into a SIP and using a circular approach. Normalisation is used to simplify the interpretation of the results, showing to what extent an impact category indicator result has a relatively high or a relatively low value compared to a reference.

From Figure 5.9 it might seem that the finned system with the night cover is the worst case scenario and that a lot of the midpoint categories have an equally high impact. However, when the results are normalised and the categories become comparable, it is evident that, for all but fresh water and marine ecotoxicity, the ICSSWH systems have a small, often negligible environmental impact.

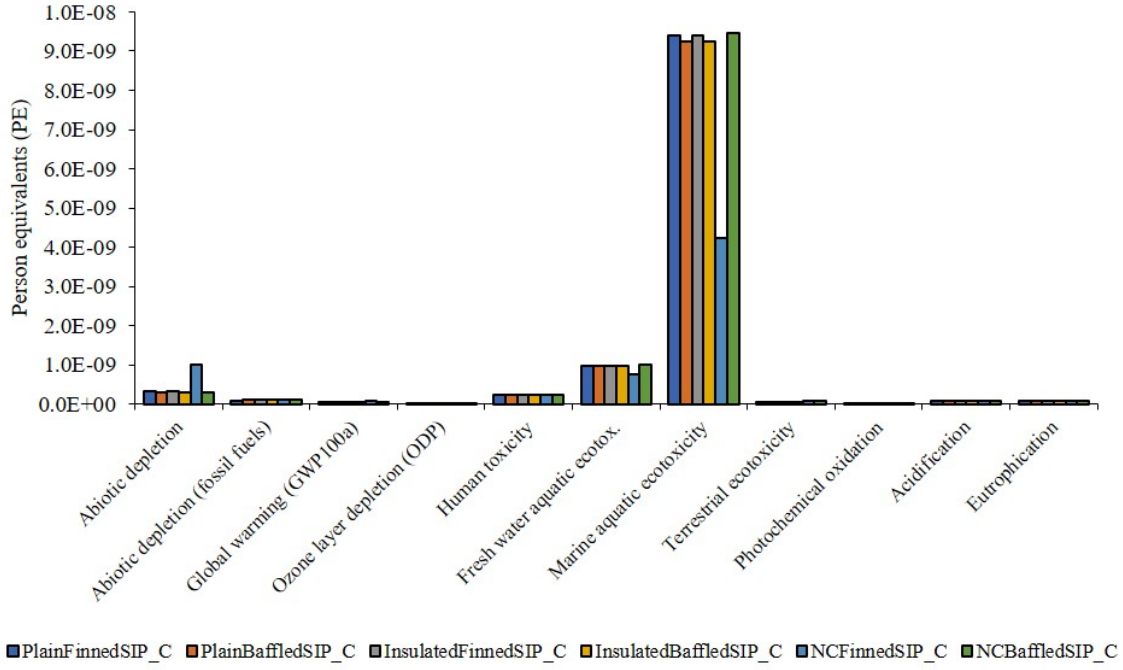

Figure 5.10: Midpoint normalisation impacts for the ICSSWH design configurations and conditions

Evaluating impact at the midpoint level shows that to look at exact numbers for energy and carbon might give the false impression that LCA provides a definitive answer; choose the highest or lowest option depending on what needs to be minimised or maximised. However, when LCA is used as intended, as a decision support tool for better environmental protection, the evidence it gives is more nuanced. It is heavily dependent on which impact categories are of the greatest concern at any given time in the decision-making process. In the current social and political climate, climate change mitigation and GHG emissions reduction have the highest priority of the impact categories reviewed. However, caution must be taken when making decisions that, by minimising one impact, the environmental burdens are not simply shifted to a different impact category.

5.3.2.2 Endpoint damage categories

Endpoint impact categories are those at the end of the impact pathway and are directly related to the areas of protection. A similar comparison to the midpoint category analysis is presented in Figure 5.11 of the design configurations/conditions when integrated into a SIP and using a circular approach. However, the insulated condition has been omitted as the EPD for aerogel insulation did not provide any data on endpoint impact. The analysis was done using ReCiPe 2016 Endpoint (H, v1.02). Endpoint impacts represent the results from the midpoint impact categories that have been characterised, normalised and combined to generate a single, cumulative score for the three damage areas, or areas of protection. Therefore, the normalised results of the endpoint impacts can vary greatly from the midpoint counterparts that contribute to them.

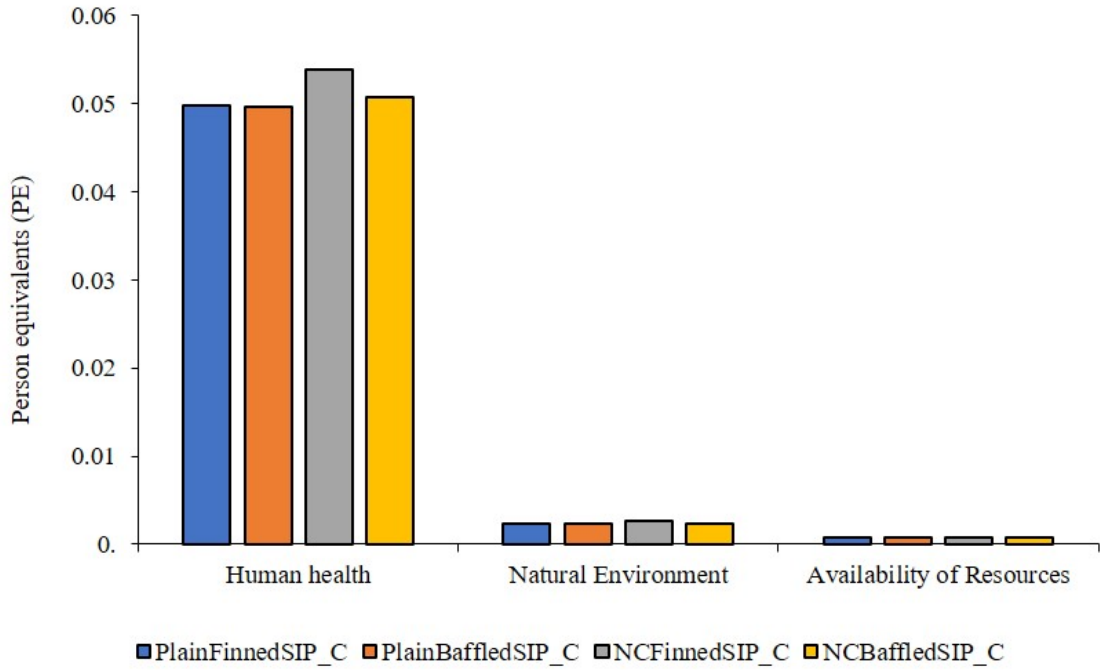

Figure 5.11: Endpoint normalisation impacts for the ICSSWH design configurations and conditions

Figure 5.11 indicates that the human health endpoint category is the most impacted for all the ICSSWH designs. This area of protection is derived from the climate change, ozone depletion, human toxicity, and photochemical oxidation midpoint categories which is at odds with the results shown in Figure 5.10 which suggests that the natural environment is at greater risk. This highlights the subjectivity involved when using

endpoint indicators over midpoint; these values have a 'panel weighting' whereby a panel assesses the relative importance of each impact category (PRé, 2016). Therefore, it is highly subjective as to which impacts are valued more highly; the panel may deem impacts on human health as much more worrying than those on the natural environment Also there is a loss of accuracy as well as transparency in terms of impact units; the endpoint score is the dimensionless person equivalents (PE) while midpoint methods offer a tangible measurement.

Table 5.3 provides a simple damage assessment comparison between two design configurations. The plain baffled configuration integrated into a SIP, from a linear and circular approach, is presented as it is the best-case scenario based on both the thermal performance and carbon impact. It provides an indication of the percentage increase in impacts when moving from a linear to circular approach. When landfilling the components in the ICSSWH design instead of reusing/recycling them, the impact on human health, the natural environment and resource availability increases by 42%, 37% and 29%, respectively.

Table 5.3: Damage assessment of the plain baffled system, integrated into a SIP, on endpoint areas of protection and the percentage increase in impacts when moving from a linear to circular approach

Damage category	**Unit**	**Plain Baffled SIP (Circular)**	**Plain Baffled SIP (Linear)**	**% increase**
Human health	DALY	0.00091	0.00129	**42%**
Natural environment	species.yr	1.355E-06	1.855E-06	**37%**
Resource availability	USD2013	16.44	21.12	**29%**

5.4 Interpretation

The results from the LCIAs are evaluated by comparing the embodied impacts against the operational savings both with and without the circular economy aspect in mind. This was done to highlight the benefit of a circular economy approach as well as emphasise the fact that the presented ICSSWH system allows for this through it design for disassembly.

5.4.1 Energy payback times

The time it takes to recoup the embodied energy expended throughout a FU's life cycle is the energy payback time. The energy the system can provide throughout its useful life is the operational energy savings, by hot water provided by the system and conventional energy avoided. This payback time is calculated both with and without a circular economy approach. Figure 5.12 illustrates the monthly operational energy savings offered by the different design configurations and conditions, extrapolated from the results presented in Chapter 4, against the energy required by the end user. All of them can provide a significant proportion of the annual energy required. Table 5.4 summarises the embodied energy, lifetime energy contribution, i.e. energy saved, and payback times for each of the design configurations and conditions under evaluation.

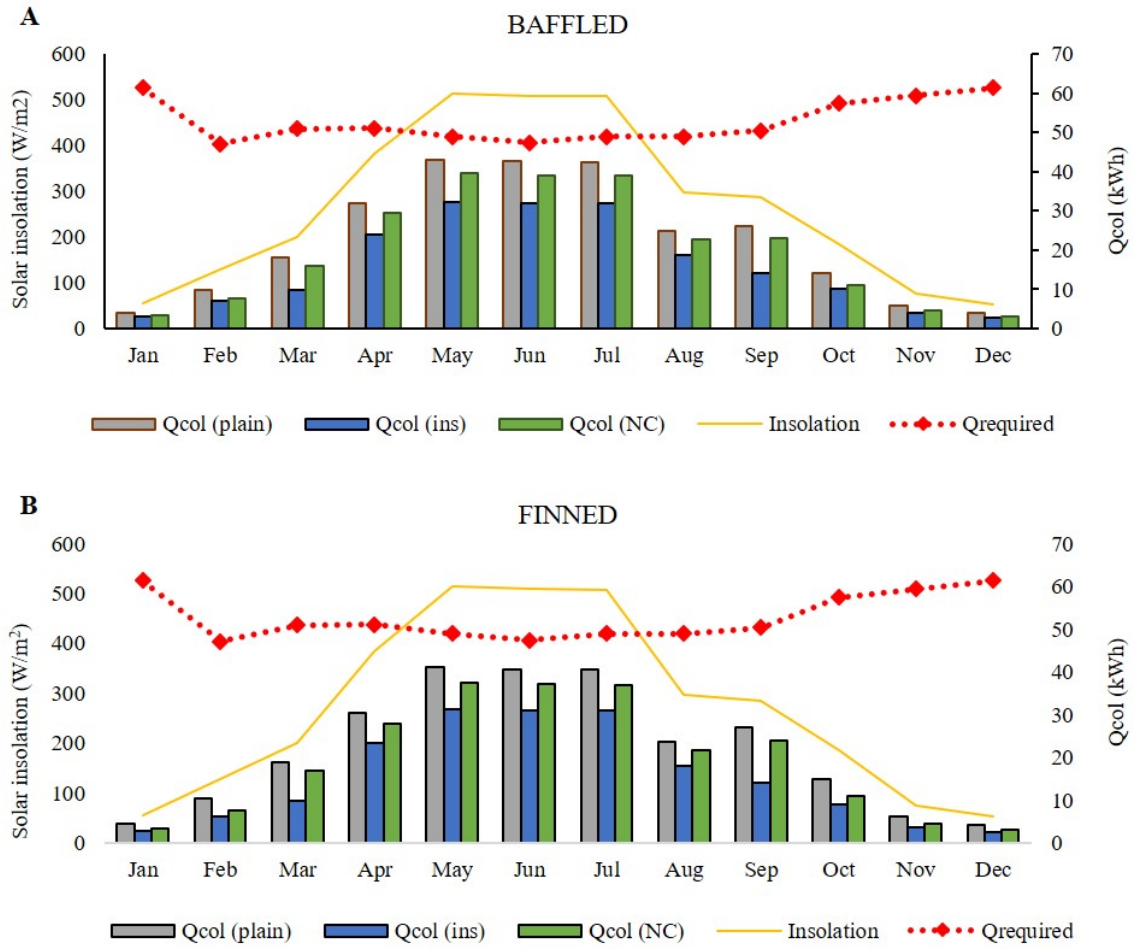

Figure 5.12: Monthly operational energy contribution from the design configurations for the A - baffled collector and B - finned collector, plotted alongside the energy required by the end user and solar insolation. Q_{col} – energy collected by the system, $Q_{required}$ – energy required by the end-user

Table 5.4: Embodied energy, energy contribution and energy payback times for the different design conditions and configurations

	Design	Embodied energy (GJ)	Energy contribution (GJ)	Payback time (years)
Linear	Baffled Plain	3.55	19.2	3.7
	Baffled Insulated	3.63	13.7	5.3
	Baffled Night Cover	3.67	17.2	4.3
	Finned Plain	3.51	18.9	3.7
	Finned Insulated	3.59	13.1	5.5
	Finned Night Cover	3.63	16.7	4.4
Circular	Baffled Plain	3.54	19.2	3.7
	Baffled Insulated	3.62	13.7	5.3
	Baffled Night Cover	3.66	17.2	4.3
	Finned Plain	3.5	18.9	3.7
	Finned Insulated	3.58	13.1	5.4
	Finned Night Cover	3.62	16.7	4.3

Note that, as evidenced through the uncertainty analysis presented in Section 5.3.1.4, there is a lot of uncertainty in LCA thus the margin for error is higher than in other types of modelling (Bamber et al., 2020). Therefore, a margin of ±10% is deemed to be insignificant in LCA modelling, as it does not support a higher level of accuracy, and comparisons made where findings fall within that margin are indicative, not conclusive.

Best-case scenario in terms of energy payback times is the plain baffled system from a circular perspective with an energy payback time of 3.7 years. However, when comparing linear and circular the differences are very minimal. The worst-case scenario is the insulated finned system when applying a linear approach, taking 5.5 years to pay back its embodied energy. When it comes to embodied energy, the end-of-life treatment has a similar energy intensity for both a circular and linear approach, as discussed in Section 5.3.1.1. Additionally, the relatively poor thermal performance of the insulated system means that it consistently has the worst payback times and is the only set-up that takes longer than 5 years to pay itself back.

5.4.2 Carbon payback times

To determine the carbon payback times, the operational energy generated by the systems needs to be converted into $kgCO_{2e}$ using a carbon conversion factor. The value of this factor depends on the carbon intensity of the energy carrier/mix. This section calculates the payback times of each collector when replacing both a natural gas and electric water heating system. The carbon intensity of electricity is steadily decreasing and is becoming comparable to natural gas (Electricity Info, 2020; National Grid ESO, 2020). To accommodate for the decarbonisation of electricity, a steady decarbonisation rate of 6.4% per year was applied as this is the rate required to limit global warming to 2°C (Grant et al., 2018). Natural gas carbon conversion factors were obtained from the UK Government GHG Conversion Factors published by the Department for Business, Energy and Industrial Strategy (DBEIS, 2019b).

Table 5.5 summarises the embodied carbon, lifetime carbon savings, and payback times for each of the design configurations and conditions under evaluation. In terms of carbon payback times, the best-case scenario is the plain baffled system when applying a circular approach at 4.9 years when replacing a natural gas system (7.6 years when replacing an electric system). Additionally, there is a negligible difference in payback times between the plain baffled and plain finned systems, under a circular approach. This highlights the benefit of keeping materials in the resource loop as opposed to disposing of them in a landfill. The worst-case scenario is the insulated finned system from a linear perspective with a payback time of 13 years when replacing an electric system (8.4 years when replacing natural gas). As with the energy impact, the insulated configuration has the worst payback times due to it poorer thermal performance. The decarbonisation of electricity has a highly significant impact on the payback times of these systems and replacing natural gas hot water systems offers the greatest benefit, with payback times as much 4.6 years sooner.

Table 5.5: Embodied carbon, carbon savings and carbon payback times for the different design conditions and configurations

	Design	Embodied carbon ($kgCO_{2e}$)	Carbon savings, NGas ($kgCO_{2e}$)	Carbon savings, Elec ($kgCO_{2e}$)	Payback time, NGas (years)	Payback time, Elec (years)
Linear	Baffled Plain	283	983	636	5.8	8.9
	Baffled Insulated	287	699	452	8.2	12.7
	Baffled Night Cover	289	880	569	6.6	10.1
	Finned Plain	280	968	626	5.8	8.9
	Finned Insulated	284	673	435	8.4	13.0
	Finned Night Cover	291	854	552	6.8	10.5
Circular	Baffled Plain	240	983	636	4.9	7.6
	Baffled Insulated	244	699	452	7.0	10.8
	Baffled Night Cover	250	880	569	5.7	8.8
	Finned Plain	238	968	626	4.9	7.6
	Finned Insulated	242	673	435	7.2	11.1
	Finned Night Cover	248	854	552	5.8	9.0

Each collector set-up under investigation can pay itself back, in terms of both energy and carbon, well within its useful life. From a carbon impact perspective, payback times range from 4.9 to 8.4 years, when replacing a natural gas system, and 7.6 to 13 years, when replacing an electric water heater. When considering the payback of embodied energy, payback times range from 3.7 to 5.5 years, considerably shorter than embodied carbon.

As shown in Section 5.3.1.4, there is some uncertainty surrounding the input data used for the LCI which would impact the interpretation of the results presented above. However, even if all the energy and carbon impact values were to increase by 50%, the ICSSWH systems can still amply recoup their embodied investments within their anticipated lifespan. Their embodied energy would take up to as long as 8.2 years to pay back and their embodied carbon up 20 years (insulated finned system). If the LCI data is assumed to be correct but the lifespan is considered optimistic and is lowered to 15 years as opposed to 20 years, the systems are still able to pay back the energy and carbon investment. Considering a worst-case scenario where the embodied impacts

increase by 50% and the lifespan reduces to 15 years, the systems could still easily payback their embodied energy. However, five scenarios would become unfeasible from a carbon payback perspective, taking between 16 and 20 years to pay off their carbon investment; NC Finned SIP L, Insulated Baffled SIP C, Insulated Finned SIP C, Insulated Baffled SIP L, and Insulated Finned SIP L. The worst payback time would be 20 years for the insulated finned system. However, based on the uncertainty analysis presented in Section 5.3.1.4, a 50% error in the LCI input data is highly unlikely. Regardless, none of the configurations that become unfeasible with a worst-case scenario exhibited the best thermal performance so they would not be recommended anyway.

5.5 Concluding remarks

This chapter presented a comprehensive carbon and energy analysis of the 24 ICSSWH scenarios under evaluation. The carbon results highlighted the importance of a circular approach, keeping materials in the resource loop and out of the landfill. Also, integrating the ICSSWH into SIPs significantly reduces the systems carbon impact, especially in a linear scenario, due to the lower mass of wood required and the loss of the PUR that insulated the collector in the frame. From an energy perspective there was a minimal difference between the circular and linear scenarios as energy cannot be emitted or sequestered like carbon so landfilling the materials does not have a significant energy impact.

An analysis of the environmental impacts at both midpoint and endpoint was also provided to show that single estimate carbon values are not a definitive measure of environmental impact. When LCA is used as intended, as a decision-making support tool for better environmental protection, the results are much more nuanced. In addition, the distinct difference in the areas impacted between the midpoint and endpoint results shows the subjective nature of normalisation in LCA and the loss of transparency and accuracy. The midpoint results suggest that the natural environment is the most heavily affected. However, when an endpoint analysis is used, the damage area that is valued more highly shifts to human health. This suggests that the panel weighting the

endpoint indicators deem impacts on human health to be much more worrying than those on the natural environment. Therefore, the LCIA results should be applied and interpreted with caution.

In terms of payback times, the design configurations are more than able to pay back their embodied carbon and energy investments within their lifespan. When testing the sensitivity of the results to uncertainty in the LCI input data or assumed collector lifespan, the systems are still sustainable with satisfactory payback times. However, assuming a worst-case scenario with uncertainty in both the LCI input data and collector lifespan, five of the 24 scenarios become unfeasible with payback times exceeding the lifespan of the collector when replacing an electric water heating system. Albeit extreme conditions are required for this to materialise, i.e. a five-year reduction in lifespan and an increase in embodied impacts of 50%. While this is useful to show that there is a degree of assumption and interpretation in the results, the numerical findings of this work are robust enough to suggest that all 24 scenarios will likely payback their embodied impacts well within their useful lives.

The decarbonisation of the electricity grid has a significant impact on the carbon payback times which is an important consideration given the current climate crisis. For ICSSWH systems to be sustainable they need to minimise their embodied carbon while maximising their operational energy savings. Based on the experimental results of thermal performance and with the LCI input data, all 24 scenarios are deemed sustainable. The interpretation of the LCA conducted in this chapter shows that the plain baffled system integrated into a SIP, under a circular approach, is the best-case scenario.

Sixth Chapter

Discussion

This thesis presented evidence on the benefits and need for solar water heating, as a solution in line with the requirements to meet carbon budgets and the goal in the Paris agreement, and the existing research concerned with their thermal and environmental performance. In a bid to improve these parameters, a novel ICSSWH was designed with the circular economy ethos in mind. The collector was specifically designed to be disassembled so that all the constituent parts can be cleanly separated and reused/recycled at the end of the collector's useful life, or help to extend its operable lifespan. Beyond this element of disassembly, two base collector configurations were developed, baffled and finned, alongside two design conditions aimed at improving heat retention. Additional insulation, covering the top third of the absorber plate, and the use of a night cover were reviewed.

These design conditions and configurations were field-tested under seasonal variation to quantify their thermal performance. Additionally, the environmental performance of these designs was assessed through life cycle assessment (LCA) and, using the data gathered from the field experiments, their energy and carbon payback times were determined. This holistic view of the ICSSWH design allowed for a more representative evaluation of environmental sustainability. The literature review presented in Chapter 2 highlighted the lack of such holistic evaluations regarding integrated collector-storage style solar water heaters, particularly in the context of a Scottish, maritime climate.

This chapter marries the results of the thermal and environmental performance of

the systems under evaluation in the context of present thinking and needs. The current discussion surrounding ICSSWH design is evaluated in the context of where this work sits in the larger picture of domestic solar water heating technologies. Finally, the novel elements of the design, and the unique contribution that ICSSWH can make to alleviate current challenges in the need for new homes without sacrificing climate targets, are highlighted to make the case for this contributing solution to renewable heating.

6.1 Thermal performance with sustainable thinking

The experimental analysis and LCA results were presented in Chapters 4 and 5, respectively. The results of the field tests showed that the baffled collector design, with a night cover as an additional heat retention method, offered the best thermal performance. In terms of environmental sustainability, the energy and carbon LCA identified the finned system as the best, in all configurations. However, the differences between the finned and baffled designs are marginal and when the thermal performance is considered alongside environmental sustainability, in terms of energy and carbon payback times, the baffled system with no additional heat retention methods is the best design, holistically. Therefore, based on the relative simplicity, lower maintenance requirements, and lower payback times, the plain baffled ICSSWH is deemed the better collector design from the configurations researched.

The results of Chapter 5 emphasised that the carbon investment required for the ICSSWH is worthwhile given the carbon savings garnered throughout the collector's service life. For the collectors under investigation, their coefficient of environmental performance (CoEP) can be determined from the ratio of operational contribution to embodied investment. Therefore, the maximum CoEP, in terms of energy, is 5.42 for the plain baffled system and 4.1, in terms of carbon, for the plain baffled configuration replacing a natural gas-fuelled water heating system. LCA is an important aspect of this research as it enables a comprehensive statement about the sustainability and suitability of the system to be made, when looking at it from a life-cycle perspective. As the ICSSWH, in all configurations, saves more energy and carbon during operation than

is embodied in the upstream and downstream activities, the environmental burden and investment is justified.

6.2 The bigger picture

6.2.1 Comparison with relevant literature

To understand the significance of this research it is important to contextualise the findings with relevant literature. This section discusses the thermal and environmental performance presented in Chapters 4 and 5 alongside the findings of other studies. Table 6.1 and Table 6.2 provide a detailed comparison of the parameters and results of this work against other relevant studies in terms of energy and carbon analyses, respectively. As discovered in Chapter 2, there is a heavy focus on the energy performance of solar water heaters (SWHs) in current research, with a marked lack of carbon/environmental analyses, which is a substantial gap in knowledge that this thesis addresses. This issue is reflected in the number of relevant references included in the tables. Also, a caveat to the comparison with other studies is that carbon payback times are difficult to compare as they depend on the carbon intensity of the electricity mix which is highly geographically variable. Additionally, the comparison studies do not consider decarbonisation of the grid. Applying a decarbonisation rate, of 6.4% in the current work, has a significant impact on the carbon payback times which might explain the difference in the observed payback values compared to those found in the literature.

Table 6.1: Comparison with relevant studies based on energy analysis

Paper	**Collector type**	**Storage tank (l)**	**Absorber area(m^2)**	**Max. outlet temp (°C)**	**Avg. ambient temp (°C)**	**Solar irradiance ($kWh/m^2/day$)**	**Collection efficiency (%)**	**Energy contribution (GJ/year)**	**Energy payback time (years)**
Smyth et al. (2000, 2001)*	ICSSWH (with reflector)	57	0.9215	60		0.7-3.5	36-52% (average)	1.83	< 2
Tripanagnostopoulos et al. (2005)	PV/T solar water heater	1500	30		12-29	2.7-6.0	14-44.4% (average)	24.9-78.9	1.1-2.7
Garnier (2009)	ICSSWH	150	3	65	12-22		65-71%	3.7-4.0	1.5-2.6
Laborderie et al. (2011)	Flat-plate	300	4.4			3.4-3.8	38% (average)	5.1	< 1-1.5
Carnevale et al. (2014)	Thermosiphon flat-plate	160	2.13	50-60	4-21.5	2.1-6.07	79%	5.07	0.7-1.2
Loumakis (2018)	Low cost flat-plate type	80	0.81	47.2	3-13.3	1.1-3.8	16.2% (average)	0.54	
Souliotis et al. (2018)	ICSSWH (with reflector)	1673	19.08	55			40-60%	46-55	< 1
Uctug and Azapagic (2018)+	Thermosiphon flat-plate	200	2.25	60	9.0-22.9	1.3-6.3	70%	5.36	1-3.3
Harmim et al. (2019)	ICSSWH (with reflector)	60	0.3	60	7.7-35.2	5.4-6.0	36.4-51.6%		
Milousi et al. (2019)	Flat-plate and Evacuated tube	200	2.32 and 2.61		8-28	4.6-5	55.3% and 62.7%	4.91 and 5.4	

Continuation of Table 6.1

Paper	Collector type	Storage tank (l)	Absorber area(m^2)	Max. outlet temp (°C)	Avg. ambient temp (°C)	Solar irradiance ($kWh/m^2/day$)	Collection efficiency (%)	Energy contribution (GJ/year)	Energy payback time (years)
Yassen et al. (2019)	ICSSWH (corrugated absorber)	140	1.85	78	5-26	5.0-5.5	40.7-45.5% average)	2.0	
Zhang et al. (2020)	Loop-thermosiphon flat-plate	150	2	70	12-30	2.4-4.6	48.4-59.5%	4.38	
Present work	**ICSSWH**	**48**	**0.96**	**72**	**4.3-18.1**	**0.1-1.8**	**32% (average)**	**0.96**	**3.7-5.5**

** based on total yearly solar energy incident and a maximum collection efficiency of 52% - in Smyth et al. (2001), the same collector has an adjusted collection efficiency of 34.5% and annual energy contribution of 0.72 GJ. Even if that value is based on 244 days, extrapolating to 365 given an energy output of 1.08 GJ.*

+ based on Istanbul (Region 2) data as the water inlet temp and average solar irradiation were the most similar. https://power.larc.nasa.gov/data-access-viewer/ for some meteorological data, https://solargis.com/maps-and-gis-data/download for kwh/m^2/day values.

Table 6.2: Comparison with relevant studies based on carbon analysis

Paper	**Collector type**	**Storage tank (l)**	**Absorber area(m^2)**	**Occupancy (persons)**	**Lifespan (years)**	**LCA stages considered**	**Carbon savings ($kgCO_{2e}$/year)**	**Carbon payback time (years)**
Tripanagnostopoulos et al. (2005)	PV/T solar water heater	1500	30		15-25	A-D	3940-8880	1.4-3.1
Garnier (2009)	ICSSWH	150	3	3	20	A-D	198-211 (vs gas)	1.6-3.1
Carnevale et al. (2014)	Thermosiphon flat-plate	160	2.13	3-4	25	A-D	211	0.65-1.1
Uctug and Azapagic (2018)[+]	Thermosiphon flat-plate	200	2.25	4	25	A-D	387 (vs gas)	1-3.2
Arnaoutakis et al. (2019)	ICSSWH (with CPC reflector)	200	2.2	4	10	A-C	400-600	
Milousi et al. (2019)	Flat-plate and Evacuated tube	200	2.32 and 2.61	4	20	A-C	1300 and 1250 (vs elec)	2.6 and 2.1
Present work	**ICSSWH**	**48**	**0.96**	**1**	**20**	**A-D**	**49.15 (vs gas); 31.8 (vs elec)**	**4.9-7.2; 7.6–11.1**

[+] *based on Istanbul (Region 2) data as the water inlet temp and average solar irradiation were the most similar.*

This theory is supported by the relatively comparable energy payback times, when viewed alongside the collector parameters/outputs. Validation is achieved by comparing like-for-like and common metrics are similar storage temperatures and ambient air temperatures. For example, Yassen et al. (2019) present a similar comparison and base their validation on similar ambient air temperatures. This is not an accurate representation of collector performance for glazed collectors as they are designed with an air cavity to prevent convective heat loss to the ambient environment and combat the effects of variations in air temperature. Therefore, validation should be based on the comparability of solar insolation levels (W/m^2), intermittency and duration (daylight hours), which can be expressed by the solar irradiance ($kWh/m^2/day$), as presented in Table 6.1.

From the data provided in Tables 6.1 and 6.2, the position of the ICSSWH evaluated in this work can be determined in terms of the wider research picture surrounding SWHs. Parallels can be drawn between average efficiencies, system life span, storage size per occupant, and storage size, annual energy contribution, and annual carbon savings per square meter of absorber area. Therefore, despite the caveats highlighted above and the clear shortcoming of the incident solar irradiance levels in this work (Table 6.1), the ICSSWH evaluated here holds its own in the field of SWH research. As mentioned above, a fair metric for comparison is solar irradiance which is significantly higher in the reviewed studies. For example, Smyth et al. (2000, 2001) evaluated an ICSSWH of similar storage volume and absorber area with comparable efficiencies yet quoted an energy contribution almost double that of the present work and thus much shorter energy payback times. The study was conducted in Northern Ireland, which is geographically close, however, there is a noticeable difference in the incident solar irradiance which had a much greater range and reached levels almost double those recorded in this study. This is most likely due to the shading on the tanks during testing, as discussed in Chapter 3, Section 3.2.6.4.

Similarly, Souliotis et al. (2018) assessed the use of ICS-type SWHs for use in social housing and found an annual energy contribution in the range of 2.4 – 2.9 GJ per square meter of absorber area. This is more than double the energy provided by the ICSSWH

in this study, yet the research was a simulation analysis using meteorological data for Greece and Cyprus. Daily solar irradiance in the regions studied ranges from 4.6 – 5.0 kWh/m^2 (Athens, Greece) and 5.2 – 5.3 kWh/m^2 (Nicosia, Cyprus) (The World Bank, 2019); several times the levels experienced in this study. In terms of carbon payback times, the results are dependent upon the carbon intensity of the energy mix, which varies geographically as well as temporally, or the type of heating system the SWHs are replacing.

6.2.1.1 Comparison of additional environmental impacts

The environmental LCA work of this thesis can be evaluated on a deeper level and compared against the recent work of Uctug and Azapagic (2018) and Milousi et al. (2019) who present comprehensive analyses of various environmental indicators that are impacted by the production of commercially available SWHs. As shown in Table 6.2, the reviewed systems are distributed flat-plate and evacuated tube SWHs designed for a 4-person dwelling with a 200-litre storage volume and 2.25 to 2.61 m^2 absorber areas. The SWH in this work is for a single occupancy dwelling with a 48-litre storage volume and 0.96 m^2 absorber area. Therefore, for this comparison, the results will be scaled to represent a 1 m^2 absorber area and normalised per kWh of useful energy generated over 20 years.

Milousi et al. (2019) used the same software and database as in the present study, SimaPro and Ecoinvent, albeit previous versions which, particularly for Ecoinvent, might well mean different underlying data, but the authors also employ a different life cycle impact assessment (LCIA) method for the quantification of midpoint impacts, ReCiPe 2016 Midpoint Hierarchist (H) versus CML-IA baseline used here. Uctug and Azapagic (2018) used CCaLC software, equipped with Ecoinvent, and the CML 2001 LCIA method; this method is no longer supported in the version of SimaPro used in this study and was superseded by the CML-IA baseline method. A common problem with LCAs, in terms of comparability, is the diversity when it comes to the LCIA method and database used. That is no exception here, thus the comparison presented is interpreted with consideration of the caveats discussed in Chapter 2, Section 2.4.1. However, there

are similarities with both studies; Ecoinvent is the common database across all three studies and both this work and Uctug and Azapagic (2018) use a version of the CML LCIA method. Using their respective methods, Uctug and Azapagic (2018) considered 6 midpoint environmental indicators while Milousi et al. (2019) consider several more and offer a broader midpoint impact assessment, as shown in Table 6.3. However, a greater number of indicators does not necessarily mean the assessment is more comprehensive. Having a broader range is only beneficial if they are interpreted with an awareness of the quality of their associated characterisation factors. The International Reference Life Cycle Data System (ILCD) Handbook classifies 16 midpoint indicators based on how recommended their use is (ILCD, 2010). The additional indicators included in the ReCiPe method are classified as 'recommended but to be applied with caution'. The indicators used in this study, with the exception of ecotoxicity, are more established and are classified as 'recommended and satisfactory' or 'recommended but in need of some improvements'.

Table 6.3: Comparison of midpoint environmental indicators considered. * Considered as a single indicator

Midpoint indicator	**Milousi et al. (2019)**	**Uctug and Azapagic (2018)**	**Present study**
Global warming	✓	✓	✓
Stratospheric ozone depletion	✓	✓	✓
Ionizing radiation	✓		
Ozone formation, human health	✓	✓*	✓*
Ozone formation, terrestrial ecosystems	✓		
Particulate matter formation	✓		
Acidification	✓	✓	✓
Eutrophication, freshwater	✓	✓	✓
Ecotoxicity, terrestrial	✓		✓
Ecotoxicity, freshwater	✓		✓
Ecotoxicity, marine	✓		✓
Human toxicity, cancer effects	✓	✓*	✓*
Human toxicity, non-cancer effects	✓		
Land use	✓		
Mineral resource scarcity	✓		✓
Fossil resource scarcity	✓		✓
Water depletion	✓		

Table 6.4 outlines the LCIA characterisation results for the additional environmental impacts at the midpoint level. Note: the results used for the present study are based on the plain baffled configuration integrated into a SIP. Only the impact categories in common with the present study are included. For every kilowatt hour of energy generated per square meter of each SWH, the ICSSWH in this study performs marginally worse in most impact categories, bar acidification compared with Uctug and Azapagic (2018) and ozone depletion and formation and terrestrial ecotoxicity when compared with Milousi et al. (2019). Terrestrial ecotoxicity, marine ecotoxicity and fossil resource scarcity are significantly different in this study compared to Milousi et al. (2019) and this is due to the LCIA method used. To check this anomaly, the life cycle inventory (LCI) of the ICSSWH in this study was modelled using the ReCiPe 2016 Midpoint Hierarchist (H) method. The results showed that terrestrial ecotoxicity is three orders of magnitude

higher using ReCiPe over CML-IA baseline and marine ecotoxicity and resource scarcity were five and three orders of magnitude smaller, respectively. This is consistent with the differences seen in Table 6.4 and reflects the different characterisation processes. The other impact categories reviewed here are also within different orders of magnitude for the ReCiPe versus CML method but less extreme. Only global warming potential, which is built on more established and less varying calculation and characterisation methods, shows similar results.

Table 6.4: Environmental impact assessment results from the present study compared to similar studies. The results for each study have been normalised to the impact per kWh generated by the SWH, per square meter absorber area. FPC – flat-plate collector, ETC – evacuated tube collector

Midpoint indicator (per kWh·m^2)	**Milousi et al. (2019)***		**Uctug and Azapagic (2018)$^+$**		**Present study**	
	FPC	*ETC*	*Landfill*	*Recycling*	*Linear*	*Circular*
Global warming (kg CO_2 eq)	0.0238	0.0222	0.0287	0.0257	0.053	0.0449
Ozone depletion (kg CFC-11 eq)	1.29E-08	1.36E-08	1.51E-09	1.51E-09	3.76E-09	3.75E-09
Ozone formation (kg C_2H_4 eq)	1.27E-04	1.29E-04	1.13E-05	1.06E-05	1.92E-05	1.80E-05
Acidification (kg SO_2 eq)	2.07E-04	2.01E-04	4.38E-04	4.27E-04	2.79E-04	2.79E-04
Eutrophication (kg PO_4 eq)	1.28E-05	1.37E-05	7.71E-05	7.56E-05	1.44E-04	1.28E-04
Ecotoxicity, terrestrial (kg 1,4-DB eq)	0.855	0.931			6.03E-04	5.92E-04
Ecotoxicity, freshwater (kg 1,4-DB eq)	6.42E-03	6.94E-03			1.03E-01	8.61E-02
Ecotoxicity, marine (kg 1,4-DB eq)	9.27E-03	1.00E-02			1.90E+02	1.82E+02
Human toxicity (kg 1,4-DB eq)	0.224	0.244	0.114	0.027	0.306	0.304
Fossil resource scarcity (MJ)	1.30E-04	1.29E-04			4.78E-01	4.78E-01

** As Milousi et al. (2019) use a different LCIA method, the indicator units are quantified differently. A conversion factor has been applied to the indicators with different units, based on the analysis of LCIA methods presented in Owsianiak et al. (2014).*

$^+$ Calculations based on a 20-year lifespan, as opposed to 25 years considered in the work, for comparability.

These results seem surprising as the ICSSWH presented here does not have an external hot water storage tank, therefore the mass of materials required for the tank and the additional fittings and components are not included. Milousi et al. (2019) do not give a detailed life cycle inventory but Uctug and Azapagic (2018) include 79 kg of steel for the storage tank and approximately 22 kg of steel for the collector, seven times the weight used for the ICSSWH. Therefore, the environmental impacts should be higher, even on a per meter squared basis. Given the method used to normalise the results, per kWh/m^2, the positive, albeit marginal, difference observed is most likely an artefact of system performance; the collectors reviewed in the two studies can provide significantly more energy throughout their useful life than the ICSSWH in this study, therefore the denominator is larger. Another way to normalise the results is simply per square meter of absorber area and, grouping the main components (steel, aluminium, copper, and glass), the weight per square meter of aluminium and glass is higher in the ICSSWH but there is significantly less steel, when compared with the flat-plate collector in Uctug and Azapagic (2018). There is 1 kg/m^2 more glass and 8.9 kg/m^2 more aluminium while there is 32.6 kg/m^2 less steel. When compared with the evacuated tube collector in Milousi et al. (2019), there is 18.1 kg/m^2 more steel, 3.9 kg/m^2 more copper and 3.2 kg/m^2 more glass than in the ICSSWH. However, there is 9.7 kg/m^2 less aluminium as the authors do not include it in their LCI. Given the energy intensity of aluminium production, this goes some way to explain the higher impacts for the ICSSWH, but this should be largely overshadowed by the steel content. Regardless of the method of normalisation, the difference between the results of the ICSSWH versus the flat-plate and evacuated tube collectors is negligible in absolute terms with the largest difference being 0.3 kg 1,4-DB eq for human toxicity.

For a linear and circular comparison, Uctug and Azapagic (2018) considered two disposal scenarios for their thermosiphon flat-plate, landfill and recycling. In essence, these scenarios are the same as those considered in this study; 'linear' assumes all components are sent to landfill while 'circular' assumes all components exit the system and the impacts associated with recycling/reuse are not a burden in the life cycle of the ICSSWH. For Uctug and Azapagic (2018), the benefits of recycling are most noticeable

in the human toxicity impact category where the impacts of landfilling are 76% higher. In terms of global warming potential, recycling offers a 12% reduction in impacts. For the other indicators, the savings are more marginal, 6% for ozone formation, 3% for acidification, and 2% for eutrophication. Based on their analysis, recycling makes no difference to ozone depletion. The linear versus circular results from the present study show a similar reduction in global warming potential, at 18%, and the same decrease in ozone formation of 6%. Eutrophication shows a greater decrease of 11% while there is only a slight difference between the linear and circular scenarios for acidification (0.2%), ozone depletion (0.2%) and human toxicity (0.5%). This shows the black-box nature of LCA tools, where ready-made processes and product stages are used in place of primary data. Additionally, Uctug and Azapagic (2018) modelled recycling as a benefit to their system thus the different reductions observed are expected. In line with existing standards, this study assumed that, in a circular scenario, product materials exit the system and the benefit of using non-virgin materials is credited to the next life cycle.

The above discussion highlights the difficultly in comparing results across studies, especially given the inconsistency in the employed LCIA method, functional unit and reporting style. For example, the assessment presented by Milousi et al. (2019) is not transparent and the results are questionable based on their process network; it is difficult to understand the functional unit they used and the extent of the inputs. However, despite the caveats discussed and considering the difference between the two methods used, Table 6.4 shows that the results for the solar water heater evaluated in this study are well aligned with commercially available systems and the differences are so small that they are negligible and justifiable due to the differences in the inventories as well as the distinctly different LCIA method. The inputs determine the outputs and given the inherent differences in the composition of the different solar collectors, the outputs from their LCIs differ accordingly. The minor differences observed are hard to understand without having access to the data and the models used and the source of discrepancies is impossible to pinpoint. For full transparency and replicability, detailed LCIs, the Ecoinvent processes used and the process networks for this study are provided for reference in Appendices B, C and D, respectively.

The ICSSWH presented here is a novel product that is not built following traditional technology, which can be seen when comparing the LCI with that of the flat-plate collector. Additionally, the results align well with existing research despite the vastly different geographic contexts of the studies which testifies to the robustness of the results. This work is built on primary data rather than secondary sources as used by Uctug and Azapagic (2018) and Milousi et al. (2019). When primary data is used it generally leads to higher impacts in LCA because more activities are considered, and more specific data is captured (Pomponi, 2015). The discussion presented here provides evidence for the viability of the ICSSWH system under investigation in northern maritime climates. The comprehensiveness of the analysis presented in this thesis is reflected in the higher impacts observed compared to literature values, as discussed above. This highlights the fact that more specific detail is captured through primary data collection which is then included in the analyses. Despite these higher impacts, and despite including a decarbonisation rate to account for the ongoing decarbonisation of the UK electricity grid to meet zero carbon targets, the systems evaluated here still amply pay back their embodied carbon, thus further confirming their viability as a net-zero carbon generating technology.

6.2.2 Influence of Covid-19 Pandemic

2020 began with the outbreak of a coronavirus, named Covid-19, which has since become a global pandemic with many countries in a state of lockdown. This has had a positive impact on global pollution levels with China experiencing a temporary decline in CO_2 emissions of 25% (Evans, 2020). The latest report released by the International Energy Agency (IEA), the Global Energy Review 2020, is the most extensive and up-to-date look at the pandemic's impact on energy use and carbon emissions, based on real-time data from the year so far (IEA, 2020). This review modelled various scenarios and found that the impact on this year's energy demand could be more than seven times larger than that of the 2008 financial crisis, and could lead to a record decrease in carbon emissions of approximately 8%, or almost 2.6 gigatonnes (Gt), taking them

to their lowest level in a decade. A recent study also estimated the decrease in CO_2 emissions as a result of the forced confinement and found it to be in the range of 4.2 to 7.5%, depending on the length of lockdown and post-pandemic recovery (Le Quéré et al., 2020).

However, after previous crises, such as the 2008 global financial crisis, the 1970s energy crisis and the Second World War, the rebound in emissions has been larger than the decline and that is likely to be the case here unless investment to restart the economy targets a cleaner and more resilient energy infrastructure. This unprecedented decline may only be temporary without structural changes, but this pandemic is bringing about some significant rethinking in terms of delivery of low-carbon objectives. The analysis conducted by the IEA (2020) observed a major shift towards low-carbon sources of electricity, such as wind and solar PV, due to their low operating costs and preferential access to many power systems. The report also highlighted that, so far in 2020, low-carbon technologies reached 40% of the global power mix, the largest source of global electricity generation. These technologies and their output are much less susceptible to changes in electricity demand unlike conventional sources of energy for electricity generation. This is a highly uncertain and unprecedented time and the full impact will depend on the duration and intensity of the lockdown measures and the stimulus packages put in place by governments around the world. This is an opportunity to shape the energy sector and make positive transitions to cleaner sources of energy whilst safeguarding energy security.

A further driver for adapting and accelerating pollution reduction policies and targets and investing in a cleaner energy infrastructure is the potential link between pollution, industrialisation, energy use, carbon emissions and highly contagious viruses. There are theories that high pollution episodes, in areas like northern Italy (Conticini et al., 2020), areas of China (Cui et al., 2003), US cities (Wu et al., 2020), etc., correlate with higher incidence of coronavirus. However, in the case of Covid-19, this is speculative and shrouded in uncertainty with no peer-reviewed evidence base to support it as-of-yet. With this pandemic highlighting the fragility of the energy market and the share of renewables jumping several years ahead of pre-pandemic estimates, economic stimulus

packages will be an opportunity to link economic recovery efforts with clean energy transitions.

Solar thermal energy could play a major role in the future energy picture and the ICSSWH evaluated in this work has an important advantage over its commercial counterparts. The physical integration into the roof structure is a critical element of this work, the ICSSWH is designed to come as part of a pre-built package, already integrated into the modern roof structure when it arrives on site, with the renewable delivery required to meet carbon objectives (Scottish Government, 2017). The thermal and environmental analysis presented in this work demonstrates the environmental sustainability of the system, but the element of integration illustrates the benefits of its practical application. The following section provides a discussion of the benefits of an integrated system.

6.3 Opportunities for ICSSWH systems

The UK Government launched the 2015 to 2018 Affordable Homes Programme which included the target to deliver 400,000 affordable homes by 2020-21 (HM Treasury, 2015) and in 2018 the UK Government announced £2 billion of new long-term funding for this programme (HM Treasury, 2018). Additionally, City of Edinburgh Council (CEC) launched its "21st Century Homes" programme which aims to deliver 10,000 affordable and mid-market homes by 2030 yet they've set an ambitious carbon neutral target for 2030 (City of Edinburgh Council, 2019). Glasgow Council is also committed to becoming net-zero (Glasgow City Council, 2019) so efforts must be made to achieve these targets. This demand for new builds will have a significant impact on national and local authority carbon budgets and their construction and service elements will need to be carefully considered.

Scottish government targets to hit zero-carbon by 2045 (Scottish Government, 2019) require drastic and immediate action. Renewable technologies already play an important role in achieving this target, with minimum requirements included in Section 7 (Sustainability) of the Building (Scotland) Regulations Technical Handbooks (Scot-

tish Government, 2014). This is a voluntary part of the Regulations that promotes a hierarchy of achievement in levels of sustainability for domestic and non-domestic buildings. These levels include; Bronze or Bronze active, Silver or Silver active, Gold and Platinum. Bronze is the lowest, baseline level for sustainability and is achieved when the home meets the functional standards set out in the first six sections of the Technical Handbooks. Beyond that, to achieve any further level of sustainability, low and zero carbon generating technology must be used to meet partial space or water heating demands. Silver requires that at least 5% of water heating should be provided by renewables and to achieve Gold, 50% of the water heating demand must be met by renewables. Platinum aspires to be carbon neutral (zero net emissions) and requires that all energy needs are met entirely by renewables.

However, government incentives for domestic renewable technology schemes in Scotland have been slashed in line with UK level scheme closures. In 2018, the Feed-in Tariffs (Closure, etc) Order 2018 signalled the end of the UK's Feed-in Tariff, which was aimed at encouraging the uptake of small scale renewable and low carbon technologies (Ofgem, 2019). More needs to be done to make these technologies economically viable as well as environmentally sustainable and to promote innovative solutions to combat the climate crisis. The Renewable Heat Incentive is still active (Ofgem, 2020b) and is a UK Government scheme, covering Scotland, which aims to encourage uptake of renewable heat technologies. Solar thermal systems are included in the Domestic Renewable Heat Incentive Product Eligibility List and are a potentially vital contributing solution to the climate crisis. However, only the more common, commercially available flat-plate and evacuated tube systems are eligible at present.

6.3.1 Benefits of an integrated system

The demand for new homes must be delivered in line with government carbon objectives therefore the need is there for efficient and sustainable integrated building energy systems. However, the application of these systems, such as solar thermal collectors, in a domestic context is still limited due to building integration issues (Buker and Riffat,

2015). To alleviate these issues, any solar thermal system needs to be properly designed and adapted for integration into the building envelope. Such an integrated system would simplify the installation process and lower overall costs. Successful integration of solar thermal systems into the building envelope is reliant on the type of building structure as well as the system design. The ICSSWH evaluated in this work was specifically engineered for integration into modern roof structures to be compatible with offsite, modular construction which is becoming increasingly popular due to its affordability, energy performance and sustainability (Smith et al., 2012, 2015). This method of construction will become more prevalent in meeting identified housing needs for the UK (Smith et al., 2012) and to achieve growth opportunities for the construction industry (Construction Scotland, 2018).

Given the current skills gap in Scotland, this shift toward offsite modular systems may accelerate due to the loss of skilled labour required to build traditional housing (Smith, 2019). Besides, offsite construction offers greater efficiency in terms of labour throughout the lifespan of a project with a significant reduction in traditional on-site labour and cleaner, safer, indoor working environments (Homes for Scotland, 2015). Currently, timber-frame construction accounts for around 75% of all new homes in Scotland (Smith, 2019) and it is well suited for building integrated systems with the added benefit of significant carbon abatement compared with an equivalent masonry or concrete structure (Spear et al., 2019). Additionally, the greater sustainability and energy performance provides a good opportunity for councils to meet their housing goals while minimising the impact on their carbon budget. The “fabric-first” approach reduces space heating needs, but hot water demand exists all year round despite the energy efficiency of the structure. For example, Figure 6.1 illustrates the relative space and water heating demand when applying a Passivhaus scenario, one of the most ambitious standards for energy efficiency, versus an average build. This shows that space heating demand can be drastically reduced with a Passivhaus design, but the hot water demand is still there; the relative demand share significantly increases with space heating savings. If this continues to be met by fossil fuel sources, carbon reduction targets will remain out of reach. Therefore, additional solutions are required to drive down the emissions

associated with hot water demand and the ICSSWH is well placed to contribute to this demand.

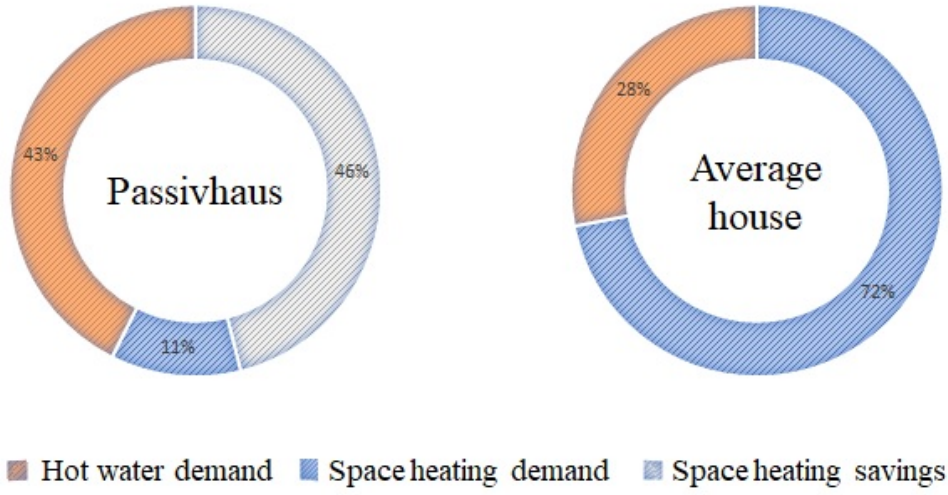

Figure 6.1: Relative space and water heating demand when applying design solutions such as Passivhaus versus average builds (Recoup, 2017)

The ICSSWH evaluated in this study was designed for integration into modern modular construction as a plug-and-play, fit-and-forget system and this could play an important role in future construction projects. This also saves travel and installation costs compared to fitting the system on site, which has associated benefits and savings. The experimental testing was conducted with the collector embedded into a structural insulated panel (SIP). This design facilitates the move from an insulated frame that is bolted on top of a roof structure to the storage tank being physically embedded in the roof itself. Figure 6.2 illustrates the benefits of this change. With the collector in the frame, the amount of insulation required to match the U-value of the SIP is impractical when mounting the system on an angled roof as it would be too bulky and aesthetically unappealing. Therefore, by embedding the panel in the SIP, the back and sides are significantly better insulated, and the absorber plate of the collector is flush to the roof surface. This installation could be finished like a Velux rooflight to ensure water and air tightness and roof tiles could be fitted around the absorber opening without impacting the collection capacity. Additionally, the system weighs approximately the same as the tiles that it would be replacing so there is no extra strain added to the roof structure.

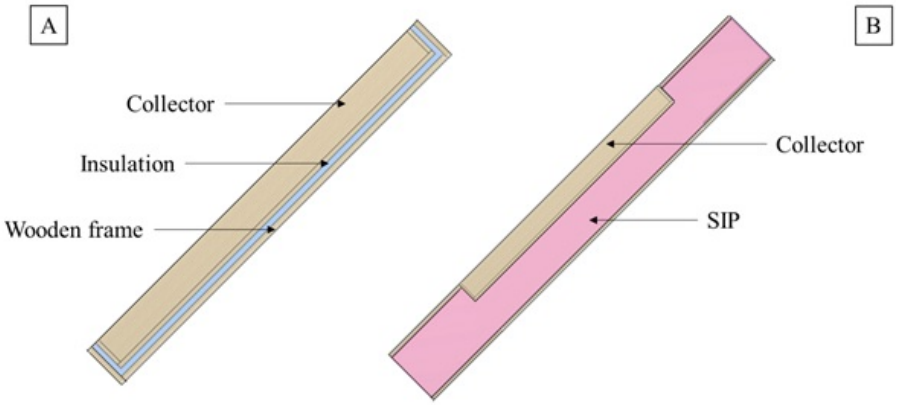

Figure 6.2: Illustration of the ICSSWH mounted in a frame [A] versus integrated into the building fabric [B]

The dimensions of the ICSSWH have been optimised for integration in SIP-type roof panels. However, given that the dimensions of the current design are 1325 x 725 x 50 mm, the height-to-width ratio (H/W) of the storage tank is 1.9 with an absorber area of 0.96 m^2 and a volume of 48 litres. Based on the review of the literature, presented in Chapter 2 Section 2.2.2, it would be justified to adapt this design to attain H/W close to 3 and a volume-to-area ratio within 51–69 l/m^2. Therefore, the following dimensions are proposed – 1800 x 560 x 60 mm, giving an increased H/W of 3.2, a slightly increased absorber area of 1 m^2, and a storage volume of 60 litres. These narrower dimensions have the added advantages of being compatible with a greater range of rafter spacings, thus making it a more desirable component in MMC, greater heat transfer through convection and conduction due to the greater vertical aspect ratio (H/L) of 30, and better freeze tolerance due to the larger storage volume. Also, the increase in depth is not so large that it significantly impacts the thermal mass of the system, the change in convective heat transfer when increasing from 50 to 60 mm is negligible, as shown in Figure 6.3.

An issue with this, however, is the alteration of the air cavity ratio. The storage tank dimensions can be adjusted for optimal performance, but this inescapably impacts upon the aspect ratio of the air cavity. Given the proposed new dimensions, the air cavity would have an aspect ratio of approximately 51, assuming the spacing between the transparent cover and absorber plate is kept at 35 mm. Increasing this air gap to 45 mm

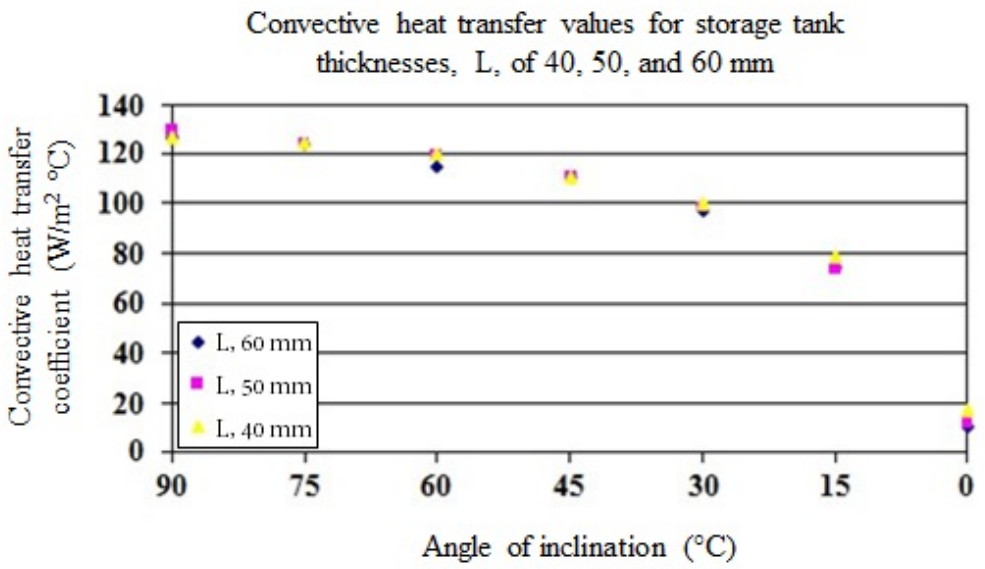

Figure 6.3: Convective heat transfer coefficient values for varying storage tank thicknesses obtained through CFD analysis of a 1000 x 1000 mm square tank. Adapted from Henderson et al. (2007)

would reduce the aspect ratio to 40 equal to that of the current design however this has its own setbacks. Not only does it increase the overall depth of the system, thus affecting its embedment in a roofing panel, it also increases the Rayleigh number which promotes heat loss through convection. The thermodynamics of the system are highly complex, but it assumed the air gap spacing of 35 mm, to maintain a lower Rayleigh number, is a more important parameter than the higher aspect ratio. Therefore, to improve the compatibility with modern roof structures as well as the convective and conductive heat transfer of the storage tank, while having minimal impact on the Rayleigh number, storage tank dimensions of 1800 x 560 x 60 mm with an air cavity gap of 35 mm are recommended.

6.3.2 Monetary payback

The average energy mix for heating of existing housing in the UK is 86% natural gas and 14% electricity, while 69% of new builds are designed to be supplied solely by electricity. Therefore, the continuing decarbonisation of the electric grid will provide significant CO_2 reductions from new homes. With a focus of energy efficient homes being on a low energy demand for space heating, the main heating demand shifts to hot water needs. As more and more services and infrastructure move towards electrification and

decarbonisation through renewable generation, there will be increasing pressure on the existing grid infrastructure which is outdated and ill-equipped to deal with renewable input (Strbac, 2010). Solar water heaters can be used to ease the burden on the grid as they heat the water directly and only require auxiliary heating. The ICSSWH in this work has been shown to provide a significant proportion of single occupancy hot water needs thus has the potential to meet demand.

Additionally, with the electrification of heating comes a marked increase in the occupant's energy bills as electricity in the UK is approximately four times the cost of natural gas at present. Once installed, ICSSWH is a free source of energy and the following cost calculation shows the potential saving and capital cost payback times for the plain baffled and finned collectors.

The collector configurations were a bespoke design fabricated by Pentland Tech Metal Fabrications; an Edinburgh based company. The following is the cost breakdown (including VAT) of the main collector components that was provided by the company when fabricated in 2017:

1.5 mm stainless steel tank base - £254.00

3mm aluminium absorber plate with three 3mm fins - £210.00

3mm aluminium plain absorber plate - £58.00

4mm polycarbonate sheet for baffle plate - £35.00

4mm float (single glazed) glass - £35.00

These costs reflect the bespoke nature of the collector and if the system was to become commercialised the production process would be streamlined and value engineered, thus greatly reducing the cost of manufacture. However, uncertain costs are not included such as the pipework, gasket and fittings due to the DIY nature of the project. Additionally, installation and maintenance costs are excluded as these tend to be quoted on an installation case-by-case basis, so any assumption would be highly speculative. Plus, if the collector comes as part of an integrated package with the roof structure, the installation costs will be absorbed in the overall cost of the modular system and no additional on-site plumbing would be required, unlike traditional SWHs. The maintenance costs should be very low as the only requirement is assumed to be a gasket

replacement every five years. Based on the cost of the rubber used for the gasket and the area required, this would be less than £2 plus the cost of labour. Therefore, the capital costs of the bespoke manufactured collectors in this study (including VAT) are estimated as £380 and £500 for the baffled and finned collectors, respectively.

Beyond this, there will be additional costs for the heat retention methods. The additional insulation method will simply be the cost of the insulation used but the method that employs a night cover will have more significant extra costs. The mechanism used in this research was very simple and required manual operation. However, for a consumer application this would have to be much more robust, using a system somewhat like a Velux solar powered blackout blind which costs upwards of £150. Based on the thermal and environmental analysis, discussed in Section 6.1, the extra cost and complexity of the additional night cover is not warranted.

The lifespan of the ICSSWH system is assumed to be 20 years and from the experimental results, the plain baffled collector can provide 5333 kWh and the plain finned collector can provide 5250 kWh throughout its useful life. The market price of energy is variable, so it is difficult to conduct an accurate life cycle payback and thus energy cost projections over the next 20 years are not considered in this estimation. The coronavirus pandemic will have an impact on energy prices, but this is assumed to be a short-term fluctuation. Given that electricity prices increase year-on-year and this trend shows no sign of changing (Ofgem, 2018), the default tariff cap levels developed by Ofgem were used in this calculation for both gas and electricity (Ofgem, 2020a). Currently the average domestic energy prices for Scotland are 24.6 p/kWh for electricity and 6.7 p/kWh for gas, when considering standing charges and a gas boiler efficiency of 80%.

Based on the capital costs of the collectors, the energy they can provide and the cost of energy from the grid, the monetary payback is presented in Table 6.5. Note that the manufacturing costs for a final, commercial collector will be different.

As the cost of the finned collector is higher and the energy contribution is lower than the baffled collector, the monetary savings and paybacks suffer accordingly. Therefore, from a monetary payback perspective, the baffled configuration is again the better-case scenario, offering approximate annual savings of £66 when replacing an electric system

Table 6.5: Total monetary savings offered by the plain baffled and finned collectors and payback times when replacing an electric system and gas boiler, based on a lifespan of 20 years

Parameter	Baffled	Finned
Capital cost	£380	£500
Lifetime energy provision (kWh)	5333	5250
Ofgem electricity tariff (p/kWh)	24.6	
Ofgem gas tariff (p/kWh)	6.7	
Savings, replacing an electric system	£1312	£1292
Savings, replacing a gas system	£357	£352
Monetary payback time (elec)	5.8 years	7.7 years
Monetary payback time (gas)	21.3 years	28.4 years

and £18 when replacing a gas boiler for water heating. This translates to monetary payback times of 5.8 years and 21.3 years, respectively. Therefore, the ICSSWH is only economically feasible when replacing a direct electric heated system, given the lifespan of the collector is assumed to be 20 years. It could not repay its capital costs through savings on the energy bill when replacing a gas boiler as the price of gas is still too competitive. However, with help from the Renewable Heat Incentive government scheme, this system could become viable regardless of the system being replaced. These schemes and incentives are important to encourage the uptake of new low and zero carbon generating technology. Additionally, with a commercial, value engineered system the capital costs, and therefore payback times will be driven down further.

Given the increased interest in offsite modular methods of construction and the shift to electrification of energy supply in the UK, the ICSSWH presented here is an excellent option for building integrated systems. The baffled collector can comfortably repay its capital costs when replacing an electric system and even if an installation cost of £500 is assumed, i.e. the average daily rate for a plumber, the payback time becomes 13.5 years which is still well within the lifespan. However, this system is anticipated to be part of a complete offsite package thus installation would be included in the construction of the house.

6.4 Concluding remarks

The discussion presented in this chapter highlights the novel elements of the design, and the unique contribution the ICSSWH can make to alleviate the current challenges and achieve carbon reduction targets. From a thermal and environmental performance perspective, the system justifies the energy and carbon investment required, offering significant savings and feasible payback times. When placed in the context of existing literature and commercially available systems, the results found in this work are well aligned. These results and the systems' ability to pay back the embodied investment attests to the robustness of the design and methodology.

The construction sector is facing a skills gap with a shortage of skilled labour for building traditional housing. Paired with an increasing need for new housing this is driving the industry toward more modern methods of construction (MMC) such as offsite modular systems. The ICSSWH evaluated in this study is specifically designed for integration into modular construction and the above discussion highlights the benefit of an integrated system. Additionally, the monetary payback times show that the system is economically sustainable even without government incentives such as the Renewable Heat Incentive due to the shift toward electrification of the energy supply. Besides, sustainability is becoming a tool for value creation as opposed to cost reduction (Bakker et al., 2014); products should be designed with a circular economy ethos in mind instead of developing a product and retrospectively assessing its impact.

Solar thermal systems offer a great opportunity for hot water demand, and MMC to meet modern housing demands. MMC is more energy efficient than traditional housing and building offsite as a modular system makes construction more streamlined, safer and cheaper. The ICSSWH presented here pairs the hot water demand with the need for modern homes as it is designed to be "plugged" into modular roof structures, as opposed to commercially available systems that tend to be bolted on to the finished roof. Building integrated systems offer a simpler solution as they come as a single package to help meet the hot water needs of the end user while contributing to emissions targets.

Seventh Chapter

Conclusions

This thesis has presented an argument for the integration of a novel solar water heater design, integrated collector-storage solar water heater (ICSSWH), into the building fabric. The ICSSWH has been specifically designed to be compatible with modern methods of construction (MMC) and offsite modular systems. This chapter first lays out the aim and objectives of this thesis, how they were approached and the valuable results and research answers that were obtained. Following this, the contributions that this piece of work makes to the greater body of knowledge will be outlined. This chapter concludes with recommendations for future work and highlights the limitations of the present research that should be considered moving forward.

7.1 Satisfying the research objectives

The aim of this research was to develop a novel unique ICSSWH design for integration into buildings and optimise its performance under Scottish weather conditions, incorporating circular economy principles. Four objectives were identified to achieve this aim and they are outlined below along with how this research harnessed existing literature and applied an appropriate methodology to accomplish them.

Objective 1

"Optimise the ICSSWH design for integration into modern offsite modular construction."

The dimensions of the ICSSWH were adapted from previous iterations to make

them more compatible with the rafter spacing in modern modular construction. The "plug-and-play" design minimises the complexity of the system and its integration into the roof structure itself means that it can come as part of a complete offsite modular package, as discussed in Chapter 6, Section 6.3. This objective was achieved through appropriate application of the methodology and the thermal analysis presented in Chapter 4, Section 4.4. This demonstrated the enhanced heat retention when embedding the collector into the building fabric as opposed to bolting an insulated frame onto the roof surface. This objective also requires the collector design and materials to be fit for purpose and be effective in terms of solar collection and heat transfer. The choice of storage tank materials was based on the review of the literature (Chapter 2, Section 2.2.1.10) and the combination of the stainless-steel storage tank and aluminium absorber plate was chosen to optimise the collection of solar energy through the absorber while minimising the losses from the back and sides of the storage tank. Additionally, the choice of a stainless-steel storage tank offers greater structural stability for integration into the roof structure. The inclusion of the elongated heat transfer fins and the internal baffle plate do not impact the critical dimensions of the tank and were added to improve heat transfer within the water store. The thermal analysis of the baseline performance illustrates the effectiveness of these elements in terms of heat transfer (Chapter 4, Section 4.1) and the integration into the structural insulated panel (SIP) reduces the thermal losses thus satisfying Objective 1.

Additional heat retention methods were evaluated to further combat the problem of night-time heat losses that these ICS systems commonly suffer from. In line with this first objective, these methods had to be easily incorporated into the system design to maintain the simple "plug-and-play" aspect. To achieve this element of the research aim, Objective 2 must also be satisfied.

Objective 2

"Establish the impact/improvement external heat retention methods have on thermal efficiency without significantly increasing the complexity of the unit."

As stated above, heat retention methods were evaluated to see if they had a signi-

ficant impact on reducing night-time losses without compromising Objective 1 and impeding solar collection or ease of integration into MMC. Based on the review of the literature there were numerous potential options including phase change materials, thermal diodes, additional insulation and baffle plates. From the methods reviewed, several were taken forward to be included in the current evaluation, presented in Chapter 3, Sections 3.2.1 and 3.2.3. Two baseline configurations were developed, one with heat transfer fins and one with an insulating baffle plate, and they were designed considering the best use of storage tank/collector material. Beyond this, two additional heat retention strategies were chosen based on the review of insulation materials in Chapter 2, Section 2.2.1.1. From these, additional opaque insulation was chosen to be applied to the top third of the absorber plate with the aim of harnessing thermal stratification and trapping the heat in the hottest portion of the storage tank. Also, a night-time cover was assessed as this offered a balance between minimising night-time heat losses while maximising day-time solar collection as the full absorber area is available for heat gain, unlike with the additional insulation. This objective sought to determine whether the greater insulating properties of the material used for the additional insulation outweighed the greater day-time heat gains but simpler thermal barrier of the night cover. The heat retention methods chosen in this research were deemed to offer the least complex option but still with significant potential performance improvements, thus aiming to satisfy Objective 2.

The results of the analysis are presented in Chapter 4, Section 4.3, and they show that Objective 2 is satisfied by both baseline configurations. It is also satisfied to an extent by the night cover heat retention method; the night cover does allow for maximum solar gain and was shown to be effective in retaining heat overnight but it did add to the complexity of the unit especially as it had to be applied and removed manually in this research. However, this could be solved, or at least improved, using a solar blind in a final installation scenario. The additional insulation as a heat retention method did not satisfy Objective 2 as the loss of a third of the absorber area reduced the solar gains significantly. Despite it being effective at retaining heat overnight, it demonstrated a much poorer thermal performance than both the baseline and night cover conditions.

Overall, the night cover proved to be an effective heat retention method and could be a simple solution easily integrated into the overall design, with the proper application to make it an integral part of the system that can be controlled remotely or automatically.

Objective 3

"Evaluate the overall performance of the design (considering Objectives 1 and 2) when it is used in a direct draw-off configuration (i.e. hot water use)."

Alongside the thermal performance in terms of improved heat gain and reduced heat loss, the system must perform effectively when used in practical application, under a direct, realistic draw-off configuration. These systems must be tested in real time and under real conditions to minimise the impact of the performance gap which is a common problem when moving from lab-based validation to in-use application. Objective 3 was identified to address this and a realistic draw-off profile, derived from the literature review (Chapter 2, Section 2.3), is applied throughout the experimental tests conducted in Chapter 4. The results of this analysis satisfied Objective 3 by demonstrating that, with the chosen design configurations and conditions and while integrated in a warm roof timber panel, the ICSSWH system could effectively and satisfactorily contribute to the hot water demand of the direct draw-off profile. With the application of the night cover, a larger proportion of the energy required for the morning and evening draw-offs could be provided; Chapter 4, Section 4.3.3.1, shows that, during the non-collection period, the night cover condition can provide temperatures 16°C higher than the baseline condition, on average. For the afternoon draw-off events, the baseline and night cover conditions could provide a similar share. As the additional insulation condition was unable to collect as much incident solar radiation as the other two conditions, its ability to meet the hot water demand throughout the collection period was diminished. Also, the heat retention method could only offer temperatures up to 3°C higher than the baseline condition for the morning and evening draw-offs.

In terms of thermal stratification, Chapter 4, Section 4.1.3 and Section 4.3.3.3, provided an analysis of the temperature stratification in the water store across draw-off events. This showed that, when hot water is drawn from the top of the storage tank and

replaced by cold water at the bottom, the water body becomes more distinctly stratified across the overall length of the tank but the bottom third of the tank does destratify, i.e. mixing occurs between the different temperature layers. For the draw-offs that occur at night, when there is no solar insolation to recharge the system, the water store becomes steadily less stratified. However, when hot water is discharged during the day, the draw-off improves temperature stratification with an increase in the temperature difference between the top and bottom layers of the water store. Therefore, the application of a realistic draw-off profile improves the efficiency of the system as the use and replacement of hot water with cold, inlet water increases the capacity for solar heat gain across the day. Considering the design configurations and conditions covered in Objectives 1 and 2, draw-off has a very similar impact on thermal stratification in all conditions with a noticeable increase in the overall stratification and mild destratification in the lower layers of the water store, as discussed in Chapter 4, Section 4.3.3.3.

Objective 4

"Determine the environmental impact and energy and carbon payback times for the ICSSWH system using Life Cycle Assessment (LCA)."

Objectives 1 to 3 were developed to investigate the practical application and performance of the novel ICSSWH. However, it is essential to evaluate the environmental sustainability of the design especially given its intention to contribute to a low-carbon future. Therefore, Objective 4 addresses the environmental impact of the ICSSWH and the proposed design configurations and conditions and this was satisfied by the analysis presented in Chapter 5. 24 scenarios were considered that evaluated the carbon and energy impact of the baffled and finned collectors with and without the heat retention methods, in an insulated frame or integrated into a SIP, and under a linear or circular end-of-life scenario. The inclusion of this objective is important as it evaluates the whole life sustainability of the system and ties this together with the thermal performance in the form of payback times. From a whole life perspective, as discussed in Chapter 5 Section 5.3, the ICSSWH in the frame has a poorer environmental performance than when embedded in the SIP and the baffled configuration has slightly higher impacts

than the finned. Additionally, the heat retention methods increase the impacts with the night cover generating more than the additional insulation. This is in line with the extra components and materials required.

When it comes to the linear and circular scenarios, a circular approach, i.e. reuse of the collector elements to keep them in the resource loop, has a significantly smaller carbon impact than in the linear case, i.e. the ICSSWH sent to landfill at the end of its useful life. To satisfactorily achieve this objective, the ICSSWH was designed to be disassembled so that all the constituent materials can be cleanly separated for reuse. This is a very important element of the design and was consciously incorporated with a circular economy ethos in mind. Therefore, from an LCA point of view, this research satisfies Objective 4 as the ICSSWH is sustainable in terms of both the energy and environmental impacts. To further validate this result, the energy contribution and carbon savings, as well as the associated payback times, offered by the ICSSWH are compared alongside existing values from the literature and a discussion surrounding this in provided in Chapter 6, Section 6.2.1.

7.2 Contribution to knowledge

In achieving the research aim through the objectives discussed above, the contribution of this thesis advances existing knowledge in different aspects which are identified and outlined below.

Innovation

An advanced ICSSWH design was developed for easier integration into modular offsite construction as well as to provide a more sustainable system. The design for disassembly, where the storage tank and absorber plate are made from different, thermally optimised, materials, is a novel and innovative element of the design that had not been applied to ICSSWH systems. The development and thermal performance evaluation of this decoupled system integrated into a SIP has demonstrated the practical feasibility of the design.

Circular economy approach

The environmental impact and benefit of the ICSSWH due to its unique design for disassembly were evaluated. The capacity to cleanly separate and reuse the system components at the end of its service life was inspired by a circular economy ethos. The analysis presented in this research fills a gap in knowledge whereby circular life cycle assessments of ICSSWHs in a northern maritime context are distinctly lacking in the literature. It also highlights the importance of promoting reuse over the simple landfilling of valuable resources.

Method for practical application

A literature review was conducted to determine a realistic and feasible draw-off profile for the ICSSWH under investigation. A method was then developed to conduct extended field tests for the ICSSWH to determine how the system performance is impacted by transient discharge and recharge cycles, mimicking practical application. The lack of realistic and extended field testing was another gap identified in the existing body of knowledge that this research aimed to fill.

Feasible prototype

Along with the innovative element of this research, the real-life performance assessment of different heat retention methods on the current ICSSWH design under Scottish weather conditions offers a valuable contribution to knowledge. Very few studies have reviewed the performance of ICS-type collectors under a Scottish climate and the combination of the design for disassembly, integration into the building fabric and the design configurations and conditions offers a new perspective for the feasibility of these systems.

These contributions have implications for both current theory surrounding solar water heaters and existing practices concerning their performance evaluation. The novel design for disassembly highlights the importance of considering sustainability in the design stage and carefully choosing materials that support both sustainable design and optimal thermal performance. The experimental tests demonstrated the practical application of the de-constructable design, promoting this as a feasible new paradigm

for SWHs. This design for disassembly also lends itself to circular life cycle thinking, challenging the existing practice of the take-make-waste extractive industrial model (Bakker et al., 2014). The ability to cleanly separate the constituent materials greatly improves the reuse/recycle potential of the system. Evaluating products/systems/services from a circular economy perspective, i.e. decoupling resource consumption from economic growth, allows waste to be turned into wealth and promotes sustainable production and consumption (Lacy and Rutqvist, 2016). Additionally, this is the first study to conduct an environmental sustainability assessment, looking at impact categories beyond carbon using LCA and life cycle thinking, on ICSSWHs in a Scottish context.

7.3 Limitations and recommendations for future work

Research inevitably has limitations. While these have been highlighted throughout the thesis, this section offers a brief recap of the main limitations of this work combined with the opportunities for future research. An important limitation is the seasonal testing methodology. To truly compare the different design conditions and configurations they should all be tested side-by-side, so they are subject to the same environmental conditions. However, due to the expenditure and space that would be required, this was not possible. Another way to conduct a fair comparison would be controlled laboratory tests using a heating pad. However, the aim of this research was to test the systems in-situ, not under 'ideal' lab conditions, thus avoiding the performance gap. Additionally, the heat pad would not have worked alongside the heat retention methods. Another limitation of this research is the location of the solar lab which suffered considerable shading. While this is a limitation to testing the full potential of the system, it represents an advantage in terms of assessing its suitability to real-world application where homes may be subject to shading from surrounding trees, buildings, and infrastructure. Limitations in the LCA component of this work included the integrity and geographic representativeness of the life cycle inventory database used and the 'black box' nature of LCA tools which made comparability with existing literature difficult.

The research design and approach aimed to minimise limitations but, as discussed in Chapter 3 Section 3.1, truly objective research is not possible here. Throughout the interpretation of the experimental results, the errors associated with the experimental apparatus were taken into consideration when assessing the conclusiveness of the findings (see Chapter 3, Section 3.2.6.3). A margin of error was also considered throughout the LCA work, given the inherent uncertainty in LCA modelling (see Chapter 5, Section 5.3.1.4).

There is no rest for the weary and this research has highlighted several avenues for future work. As discussed in Chapter 6, Section 6.3.1, to be compatible with a broader range of modular systems, the tank dimensions could be further adapted to make a longer, slimmer design and this has the added benefit of a better storage tank aspect ratio which improves thermal stratification and thus system performance. An obvious drawback of the ICSSWH presented here, as well as traditional solar water heaters in a northern climate, is the poor energy contribution in the winter months. Therefore, it would be valuable to research the integration of a heating element which could also address the issue of Legionella. The design of the ICSSWH allows for easy incorporation of an immersion heater inside the storage tank; an outlet manifold could run down the centre and the heater would sit inside it. This would work well with the finned design as the manifold would replace the middle fin. Taking this recommendation forward would require extensive thermal analysis to determine the internal thermodynamics as well as a review of the environmental impact as the immersion heater will have an associated impact on both embodied and operational energy and emissions. In terms of integration into offsite modular construction, feasibility studies and structural analyses would need to be conducted to determine the best way to embed and finish the ICSSWH for a final commercial product. For example, in a future installation an insulated blackout blind could be used for the night cover condition. Structural stability would need to be determined through racking tests as well as value engineering the system for commercialisation.

7.4 Concluding remarks

This thesis presented a comprehensive and holistic view of a novel ICSSWH design for disassembly and for integration into modern modular offsite construction. This chapter tied together the aim and objectives of this research with the results of the work that strived to satisfy them. This work has achieved these objectives and the ICSSWH evaluated has been shown to be a feasible prototype from a thermal, sustainable, and practical perspective. Based on the interpretation presented in Chapter 5, Section 5.4, the energy required to meet the hot water demand per person (i.e. one ICSSWH) in Scotland in any given year is 633 kWh and, considering the plain baffled configuration, the ICSSWH can provide 267 kWh. With extensive uptake of this technology, significant carbon savings could be achieved; for example, if ICSSWHs were integrated into all the 10,000 new builds promised by the City of Edinburgh Council's 21st Century Homes programme (discussed in Chapter 6, Section 6.3). The average household size in Edinburgh is 2.07 people and, considering the replacement of an electric system and decarbonisation of the electricity grid given the drive toward low carbon and non-gas heating technologies, the potential carbon savings over the 20-year useful life of the collectors would be approximately 13,200 tonnes of CO_{2e}. This would bring the operational carbon emissions associated with the hot water demand of the new homes down by 42%.

Due to Covid-19, there is a lot of uncertainty in the energy sector and in future government policies. With this pandemic highlighting the fragility of the energy market and the share of renewables jumping several years ahead of pre-pandemic estimates, economic stimulus packages will be an opportunity to link economic recovery efforts with clean energy transitions. Solar thermal energy could play a major role in the future energy picture and the ICSSWH evaluated in this work has an important advantage over its commercial counterparts. The physical integration into the roof structure is a critical element; the ICSSWH is designed to come as part of a pre-built package, already integrated into the modular roof structure when it arrives on site, with the renewable

delivery required to meet carbon objectives. The thermal and environmental analysis presented in this work demonstrates the environmental sustainability of the system, and the element of integration illustrates the benefits of its practical application.

References

Ahmadzadeh, J. and M. Gascoigne (1976). “Efficiency of solar collectors”. In: *Energy Conversion and Management* 16, pp. 13–17 (cit. on p. 32).

Allen, S R, G P Hammond, H A Harajli, M C Mcmanus and A B Winnett (2010). “Integrated appraisal of a Solar Hot Water system”. In: *Energy* 35.3, pp. 1351–1362. DOI: 10.1016/j.energy.2009.11.018 (cit. on pp. 59, 60, 62).

Araya, R., F. Bustos, J. Contreras and A. Fuentes (2017). “Life-cycle savings for a flat-plate solar water collector plant in Chile”. In: *Renewable Energy* 112, pp. 365–377. DOI: 10.1016/j.renene.2017.05.036 (cit. on p. 59).

Ardente, Fulvio, Giorgio Beccali, Maurizio Cellura and Valerio Lo Brano (2005). “Life cycle assessment of a solar thermal collector”. In: *Renewable Energy* 30, pp. 1031–1054. DOI: 10.1016/j.renene.2004.09.009 (cit. on pp. 60, 68).

Arnaoutakis, N., M. Souliotis and S. Papaefthimiou (2017). “Comparative experimental Life Cycle Assessment of two commercial solar thermal devices for domestic applications”. In: *Renewable Energy* 111, pp. 187–200. DOI: 10.1016/j.renene.2017.04.008 (cit. on p. 61).

Arnaoutakis, Nektarios, Maria Milousi, Spiros Papaefthimiou, Paris A Fokaides, Yannis G Caouris and Manolis Souliotis (2019). “Life cycle assessment as a methodological tool for the optimum design of integrated collector storage solar water heaters”. In: *Energy* 182, pp. 1084–1099. DOI: 10.1016/j.energy.2019.06.097 (cit. on p. 187).

Ates, Aylin (2008). “Strategy Process in Manufacturing SMEs”. PhD thesis. University of Strathclyde, p. 344. ISBN: 2005020621 (cit. on p. 73).

Bainbridge, D.A. (1981). “Integral passive solar water heater performance”. In: *Proceedings of the sixth National Passive Solar Conference*. Portland, Oregon, USA, pp. 163–167 (cit. on pp. 32, 40).

Bakker, Conny, Cornelia Ariadne Bakker, Marcel den Hollander, Ed van Hinte and Yvo Zijlstra (2014). “Chapter 5: Which product design strategies apply to your product?” In: *Products that Last: Product design for circular business models*. 1st. TU Delft Library. Chap. 5, pp. 97–118. ISBN: 9461863861 (cit. on pp. 206, 214).

Balaji, K., S. Iniyan and Muthusamy V. Swami (2018). “Exergy, economic and environmental analysis of forced circulation flat plate solar collector using heat transfer enhancer in riser tube”. In: *Journal of Cleaner Production* 171, pp. 1118–1127. DOI: 10.1016/j.jclepro.2017.10.093 (cit. on p. 59).

Bamber, Nicole, Ian Turner, Vivek Arulnathan, Yang Li, Shiva Zargar Ershadi, Alyssa Smart and Nathan Pelletier (2020). “Comparing sources and analysis of uncertainty in consequential and attributional life cycle assessment: review of current practice and recommendations”. In: *International Journal of Life Cycle Assessment* 25.1, pp. 168–180. DOI: 10.1007/s11367-019-01663-1 (cit. on pp. 172, 177).

Battisti, Riccardo and Annalisa Corrado (2005). “Environmental assessment of solar thermal collectors with integrated water storage”. In: *Journal of Cleaner Production* 13, pp. 1295–1300. DOI: 10.1016/j.jclepro.2005.05.007 (cit. on p. 60).

Birley, Peter, Celine Garnier, John Currie, Tariq Muneer and Corresponding Author (2012). “CFD Study of an Integrated Collector Storage Domestic Solar Hot Water System”. In: *Eurosun 2012* (cit. on pp. 5, 76, 77, 80, 82, 92, 103).

Bishop, R.C. (1983). “Superinsulated batch heaters for freezing climates”. In: *Eighth National Passive Solar Conference*, pp. 807–810 (cit. on p. 30).

BP (2019). *BP Energy Outlook: 2019 edition*. Tech. rep., pp. 1–73 (cit. on p. 1).

BSI (2011). *BS EN 15978:2011 Standards Publication Sustainability of construction works — Assessment of environmental performance of buildings — Calculation method*. Tech. rep. November. London: British Standards Institution (cit. on p. 62).

BSI (2012). *BS EN 12977-2: Thermal solar systems and components — Custom built systems*. Tech. rep. Brussels: CEN; 2012 (cit. on p. 53).

BSI (2013). *BS ISO 9459-4: Solar heating — Domestic water heating systems*. Tech. rep. Switzerland, p. 80 (cit. on pp. 53, 125).

Building Scottish Standards (2013). *Building (Scotland) Regulations 2004 Technical Handbook - Domestic*. URL: https://www2.gov.scot/resource/buildingstandards/2013Domestic/chunks/index.html (visited on 01/08/2019) (cit. on p. 95).

Buker, Mahmut Sami and Saffa B. Riffat (2015). "Building integrated solar thermal collectors - A review". In: *Renewable and Sustainable Energy Reviews* 51, pp. 327–346. DOI: 10.1016/j.rser.2015.06.009 (cit. on pp. 43, 44, 198).

Burgess, Paul (2009). "Variation in Light Intensity At Different Latitudes and Seasons, Effects of Cloud Cover, and the Amounts of Direct and Diffused Light". In: *Continuous Cover Forestry Group (CCFG) Scientific Meeting*, pp. 1–10. URL: http://www.ccfg.org.uk/conferences/downloads/P%7B%5C_%7DBurgess.pdf (cit. on p. 101).

Burton, J.W. and P.R Zweig (1981). "Side by side comparison of integral passive solar water heaters". In: *Proceedings of the sixth National Passive Solar Conference*. Portland, Oregon, USA, pp. 136–140 (cit. on p. 40).

Carbon Trust (2017). *Carbon footprinting*. Tech. rep., p. 27. URL: https://www.carbontrust.com/resources/guides/carbon-footprinting-and-reporting/carbon-footprinting/ (cit. on pp. 63, 159).

Carlsson, P.F. (1993). "Heat storage for large low flow solar heating systems." In: *Proceedings of the ISES Solar World Conference*. Budapest, Hungary, pp. 441–445 (cit. on p. 33).

Carnevale, E, L Lombardi and L Zanchi (2014). "Life Cycle Assessment of solar energy systems: Comparison of photovoltaic and water thermal heater at domestic scale". In: *Energy* 77, pp. 434–446. DOI: 10.1016/j.energy.2014.09.028 (cit. on pp. 61, 185, 187).

Chaabane, Monia, Hatem Mhiri and Philippe Bournot (2013). "Thermal performance of an integrated collector storage solar water heater (ICSSWH) with a storage tank equipped with radial fins of rectangular profile". In: *Heat and Mass Transfer/Waerme- und Stoffuebertragung* 49.1, pp. 107–115. DOI: 10.1007/s00231-012-1065-z (cit. on p. 29).

Chaabane, Monia, Hatem Mhiri and Philippe Bournot (2014). "Thermal performance of an integrated collector storage solar water heater (ICSSWH) with phase change materials (PCM)". In: *Energy Conversion and Management* 78, pp. 897–903. DOI: 10.1016/j.enconman.2013.07.089 (cit. on pp. 19, 35, 37, 94).

Chaouachi, B. and S. Gabsi (2006). “Experimental study of integrated collector storage solar water heater under real conditions”. In: *Renew Energy Revue* 9.2, pp. 75–82 (cit. on p. 29).

Chaurasia, P. B L and John Twidell (2001). “Collector cum storage solar water heaters with and without transparent insulation material”. In: *Solar Energy* 70.5, pp. 403–416. DOI: 10.1016/S0038-092X(00)00158-4 (cit. on p. 18).

Chen, Guangming, Alexander Doroshenko, Paul Koltun and Kostyantyn Shestopalov (2015). “Comparative field experimental investigations of different flat plate solar collectors”. In: *Solar Energy* 115, pp. 577–588. DOI: 10.1016/j.solener.2015.03.021 (cit. on p. 61).

Chen, J. F., L. Zhang and Y. J. Dai (2018). “Performance analysis and multi-objective optimization of a hybrid photovoltaic/thermal collector for domestic hot water application”. In: *Energy* 143, pp. 500–516. DOI: 10.1016/j.energy.2017.10.143 (cit. on p. 59).

Chung, Jae Dong, Sung Hwan Cho, Choon Seob Tae and Hoseon Yoo (2008). “The effect of diffuser configuration on thermal stratification in a rectangular storage tank”. In: *Renewable Energy* 33.10, pp. 2236–2245. DOI: 10.1016/j.renene.2007.12.013 (cit. on p. 33).

City of Edinburgh Council (2019). *Capital sets ambitious neutral carbon target of 2030*. URL: https://www.edinburgh.gov.uk/news/article/12648/capital-sets-ambitious-neutral-carbon-target-of-2030 (visited on 20/05/2020) (cit. on p. 197).

Colangelo, Gianpiero, Ernani Favale, Paola Miglietta and Arturo De Risi (2016). “Innovation in flat solar thermal collectors: A review of the last ten years experimental results”. In: *Renewable and Sustainable Energy Reviews* 57, pp. 1141–1159. DOI: 10.1016/j.rser.2015.12.142. URL: http://dx.doi.org/10.1016/j.rser.2015.12.142 (cit. on pp. 15, 57).

Collinge, William O., Amy E. Landis, Alex K. Jones, Laura A. Schaefer and Melissa M. Bilec (2013). “Dynamic life cycle assessment: Framework and application to an institutional building”. In: *International Journal of Life Cycle Assessment* 18.3, pp. 538–552. DOI: 10.1007/s11367-012-0528-2 (cit. on p. 69).

Comodi, G, M Bevilacqua, F Caresana, L Pelagalli, P Venella and C Paciarotti (2014). “LCA analysis of renewable domestic hot water systems with unglazed and glazed solar thermal panels”. In: *Energy Procedia* 61, pp. 234–237. DOI: 10.1016/j.egypro.2014.11.1096 (cit. on p. 61).

Consoli, F. et al. (1993). “Guidelines for Life-Cycle Assessment: A ’Code of Practice’”. In: *5th technical workshop on LCA sponsored by the Society of Environmental Toxicology and Chemistry (SETAC)*. Sesimbra, Portugal (cit. on p. 62).

Construction Scotland (2018). *The Scottish Construction Industry Strategy 2019-2022*. Tech. rep. Blantyre, Scotland. URL: https://www.cs-ic.org/media/3353/construction-industry-strategy2-for-web-copy.pdf (cit. on p. 199).

Conticini, Edoardo, Bruno Frediani and Dario Caro (2020). “Can atmospheric pollution be considered a co-factor in extremely high level of SARS-CoV-2 lethality in Northern Italy?” In: *Environmental Pollution*. DOI: 10.1016/j.envpol.2020.114465 (cit. on p. 196).

Crawford, Robert H. (2008). “Validation of a hybrid life-cycle inventory analysis method”. In: *Journal of Environmental Management* 88.3, pp. 496–506. DOI: 10.1016/j.jenvman.2007.03.024 (cit. on p. 69).

Crawford, Robert H. (2011). *Life cycle assessment in the built environment*. Taylor & Francis (cit. on p. 69).

Crawford, Robert H., Paul Antoine Bontinck, André Stephan and Thomas Wiedmann (2017). “Towards an Automated Approach for Compiling Hybrid Life Cycle Inventories”. In: *Procedia Engineering* 180, pp. 157–166. DOI: 10.1016/j.proeng.2017.04.175 (cit. on p. 69).

Crawford, Robert H. and André Stephan (2013). “The Significance of Embodied Energy in Certified Passive Houses”. In: *International Journal of Civil, Environmental, Structural, Construction and Architectural Engineering* 7.6, pp. 427–433 (cit. on p. 69).

Creswell, John W. (2014). *Research design: Qualitative, quantitative, and mixed methods approaches*. 4th. California: SAGE Publications, Inc., p. 342. ISBN: 978-1-4522-2610-1 (cit. on p. 73).

Cuce, Erdem and Saffa B. Riffat (2015a). “A state-of-the-art review on innovative glazing technologies”. In: *Renewable and Sustainable Energy Reviews* 41, pp. 695–714. DOI: 10.1016/j.rser.2014.08.084 (cit. on pp. 29, 31, 32).

Cuce, Erdem and Saffa B. Riffat (2015b). “Aerogel-Assisted Support Pillars for Thermal Performance Enhancement of Vacuum Glazing: A CFD Research for a Commercial Product”. In: *Arabian Journal for Science and Engineering* 40.8, pp. 2233–2238. DOI: 10.1007/s13369-015-1727-5 (cit. on p. 31).

Cui, Yan, Zuo-Feng Zhang, John Friones, Jinkou Zhao, Hua Wang, Shun-Zhang Yu and Roger Detels (2003). "Air pollution and case fatality of SARS in the People's Republic of China: an ecologic study". In: *Environmental Health* 2.15. DOI: https://doi.org/10.1186/1476-069X-2-15 (cit. on p. 196).

Cummings, J. and G. Clark (1983). "Performance of integrated passive solar water heaters in US climates". In: *Proceedings of the eighth National Passive Solar Conference*. Santa Fe, New Mexico, USA, pp. 791–796 (cit. on p. 40).

Currie, John, Celine Garnier, Tariq Muneer, Tom Grassie and Douglas Henderson (2008). "Modelling bulk water temperature in integrated collector storage systems". In: *Building Service Engineering* 29.2, pp. 203–218. DOI: 10.1177/0143624408094277 (cit. on pp. 3, 13, 28, 46, 49).

DBEIS (2019a). *UK becomes first major economy to pass net zero emissions law*. URL: https://www.gov.uk/government/news/uk-becomes-first-major-economy-to-pass-net-zero-emissions-law (visited on 17/09/2019) (cit. on p. 2).

DBEIS (2019b). *Valuation of energy use and greenhouse gas*. Tech. rep. April, p. 48 (cit. on p. 178).

DECC (2015). *The Non-Domestic National Energy Efficiency Data-Framework : Energy Statistics 2006-12*. Tech. rep. March, p. 61. URL: https://assets.publishing.service.gov.uk/government/uploads/system/uploads/attachment%7B%5C_%7Ddata/file/416369/non%7B%5C_%7Ddomestic%7B%5C_%7Dnational%7B%5C_%7Denergy%7B%5C_%7Defficiency%7B%5C_%7Ddata%7B%5C_%7Dframework%7B%5C_%7Denergy%7B%5C_%7Dstatistics%7B%5C_%7D2006-12.pdf (cit. on p. 2).

Devanarayanan, K. and K. Kalidasa Murugavel (2014). "Integrated collector storage solar water heater with compound parabolic concentrator - Development and progress". In: *Renewable and Sustainable Energy Reviews* 39, pp. 51–64. DOI: 10.1016/j.rser.2014.07.076 (cit. on p. 37).

Dragsted, Janne, Simon Furbo, Mark Dannemand and Federico Bava (2017). "Thermal stratification built up in hot water tank with different inlet stratifiers". In: *Solar Energy* 147, pp. 414–425. DOI: 10.1016/j.solener.2017.03.008 (cit. on p. 34).

Drück, H and E Hahne (1998). "Test and Comparison of Hot Water Stores for Solar Combisystems". In: *Eurosun '98* III, pp. 3.3.1–7. URL: http://kske.fgg.uni-lj.si/eurosun98/abstracts/III%7B%5C_%7D3.html (cit. on p. 22).

Duffie, J. and W Beckman (2006). *Solar Engineering of Thermal Processes, 3th ed.* Vol. 116, p. 67. ISBN: 1118418123. DOI: 10.1115/1.2930068. arXiv: arXiv:1011.1669v3. URL: http://books.google.com/books?hl=en%7B%5C&%7Dlr=%7B%5C&%7Did=qkaWBrOuAEgC%7B%5C&%7Dpgis=1 (cit. on p. 29).

Eames, P. C. and B. Norton (1998). "The effect of tank geometry on thermally stratified sensible heat storage subject to low Reynolds number flows". In: *International Journal of Heat and Mass Transfer* 41.14, pp. 2131–2142. DOI: 10.1016/S0017-9310(97)00349-9 (cit. on p. 48).

Ecevit, A., M.A.M. Chaikh Wais and A.M. Al-Shariah (1990). "A comparative evaluation of the performances of three built-in-storage-type solar water heaters". In: *Solar Energy* 44.1, pp. 23–26 (cit. on p. 48).

Ecevit, A., A.M. Al-Shariah and E.D. Apaydin (1989). "Triangular built-in-storage solar water heater". In: *Solar Energy* 42.3, pp. 253–265 (cit. on p. 48).

Electricity Info (2020). *Real Time British Electricity Fuel Mix*. URL: http://electricityinfo.org/real-time-british-electricity-supply/ (visited on 30/01/2020) (cit. on p. 178).

Elsherbiny, S.M., G.D. Raithby and K.G.T. Hollands (1982). "Heat transfer by natural convection across vertical and incline air layers". In: *Journal of Heat Transfer* 104, pp. 96–102 (cit. on p. 49).

Energy Saving Trust (2008). *Measurement of Domestic Hot Water Consumption in Dwellings*. Tech. rep. URL: https://www.gov.uk/government/uploads/system/uploads/attachment%7B%5C%%7D7B%7B%5C_%7D%7B%5C%%7D7Ddata/file/48188/3147-measure-domestic-hot-water-consump.pdf (cit. on pp. 55, 57, 97, 125).

Erlandsson, Martin and Mathias Borg (2003). "Generic LCA-methodology applicable for buildings, constructions and operation services - today practice and development needs". In: *Building and Environment* 38.7, pp. 919–938. DOI: 10.1016/S0360-1323(03)00031-3 (cit. on p. 69).

European Commission (2002). "Mandate to CEN and CENELEC for the elaboration and adoption of measurement standards for household appliances: water-heaters, hot water storage appliances and water heating systems." In: September, pp. 1–14 (cit. on pp. 53, 97, 125, 126).

European Commission (2003). *Report from the Commission under Council Decision 93/389/EEC as amended by Decision 99/296/EC for a monitoring mechanism of Community greenhouse gas emissions*. Tech. rep. (cit. on p. 2).

European Commission (2012). *Characterisation factors of the ILCD Recommended Life Cycle Impact Assessment methods: database and supporting information*, p. 31. DOI: 10.2788/60825 (cit. on p. 2).

Evans, Simon (2020). *Analysis: Coronavirus set to cause largest ever annual fall in CO2 emissions*. URL: https://www.carbonbrief.org/analysis-coronavirus-set-to-cause-largest-ever-annual-fall-in-co2-emissions (visited on 11/05/2020) (cit. on p. 195).

Faiman, David, Haim Hazan and Ido Laufer (2001). "Reducing the heat loss at night from solar water heaters of the integrated collector-storage variety". In: *Solar Energy* 71.2, pp. 87–93. DOI: 10.1016/S0038-092X(01)00021-4 (cit. on p. 24).

Fang, Yueping, Trevor J. Hyde and Neil Hewitt (2010). "Predicted thermal performance of triple vacuum glazing". In: *Solar Energy* 84.12, pp. 2132–2139. DOI: 10.1016/j.solener.2010.09.002 (cit. on p. 32).

Fasulo, A., L. Odicino and D. Perello (1987). "Development of CPC with low thermal losses". In: *Solar Wind Technology* 4, pp. 157–162 (cit. on p. 40).

Fertahi, Saïf ed Dîn, T. Bouhal, F. Gargab, A. Jamil, T. Kousksou and A. Benbassou (2018). "Design and thermal performance optimization of a forced collective solar hot water production system in Morocco for energy saving in residential buildings". In: *Solar Energy* 160.December 2017, pp. 260–274. DOI: 10.1016/j.solener.2017.12.015 (cit. on p. 59).

Finnveden, G. (1997). "Valuation methods within LCA - Where are the values?" In: *The International Journal of Life Cycle Assessment* 2, pp. 163–169 (cit. on p. 74).

Frid, S. E., A. V. Arsatov and M. Yu. Oshchepkov (2016). "Engineering solutions for polymer composites solar water heaters production". In: *Thermal Engineering* 63.6, pp. 399–403. DOI: 10.1134/S0040601516060021 (cit. on pp. 33, 43, 44).

Frischknecht, R, A Braunschweig, P. Hofstetter and P. Suter (2000). “Human health damages due to ionising radiation in life cycle impact assessment”. In: *Environmental Impact Assessment Review* 20, pp. 159–189 (cit. on p. 66).

Frischknecht, R, R Steiner and N Jungbluth (2009). *The Ecological Scarcity Method - Eco-factors 2006: A method for impact assessment in LCA*. Umwelt-Wissen Nr.0906: Swiss Federal Office for the Environment (FOEN), Bern (cit. on p. 66).

Gardner, Leroy (2005). “The use of stainless steel in structures”. In: *Progress in Structural Engineering and Materials* 7.2, pp. 45–55. DOI: 10.1002/pse.190 (cit. on p. 42).

Garnier, C, J I Currie, T Muneer and A Girard (2008). “Computational study of an integrated collector storage solar water heater”. In: *Eurosun 2008*, pp. 1–8 (cit. on pp. 28, 80).

Garnier, C. (2009). “Performance measurement and mathematical modelling of integrated solar water heaters”. PhD thesis. Edinburgh Napier University (cit. on pp. 5, 21, 22, 28, 42, 49, 56, 59, 60, 70, 76, 77, 81, 87, 116, 122, 168, 185, 187).

Garnier, Celine, Tariq Muneer and John Currie (2018). “Numerical and empirical evaluation of a novel building integrated collector storage solar water heater”. In: *Renewable Energy* 126, pp. 281–295. DOI: 10.1016/j.renene.2018.03.041 (cit. on pp. 22, 23, 82).

Gertzos, K. P. and Y. G. Caouris (2008). “Optimal arrangement of structural and functional parts in a flat plate integrated collector storage solar water heater (ICSSWH)”. In: *Experimental Thermal and Fluid Science* 32.5, pp. 1105–1117. DOI: 10.1016/j.expthermflusci.2008.01.003 (cit. on p. 27).

Ghoneim, A. A. (2005). “Performance optimization of solar collector equipped with different arrangements of square-celled honeycomb”. In: *International Journal of Thermal Sciences* 44.1, pp. 95–105. DOI: 10.1016/j.ijthermalsci.2004.03.008 (cit. on p. 19).

Ghosh, Aritra and Brian Norton (2017). “Solar Energy Materials & Solar Cells Interior colour rendering of daylight transmitted through a suspended particle device switchable glazing”. In: *Solar Energy Materials and Solar Cells* 163.October 2016, pp. 218–223. DOI: 10.1016/j.solmat.2017.01.041 (cit. on p. 41).

Grant, J, L Ping Low, S Unsworth, C Hornwall and M Davies (2018). *Time to get on with it - The Low Carbon Index 2018*. Tech. rep. PwC, p. 16 (cit. on p. 178).

Grassie, T., H. Junaidi, T. Muneer, J. Currie and D. Henderson (2006). "Study of the Modified Built-in Storage (Integrated Collector Storage) Solar Water Heater for Scottish Weather Conditions". In: *EuroSun 2006*. Groenhout (cit. on pp. 16, 116).

Gray, David E. (2011). *Doing research in the real world*. California: SAGE Publications, Inc., p. 441 (cit. on p. 73).

Greening, Benjamin and Adisa Azapagic (2014). "Domestic solar thermal water heating: A sustainable option for the UK?" In: *Renewable Energy* 63, pp. 23–36. DOI: 10.1016/j.renene.2013.07.048 (cit. on pp. 58, 59, 61).

Guinée, J.B. et al. (2002). *Handbook on Life Cycle Assessment: Operational Guide to the ISO Standards Series: Eco-efficiency in industry and science*. Ed. by J. Guinée. Dordrecht: Kluwer Academic Publishers (cit. on p. 66).

Hahne, E. and Y. Chen (1998). "Numerical study of flow and heat transfer characteristics in hot water stores". In: *Solar Energy* 64.1-3, pp. 9–18. DOI: 10.1016/S0038-092X(98)00051-6 (cit. on p. 47).

Haillot, D., F. Nepveu, V. Goetz, X. Py and M. Benabdelkarim (2012). "High performance storage composite for the enhancement of solar domestic hot water systems. Part 2: Numerical system analysis". In: *Solar Energy* 86.1, pp. 64–77. DOI: 10.1016/j.solener.2011.09.006 (cit. on p. 35).

Hamed, Mouna, Ali Fallah and Ammar Ben Brahim (2017). "Numerical analysis of charging and discharging performance of an integrated collector storage solar water heater". In: *International Journal of Hydrogen Energy* 42.13, pp. 8777–8789. DOI: 10.1016/j.ijhydene.2016.11.179 (cit. on pp. 35, 36, 37).

Han, Z.M., Y.W. Bao, W.D. Wu, Z.Q Liu, X.G. Liu and Y. Tian (2012). "Evaluation of thermal performance for vacuum glazing by using three-dimensional finite element model". In: *Key Engineering Materials* 492, pp. 328–332 (cit. on p. 31).

Harmim, A., M. Boukar, M. Amar and Aek Haida (2019). "Simulation and experimentation of an integrated collector storage solar water heater designed for integration into building facade". In: *Energy* 166, pp. 59–71. DOI: 10.1016/j.energy.2018.10.069 (cit. on p. 185).

Haskell, C.L. (1907). *Solar heater. US 842658 A* (cit. on pp. 26, 27).

Hegazy, Adel A. (2007). “Effect of inlet design on the performance of storage-type domestic electrical water heaters”. In: *Applied Energy* 84.12, pp. 1338–1355. DOI: 10.1016/j.apenergy.2006.09.014 (cit. on pp. 33, 34).

Hegazy, Adel A. and M. R. Diab (2002). “Performance of an improved design for storage-type domestic electrical water-heaters”. In: *Applied Energy* 71.4, pp. 287–306. DOI: 10.1016/S0306-2619(02)00006-5 (cit. on p. 33).

Heijungs, R. (1998). “Towards eco-efficiency with LCA’s prevention principle: an epistemological foundation of LCA using axioms”. In: *Product Innovation and Eco-efficiency*. Ed. by J.M. Klostermann and A. Tukker. The Netherlands: Springer (cit. on p. 74).

Henderson, D., H. Junaidi, T. Muneer, T. Grassie and J. Currie (2007). “Experimental and CFD investigation of an ICSSWH at various inclinations”. In: *Renewable and Sustainable Energy Reviews* 11.6, pp. 1087–1116. DOI: 10.1016/j.rser.2005.11.003 (cit. on pp. 5, 48, 49, 50, 81, 92, 202).

Hertwich, E.G., J.K. Hammitt and W.S. Pease (2000). “A Theoretical Foundation for Life-Cycle Assessment”. In: *Journal of Industrial Ecology* 4, pp. 13–28 (cit. on p. 74).

HM Treasury (2015). *Spending Review and Autumn Statement 2015*. Tech. rep. URL: https://assets.publishing.service.gov.uk/government/uploads/system/uploads/attachment%7B%5C_%7Ddata/file/479749/52229%7B%5C_%7DBlue%7B%5C_%7DBook%7B%5C_%7DPU1865%7B%5C_%7DWeb%7B%5C_%7DAccessible.pdf%7B%5C%%7D0Ahttp://www.publications.parliament.uk/pa/cm201516/cmselect/cmtreasy/638/63805.htm%7B%5C#%7Dfootnote-050-backlink (cit. on p. 197).

HM Treasury (2018). *Budget 2018*. Tech. rep. October. House of Commons. URL: https://assets.publishing.service.gov.uk/government/uploads/system/uploads/attachment%7B%5C_%7Ddata/file/752202/Budget%7B%5C_%7D2018%7B%5C_%7Dred%7B%5C_%7Dweb.pdf (cit. on p. 197).

Homes for Scotland (2015). “Mainstreaming Offsite Modern Methods of Construction (MMC) in House Building”. In: August. URL: http://www.homesforscotland.com/Our-work/Publications (cit. on p. 199).

Ibrahim, Oussama, Farouk Fardoun, Rafic Younes and Hasna Louahlia-Gualous (2014). “Review of water-heating systems: General selection approach based on energy and environmental

aspects". In: *Building and Environment* 72, pp. 259–286. DOI: 10.1016/j.buildenv.2013.09.006 (cit. on p. 15).

IEA (2020). *Global Energy Review 2020*. Tech. rep. Paris: International Energy Agency (IEA). URL: https://www.iea.org/reports/global-energy-review-2020 (cit. on pp. 195, 196).

ILCD (2010). *Framework and Requirements for Life Cycle Impact Assessment Models and Indicators*. 1st, p. 105. DOI: 10.2788/38719. URL: http://eplca.jrc.ec.europa.eu/uploads/ILCD-Handbook-LCIA-Framework-Requirements-ONLINE-March-2010-ISBN-fin-v1.0-EN.pdf%7B%5C%%7D0Ahttp://eplca.jrc.ec.europa.eu/ (cit. on pp. 63, 65, 170, 190).

ILCD (2011). *Recommendations for Life Cycle Impact Assessment in the European context - based on existing environmental impact assessment models and factors*. Tech. rep. DOI: 10.278/33030 (cit. on p. 66).

Incropera, F.P., D.P. DeWitt, T.L. Bergmann and A.S. Lavine (2013). *Principles of Heat and Mass Transfer*. 7th. New York: Wiley & Sons (cit. on pp. 40, 42).

IPCC (2014a). *Climate Change 2014: Mitigation of Climate Change*. Tech. rep., p. 1454. DOI: 10.1017/CBO9781107415416. arXiv: arXiv:1011.1669v3 (cit. on p. 11).

IPCC (2014b). *Climate Change 2014: Synthesis Report. Contribution of Working Groups I, II and III to the Fifth Assessment Report of the Intergovernmental Panel on Climate Change*. Tech. rep. Geneva, Switzerland: IPCC, p. 151 (cit. on pp. 63, 66).

ISO14040 (2006). "Environmental management — Life cycle assessment — Principles and framework". In: (cit. on pp. 62, 65, 108, 155).

Jaisankar, S., J. Ananth, S. Thulasi, S. T. Jayasuthakar and K. N. Sheeba (2011). "A comprehensive review on solar water heaters". In: *Renewable and Sustainable Energy Reviews* 15.6, pp. 3045–3050. DOI: 10.1016/j.rser.2011.03.009 (cit. on p. 57).

Jamar, A., Z.A.A. Majid, W.H. Azmi, M. Norhafana and A.A. Razak (2016). "A review of water heating system for solar energy applications". In: *International Communications in Heat and Mass Transfer* 76, pp. 178–187. DOI: 10.1016/j.icheatmasstransfer.2016.05.028 (cit. on p. 15).

Jelle, B.P., A. Hynd, A. Gustavsen, D. Arasteh, H. Goudey and R. Hart (2012). “Fenestration of today and tomorrow: a state-of-the-art review and future research opportunities”. In: *Solar Energy Materials and Solar Cells* 96, pp. 1–28 (cit. on p. 31).

Jordan, U and Klaus Vajen (2000). “Influence of the DHW profile on the Fractional Energy\rSavings: A Case Study of a Solar Combi-System”. In: *Solar Energy* 69.1-6, pp. 197–208. DOI: http://dx.doi.org/10.1016/S0038-092X(00)00154-7 (cit. on p. 55).

Junaidi, H.A. A, D. Henderson, T. Muneer, T. Grassie and J. Currie (2006). “Study of Stratification in ICSSWH (Integrated Collector Storage Solar Water Heater)”. In: *9th AIAA/ASME Joint Thermophysis & Heat Transfer Conference* June, pp. 1–7 (cit. on p. 49).

Junaidi, Haroon A (2007). “Optimized Solar Water Heater for Scottish Weather Conditions”. PhD thesis. Edinburgh Napier University (cit. on pp. 5, 11, 28, 49, 51, 122).

Kablan, M. M. (2004). “Techno-economic analysis of the Jordanian solar water heating system”. In: *Energy* 29.7, pp. 1069–1079. DOI: 10.1016/j.energy.2004.01.003 (cit. on p. 22).

Kalogirou, Soteris (2009). “Thermal performance , economic and environmental life cycle analysis of thermosiphon solar water heaters”. In: *Solar Energy* 83.1, pp. 106–115. DOI: 10.1016/j.solener.2008.06.005 (cit. on p. 60).

Kaushik, S. C., R. Kumar and H. P. Garg (1995). “Effect of baffle plate on the performance of a triangular built-in-storage solar water heater”. In: *Energy Conversion and Management* 36.5, pp. 337–342. DOI: 10.1016/0196-8904(95)98898-W (cit. on pp. 24, 26).

Kaushik, S. C., Rakesh Kumar, H. P. Garg and J. Prakash (1994). “Transient analysis of a triangular built-in-storage solar water heater under winter conditions”. In: *Heat Recovery Systems and CHP* 14.4, pp. 337–341. DOI: 10.1016/0890-4332(94)90037-X (cit. on p. 48).

Kaushika, N D and K S Reddy (1999). “Thermal design and field experiment of transparent honeycomb insulated integrated-collector-storage solar water heater”. In: *Applied Thermal Engineering* 19, pp. 145–161. DOI: 10.1016/S1359-4311(98)00033-7 (cit. on p. 19).

Kaushika, N. D. and K. Sumathy (2003). “Solar transparent insulation materials: A review”. In: *Renewable and Sustainable Energy Reviews* 7.4, pp. 317–351. DOI: 10.1016/S1364-0321(03)00067-4 (cit. on p. 18).

Al-Kayiem, Hussain H. and Saw C. Lin (2014). “Performance evaluation of a solar water heater integrated with a PCM nanocomposite TES at various inclinations”. In: *Solar Energy* 109.1, pp. 82–92. DOI: 10.1016/j.solener.2014.08.021 (cit. on p. 35).

Khalifa, N (1998). “Forced versus natural circulation solae water heaters: A comparative performance study”. In: *Renewable Energy* 14, pp. 77–82. DOI: 10.1016/S0960-1481(98)00050-0 (cit. on p. 13).

AL-Khaliffajy, M. and R. Mossad (2011). “Optimization of the Air Gap Spacing In a Solar Water Heater with Double Glass”. In: *9th Australasian Heat and Mass Transfer Conference*. 1. Melbourne, Victoria, Australia (cit. on p. 30).

Knight, A. and N. Turnbull (2008). “Epistemology”. In: *Advanced Research Methods in the Built Environment*. Ed. by A. Knight and L. Ruddock. Oxford, UK: Wiley-Blackwell (cit. on p. 73).

Koroneos, Christopher J and Evanthia A Nanaki (2012). “Life cycle environmental impact assessment of a solar water heater”. In: *Journal of Cleaner Production* 37, pp. 154–161. DOI: 10.1016/j.jclepro.2012.07.001 (cit. on p. 61).

Kottek, Markus, Jürgen Grieser, Christoph Beck, Bruno Rudolf and Franz Rubel (2006). “World map of the Köppen-Geiger climate classification updated”. In: *Meteorologische Zeitschrift* 15.3, pp. 259–263. ISSN: 09412948. DOI: 10.1127/0941-2948/2006/0130 (cit. on pp. 76, 77).

Kumar, Rakesh and Marc A. Rosen (2010). “Thermal performance of integrated collector storage solar water heater with corrugated absorber surface”. In: *Applied Thermal Engineering* 30.13, pp. 1764–1768. DOI: 10.1016/j.applthermaleng.2010.04.007 (cit. on p. 41).

Kumar, Rakesh and Marc A. Rosen (2011a). “Comparative performance investigation of integrated collector-storage solar water heaters with various heat loss reduction strategies”. In: *International Journal of Energy Research* 35.13, pp. 1179–1187. DOI: 10.1002/er.1764. eprint: arXiv:1011.1669v3 (cit. on pp. 20, 21, 30, 33, 49, 94).

Kumar, Rakesh and Marc A. Rosen (2011b). “Integrated collector-storage solar water heater with extended storage unit”. In: *Applied Thermal Engineering* 31.2-3, pp. 348–354. DOI: 10.1016/j.applthermaleng.2010.09.021 (cit. on p. 25).

Kumar, Rakesh and Marc A. Rosen (2013). “Review of solar water heaters with integrated collector-storage units”. In: *International Journal of Energy, Environment, and Economics* 21.4, pp. 343–382 (cit. on pp. 14, 15, 29, 33, 57).

Kylili, Angeliki, Paris A. Fokaides, Andreas Ioannides and Soteris Kalogirou (2018). “Environmental assessment of solar thermal systems for the industrial sector”. In: *Journal of Cleaner*

Production 176, pp. 99–109. DOI: 10.1016/j.jclepro.2017.12.150 (cit. on pp. 58, 61).

Laborderie, Alexis De, Clément Puech, Nadine Adra, Isabelle Blanc, Didier Beloin-Saint-Pierre, Pierryves Padey, Jérôme Payet, Marion Sie and Philippe Jacquin (2011). "Environmental Impacts of Solar Thermal Systems with Life Cycle Assessment". In: *World Renewable Energy Congress 2011 - 8-13 May 2011, Linkoping, Sweden*. Vol. 57. 14, pp. 3678–3685. DOI: 10.3384/ecp110573678 (cit. on pp. 60, 185).

Lacy, P and J Rutqvist (2016). *Waste to wealth: The circular economy advantage*, p. 264. DOI: 10.1057/9781137530707 (cit. on pp. 162, 214).

Lamnatou, Chr, G Notton, D Chemisana and C Cristofari (2015). "The environmental performance of a building-integrated solar thermal collector , based on multiple approaches and life-cycle impact assessment methodologies". In: *Building and Environment* 87, pp. 45–58. DOI: 10.1016/j.buildenv.2015.01.011 (cit. on p. 61).

Lavan, Z. and J. Thompson (1977). "Experimental study of thermally stratified hot water storage tanks". In: *Solar Energy* 19.5, pp. 519–524 (cit. on pp. 33, 47).

Le Quéré, Corinne et al. (2020). "Temporary reduction in daily global CO2 emissions during the COVID-19 forced confinement". In: *Nature Climate Change*, pp. 1–7. DOI: 10.1038/s41558-020-0797-x (cit. on p. 196).

Lefkow, A.R. and J.C. Lee (1980). "Selective IR reflective coatings". In: *Annual DOE active solar heating and cooling contractors review meeting* (cit. on p. 32).

Lenzen, Manfred (2001). "Errors in Conventional and Input-Output-based Life-Cycle Inventories". In: *Journal of Industrial Ecology* 4.4, pp. 127–148. DOI: 10.1162/10881980052541981 (cit. on pp. 69, 170).

Lenzen, Manfred and Christopher Dey (2000). "Truncation error in embodied energy analyses of basic iron and steel products". In: *Energy* 25.6, pp. 577–585. DOI: 10.1016/S0360-5442(99)00088-2 (cit. on p. 68).

Li, Zhuo and Zhi Gen Wu (2015). "Analysis of HTFs, PCMs and fins effects on the thermal performance of shell-tube thermal energy storage units". In: *Solar Energy* 122, pp. 382–395. DOI: 10.1016/j.solener.2015.09.019 (cit. on p. 28).

Loumakis, George (2018). "Development and testing of a low cost solar thermal collector". PhD thesis. Glasgow Caledonian University (cit. on p. 185).

Majeau-Bettez, Guillaume, Anders Hammer Strømman and Edgar G. Hertwich (2011). "Evaluation of process- and input-output-based life cycle inventory data with regard to truncation and aggregation issues". In: *Environmental Science and Technology* 45.23, pp. 10170–10177. DOI: 10.1021/es201308x (cit. on p. 69).

Martínez, E., J. Blanco, E. Jiménez, J. C. Saenz-Díez and F. Sanz (2015). "Comparative evaluation of life cycle impact assessment software tools through a wind turbine case study". In: *Renewable Energy* 74, pp. 237–246. DOI: 10.1016/j.renene.2014.08.004 (cit. on pp. 68, 112).

Martínez-Rocamora, A., J. Solís-Guzmán and M. Marrero (2016). "LCA databases focused on construction materials: A review". In: *Renewable and Sustainable Energy Reviews* 58, pp. 565–573. DOI: 10.1016/j.rser.2015.12.243 (cit. on p. 68).

McCracken, H. (1978). *How to build a passive solar water heater*. Alturas, California, USA: Carlos (cit. on pp. 17, 19).

McLennan, C. (2006). *Solar water heating*. Tech. rep. Edinburgh: School of Engineering, Edinburgh Napier University (cit. on pp. 55, 56, 125).

Menzies, Gillian and Y Roderick (2010). "Energy and carbon impact analysis of a solar thermal collector system". In: *International Journal of Sustainable Engineering* 3.1, pp. 1–8. DOI: 10.1080/19397030903362869 (cit. on pp. 59, 60).

Mila i Canals, L, J. Romanya, Sarah J. Cowell, Llorenç Milà i Canals, Joan Romanyà and Sarah J. Cowell (2007). "Method for assessing impacts on life support functions (LSF) related to the use of 'fertile land' in Life Cycle Assessment (LCA)". In: *Journal of Cleaner Production* 15.15, pp. 1426–1440. ISSN: 09596526. DOI: 10.1016/j.jclepro.2006.05.005 (cit. on p. 66).

Milousi, Maria, Manolis Souliotis, George Arampatzis and Spiros Papaefthimiou (2019). "Evaluating the Environmental Performance of Solar Energy Systems Through a Combined Life Cycle Assessment and Cost Analysis". In: *Sustainability* 11.9, p. 2539. DOI: https://doi.org/10.3390/su11092539 (cit. on pp. 185, 187, 189, 190, 191, 192, 193, 194, 195).

Mohamad, A. A. (1997). "Integrated Solar Collector - Storage Tank System with Thermal Diode". In: *Solar Energy* 61.3, pp. 211–218. ISSN: 0038092X. DOI: 10.1016/S0038-092X(97)00046-7 (cit. on pp. 24, 44, 45).

Mohsen, M.S. and B.A. Akash (2002). "On integrated solar water heating system". In: *International Communications in Heat and Mass Transfer* 29.1, pp. 135–140 (cit. on p. 28).

Moncaster, A. M. and J. Y. Song (2012). "A comparative review of existing data and methodologies for calculating embodied energy and carbon of buildings". In: *International Journal of Sustainable Building Technology and Urban Development* 3.1, pp. 26–36. ISSN: 20937628. DOI: 10.1080/2093761X.2012.673915 (cit. on p. 69).

Moore, A. D., T. Urmee, P. A. Bahri, S. Rezvani and G. F. Baverstock (2017). "Life cycle assessment of domestic hot water systems in Australia". In: *Renewable Energy* 103, pp. 187–196. DOI: 10.1016/j.renene.2016.09.062 (cit. on p. 59).

Muneer, T, S Younes, N Lambert and J Kubie (2006). "Life cycle assessment of a medium-sized photovoltaic facility at a high latitude location". In: *Proceedings of the Institution of Mechanical Engineers, Part A: Journal of Power and Energy* 220.6, pp. 517–524. DOI: 10.1243/09576509JPE253. URL: http://dx.doi.org/10.1243/09576509JPE253 (cit. on pp. 17, 28, 81).

Muneer, T., N. Adodahab, G. Weir and J. Kubie (2000). *Windows in Buildings*. Oxford, UK: Architectural Press. ISBN: 0 7506 4209 2 (cit. on pp. 32, 101).

NASA (2008). *Surface meteorology and Solar Energy (SSE) Release 6.0 Data Set*. URL: https://power.larc.nasa.gov/ (cit. on pp. 51, 101).

National Grid ESO (2020). *Carbon intensity API*. URL: https://carbonintensity.org.uk/ (visited on 30/01/2020) (cit. on p. 178).

Nelson, J E B, A R Balakrishnan and S Srinivasa Murthy (1999). "Experiments on stratified chilled-water tanks". In: *International Journal of Refrigeration* 22.3, pp. 216–234. DOI: 10.1016/S0140-7007(98)00055-3 (cit. on p. 47).

Norton, B. and S. Lo (2006). "Anatomy of a solar collector". In: *Refocus* 7.3, pp. 32–35. DOI: 10.1016/S1471-0846(06)70570-4. URL: http://www.sciencedirect.com/science/article/pii/S1471084606705704 (cit. on pp. 29, 33, 40).

NSG Group (2003). *Nippon Sheet Glass Spacia - The principle*. URL: http://www.nsg-spacia.co.jp/tech/index.html (visited on 24/01/2018) (cit. on p. 31).

Office for National Statistics (2013). *Population and Household Estimates for the United Kingdom, March 2011*. Tech. rep. March 2011, Statistical Bulletin (cit. on p. 55).

Ofgem (2018). *Supplier cost index by fuel type (GB)*. URL: https://www.ofgem.gov.uk/data-portal/supplier-cost-index-fuel-type-gb (visited on 21/05/2020) (cit. on p. 204).

Ofgem (2019). *Feed-in Tariffs: Essential Guide to Closure of the Scheme*. Tech. rep. March, p. 17. URL: https://www.ofgem.gov.uk/system/files/docs/2019/03/guide%7B%5C_%7Dto%7B%5C_%7Dclosure.pdf (cit. on p. 198).

Ofgem (2020a). *Default tariff cap level: 1 April 2020 to 30 September 2020*. Tech. rep. London: Ofgem. URL: https://www.ofgem.gov.uk/system/files/docs/2020/02/default%7B%5C_%7Dtariff%7B%5C_%7Dcap%7B%5C_%7Dlevel%7B%5C_%7D-%7B%5C_%7D1%7B%5C_%7Dapril%7B%5C_%7D2020%7B%5C_%7D-%7B%5C_%7D30%7B%5C_%7Dseptember%7B%5C_%7D2020%7B%5C_%7D0.pdf (cit. on p. 204).

Ofgem (2020b). *Domestic Renewable Heat Incentive Quarterly Report Issue 23*. Tech. rep., pp. 1–6. URL: www.ofgem.gov.uk/drhi (cit. on p. 198).

Oshchepkov, M. Yu. and S. E. Frid (2016). "Modeling of the Warm Water Displacement from Stratified Tanks of Integrated Collector Storage Solar Water Heaters". In: *Applied Solar Energy* 52.3, pp. 173–177. DOI: 10.3103/S0003701X15010107 (cit. on p. 43).

Owens, J.W. (1998). " Life cycle impact assessment: The use of subjective judgements in classification and characterization". In: *The International Journal of Life Cycle Assessment* 3, pp. 43–46 (cit. on p. 74).

Owsianiak, Mikołaj, Alexis Laurent, Anders Bjørn and Michael Z. Hauschild (2014). "IMPACT 2002+, ReCiPe 2008 and ILCD's recommended practice for characterization modelling in life cycle impact assessment: A case study-based comparison". In: *International Journal of Life Cycle Assessment* 19.5, pp. 1007–1021. DOI: 10.1007/s11367-014-0708-3 (cit. on p. 192).

Pandey, A. K., M. S. Hossain, V. V. Tyagi, Nasrudin Abd Rahim, Jeyraj A.L. Selvaraj and Ahmet Sari (2018). "Novel approaches and recent developments on potential applications of phase change materials in solar energy". In: *Renewable and Sustainable Energy Reviews* 82, pp. 281–323. DOI: 10.1016/j.rser.2017.09.043 (cit. on pp. 35, 36, 37).

Pereira da Cunha, Jose and Philip Eames (2016). “Thermal energy storage for low and medium temperature applications using phase change materials - A review”. In: *Applied Energy* 177, pp. 227–238. DOI: 10.1016/j.apenergy.2016.05.097 (cit. on p. 35).

Philibert, C (2006). *Barriers to technology diffusion: the case of solar thermal techologies*. Tech. rep. October. DOI: 10.1177/0160017604266026 (cit. on p. 3).

Piroozfar, Poorang, Francesco Pomponi and Eric R P Farr (2016). “Life cycle assessment of domestic hot water systems : a comparative analysis”. In: *International Journal of Construction Management* 16.2, pp. 109–125. DOI: 10.1080/15623599.2016.1146111 (cit. on pp. 59, 61).

Polentini, M.S., S. Ramadhyani and F.P. Incropera (1993). “Single-phase thermosyphon cooling of an array of discrete heat sources in a rectangular cavity”. In: *International Journal of Heat and Mass Transfer* 36.16, pp. 3983–3996 (cit. on p. 47).

Pomponi, Francesco (2015). “Operational performance and life cycle assessment of double skin façades for office refurbishments in the UK”. PhD thesis. University of Brighton (cit. on pp. 115, 195).

Pomponi, Francesco and Manfred Lenzen (2018). “Hybrid life cycle assessment (LCA) will likely yield more accurate results than process-based LCA”. In: *Journal of Cleaner Production* 176, pp. 210–215. DOI: 10.1016/j.jclepro.2017.12.119 (cit. on p. 69).

Pomponi, Francesco and Alice Moncaster (2016). “Embodied carbon mitigation and reduction in the built environment – What does the evidence say?” In: *Journal of Environmental Management* 181, pp. 687–700. DOI: 10.1016/j.jenvman.2016.08.036 (cit. on p. 68).

Pomponi, Francesco and Alice Moncaster (2017). “Research dimensions for circular economy studies in the built environment”. In: April. DOI: 10.1007/978-3-319-50346-2 (cit. on p. 59).

Popel’, O. S., S. E. Frid, A. V. Mordynskii, M. Zh. Suleimanov, A. V. Arsatov and M. Yu. Oschepkov (2013). “Results of the development of a solar accumulation-type water heater made of polymer and composite materials”. In: *Thermal Engineering* 60.4, pp. 267–269. DOI: 10.1134/S0040601513040101 (cit. on pp. 43, 44).

Posch, Maximilian, Jyri Seppälä, Jean-paul Hettelingh, Matti Johansson, Manuele Margni and Olivier Jolliet (2008). “The role of atmospheric dispersion models and ecosystem sensitivity

in the determination of characterisation factors for acidifying and eutrophying emissions in LCIA". In: *International Journal of Life Cycle Assessment* 13, pp. 477–486. DOI: 10.1007/s11367-008-0025-9 (cit. on p. 66).

Prabhu, P.A., N N Shinde and P.S Patil (2012). "Review of Phase Change Materials For Thermal Energy Storage Applications". In: *International Journal of Engineering Research and Applications* 2.3, pp. 871–875 (cit. on p. 35).

Prakash, J., H.P. Garg, R. Kumar and S. C. Kaushik (1992). "Triangular built-in-storage solar water heater". In: *Proceedings of the National Energy Conference*. Dehli, India, pp. 28–31 (cit. on p. 48).

PRé (2016). *Introduction to LCA with SimaPro*. Tech. rep., p. 80. URL: https://www.pre-sustainability.com/download/SimaPro8IntroductionToLCA.pdf (cit. on pp. 67, 112, 175).

Rabl, A. and J.V. Sparado (2004). *The RiskPoll software, version 1.051* (cit. on p. 66).

Raisul Islam, M., K. Sumathy and S. Ullah Khan (2013). "Solar water heating systems and their market trends". In: *Renewable and Sustainable Energy Reviews* 17, pp. 1–25. DOI: 10.1016/j.rser.2012.09.011 (cit. on p. 15).

Recoup (2017). *WWHRS for Passive Houses*. URL: https://recoupwwhrs.co.uk/technical/passive-house/ (visited on) (cit. on p. 200).

Reddy, K. S. and N. D. Kaushika (1999). "Comparative study of transparent insulation materials cover systems for integrated-collector-storage solar water heaters". In: *Solar Energy Materials and Solar Cells* 58.4, pp. 431–446. DOI: 10.1016/S0927-0248(99)00018-5 (cit. on pp. 18, 19).

Renuables (2015). *Environmental Product Declaration: Spaceloft Aerogel Insulation*. Tech. rep., p. 13. URL: https://www.thermablok.co.uk/site/wp-content/uploads/2019/02/epd725-Spaceloft-Aerogel-Insulation.pdf (cit. on p. 159).

Rosenbaum, Ralph K, Till M Bachmann, Olivier Jolliet, Ronnie Juraske, Annette Koehler and Michael Z Hauschild (2008). "USEtox — the UNEP-SETAC toxicity model : recommended characterisation factors for human toxicity and freshwater ecotoxicity in life cycle impact assessment". In: *International Journal of Life Cycle Assessment* 13, pp. 532–546. DOI: 10.1007/s11367-008-0038-4 (cit. on p. 66).

Rout, Auroshis, Sudhansu S. Sahoo and Sanju Thomas (2018). “Risk modeling of domestic solar water heater using Monte Carlo simulation for east-coastal region of India”. In: *Energy* 145, pp. 548–556. DOI: 10.1016/j.energy.2018.01.018 (cit. on p. 59).

Saint, Ruth M, Céline Garnier, Francesco Pomponi and John Currie (2018). “Thermal Performance through Heat Retention in Integrated Collector-Storage Solar Water Heaters : A Review”. In: *Energies* 11, p. 1615. DOI: 10.3390/en11061615 (cit. on p. 10).

Saint, Ruth M R.M, Francesco Pomponi, Céline Garnier and John I Currie (2019). “Whole-life design and resource reuse of a solar water heater in the UK”. In: *Proceedings of the Institution of Civil Engineers – Engineering Sustainability* 172.3, pp. 153–164. DOI: 10.1680/jensu.17.00068Engineering (cit. on p. 10).

Saltelli, A., S. Tarantola, F. Campolongo and M. Ratto (2004). *Sensitivity in practice: A guide to assessing scientific models*. England: John Wiley & Sons Ltd (cit. on pp. 113, 114).

Sarbu, Ioan and Calin Sebarchievici (2017). *Chapter 5 – Solar Water and Space-Heating Systems*. 1st. Academic Press, pp. 139–206. DOI: 10.1016/B978-0-12-811662-3.00005-0 (cit. on p. 22).

Schmidt, C. and A. Goetzberger (1990). “Single-tube integrated collector storage systems with transparent insulation and involute reflector”. In: *Solar Energy* 45.2, pp. 93–100 (cit. on pp. 18, 24).

Scottish Government (2014). *Technical Handbook - Domestic - Section 7 (Sustainability)*. Tech. rep. Livingston, Scotland: Scottish Building Standards - Scottish Government, pp. 379–399 (cit. on p. 197).

Scottish Government (2017). *Draft Climate Change Plan: The draft third report on policies and proposals 2017-2032*. Tech. rep. January, available from: http://www.official–documents.gov. (Cit. on pp. 2, 197).

Scottish Government (2019). *Reaching net zero*. URL: https://www.gov.scot/news/reaching-net-zero/ (visited on 17/09/2019) (cit. on pp. 3, 197).

El-Sebaii, A. A. (2005). “Thermal performance of a shallow solar-pond integrated with a baffle plate”. In: *Applied Energy* 81.1, pp. 33–53. DOI: 10.1016/j.apenergy.2004.05.003 (cit. on p. 26).

Seppälä, Jyri, Maximilian Posch, Matti Johansson and Jean-paul Paul Hettelingh (2006). “Country-dependent characterisation factors for acidification and terrestrial eutrophication based on

accumulated exceedance as an impact category indicator". In: *International Journal of Life Cycle Assessment* 11.6, pp. 403–416. DOI: 10.1065/lca2005.06.215 (cit. on p. 66).

Shukla, Ruchi, K. Sumathy, Phillip Erickson and Jiawei Gong (2013). "Recent advances in the solar water heating systems: A review". In: *Renewable and Sustainable Energy Reviews* 19, pp. 173–190. DOI: 10.1016/j.rser.2012.10.048 (cit. on pp. 43, 44).

Singh, Ramkishore, Ian J. Lazarus and Manolis Souliotis (2016). "Recent developments in integrated collector storage (ICS) solar water heaters: A review". In: *Renewable and Sustainable Energy Reviews* 54, pp. 270–298. DOI: 10.1016/j.rser.2015.10.006 (cit. on pp. 13, 15, 57).

Smith, S., R. Hairstans, R. Macdonald and F. Sanna (2012). *A strategic review of the offsite construction sector in Scotland*. Tech. rep. Edinburgh, Scotland: Scottish Government (cit. on p. 199).

Smith, S., J.B. Wood and R Hairstans (2015). "Increasing need for Offsite Construction and Manufactured Infrastructure in the UK Economy". In: *Chartered Institute of Architectural Technologist Symposium 2016* December (cit. on p. 199).

Smith, Sean (2019). *New Housing & Future Construction Skills; Adapting and Modernising for Growth*. Tech. rep. May. Edinburgh, Scotland: Scottish Government. URL: https://www.gov.scot/publications/new-housing-future-construction-skills-adapting-modernising-growth/pages/2/ (cit. on p. 199).

Smyth, M., P.C. Eames and B. Norton (1999). "A comparative performance rating for an integrated solar collector/storage vessel with inner sleeves to increase heat retention". In: *Solar Energy* 66.4, pp. 291–303. DOI: 10.1016/S0038-092X(99)00027-4 (cit. on p. 25).

Smyth, M., P.C. Eames and B. Norton (2000). "Life Cycle Assessment of a Heat Retaining Integrated Collector/Storage Solar Water Heater (ICSSWH)". In: *The Energy for the 21st Century World Renewable Energy Congress VI*. Brighton., pp. 1036–1040 (cit. on pp. 59, 60, 70, 185, 188).

Smyth, M., P.C. Eames and B. Norton (2001). "Evaluation of a freeze resistant integrated collector/storage solar water-heater for northern Europe". In: *Applied Energy* 68.3, pp. 265–274. DOI: 10.1016/S0306-2619(00)00049-0 (cit. on pp. 25, 185, 186, 188).

Smyth, M., P.C. Eames and B. Norton (2003). “Heat retaining integrated collector / storage solar water heaters”. In: *Solar Energy* 75.6, pp. 27–34. DOI: 10.1016/j.rser.2004.11.001 (cit. on pp. 19, 25, 94).

Smyth, M., P.C. Eames and B. Norton (2006). “Integrated collector storage solar water heaters”. In: *Renewable and Sustainable Energy Reviews* 10.6, pp. 503–538. DOI: 10.1016/j.rser.2004.11.001 (cit. on pp. 11, 14, 15, 16, 24, 33, 40, 42, 44, 48).

Smyth, M., A. Pugsley, G. Hanna, A. Zacharopoulos, J. Mondol, A. Besheer and A. Savvides (2019). “Experimental performance characterisation of a Hybrid Photovoltaic/Solar Thermal Façade module compared to a flat Integrated Collector Storage Solar Water Heater module”. In: *Renewable Energy* 137, pp. 137–143. DOI: 10.1016/j.renene.2018.04.017 (cit. on p. 149).

Smyth, M., P. Quinlan, J. D. Mondol, A. Zacharopoulos, D. McLarnon and A. Pugsley (2017). “The evolutionary thermal performance and development of a novel thermal diode pre-heat solar water heater under simulated heat flux conditions”. In: *Renewable Energy* 113, pp. 1160–1167. DOI: 10.1016/j.renene.2017.06.080 (cit. on pp. 45, 46).

Smyth, M., P. Quinlan, J. D. Mondol, A. Zacharopoulos, D. McLarnon and A. Pugsley (2018). “The experimental evaluation and improvements of a novel thermal diode pre-heat solar water heater under simulated solar conditions”. In: *Renewable Energy* 121, pp. 116–122. DOI: 10.1016/j.renene.2017.12.083 (cit. on p. 151).

Sokolov, M. and M. Vaxman (1983). “Analysis of an integral compact solar water heater”. In: *Solar Energy* 30.3, pp. 237–246 (cit. on p. 25).

Sopian, K., M. Syahri, S. Abdullah, M. Y. Othman and B. Yatim (2004). “Performance of a non-metallic unglazed solar water heater with integrated storage system”. In: *Renewable Energy* 29.9, pp. 1421–1430. DOI: 10.1016/j.renene.2004.01.002 (cit. on p. 44).

Soponronnarit, S., C. Taechapiroj and S. Tia (1994). “Comparative Studies of Built-in-Storage Solar Water Heaters”. In: *International Energy Journal* 16.1, pp. 11–26 (cit. on p. 48).

Souliotis, M., D. Chemisana, Y. G. Caouris and Y. Tripanagnostopoulos (2013). “Experimental study of integrated collector storage solar water heaters”. In: *Renewable Energy* 50.April 2014, pp. 1083–1094. DOI: 10.1016/j.renene.2012.08.061 (cit. on p. 38).

Souliotis, M., P. Quinlan, M. Smyth, Y. Tripanagnostopoulos, A. Zacharopoulos, M. Ramirez and P. Yianoulis (2011). “Heat retaining integrated collector storage solar water heater with

asymmetric CPC reflector". In: *Solar Energy* 85.10, pp. 2474–2487. DOI: 10.1016/j.solener.2011.07.005 (cit. on pp. 37, 38, 45).

Souliotis, M., R. Singh, S. Papaefthimiou, I. J. Lazarus and K. Andriosopoulos (2015). "Integrated collector storage solar water heaters: survey and recent developments". In: *Energy Systems* 7.1, pp. 49–72. DOI: 10.1007/s12667-014-0139-z (cit. on pp. 15, 35).

Souliotis, Manolis, Giorgos Panaras, Paris A. Fokaides, Spiros Papaefthimiou and Soteris A. Kalogirou (2018). "Solar water heating for social housing: Energy analysis and Life Cycle Assessment". In: *Energy and Buildings* 169, pp. 157–171. DOI: 10.1016/j.enbuild.2018.03.048 (cit. on pp. 185, 188).

Souliotis, Manolis, Spiros Papaefthimiou, Yiannis G. Caouris, Aggelos Zacharopoulos, Patrick Quinlan and Mervyn Smyth (2017). "Integrated collector storage solar water heater under partial vacuum". In: *Energy* 139, pp. 991–1002. DOI: 10.1016/j.energy.2017.08.074 (cit. on p. 45).

Souza, Jeronimo V D, Gilles Fraisse, Mickael Pailha and Shihe Xin (2014). "Experimental study of a partially heated cavity of an integrated collector storage solar water heater (ICSSWH)". In: *Solar Energy* 101, pp. 53–62. DOI: 10.1016/j.solener.2013.11.023 (cit. on pp. 20, 24, 25, 50, 76, 77, 80, 94).

Spear, M., C. Hill, A. Norton and C. Price (2019). *Wood in Construction in the UK: An Analysis of Carbon Abatement Potential*. Tech. rep. Bangor, pp. 1–28. URL: https://www.theccc.org.uk/wp-content/uploads/2019/07/Wood-in-Construction-in-the-UK-An-Analysis-of-Carbon-Abatement-Potential-BioComposites-Centre.pdf (cit. on p. 199).

Spur, Roman, Dusan Fiala, Dusan Nevrala and Doug Probert (2006). "Influence of the domestic hot-water daily draw-off profile on the performance of a hot-water store". In: *Applied Energy* 83.7, pp. 749–773. DOI: 10.1016/j.apenergy.2005.07.001 (cit. on pp. 54, 55, 56, 97, 125).

Stickney, B.L. and C. Nagy (1980). "Performance comparisons of several passive solar water heaters". In: *Proceedings of the fifth National Passive Solar Conference*. Amherst, Massachusetts, USA, pp. 1071–1075 (cit. on p. 40).

Strbac, Goran (2010). “Technical and regulatory framework for smart grid infrastructure: A review of current UK initiatives”. In: *IEEE PES General Meeting, PES 2010*, pp. 20–22. DOI: 10.1109/PES.2010.5590085 (cit. on p. 203).

Struijs, Jaap, A Beusen, Hans van Jaarsveld and Mark A J Huijbregts (2013). “Chapter 6: Aquatic Eutrophication”. In: *ReCiPe 2008 A life cycle impact assessment method which comprises harmonised category indicators at the midpoint and the endpoint level. Report I: Characterisation factors*. Ed. by M. Goedkoop, R. Heijungs, M.A.J. Huijbregts, A. De Schryver, J. Struijs and R. Van Zelm. Chap. 6 (cit. on p. 66).

Swiatek, Marie, Gilles Fraisse and Mickael Pailha (2015). “Stratification enhancement for an integrated collector storage solar water heater (ICSSWH)”. In: *Energy and Buildings* 106, pp. 35–43. DOI: 10.1016/j.enbuild.2015.07.005 (cit. on pp. 20, 25, 50, 76, 77, 80, 94).

Tanishita, I. (1955). “Present situation of commercial solar water heaters in Japan”. In: *Transactions on the use of Solar Energy*, pp. 67–78 (cit. on p. 11).

Tarhan, Sefa, Ahmet Sari and M. Hakan Yardim (2006). “Temperature distributions in trapezoidal built in storage solar water heaters with/without phase change materials”. In: *Energy Conversion and Management* 47.15-16, pp. 2143–2154. DOI: 10.1016/j.enconman.2005.12.002 (cit. on pp. 35, 36).

Teixeira, V., E. Sousa, M. F. Costa, C. Nunes, L. Rosa, M. J. Carvalho, M. Collares-Pereira, E. Roman and J. Gago (2001). “Spectrally selective composite coatings of Cr-Cr2O3 and Mo-Al2O3 for solar energy applications”. In: *Thin Solid Films* 392.2, pp. 320–326. DOI: 10.1016/S0040-6090(01)01051-3 (cit. on pp. 32, 40, 41).

The World Bank (2019). *Global Solar Atlas 2.0, Solar resource data: Solargis*. URL: https://solargis.com/maps-and-gis-data/download (cit. on p. 189).

Tiller, J.S. and V. Wochatz (1982). “Performance of integrated passive solar water heaters (Breadbox-type) under varying design conditions in the South-eastern US.” In: *Proceedings of the Seventh National Passive Solar Conference*. Knoxville, Tennesse, pp. 975–80 (cit. on pp. 40, 48).

Tou, S.K.W., C.P. Tso and X. Zhang (1999). “3-D numerical anaylsis of natural convective liquid cooling in a 3x3 heater array in rectangular enclosures”. In: *International Journal of Heat and Mass Transfer* 42.17, pp. 3231–3244 (cit. on pp. 47, 48).

Tripanagnostopoulos, Y., M. Souliotis, R. Battisti and A. Corrado (2005). "Energy, Cost and LCA Results of PV and Hybrid PV/T Solar Systems". In: *Progress in Photovoltaics: Research and Applications* 13.January, pp. 235–250. DOI: 10.1002/pip.590 (cit. on pp. 60, 185, 187).

Tripanagnostopoulos, Y., M. Souliotis and Th. Nousia (1999). "Solar ICS systems with two cylindrical storage tanks". In: *Renewable Energy* 16.1-4, pp. 665–668. DOI: 10.1016/S0960-1481(98)00248-1 (cit. on p. 19).

Tripanagnostopoulos, Yiannis and P. Yianoulis (1992). "Integrated collector/storage systems with suppressed thermal losses". In: *Solar Energy* 48.1, pp. 31–43 (cit. on p. 40).

Tsilingiridis, G., G. Martinopoulos and N. Kyriakis (2004). "Life cycle environmental impact of a thermosyphonic domestic solar hot water system in comparison with electrical and gas water heating". In: *Renewable Energy* 29.8, pp. 1277–1288. DOI: 10.1016/j.renene.2003.12.007 (cit. on p. 60).

Uctug, Fehmi Gorkem and Adisa Azapagic (2018). "Life cycle environmental impacts of domestic solar water heaters in Turkey: The effect of different climatic regions". In: *Science of the Total Environment* 622-623, pp. 1202–1216. DOI: 10.1016/j.scitotenv.2017.12.057 (cit. on pp. 58, 185, 187, 189, 190, 191, 192, 193, 194, 195).

UNFCC (2016). *Status of Ratification of the Kyoto Protocol* (cit. on p. 1).

United Nations (1998). "Kyoto Protocol To the United Nations Framework". In: *Review of European Community and International Environmental Law* 7, pp. 214–217. DOI: 10.1111/1467-9388.00150 (cit. on p. 11).

United Nations (2015). "Paris Agreement". In: *21st Conference of the Parties*, p. 3. DOI: FCCC/CP/2015/L.9. arXiv: arXiv:1011.1669v3 (cit. on p. 1).

Varghese, Jaji and K Manjunath (2017). "Techno-economic analysis of an integrated collector storage solar water heater with CPC reflector for households Techno-economic analysis of an integrated collector storage solar water heater with CPC reflector for households". In: *International Journal of Ambient Energy* 0.0, pp. 1–6. DOI: 10.1080/01430750.2017.1354327 (cit. on p. 38).

Vaxman, M. and M. Sokolov (1985). "Experiments with an integral compact solar water heater". In: *Solar Energy* 34.6, pp. 447–454 (cit. on p. 25).

Velraj, R (2016). *Sensible heat storage for solar heating and cooling systems*, pp. 399–428. DOI: 10.1016/B978-0-08-100301-5.00015-1 (cit. on p. 152).

Wang, Zhangyuan, Wansheng Yang, Feng Qiu, Xiangmei Zhang and Xudong Zhao (2015). "Solar water heating: From theory, application, marketing and research". In: *Renewable and Sustainable Energy Reviews* 41, pp. 68–84. DOI: 10.1016/j.rser.2014.08.026 (cit. on pp. 1, 13).

WHO (2007). *Legionella and the prevention of legionellosis*. Ed. by J. Bartam and K. Pond. Geneva. ISBN: 9241562978. DOI: 10.3201/eid1406.080345 (cit. on p. 23).

WMO (1999). *Scientific Assessment of Ozone Depletion: 1998. Global Ozone Research and Monitoring Project - Report No. 44*. Tech. rep. ISBN 92-807-1722-7, Geneva (cit. on p. 66).

Wozniak, S.J. (1979). *Solar heating systems for the UK: design, installation and economic aspects*. Watford, UK: Building Research Establishment (cit. on p. 32).

Wu, Xiao, Rachel C Nethery, M Benjamin Sabath, Danielle Braun and Francesca Dominici (2020). "Exposure to air pollution and COVID-19 mortality in the United States: A nationwide cross-sectional study". In: *medRxiv* Preprint. DOI: https://doi.org/10.1101/2020.04.05.20054502 (cit. on p. 196).

Yassen, Tadahmun A, Nassir D Mokhlif and Muhammad Asmail (2019). "Performance investigation of an integrated solar water heater with corrugated absorber surface for domestic use". In: *Renewable Energy* 138, pp. 852–860. ISSN: 0960-1481. DOI: 10.1016/j.renene.2019.01.114. URL: https://doi.org/10.1016/j.renene.2019.01.114 (cit. on pp. 186, 188).

Youcef-Ali, S. (2005). "Study and optimization of the thermal performances of the offset rectangular plate fin absorber plates, with various glazing". In: *Renewable Energy* 30.2, pp. 271–280. DOI: 10.1016/j.renene.2004.04.009 (cit. on pp. 27, 30).

Zambrana-Vasquez, David, Alfonso Aranda-Usón, Ignacio Zabalza-Bribián, Alberto Jañez, Eva Llera-Sastresa, Patxi Hernandez and Eneko Arrizabalaga (2015). "Environmental assessment of domestic solar hot water systems: A case study in residential and hotel buildings". In: *Journal of Cleaner Production* 88, pp. 29–42. DOI: 10.1016/j.jclepro.2014.06.035 (cit. on p. 61).

Zelm, Rosalie van et al. (2008). "European characterization factors for human health damage of PM10 and ozone in life cycle impact assessment". In: *Atmospheric Environment* 42.3, pp. 441–453. DOI: 10.1016/j.atmosenv.2007.09.072 (cit. on p. 66).

Zhang, T., Z. W. Yan, L. Y. Wang, W. J. Zheng and Y. H. Su (2020). "Comparative study on the annual performance between loop thermosyphon solar water heating system and conventional solar water heating system". In: *Solar Energy* 197.December 2019, pp. 433–442. DOI: 10.1016/j.solener.2020.01.019 (cit. on p. 186).

Ziapour, Behrooz M. and Azad Aghamiri (2014). "Simulation of an enhanced integrated collector-storage solar water heater". In: *Energy Conversion and Management* 78, pp. 193–203. DOI: 10.1016/j.enconman.2013.10.068 (cit. on pp. 25, 42).

Ziapour, Behrooz M., Vahid Palideh and Farhad Mokhtari (2016). "Performance improvement of the finned passive PVT system using reflectors like removable insulation covers". In: *Applied Thermal Engineering* 94, pp. 341–349. DOI: 10.1016/j.applthermaleng.2015.10.143 (cit. on pp. 38, 39).

Zombeck, M.V. (2007). *Handbook of Space Astronomy and Astrophysics*. Third. Cambridge: Cambridge University Press (cit. on p. 3).

Zurigat, Y.H., A.J. Ghajar and P.M. Moretti (1988). "Stratified thermal storage tank inlet mixing characterization". In: *Applied Energy* 30, pp. 99–111 (cit. on p. 33).

Appendices

Appendix A

Technical drawings

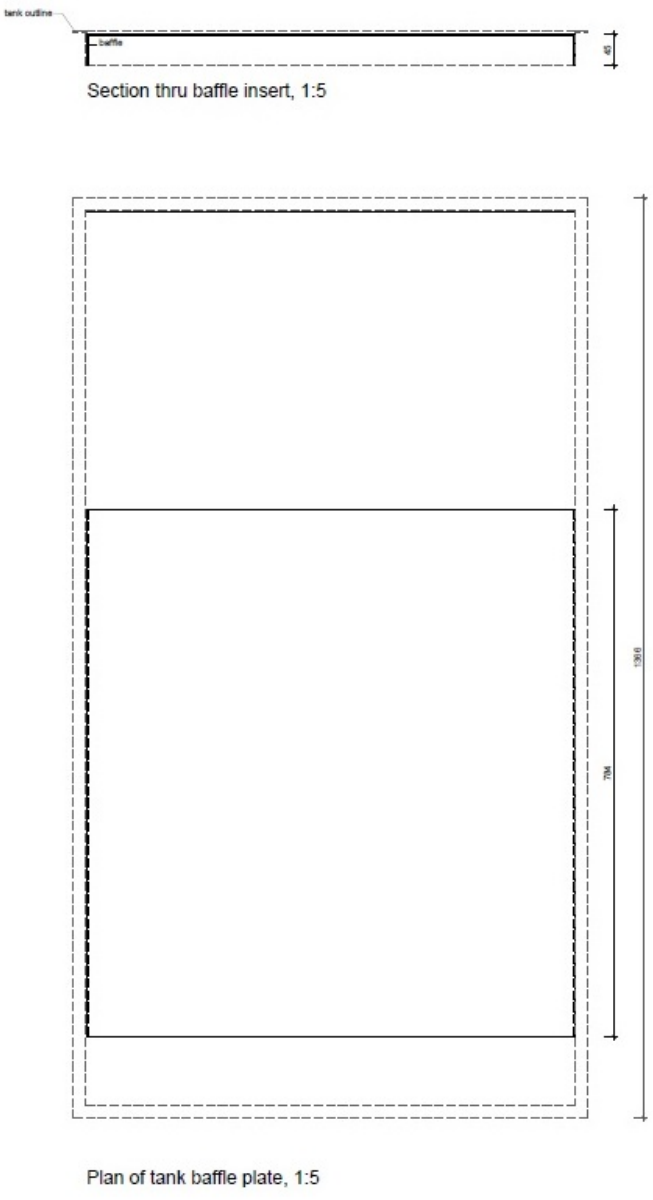

Figure A.1: Technical drawing of the baffle plate placement

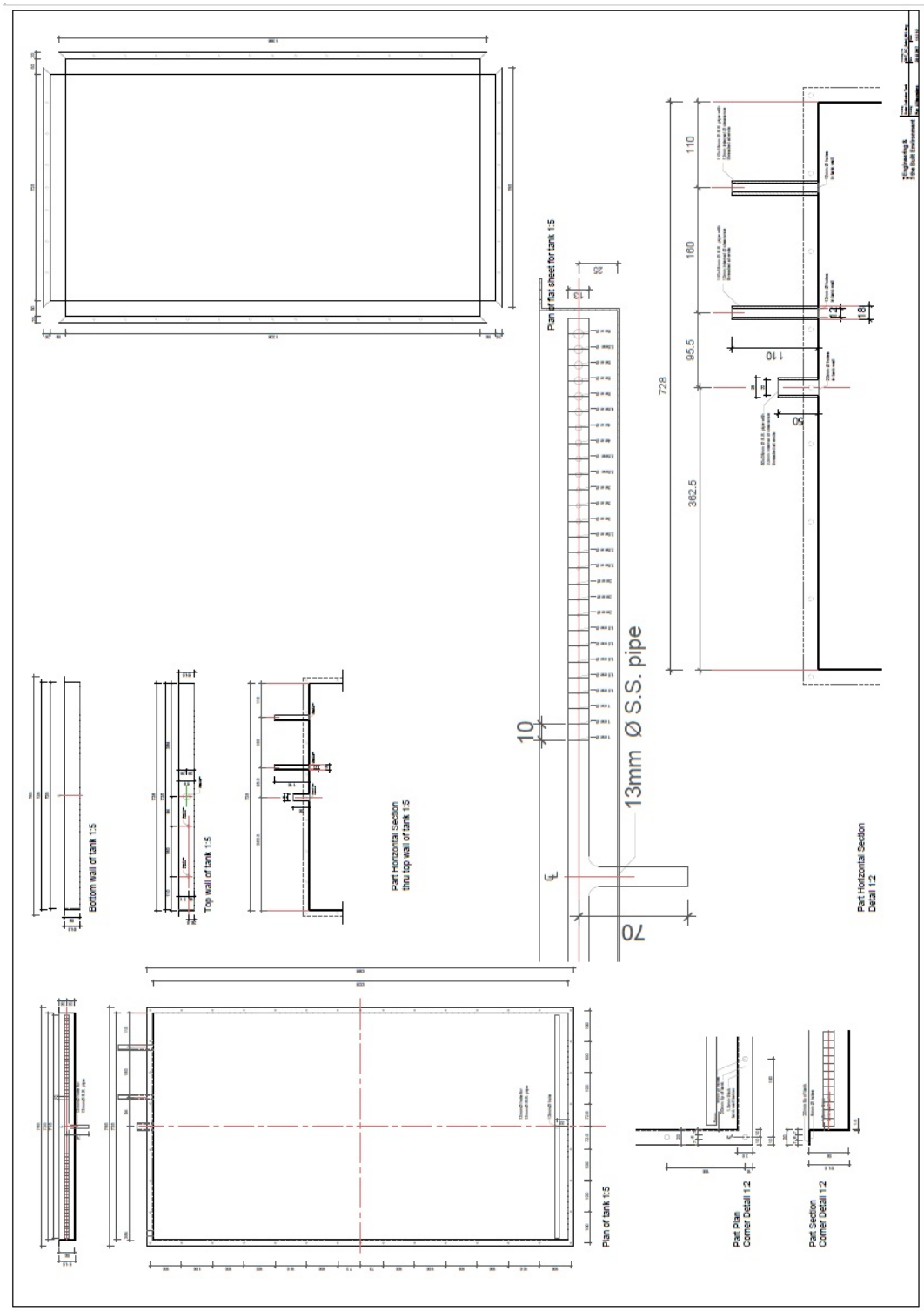

Figure A.2: Technical drawing of the tank base

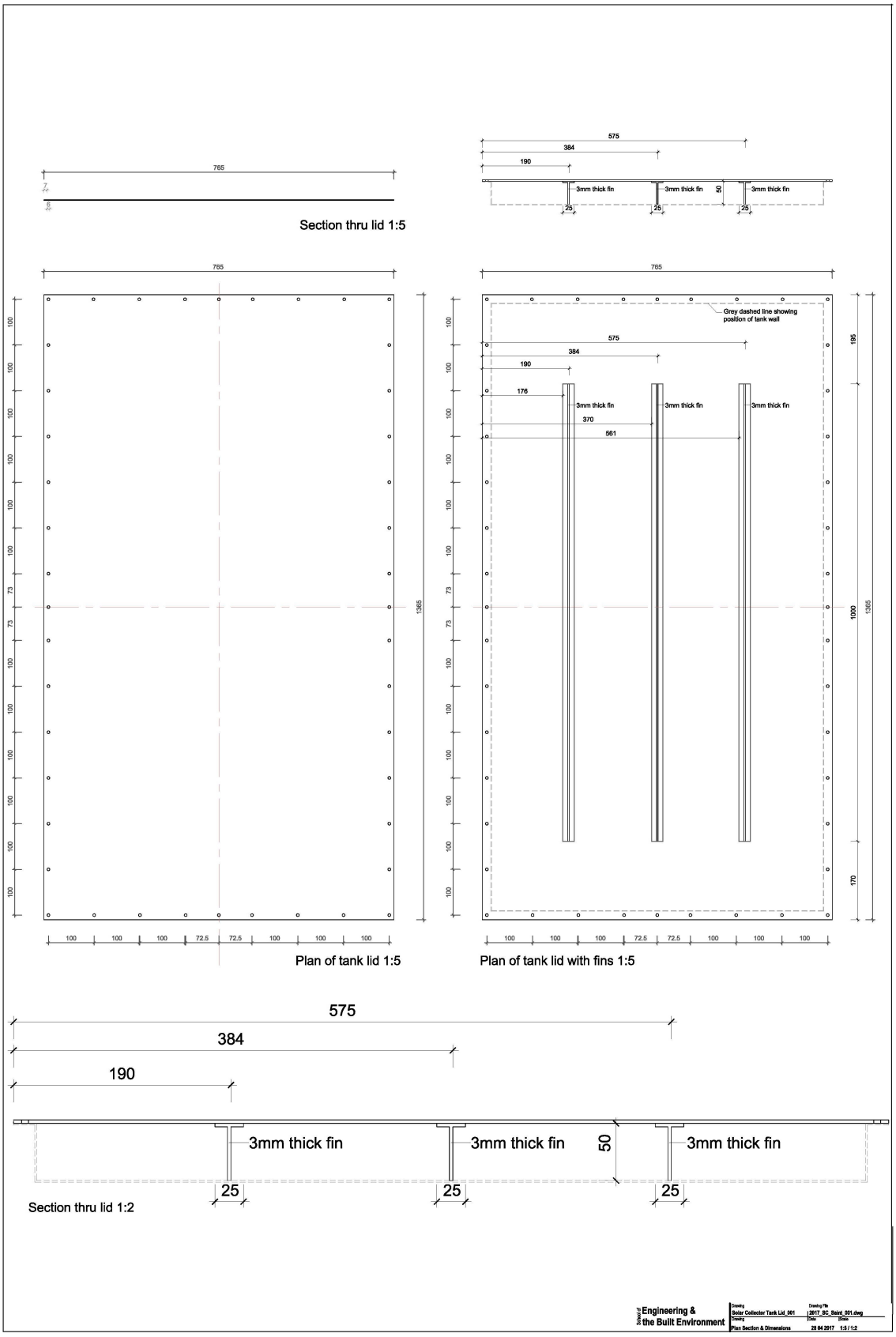

Figure A.3: Technical drawing of the finned lid

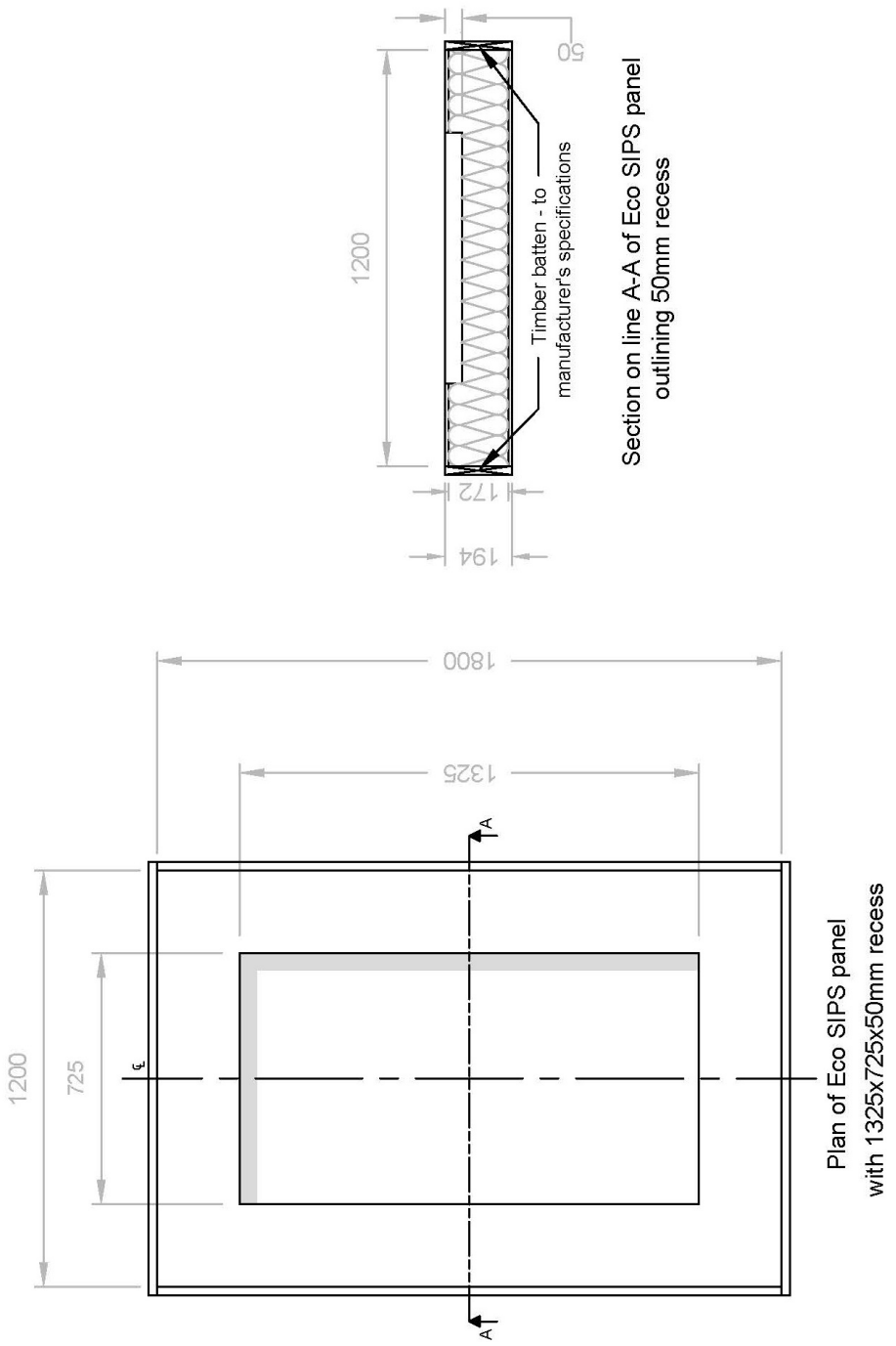

Figure A.4: Technical drawing of integration into EcoSIP panel

Appendix B

Life cycle inventories

Table B.1: Plain baffled tank in frame

	Component	Material	Quantity	Mass, 1 unit (kg)	Mass, total (kg)	% Total weight
Collector	Tank base	1.5 mm Stainless steel	1	14.4	14.4	20.8
	Absorber plate	3 mm aluminium	1	8.5	8.5	12.3
	Absorber plate coating	Black spray paint	4 coats	0.7	0.7	1.0
	Sparge tube	Copper	1	0.58	0.58	0.8
	Gasket	EPDM rubber	1	0.37	0.37	0.54
	Gasket sealant	Hylomar	1	0.1	0.1	0.14
	Compression Reducing Coupling	Copper, brass finish	1	0.1	0.1	0.14
	Compression Straight Coupling	Copper, brass finish	1	0.07	0.07	0.1
	Hose fitting	Copper, brass finish	1	0.014	0.014	0.02
	6 mm screws	Steel	44	0.023	1.01	1.46
	6 mm Nylock nuts	Stainless steel	44	0.003	0.13	0.19
	6 mm washers	Steel	88	0.003	0.26	0.37
	Sparge tube supports	Polycarbonate	2	0.0009	0.0018	0.0026
	Baffle plate	4 mm Polycarbonate	1	1.55	1.55	2.2
	Baffle plate supports	Polycarbonate	3	0.0003	0.0009	0.001
Frame	Glazing	4 mm Glass	1	11.0	11.0	15.9
	Frame	18 mm Plywood	1	28.3	28.3	40.9
	Screws	Steel	32	0.00063	0.02	0.03
	Sealant	Silicon	1	0.005	0.005	0.007
	Insulation	40 mm Celotex	1	2.0	2.0	2.9
	Waterproofing	Black paint	1	0.005	0.005	0.007
					Total	**69.1**	**100**

Table B.2: Insulated baffled tank in frame

	Component	Material	Quantity	Mass, 1 unit (kg)	Mass, total (kg)	% Total weight
Collector	Tank base	1.5 mm Stainless steel	1	14.4	14.4	20.6
	Absorber plate	3 mm aluminium	1	8.5	8.5	12.1
	Absorber plate coating	Black spray paint	4 coats	0.7	0.7	1.0
	Sparge tube	Copper	1	0.58	0.58	0.8
	Gasket	EPDM rubber	1	0.37	0.37	0.5
	Gasket sealant	Hylomar	1	0.1	0.1	0.14
	Compression Reducing Coupling	Copper, brass finish	1	0.1	0.1	0.14
	Compression Straight Coupling	Copper, brass finish	1	0.07	0.07	0.1
	Hose fitting	Copper, brass finish	1	0.014	0.014	0.02
	6 mm screws	Steel	44	0.023	1.01	1.4
	6 mm Nylock nuts	Stainless steel	44	0.003	0.13	0.19
	6 mm washers	Steel	88	0.003	0.26	0.36
	Sparge tube supports	Polycarbonate	2	0.0009	0.0018	0.0026
	Baffle plate	4 mm Polycarbonate	1	1.55	1.55	2.2
	Baffle plate supports	Polycarbonate	3	0.0003	0.0009	0.001
Frame	Glazing	4 mm Glass	1	11.0	11.0	15.7
	Frame	18 mm Plywood	1	28.3	28.3	40.4
	Screws	Steel	32	0.00063	0.02	0.029
	Sealant	Silicon	1	0.005	0.005	0.007
	Insulation	40 mm Celotex	1	2.0	2.0	2.9
	Waterproofing	Black paint	1	0.005	0.005	0.007
Additions	Absorber insulation	Spacetherm© Areogel	1	0.96	0.96	1.37
				Total	**70.1**	**100**

Table B.3: Baffled tank with night cover in frame

	Component	Material	Quantity	Mass, 1 unit (kg)	Mass, total (kg)	% Total weight
Collector	Tank base	1.5 mm Stainless steel	1	14.4	14.4	20.4
	Absorber plate	3 mm aluminium	1	8.5	8.5	12.0
	Absorber plate coating	Black spray paint	4 coats	0.7	0.7	1.0
	Sparge tube	Copper	1	0.58	0.58	0.8
	Gasket	EPDM rubber	1	0.37	0.37	0.5
	Gasket sealant	Hylomar	1	0.1	0.1	0.14
	Compression Reducing Coupling	Copper, brass finish	1	0.1	0.1	0.14
	Compression Straight Coupling	Copper, brass finish	1	0.07	0.07	0.1
	Hose fitting	Copper, brass finish	1	0.014	0.014	0.02
	6 mm screws	Steel	44	0.023	1.01	1.4
	6 mm Nylock nuts	Stainless steel	44	0.003	0.13	0.19
	6 mm washers	Steel	88	0.003	0.26	0.36
	Sparge tube supports	Polycarbonate	2	0.0009	0.0018	0.003
	Baffle plate	4 mm Polycarbonate	1	1.55	1.55	2.2
	Baffle plate supports	Polycarbonate	3	0.0003	0.0009	0.001
Frame	Glazing	4 mm Glass	1	11.0	11.0	15.5
	Frame	18 mm Plywood	1	28.3	28.3	40.1
	Screws	Steel	32	0.00063	0.02	0.028
	Sealant	Silicon	1	0.005	0.005	0.007
	Insulation	40 mm Celotex	1	2.0	2.0	2.9
	Waterproofing	Black paint	1	0.005	0.005	0.007
Additions	Channels	Aluminium	2	0.35	0.7	1.0
	Insulating blind	Airtec foil	1	0.35	0.35	0.5
	Roller for blind	Aluminium	1	0.28	0.28	0.39
	Supports for roller	Plywood	2	0.04	0.08	0.11
	Stabilising band	Polycarbonate	1	0.11	0.11	0.15
	Screws	Steel	8	0.00063	0.005	0.007
				Total	**70.6**	**100**

Table B.4: Plain baffled tank in SIP

	Component	Material	Quantity	Mass, 1 unit (kg)	Mass, total (kg)	% Total weight
Collector	Tank base	1.5 mm Stainless steel	1	14.4	14.4	30.7
	Absorber plate	3 mm aluminium	1	8.5	8.5	18.1
	Absorber plate coating	Black spray paint	4 coats	0.7	0.7	1.5
	Sparge tube	Copper	1	0.58	0.58	1.2
	Gasket	EPDM rubber	1	0.37	0.37	0.8
	Gasket sealant	Hylomar	1	0.1	0.1	0.2
	Compression Reducing Coupling	Copper, brass finish	1	0.1	0.1	0.2
	Compression Straight Coupling	Copper, brass finish	1	0.07	0.07	0.15
	Hose fitting	Copper, brass finish	1	0.014	0.014	0.03
	6 mm screws	Steel	44	0.023	1.01	2.16
	6 mm Nylock nuts	Stainless steel	44	0.003	0.13	0.28
	6 mm washers	Steel	88	0.003	0.26	0.54
	Sparge tube supports	Polycarbonate	2	0.0009	0.0018	0.004
	Baffle plate	4 mm Polycarbonate	1	1.55	1.55	3.3
	Baffle plate supports	Polycarbonate	3	0.0003	0.0009	0.002
Frame	Glazing	4 mm Glass	1	11.0	11.0	23.4
	Frame	18 mm Plywood	1	8.13	8.13	17.3
	Screws	Steel	12	0.00063	0.01	0.016
	Sealant	Silicon	1	0.005	0.005	0.0011
	Waterproofing	Black paint	1	0.005	0.005	0.0011
				Total	**46.9**	**100**

Table B.5: Insulated baffled tank in SIP

	Component	Material	Quantity	Mass, 1 unit (kg)	Mass, total (kg)	% Total weight
Collector	Tank base	1.5 mm Stainless steel	1	14.4	14.4	30.1
	Absorber plate	3 mm aluminium	1	8.5	8.5	17.8
	Absorber plate coating	Black spray paint	4 coats	0.7	0.7	1.5
	Sparge tube	Copper	1	0.58	0.58	1.2
	Gasket	EPDM rubber	1	0.37	0.37	0.77
	Gasket sealant	Hylomar	1	0.1	0.1	0.2
	Compression Reducing Coupling	Copper, brass finish	1	0.1	0.1	0.2
	Compression Straight Coupling	Copper, brass finish	1	0.07	0.07	0.1
	Hose fitting	Copper, brass finish	1	0.014	0.014	0.029
	6 mm screws	Steel	44	0.023	1.01	2.1
	6 mm Nylock nuts	Stainless steel	44	0.003	0.13	0.28
	6 mm washers	Steel	88	0.003	0.26	0.53
	Sparge tube supports	Polycarbonate	2	0.0009	0.0018	0.004
	Baffle plate	4 mm Polycarbonate	1	1.55	1.55	3.24
	Baffle plate supports	Polycarbonate	3	0.0003	0.0009	0.002
Frame	Glazing	4 mm Glass	1	11.0	11.0	22.9
	Frame	18 mm Plywood	1	8.13	8.13	17
	Screws	Steel	12	0.00063	0.01	0.016
	Sealant	Silicon	1	0.005	0.005	0.001
	Waterproofing	Black paint	1	0.005	0.005	0.001
Additions	Absorber insulation	Spacetherm© Areogel	1	0.96	0.96	2.01
				Total	**47.9**	**100**

Table B.6: Baffled tank with night cover in SIP

	Component	Material	Quantity	Mass, 1 unit (kg)	Mass, total (kg)	% Total weight
Collector	Tank base	1.5 mm Stainless steel	1	14.4	14.4	29.7
	Absorber plate	3 mm aluminium	1	8.5	8.5	17.6
	Absorber plate coating	Black spray paint	4 coats	0.7	0.7	1.5
	Sparge tube	Copper	1	0.58	0.58	1.2
	Gasket	EPDM rubber	1	0.37	0.37	0.8
	Gasket sealant	Hylomar	1	0.1	0.1	0.2
	Compression Reducing Coupling	Copper, brass finish	1	0.1	0.1	0.2
	Compression Straight Coupling	Copper, brass finish	1	0.07	0.07	0.1
	Hose fitting	Copper, brass finish	1	0.014	0.014	0.03
	6 mm screws	Steel	44	0.023	1.01	2.1
	6 mm Nylock nuts	Stainless steel	44	0.003	0.13	0.28
	6 mm washers	Steel	88	0.003	0.26	0.53
	Sparge tube supports	Polycarbonate	2	0.0009	0.0018	0.004
	Baffle plate	4 mm Polycarbonate	1	1.55	1.55	3.2
	Baffle plate supports	Polycarbonate	3	0.0003	0.0009	0.002
Frame	Glazing	4 mm Glass	1	11.0	11.0	22.7
	Frame	18 mm Plywood	1	8.13	8.13	16.8
	Screws	Steel	12	0.00063	0.01	0.015
	Sealant	Silicon	1	0.005	0.005	0.001
	Waterproofing	Black paint	1	0.005	0.005	0.001
Additions	Channels	Aluminium	2	0.35	0.7	1.4
	Insulating blind	Airtec foil	1	0.35	0.35	0.7
	Roller for blind	Aluminium	1	0.28	0.28	0.6
	Supports for roller	Plywood	2	0.04	0.08	0.2
	Stabilising band	Polycarbonate	1	0.11	0.11	0.2
	Screws	Steel	8	0.00063	0.005	0.007
				Total	**48.4**	**100**

Table B.7: Plain finned tank in frame

	Component	Material	Quantity	Mass, 1 unit (kg)	Mass, total (kg)	% Total weight
Collector	Tank base	1.5 mm Stainless steel	1	14.4	14.4	20.9
	Absorber plate (w. fins)	3 mm aluminium	1	9.7	9.7	14.1
	Absorber plate coating	Black spray paint	4 coats	0.7	0.7	1.0
	Sparge tube	Copper	1	0.58	0.58	0.8
	Gasket	EPDM rubber	1	0.37	0.37	0.54
	Gasket sealant	Hylomar	1	0.1	0.1	0.14
	Compression Reducing Coupling	Copper, brass finish	1	0.1	0.1	0.14
	Compression Straight Coupling	Copper, brass finish	1	0.07	0.07	0.1
	Hose fitting	Copper, brass finish	1	0.014	0.014	0.02
	6 mm screws	Steel	44	0.023	1.01	1.5
	6 mm Nylock nuts	Stainless steel	44	0.003	0.13	0.2
	6 mm washers	Steel	88	0.003	0.26	0.4
	Sparge tube supports	Polycarbonate	2	0.0009	0.0018	0.003
Frame	Glazing	4 mm Glass	1	11.0	11.0	16.0
	Frame	18 mm Plywood	1	28.3	28.3	41.2
	Screws	Steel	32	0.00063	0.02	0.03
	Sealant	Silicon	1	0.005	0.005	0.007
	Insulation	40 mm Celotex	1	2.0	2.0	2.9
	Waterproofing	Black paint	1	0.005	0.005	0.007
				Total	**68.8**	**100**

Table B.8: Insulated finned tank in frame

	Component	Material	Quantity	Mass, 1 unit (kg)	Mass, total (kg)	% Total weight
Collector	Tank base	1.5 mm Stainless steel	1	14.4	14.4	20.7
	Absorber plate (w. fins)	3 mm aluminium	1	9.7	9.7	13.9
	Absorber plate coating	Black spray paint	4 coats	0.7	0.7	1.0
	Sparge tube	Copper	1	0.58	0.58	0.83
	Gasket	EPDM rubber	1	0.37	0.37	0.53
	Gasket sealant	Hylomar	1	0.1	0.1	0.14
	Compression Reducing Coupling	Copper, brass finish	1	0.1	0.1	0.14
	Compression Straight Coupling	Copper, brass finish	1	0.07	0.07	0.1
	Hose fitting	Copper, brass finish	1	0.014	0.014	0.02
	6 mm screws	Steel	44	0.023	1.01	1.45
	6 mm Nylock nuts	Stainless steel	44	0.003	0.13	0.19
	6 mm washers	Steel	88	0.003	0.26	0.37
	Sparge tube supports	Polycarbonate	2	0.0009	0.0018	0.003
Frame	Glazing	4 mm Glass	1	11.0	11.0	15.7
	Frame	18 mm Plywood	1	28.3	28.3	40.6
	Screws	Steel	32	0.00063	0.02	0.029
	Sealant	Silicon	1	0.005	0.005	0.007
	Insulation	40 mm Celotex	1	2.0	2.0	2.9
	Waterproofing	Black paint	1	0.005	0.005	0.007
Additions	Absorber insulation	Spacetherm© Areogel	1	0.96	0.96	1.38
					Total	**69.7**	**100**

Table B.9: Finned tank with night cover in frame

	Component	Material	Quantity	Mass, 1 unit (kg)	Mass, total (kg)	% Total weight
Collector	Tank base	1.5 mm Stainless steel	1	14.4	14.4	20.5
	Absorber plate (w. fins)	3 mm aluminium	1	9.7	9.7	13.8
	Absorber plate coating	Black spray paint	4 coats	0.7	0.7	1.0
	Sparge tube	Copper	1	0.58	0.58	0.8
	Gasket	EPDM rubber	1	0.37	0.37	0.5
	Gasket sealant	Hylomar	1	0.1	0.1	0.1
	Compression Reducing Coupling	Copper, brass finish	1	0.1	0.1	0.1
	Compression Straight Coupling	Copper, brass finish	1	0.07	0.07	0.1
	Hose fitting	Copper, brass finish	1	0.014	0.014	0.02
	6 mm screws	Steel	44	0.023	1.01	1.4
	6 mm Nylock nuts	Stainless steel	44	0.003	0.13	0.19
	6 mm washers	Steel	88	0.003	0.26	0.37
	Sparge tube supports	Polycarbonate	2	0.0009	0.0018	0.003
Frame	Glazing	4 mm Glass	1	11.0	11.0	15.6
	Frame	18 mm Plywood	1	28.3	28.3	40.3
	Screws	Steel	32	0.00063	0.02	0.028
	Sealant	Silicon	1	0.005	0.005	0.007
	Insulation	40 mm Celotex	1	2.0	2.0	2.9
	Waterproofing	Black paint	1	0.005	0.005	0.007
Additions	Channels	Aluminium	2	0.35	0.7	1.0
	Insulating blind	Airtec foil	1	0.35	0.35	0.5
	Roller for blind	Aluminium	1	0.28	0.28	0.4
	Supports for roller	Plywood	2	0.04	0.08	0.11
	Stabilising band	Polycarbonate	1	0.11	0.11	0.15
	Screws	Steel	8	0.00063	0.005	0.007
				Total	**70.3**	**100**

Table B.10: Plain finned tank in SIP

	Component	Material	Quantity	Mass, 1 unit (kg)	Mass, total (kg)	% Total weight
Collector	Tank base	1.5 mm Stainless steel	1	14.4	14.4	30.9
	Absorber plate (w. fins)	3 mm aluminium	1	9.7	9.7	20.8
	Absorber plate coating	Black spray paint	4 coats	0.7	0.7	1.5
	Sparge tube	Copper	1	0.58	0.58	1.2
	Gasket	EPDM rubber	1	0.37	0.37	0.8
	Gasket sealant	Hylomar	1	0.1	0.1	0.2
	Compression Reducing Coupling	Copper, brass finish	1	0.1	0.1	0.2
	Compression Straight Coupling	Copper, brass finish	1	0.07	0.07	0.2
	Hose fitting	Copper, brass finish	1	0.014	0.014	0.03
	6 mm screws	Steel	44	0.023	1.01	2.2
	6 mm Nylock nuts	Stainless steel	44	0.003	0.13	0.3
	6 mm washers	Steel	88	0.003	0.26	0.5
	Sparge tube supports	Polycarbonate	2	0.0009	0.0018	0.004
Frame	Glazing	4 mm Glass	1	11.0	11.0	23.6
	Frame	18 mm Plywood	1	8.13	8.13	17.5
	Screws	Steel	12	0.00063	0.01	0.02
	Sealant	Silicon	1	0.005	0.005	0.001
	Waterproofing	Black paint	1	0.005	0.005	0.001
				Total	**46.6**	**100**

Table B.11: Insulated finned tank in SIP

	Component	Material	Quantity	Mass, 1 unit (kg)	Mass, total (kg)	% Total weight
Collector	Tank base	1.5 mm Stainless steel	1	14.4	14.4	30.3
	Absorber plate (w. fins)	3 mm aluminium	1	9.7	9.7	20.4
	Absorber plate coating	Black spray paint	4 coats	0.7	0.7	1.5
	Sparge tube	Copper	1	0.58	0.58	1.2
	Gasket	EPDM rubber	1	0.37	0.37	0.8
	Gasket sealant	Hylomar	1	0.1	0.1	0.2
	Compression Reducing Coupling	Copper, brass finish	1	0.1	0.1	0.2
	Compression Straight Coupling	Copper, brass finish	1	0.07	0.07	0.1
	Hose fitting	Copper, brass finish	1	0.014	0.014	0.03
	6 mm screws	Steel	44	0.023	1.01	2.13
	6 mm Nylock nuts	Stainless steel	44	0.003	0.13	0.3
	6 mm washers	Steel	88	0.003	0.26	0.5
	Sparge tube supports	Polycarbonate	2	0.0009	0.0018	0.004
Frame	Glazing	4 mm Glass	1	11.0	11.0	23.1
	Frame	18 mm Plywood	1	8.13	8.13	17.1
	Screws	Steel	12	0.00063	0.01	0.016
	Sealant	Silicon	1	0.005	0.005	0.001
	Waterproofing	Black paint	1	0.005	0.005	0.001
Additions	Absorber insulation	Spacetherm© Areogel	1	0.96	0.96	2.02
					Total	**47.5**	**100**

Table B.12: Finned tank with night cover in SIP

	Component	Material	Quantity	Mass, 1 unit (kg)	Mass, total (kg)	% Total weight
Collector	Tank base	1.5 mm Stainless steel	1	14.4	14.4	30.
	Absorber plate (w. fins)	3 mm aluminium	1	9.7	9.7	20.2
	Absorber plate coating	Black spray paint	4 coats	0.7	0.7	1.46
	Sparge tube	Copper	1	0.58	0.58	1.2
	Gasket	EPDM rubber	1	0.37	0.37	0.77
	Gasket sealant	Hylomar	1	0.1	0.1	0.2
	Compression Reducing Coupling	Copper, brass finish	1	0.1	0.1	0.2
	Compression Straight Coupling	Copper, brass finish	1	0.07	0.07	0.1
	Hose fitting	Copper, brass finish	1	0.014	0.014	0.03
	6 mm screws	Steel	44	0.023	1.01	2.11
	6 mm Nylock nuts	Stainless steel	44	0.003	0.13	0.27
	6 mm washers	Steel	88	0.003	0.26	0.5
	Sparge tube supports	Polycarbonate	2	0.0009	0.0018	0.004
Frame	Glazing	4 mm Glass	1	11.0	11.0	22.8
	Frame	18 mm Plywood	1	8.13	8.13	16.9
	Screws	Steel	12	0.00063	0.01	0.015
	Sealant	Silicon	1	0.005	0.005	0.001
	Waterproofing	Black paint	1	0.005	0.005	0.001
Additions	Channels	Aluminium	2	0.35	0.7	1.46
	Insulating blind	Airtec foil	1	0.35	0.35	0.73
	Roller for blind	Aluminium	1	0.28	0.28	0.6
	Supports for roller	Plywood	2	0.04	0.08	0.2
	Stabilising band	Polycarbonate	1	0.11	0.11	0.22
	Screws	Steel	8	0.00063	0.005	0.007
				Total	**48.1**	**100**

Appendix C

LCI: Ecoinvent processes

Input/output | Parameters

Name	Status	Comment
Plain baffled collector in frame	None	

Materials/Assemblies	Amount	Unit
Aluminium, primary, ingot {IAI Area, EU27 & EFTA}| production | APOS, U	8.5	kg
Acrylic varnish, without water, in 87.5% solution state {RER}| acrylic varnish production, product in 87.5% solution state | APOS, U	0.7	kg
Copper {RER}| production, primary | APOS, U	0.8	kg
Synthetic rubber {RER}| production | APOS, U	0.37	kg
Polycarbonate {RER}| production | APOS, U	1.6	kg
Flat glass, uncoated {RER}| production | APOS, U	11	kg
Polyurethane, rigid foam {RER}| production | APOS, U	2	kg
ICS_Plywood by mass, for outdoor use {RER}| production | APOS, U	28.3	kg
Steel, chromium steel 18/8 {RER}| steel production, electric, chromium steel 18/8 | APOS, U	15.8	kg
Add line		

Processes	Amount	Unit	Distribution	SD2 or 2SD	Min	Max	Comment
Add line							

Figure C.1: Plain baffled collector in frame

Input/output | Parameters

Name	Status	Comment
Plain baffled collector in SIP	None	

Materials/Assemblies	Amount	Unit
Aluminium, primary, ingot {IAI Area, EU27 & EFTA}| production | APOS, U	8.5	kg
Acrylic varnish, without water, in 87.5% solution state {RER}| acrylic varnish production, product in 87.5% solution state | APOS, U	0.7	kg
Copper {RER}| production, primary | APOS, U	0.8	kg
Synthetic rubber {RER}| production | APOS, U	0.37	kg
Polycarbonate {RER}| production | APOS, U	1.6	kg
Flat glass, uncoated {RER}| production | APOS, U	11	kg
ICS_Plywood by mass, for outdoor use {RER}| production | APOS, U	8.13	kg
Steel, chromium steel 18/8 {RER}| steel production, electric, chromium steel 18/8 | APOS, U	15.8	kg
Add line		

Processes	Amount	Unit	Distribution	SD2 or 2SD	Min	Max	Comment
Add line							

Figure C.2: Plain baffled collector in SIP

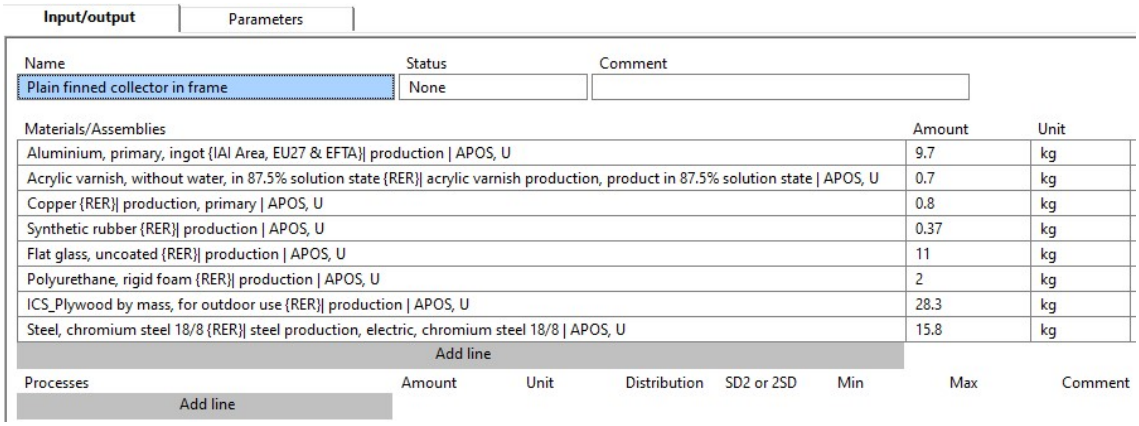

Input/output | Parameters

Name	Status	Comment
Plain finned collector in frame	None	

Materials/Assemblies	Amount	Unit
Aluminium, primary, ingot {IAI Area, EU27 & EFTA}| production | APOS, U	9.7	kg
Acrylic varnish, without water, in 87.5% solution state {RER}| acrylic varnish production, product in 87.5% solution state | APOS, U	0.7	kg
Copper {RER}| production, primary | APOS, U	0.8	kg
Synthetic rubber {RER}| production | APOS, U	0.37	kg
Flat glass, uncoated {RER}| production | APOS, U	11	kg
Polyurethane, rigid foam {RER}| production | APOS, U	2	kg
ICS_Plywood by mass, for outdoor use {RER}| production | APOS, U	28.3	kg
Steel, chromium steel 18/8 {RER}| steel production, electric, chromium steel 18/8 | APOS, U	15.8	kg
Add line		

Processes	Amount	Unit	Distribution	SD2 or 2SD	Min	Max	Comment
Add line							

Figure C.3: Plain finned collector in frame

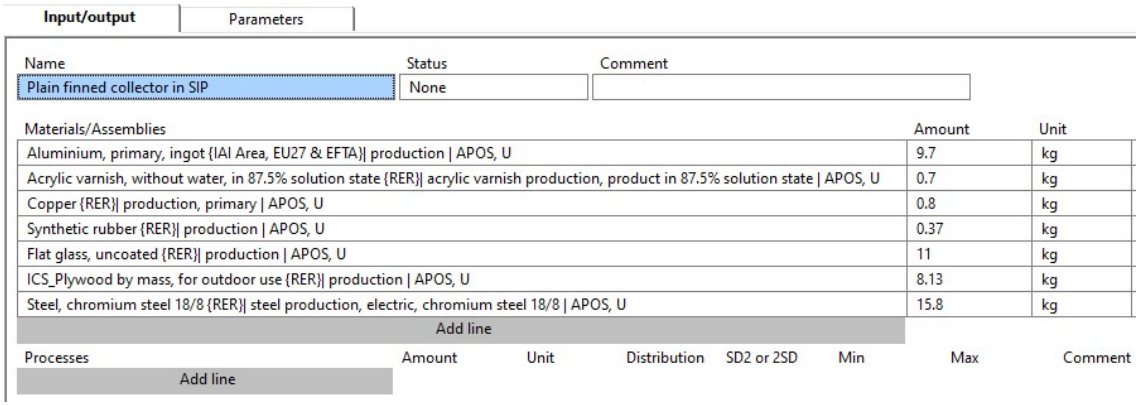

Input/output | Parameters

Name	Status	Comment
Plain finned collector in SIP	None	

Materials/Assemblies	Amount	Unit
Aluminium, primary, ingot {IAI Area, EU27 & EFTA}| production | APOS, U	9.7	kg
Acrylic varnish, without water, in 87.5% solution state {RER}| acrylic varnish production, product in 87.5% solution state | APOS, U	0.7	kg
Copper {RER}| production, primary | APOS, U	0.8	kg
Synthetic rubber {RER}| production | APOS, U	0.37	kg
Flat glass, uncoated {RER}| production | APOS, U	11	kg
ICS_Plywood by mass, for outdoor use {RER}| production | APOS, U	8.13	kg
Steel, chromium steel 18/8 {RER}| steel production, electric, chromium steel 18/8 | APOS, U	15.8	kg
Add line		

Processes	Amount	Unit	Distribution	SD2 or 2SD	Min	Max	Comment
Add line							

Figure C.4: Plain finned collector in SIP

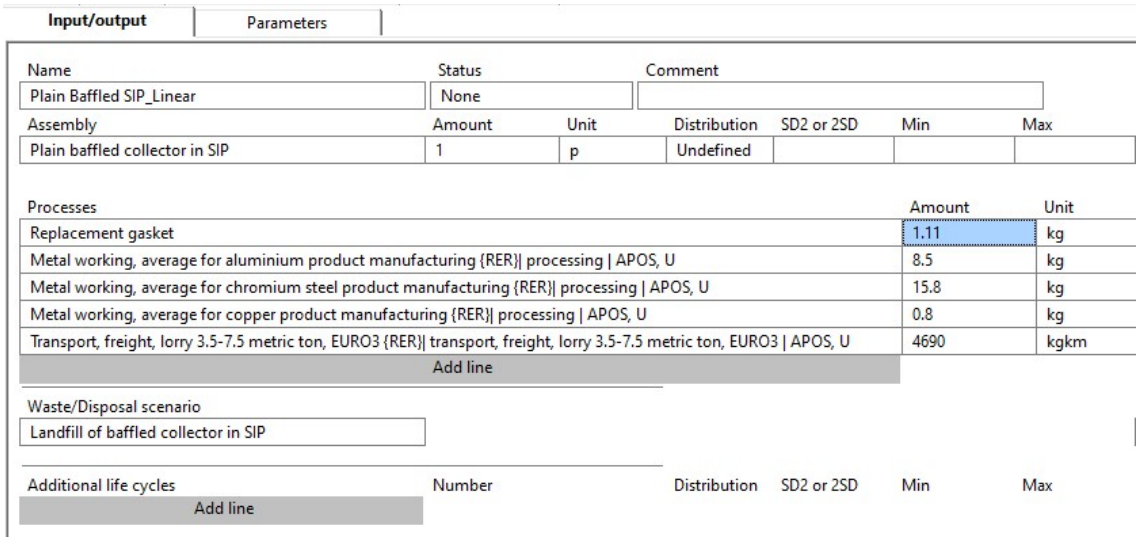

Input/output | Parameters

Name	Status	Comment
Plain Baffled SIP_Linear	None	

Assembly	Amount	Unit	Distribution	SD2 or 2SD	Min	Max
Plain baffled collector in SIP	1	p	Undefined			

Processes	Amount	Unit
Replacement gasket	1.11	kg
Metal working, average for aluminium product manufacturing {RER}| processing | APOS, U	8.5	kg
Metal working, average for chromium steel product manufacturing {RER}| processing | APOS, U	15.8	kg
Metal working, average for copper product manufacturing {RER}| processing | APOS, U	0.8	kg
Transport, freight, lorry 3.5-7.5 metric ton, EURO3 {RER}| transport, freight, lorry 3.5-7.5 metric ton, EURO3 | APOS, U	4690	kgkm
Add line		

Waste/Disposal scenario

Landfill of baffled collector in SIP

Additional life cycles	Number	Distribution	SD2 or 2SD	Min	Max
Add line					

Figure C.5: Product stages of the life cycle assessment - plain baffled collector in SIP under a linear scenario. Plain finned collector in SIP under a linear scenario has the same processes but the assembly and waste/disposal scenario are specific to the finned collector

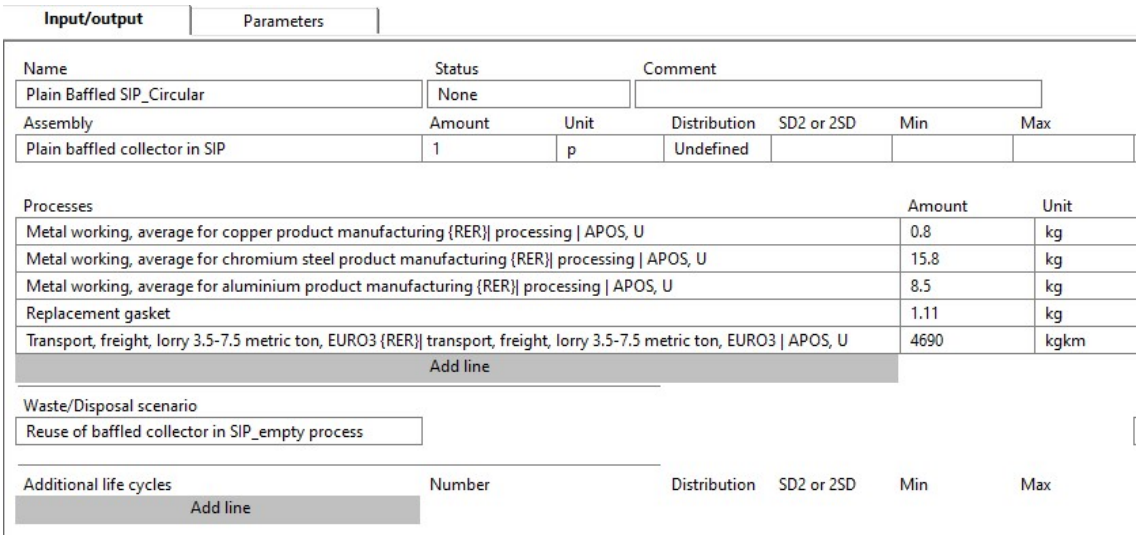

Input/output | Parameters

Name	Status	Comment
Plain Baffled SIP_Circular	None	

Assembly	Amount	Unit	Distribution	SD2 or 2SD	Min	Max
Plain baffled collector in SIP	1	p	Undefined			

Processes	Amount	Unit
Metal working, average for copper product manufacturing {RER}| processing | APOS, U	0.8	kg
Metal working, average for chromium steel product manufacturing {RER}| processing | APOS, U	15.8	kg
Metal working, average for aluminium product manufacturing {RER}| processing | APOS, U	8.5	kg
Replacement gasket	1.11	kg
Transport, freight, lorry 3.5-7.5 metric ton, EURO3 {RER}| transport, freight, lorry 3.5-7.5 metric ton, EURO3 | APOS, U	4690	kgkm

Add line

Waste/Disposal scenario

Reuse of baffled collector in SIP_empty process

Additional life cycles	Number	Distribution	SD2 or 2SD	Min	Max

Add line

Figure C.6: Product stages of the life cycle assessment - plain baffled collector in SIP under a circular scenario. Note that the waste/disposal scenario is an empty process to represent the reusable materials exiting the system. Plain finned collector in SIP under a circular scenario has the same processes but the assembly and waste/disposal scenario are specific to the finned collector

Appendix D

LCA process flows

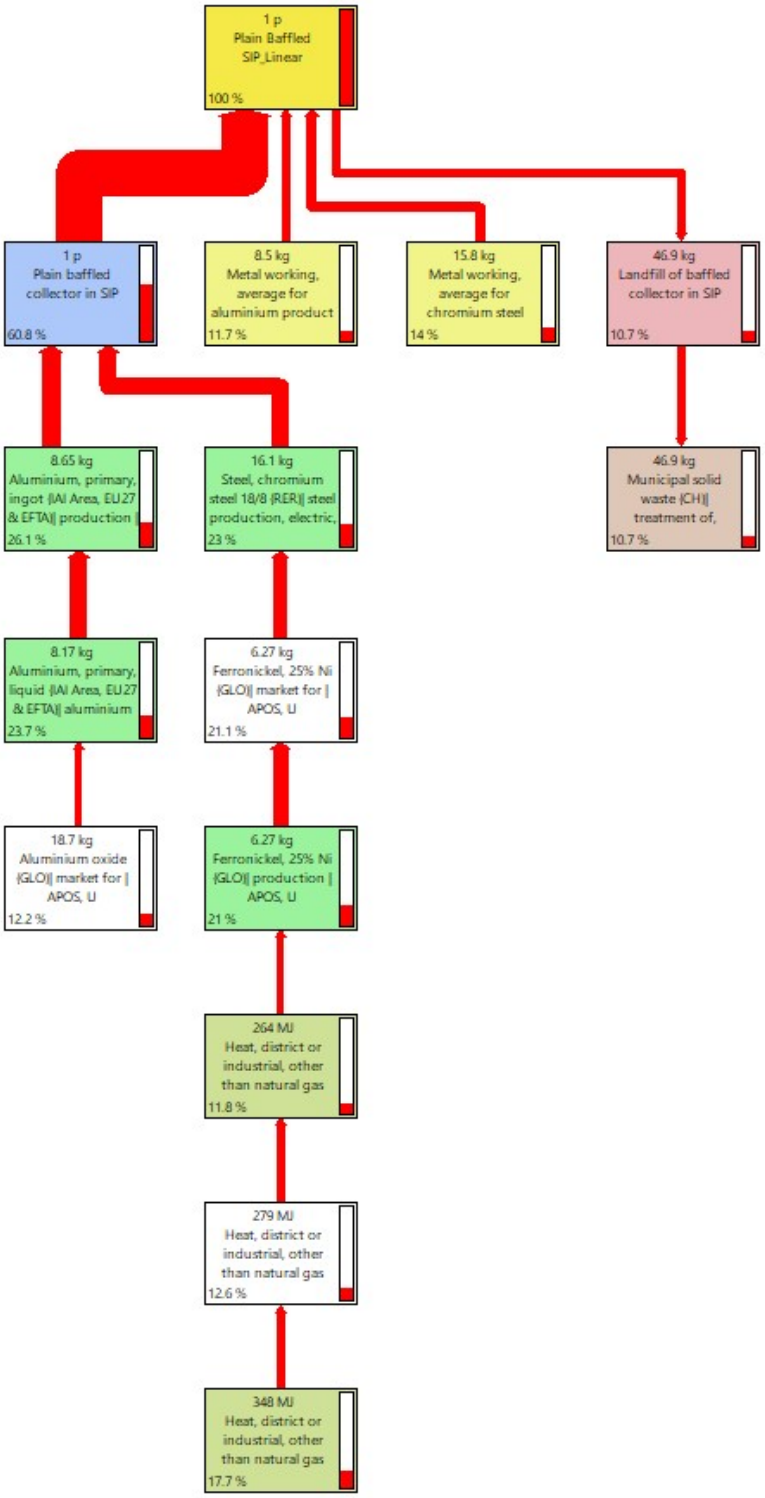

Figure D.1: Process network for the plain baffled collector integrated into the SIP, under a linear scenario, using the IPCC 2013 GWP (100a) LCIA method. Node cut-off threshold: 10%, visible nodes: 15, total nodes: 12,730

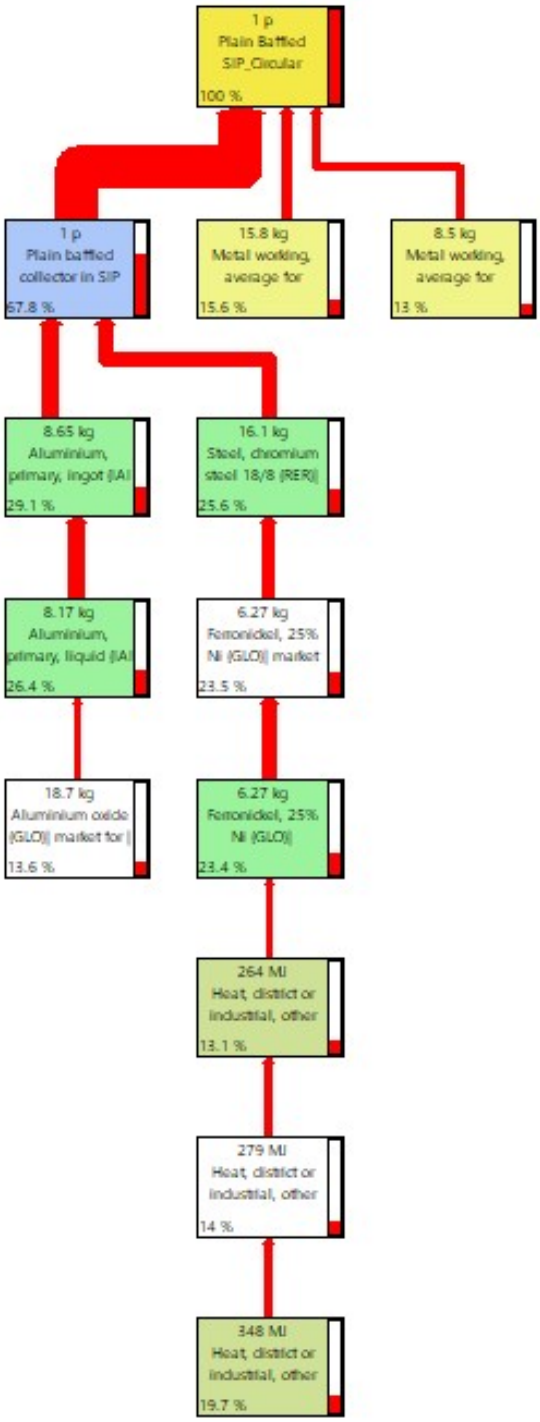

Figure D.2: Process network for the plain baffled collector integrated into the SIP, under a circular scenario, using the IPCC 2013 GWP (100a) LCIA method. Node cut-off threshold: 10%, visible nodes: 13, total nodes: 12,732

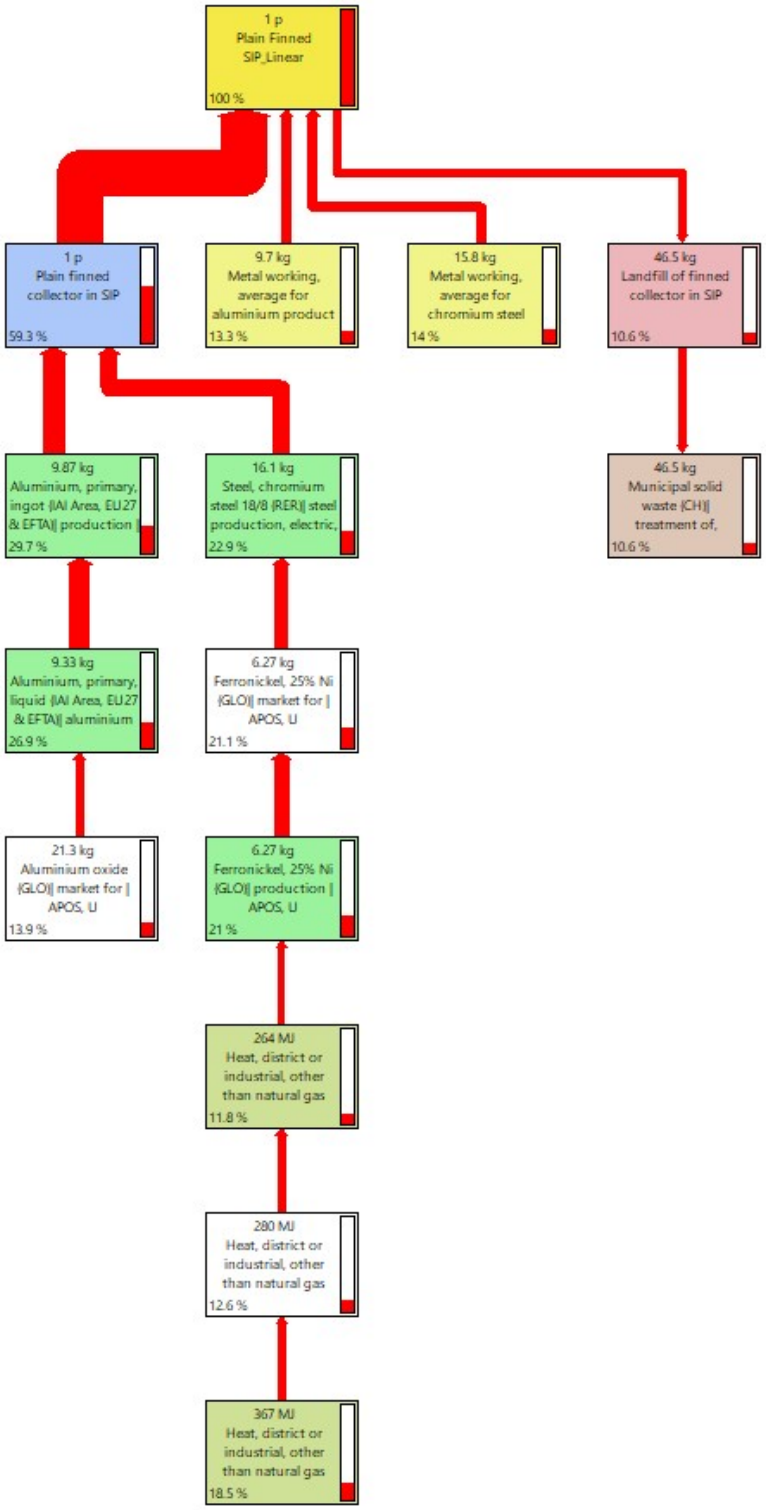

Figure D.3: Process network for the plain finned collector integrated into the SIP, under a linear scenario, using the IPCC 2013 GWP (100a) LCIA method. Node cut-off threshold: 10%, visible nodes: 15, total nodes: 12,730

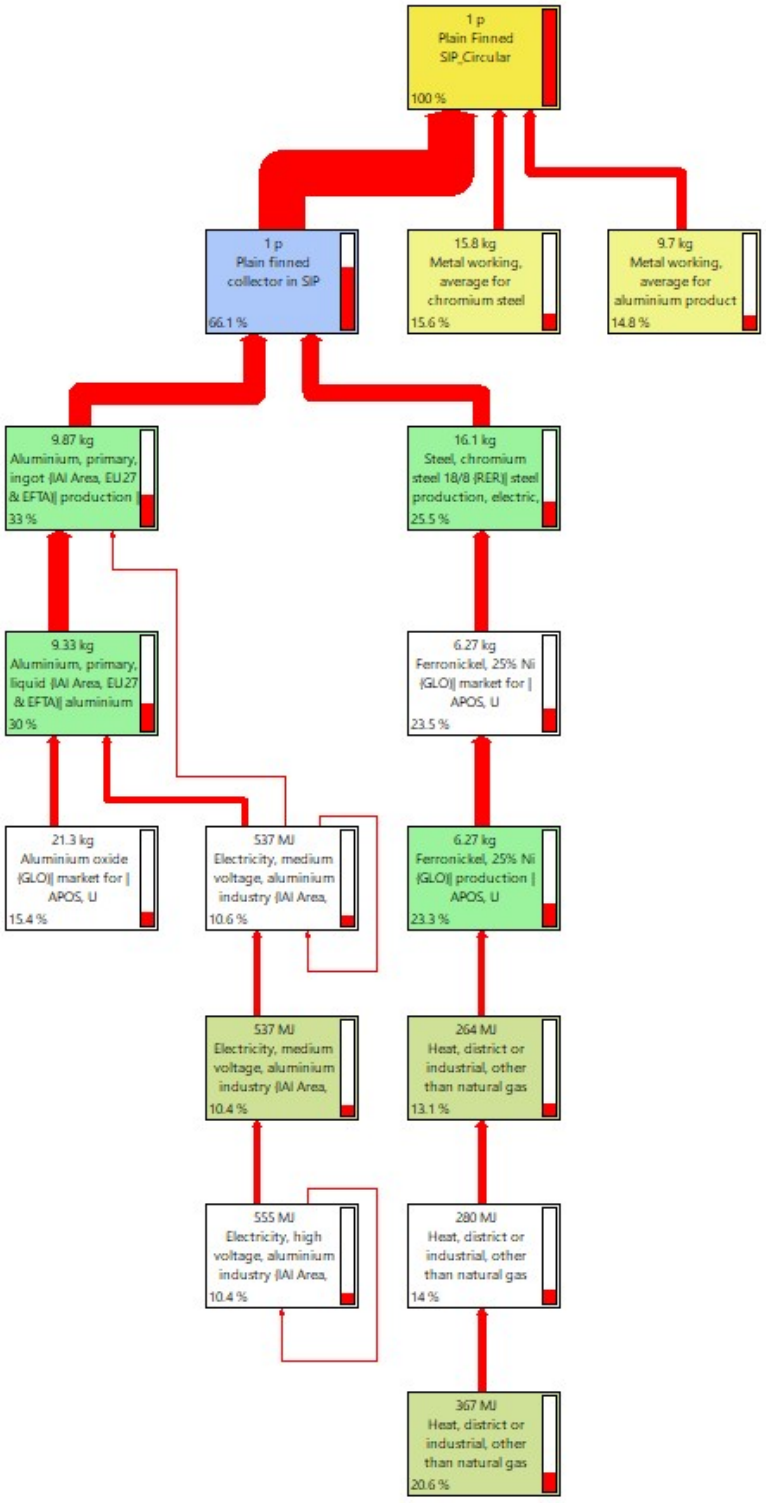

Figure D.4: Process network for the plain finned collector integrated into the SIP, under a circular scenario, using the IPCC 2013 GWP (100a) LCIA method. Node cut-off threshold: 10%, visible nodes: 16, total nodes: 12,732

Appendix E

Uncertainty analysis

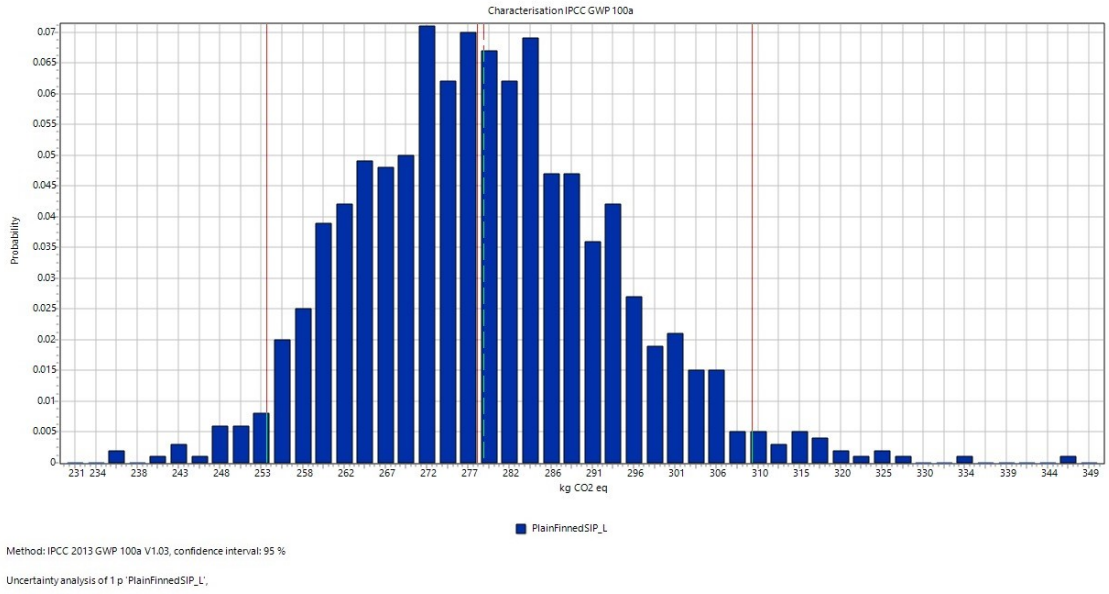

Figure E.1: GWP uncertainty analysis for the plain finned system integrated into a SIP, under a linear scenario

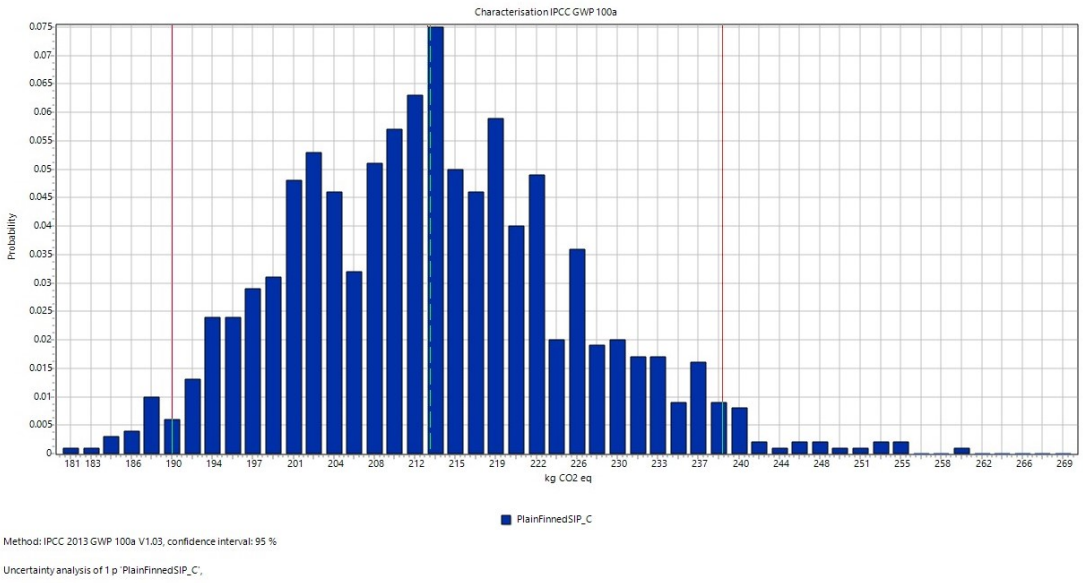

Figure E.2: GWP uncertainty analysis for the plain finned system integrated into a SIP, under a circular scenario

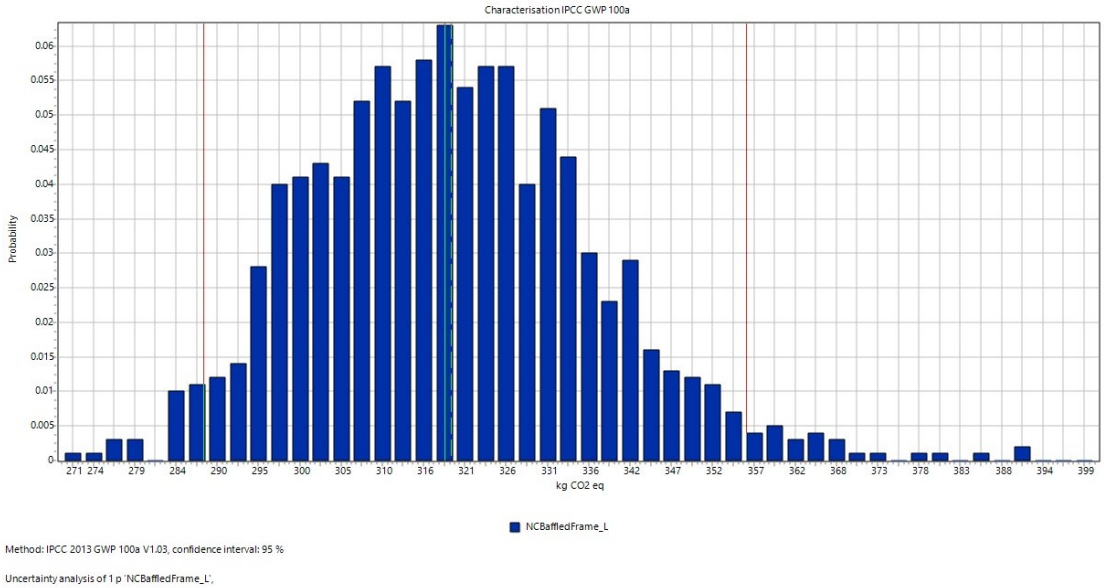

Figure E.3: GWP uncertainty analysis for the baffled system with a night cover mounted in a frame, under a linear scenario

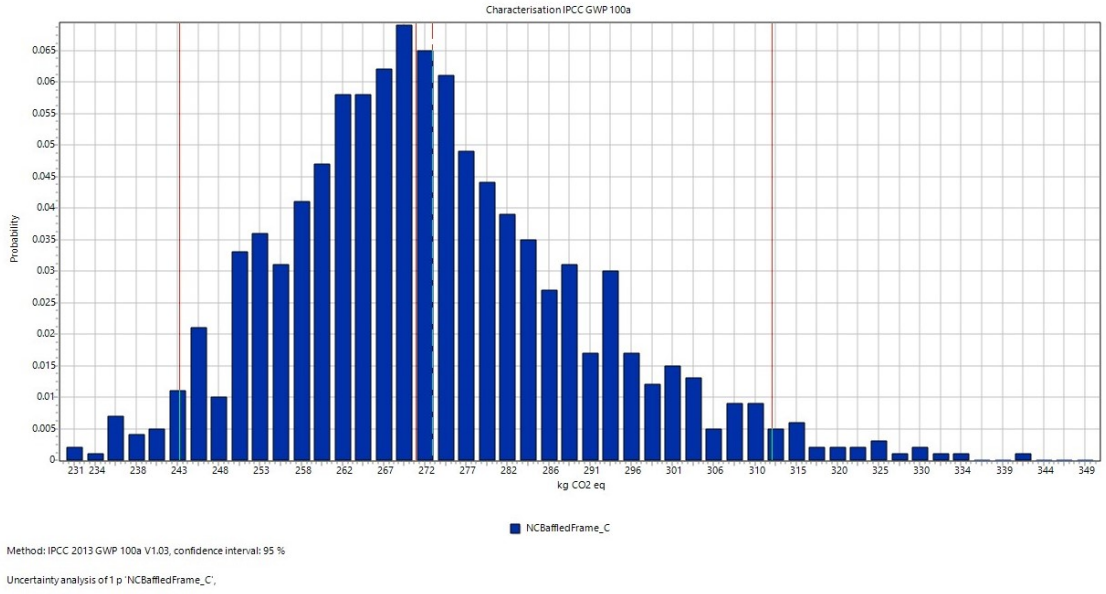

Figure E.4: GWP uncertainty analysis for the baffled system with a night cover mounted in a frame, under a circular scenario

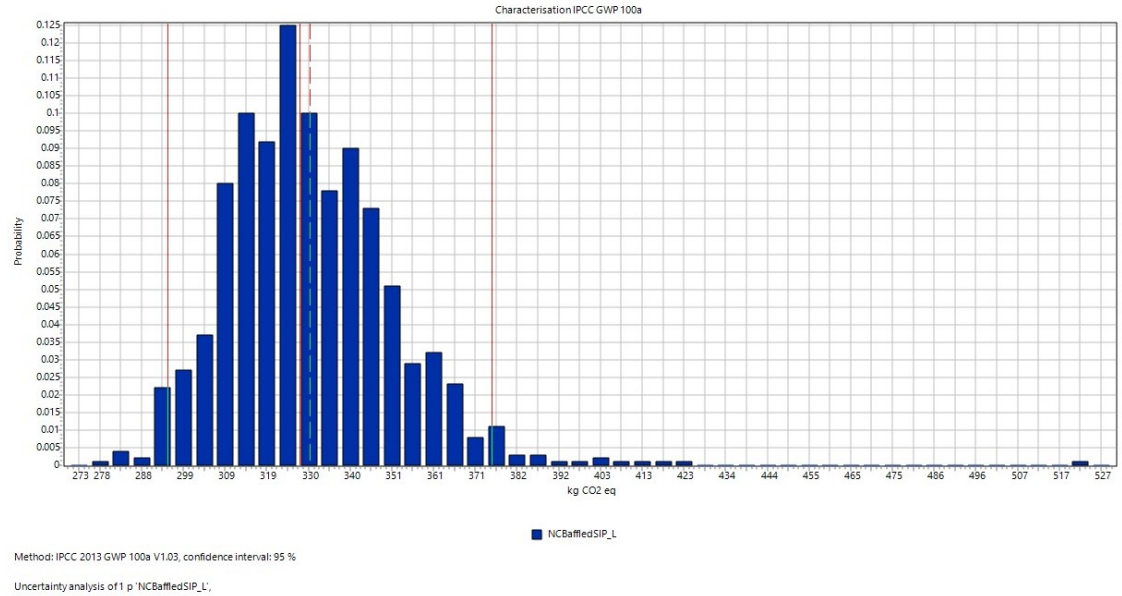

Figure E.5: GWP uncertainty analysis for the baffled system with a night cover integrated into a SIP, under a linear scenario

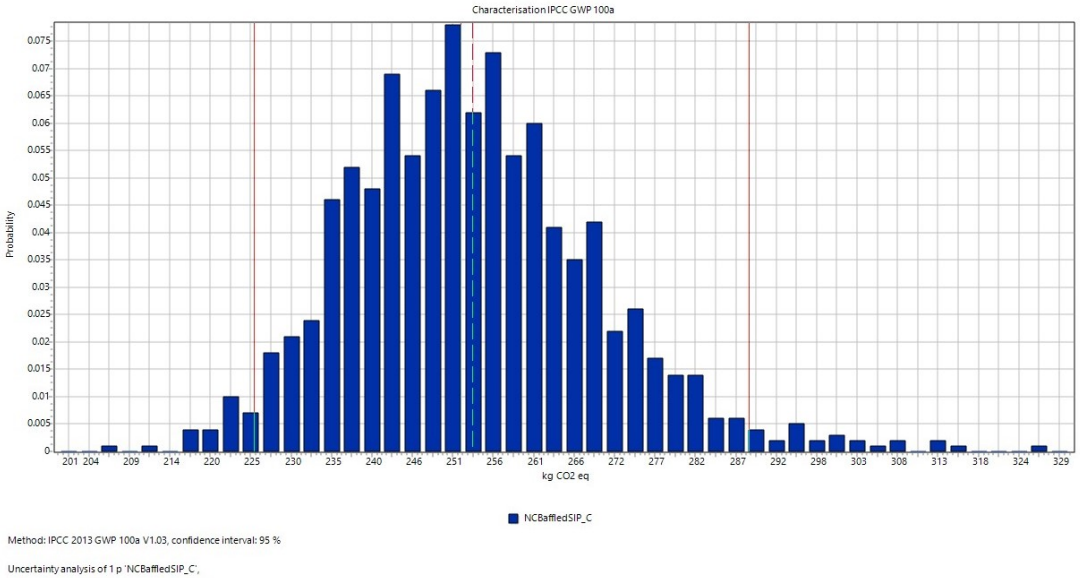

Figure E.6: GWP uncertainty analysis for the baffled system with a night cover integrated into a SIP, under a circular scenario

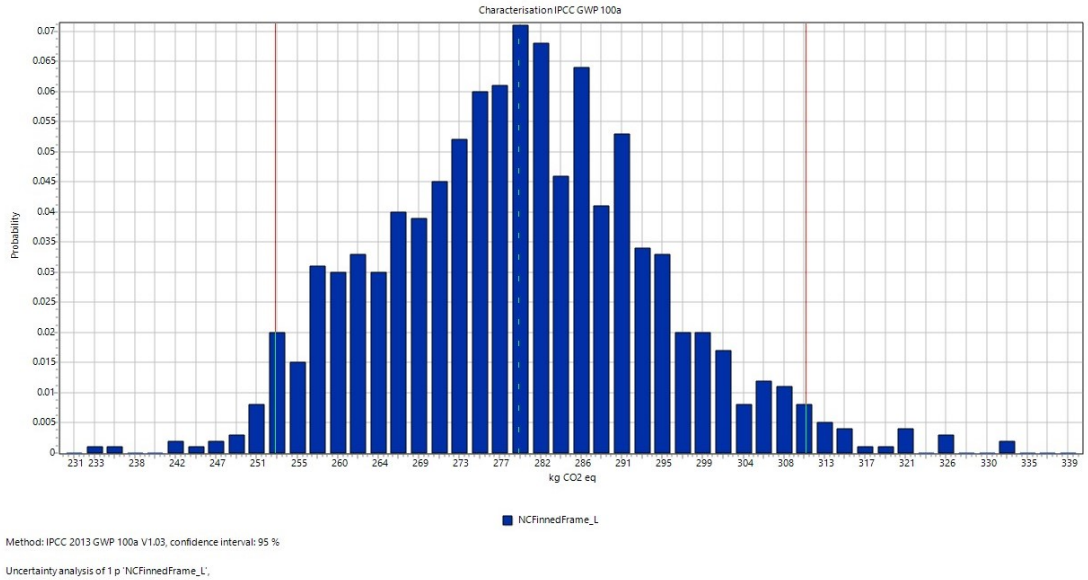

Figure E.7: GWP uncertainty analysis for the finned system with a night cover mounted in a frame, under a linear scenario

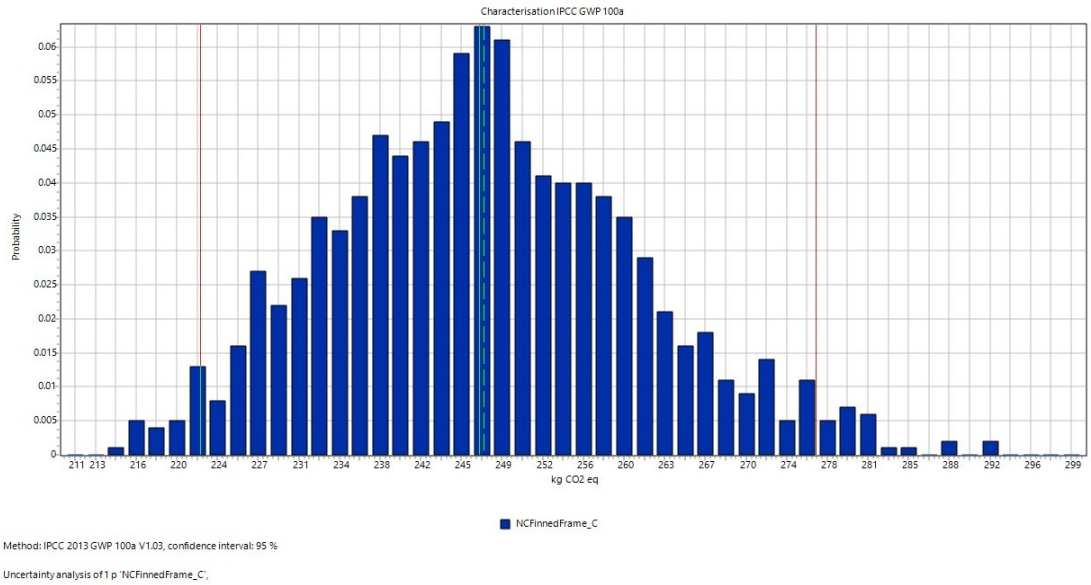

Figure E.8: GWP uncertainty analysis for the finned system with a night cover mounted in a frame, under a circular scenario

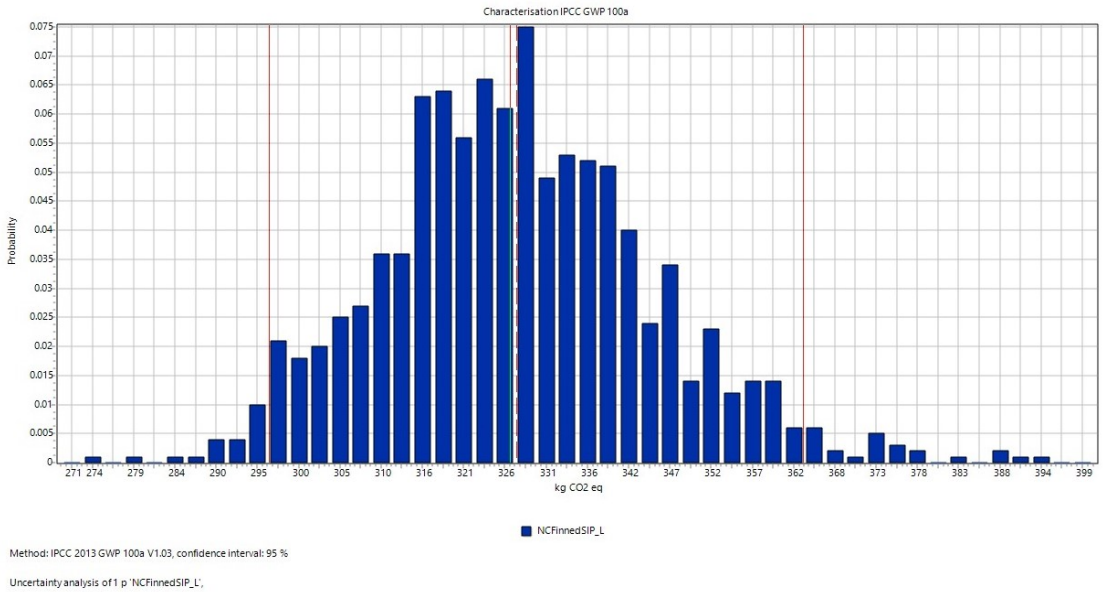

Figure E.9: GWP uncertainty analysis for the finned system with a night cover integrated into a SIP, under a linear scenario

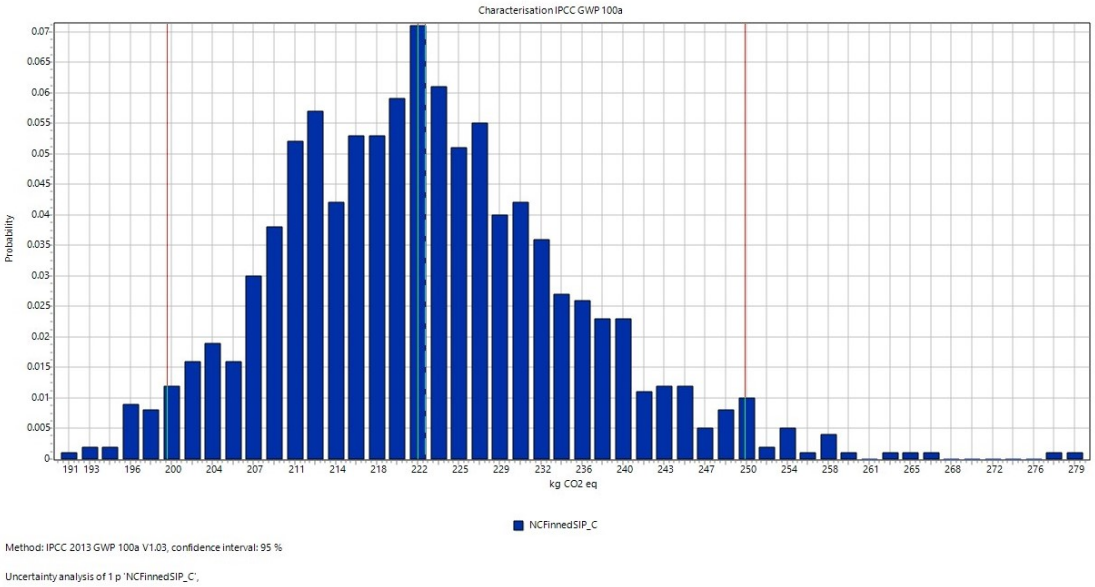

Figure E.10: GWP uncertainty analysis for the finned system with a night cover integrated into a SIP, under a circular scenario

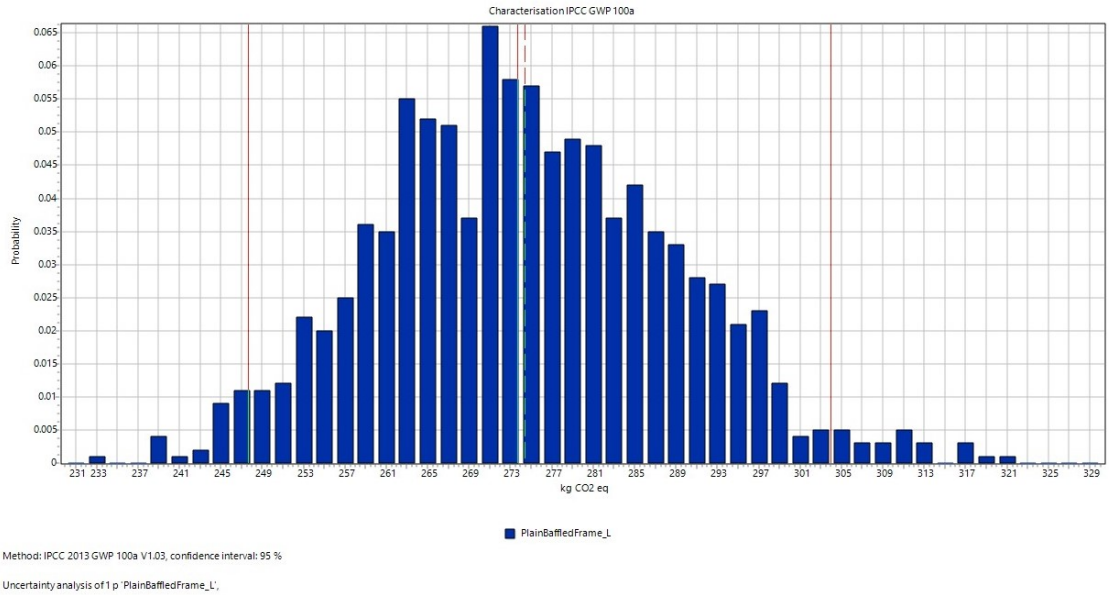

Figure E.11: GWP uncertainty analysis for the plain baffled system mounted in a frame, under a linear scenario

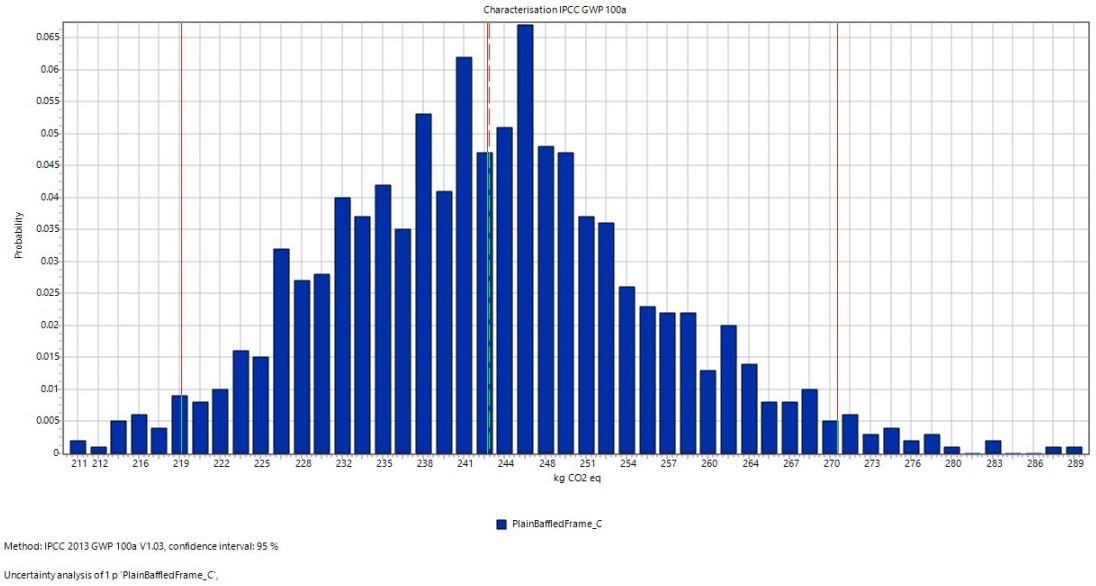

Figure E.12: GWP uncertainty analysis for the plain baffled system mounted in a frame, under a circular scenario

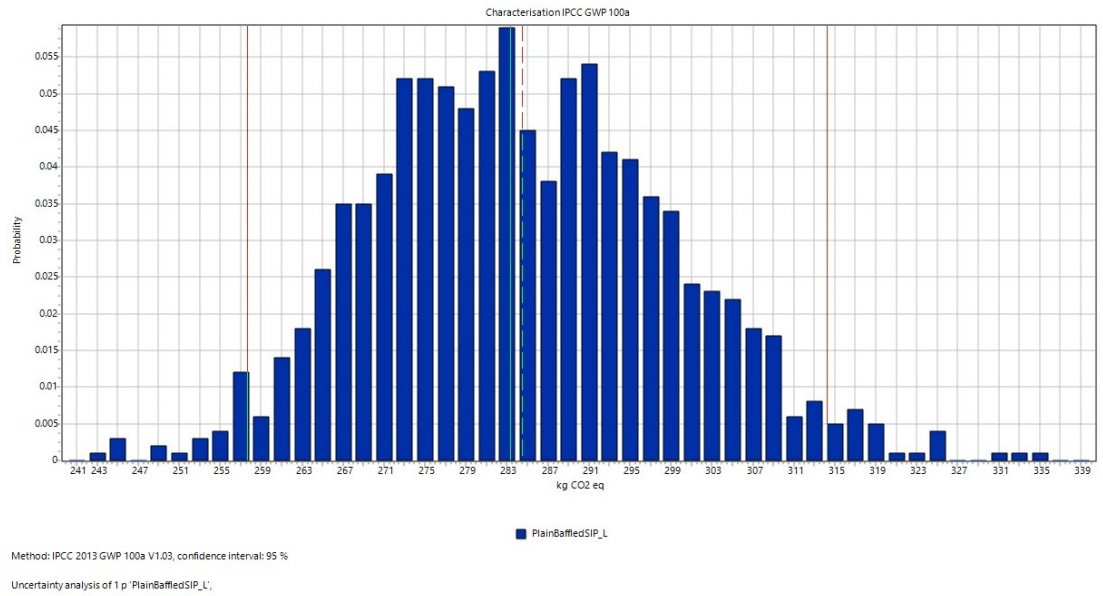

Figure E.13: GWP uncertainty analysis for the plain baffled system integrated into a SIP, under a linear scenario

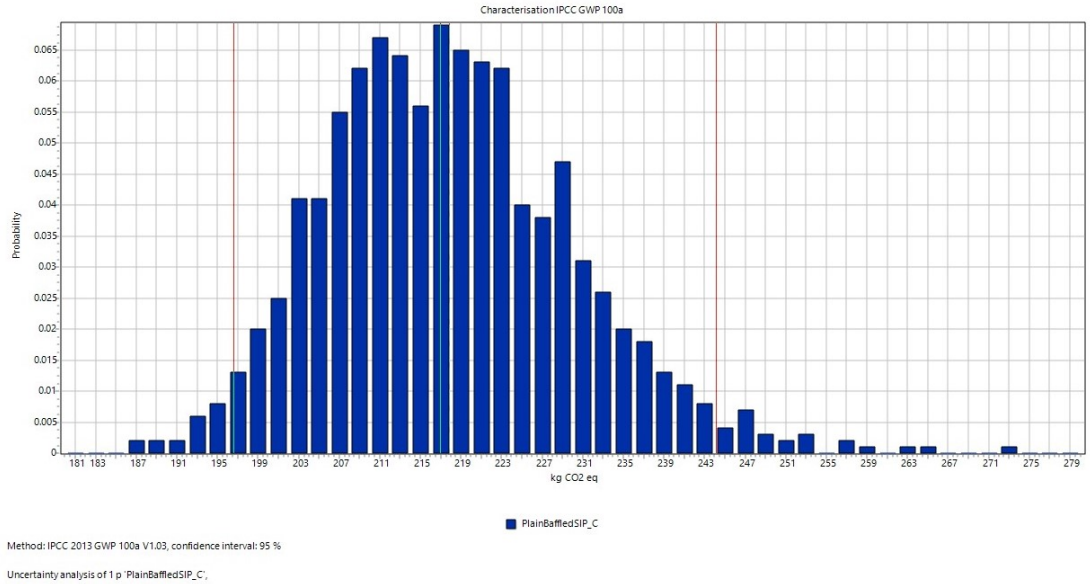

Figure E.14: GWP uncertainty analysis for the plain baffled system integrated into a SIP, under a circular scenario

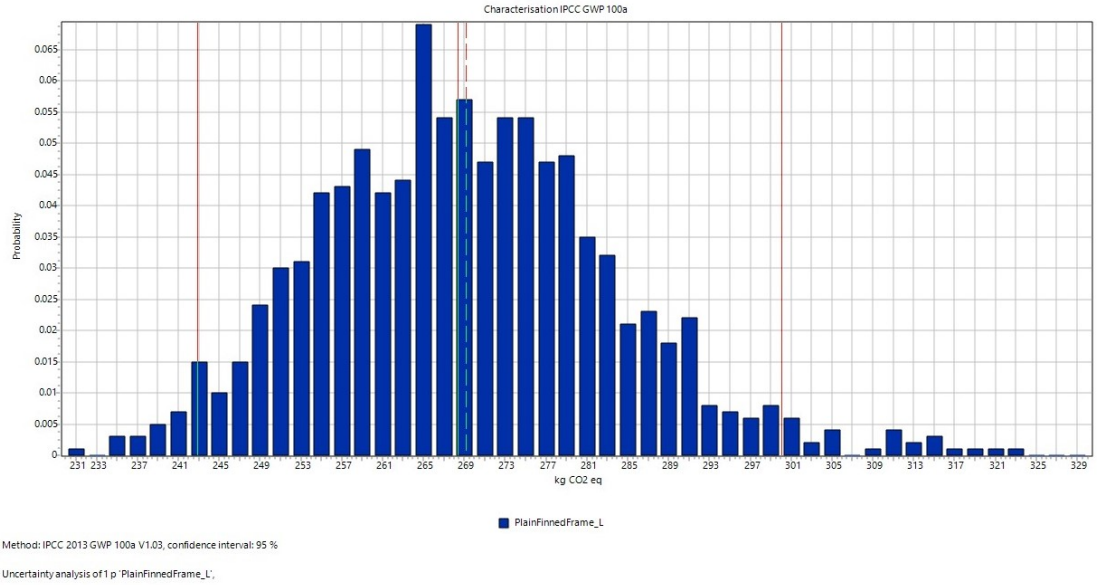

Figure E.15: GWP uncertainty analysis for the plain finned system mounted in a frame, under a linear scenario

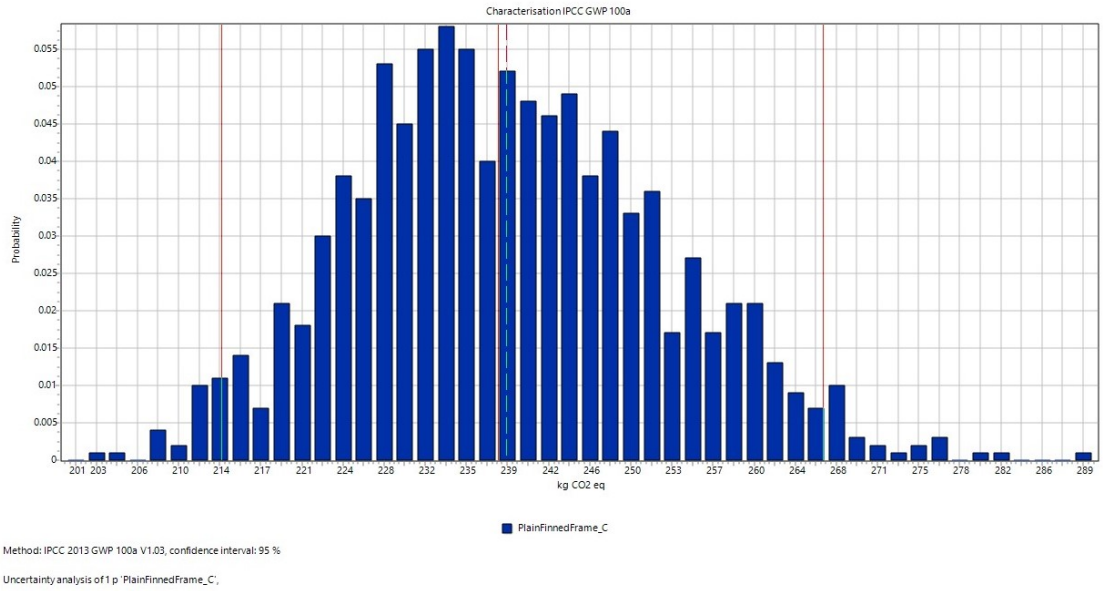

Figure E.16: GWP uncertainty analysis for the plain finned system mounted in a frame, under a circular scenario

Appendix F

Glossary of terms

Aspect ratio Internal geometric dimensions of a cavity. Vertical aspect ratio = height/length; Horizontal aspect ratio = width/length.

Baffle plate An insulating plate, inserted parallel to the absorber plate, which creates a narrow channel with a thin layer of water which can reach much higher temperatures than the main water body.

Blackbody radiation A blackbody absorbs all incident radiation, regardless of wavelength and direction. A blackbody is a diffuse emitter. As a perfect absorber and emitter, the blackbody serves as a standard against which the radiative properties of actual surfaces may be compared.

Buoyancy effect Water at a given temperature will settle down at an appropriate height in accordance with the prevalent density of the fluid. I.e. hot, lower density water naturally rises to upper layers and cold, higher density water sinks to bottom layers.

Conduction The transfer of energy, such as heat, through a substance. Heat energy is transmitted through collisions with neighbouring molecules.

Convection Transfer of heat by circulation/movement of heated parts of a liquid/gas, thermal energy expands the fluid causing buoyant movement.

Cost Analysis An economic evaluation technique to determine the total cost of owning and operating a product with time.

Destratification The breakdown of stratification or the mixing of different temperature layers.

Draw-off The removal of water from the storage tank.

Ecoinvent Life cycle inventory database containing life cycle processes for thousands of materials.

Embodied Hidden carbon generated in the extraction and production of raw materials, the manufacture of the system components, the construction of the product and its deconstruction at the end of its useful life, and the transportation required between each of these stages.

Embodied carbon payback time The time necessary for a product to save or offset the CO_2 emissions released during the production and use of the installation itself, i.e. embodied carbon.

Energy payback time The time necessary for a product to collect the energy equivalent to that used to produce it, i.e. embodied energy.

Fins Sections/struts that extend the length and depth of the water body to improve conductive heat transfer.

Heat transfer coefficient The proportionality constant between the heat flux and the thermodynamic driving force for the flow of heat (i.e., ΔT).

Heating load The amount of heat energy that would need to be added to a space to maintain the temperature in an acceptable range.

Life cycle assessment An environmental management tool that allows the environmental impact of a product to be evaluated. LCA consists of four steps: goal and scope identification, life cycle inventory, life cycle impact assessment and interpretation of results.

Monetary payback time The time necessary for a product to achieve the monetary equivalent to its capital cost.

Nusselt (Nu) Number Ratio of convective to conductive heat transfer across a boundary within a fluid. A larger Nu number means more active convection. A Nu close to 1 means convection and conduction are of similar magnitude creating sluggish flow. Depends on Rayleigh and Prandtl numbers, vertical and horizontal aspect ratios, angle of inclination and end wall boundary conditions.

Policy A committed course of action which has been wholly decided upon, and to which a policy outcome can be attributed to with a reasonable level of confidence.

Pyranometer A device that is used to measure the intensity of solar radiation.

Rayleigh Number (Ra) For a fluid – dimensionless, associated with buoyancy driven flow, also known as free or natural convection. Defined as the product of the Grashof number, which describes the relationship between buoyancy and viscosity within a fluid, and the Prandtl number, which describes the relationship between momentum diffusivity and thermal diffusivity.

Regression analysis A statistical process for estimating the relationships among variables. It includes many techniques for modelling and analysing several variables, when the focus is on the relationship between a dependent variable and one or more independent variables (or 'predictors').

SimaPro Software tool for conducting life cycle assessment. Contained various database libraries, including ecoinvent, and life cycle impact assessment methods, including CML-IA baseline and CED demand.

Stratification The degree of temperature difference between different points along the vertical length of a body of water.

Thermocouple Temperature-dependent voltage, two different conductors forming electrical junctions at different temperatures, interpreted to measure temperature. K-type = general purpose due to low cost and temperature range.

Thermosyphon A physical effect and refers to a method of passive heat exchange based on natural convection, which circulates a fluid without the necessity of a mechanical pump.

U-value Depends on the thermal resistance of the material. Every material has its own thermal resistivity and, therefore, its own U-value. It is the overall heat transfer coefficient that describes how well a building element conducts heat or the rate of transfer of heat (in watts) through one square metre of a structure divided by the difference in temperature across the structure. Measures the effectiveness of a material as an insulator – lower U-value equals better insulator.